Behaviour of hydrogels swollen in polymer solutions under mechanical action

Sylvie Vervoort

ECOLE DES MINES
DE PARIS

Ecole Doctorale 364 : Sciences Fondamentales et Appliquées

N° attribué par la bibliothèque

|__|__|__|__|__|__|__|__|__|__|

T H E S E

pour obtenir le grade de
Docteur de l'Ecole des Mines de Paris
Spécialité «Science et génie des matériaux»

présentée et soutenue publiquement par

Mlle Sylvie Vervoort

le 19 mai 2006

COMPORTEMENT D'HYDROGELS GONFLES DE SOLUTIONS DE POLYMERES SOUS ACTION MECANIQUE

Directeur de thèse : Tatiana Budtova

Jury :

M Dominique Durand	Rapporteur
Mme Paula Moldenaers	Rapporteur
M Denis Poncelet	Examinateur
M Jean-François Tranchant	Examinateur
Mme Tatiana Budtova	Examinateur
M Patrick Navard	Invité

ECOLE DES MINES
DE PARIS

Ecole Doctorale 364 : Sciences Fondamentales et Appliquées

N° attribué par la bibliothèque

|__|__|__|__|__|__|__|__|__|__|__|__|

T H E S E

pour obtenir le grade de
Docteur de l'Ecole des Mines de Paris
Spécialité «Sciences et génie des matériaux»

présentée et soutenue publiquement par

Mlle Sylvie Vervoort

le 19 mai 2006

BEHAVIOUR OF HYDROGELS SWOLLEN IN POLYMER SOLUTIONS UNDER MECHANICAL STRESS

Directeur de thèse : Tatiana Budtova

Jury :

M Dominique Durand	Rapporteur
Mme Paula Moldenaers	Rapporteur
M Denis Poncelet	Examinateur
M Jean-François Tranchant	Examinateur
Mme Tatiana Budtova	Examinateur
M Patrick Navard	Invité

Liberté

Prenez du soleil
Dans les creux des mains,
Un peu de soleil
Et partez au loin.

Partez dans le vent,
Suivez votre rêve;
Partez à l’instant,
La jeunesse est brève!

Il y a des chemins
Inconnus des hommes
Il y a des chemins
Si aériens.

Ne regrettez pas
Ce que vous quittez
Regardez là-bas,
L’horizon briller.

Loin, toujours plus loin,
Partez en chantant.
Le monde appartient
À ceux qui n’ont rien.

[Maurice Carême]

Remerciements

Cette thèse n'a non seulement été un premier projet professionnel, mais également une grande aventure personnelle. Maintenant qu'elle est soutenue et corrigée, le moment est venu de faire honneur à toutes ces personnes qui m'ont assistée et accompagnée tout au long de cette expédition. Elles m'ont laissée profiter de leurs compétences ou juste prêté oreille à mon enthousiasme et mes frustrations. Sachez que sans vous, ce travail ne serait pas devenu ce que c'est !

Ce travail a été effectué au Centre de Mise en Forme des Matériaux de l'Ecole des Mines de Paris. Je remercie les directions de m'avoir offert la possibilité de faire cette thèse. Je remercie également M. Patrick Navard, chef du groupe Physico-chimie des polymères de m'avoir accueillie dans son groupe, mais également pour ses idées et sa confiance. Je dois beaucoup à Mme Tania Budtova, ma directrice de thèse, qui a encadré ce travail avec beaucoup d'enthousiasme et sa note d'optimisme. Nos discussions ont traversé toutes les frontières entre la France, la Russie et même la Hollande et la Belgique pendant la rédaction.

Je remercie sincèrement les membres du jury : son président Mr Denis Poncelet, les rapporteurs Mme Paula Moldenaers et Mr Dominique Durand et Mr Jean-François Tranchant, représentant de la société Dior, pour l'intérêt qu'ils ont porté à mon travail et pour leurs commentaires instructeurs. La Professeur Moldenaers mérite une mention spéciale ici, car c'est grâce à ses efforts pour les échanges Erasmus que j'ai atterri au Cemef..

Le sujet s'inscrit dans le projet 'Gels polyélectrolytiques adaptatifs' du Réseau National d'Innovation Matériaux et Procédés (RNMP) et est financé par le Ministère de la recherche. Je remercie nos partenaires Dominique Durand de l'Université du Maine, Jean-François Tranchant de Parfums Dior et Jeoffrey Nicq de la société Hutchinson pour les échanges constructifs lors de nos réunions.

Je suis très reconnaissante à Bernard Pouligny du CRPP à Bordeaux qui m'a permis de faire les mesures d'orientation dans son laboratoire et aux messieurs Ferenc Horkay et Eric Geissler pour leurs conseils à propos de la synthèse de gel. Je remercie également Stanislav Patlazhan pour sa contribution à la modélisation du gel sous compression.

Le travail de thèse serait beaucoup plus dur sans les services du secrétariat, la bibliothèque, la reprographie et de l'équipe informatique. Je remercie l'équipe 'soignante' du contra-rotatif, Roland, Francis et Jo, de toujours avoir su le réparer avec le sourire (parce que j'étais bien belge…).

Je salue chaleureusement les autres thésards qui ont fait un bout de chemin avec moi et qui ont sûrement rendu la vie au labo plus agréable. Mention spéciale pour les championnes du foot, mes

coéquipiers du volley et les accros de la rando et des bons repas: Karine, Danielle, Olga, Arnaud, Céline, les Laurent, Josué, Luísa, Hugues, …: avec vous j'ai connu bien plus du sud que l'intérieur des salles-Cemef ! Merci également d'avoir voulu (ou plutôt 'osé'?) goûter de mes gâteaux, gaufres, spéculoos… faits-maison. Je ne pourrais pas m'imaginer de panel meilleur!

Les autres 'filles PCP', Karine, Olga, Véro, Edith, Magali et Alice avec qui je n'ai non seulement partagé des salles de manip au sous-sol, mais aussi des séances de rangement, le recyclage papier (Véro) et de nombreuses pauses-café-décompression.

Une pensée très affective et des verres à Kwak pour Luísa et Hugues pour tous les bons moments que nous avons passés ensemble. Je n'oublierai jamais les accueils chaleureux qui m'attendaient chez vous lorsque je revenais travailler au CEMEF après mon départ. Il est temps maintenant que vous veniez loger chez moi !

Venue au terme de cette aventure française, je n'oublie pas non plus les amis de Belgique qui sont restés fidèles malgré la distance et qui m'ont tenue au courant de la vie belge : Ann D, Ann V, An, Els, en 't Clubke.

Enfin j'embrasse mes parents et ma sœur de m'encourager et de me soutenir dans tout ce que j'entreprends.

Table of contents

Nomenclature

Standard generally accepted notation has been used throughout this text. The important symbols are defined in this list. Standard International Units have to be used, unless mentioned differently.

Latin characters

a	Monomer length	[Å]
A	Number of monomers between effective charges	[-]
B	Parameter regrouping network preparation conditions **[1.24]**	[-]
B	Second virial coefficient	[-]
C	Third virial coefficient	[-]
C_p	Concentration by weight of product p	[w/w]
Ca	Capillary number	[-]
d	Monomer persistent length	[m]
D_{Taylor}	Deformation as defined by Taylor	[-]
E	Elastic (Young's) modulus	[Pa]
f	Functionality of crosslinks	[-]
F	Force	[N]
G, ΔG	Gibbs free energy, Gibbs free energy change	[J]
G', G", G*	Storage modulus, loss modulus, complex modulus	[Pa]
h	Gap width	[m]
H	Particle height	[m]
H, ΔH	Heat content or enthalpy, enthalpy change	[J]
i	Degree of ionisation	[-]
k_B	Boltzmann constant $1{,}380658.10^{-23}$	$[J.K^{-1}]$
ℓ_B	Bjerrum length	[m]
L	Particle length	[m]
L'	Length of particle with tips	[m]
m	Mass	[g]
M_w	Molar mass	$[g.mol^{-1}]$
M_c	Molar chain mass between crosslinks	$[g.mol^{-1}]$
n	Monomer concentration in gel	$[V^{-1}]$
N	Number of monomers in a strand of an ideal network	[-]
N_{AV}	Avogadro constant $6{,}023.10^{23}$	$[mol^{-1}]$
p	Viscosity ratio droplet - matrix	[-]
P	Pressure	[Pa]
q	Volume degree of swelling	$[m^3/m^3]$

Q	Mass degree of swelling	[g/g]
r	Radial position from the rotation centre in the shear cell	[m]
r_g	Radius of gyration	[m]
R	Ideal gas constant, 8.314	[$J.mol^{-1}.K^{-1}$]
R	Radius	[m]
S, ΔS	Entropy, Entropy change	[$J.K^{-1}$]
t	Time	[s]
t_{SS}	Time needed to reach a steady state	[s]
T	Absolute temperature	[K]
U	Velocity	[$m.s^{-1}$]
v	Molar volume	[$m^3.mol^{-1}$],
v^*	Specific volume = $1/\rho$	[$m^3.kg^{-1}$]
V	Volume	[m^3]
W	Particle width	[m]
X	Arbitrary parameter, related to the calibration of motors	

Greek characters

α	Degree of swelling with respect to the reference state	
γ	Shear strain	[s.u.]
$\dot{\gamma}$	Shear rate	[s^{-1}]
Γ	Interfacial tension	[$mN.m^{-1}$]
$\delta(x)$	Relative error on x	[-]
$\Delta(x)$	Absolute error on x	[units of x]
ε	Strain	[s.u.]
η	Viscosity	[Pa.s]
ϑ	Orientation angle with respect to the flow direction	[rad]
θ	Temperature at state 'theta'	[K]
λ	Deformation ratio (compression) = h/h_o	[-]
μ	Shear modulus	[Pa]
ν	Number of chains in a network	[mol]
ν_e	Effective number of chains in a network	[mol]
π	Swelling pressure	[Pa]
ρ	Mass density = 1/v*	[$kg.m^{-3}$]
σ	Stress	[Pa]
τ	Reduced temperature = $(T-\theta)/\theta$	[-]
υ	Excluded volume parameter = $a^3(1-2\chi)$	[m^3]
ϕ	Volume fraction	[-]
χ_{ij}	Flory-Huggins affinity parameter between products i and j	[-]
ω	Angular rotation speed	[$rad.s^{-1}$]

Sub- and superscripts

c	Chain; the segment between two crosslinks
	Complex
crit	Critical
d	Droplet
E	Engineering
ej	Ejection
el	Elastic
f	Final
F	Projection on the Flow direction
gel	Gel phase
H	Corresponding to the height dimension of a gel particle
i	Initial
int	Interfacial
ion	Ionic
Jeff	Jefferey
L	Corresponding to the length dimension of a gel particle
lower	Lower plate
m	Matrix
mix	Mixing
n	Network
N	Normal
o	Reference state
p	Polymer
p	Projection
ref	Reference
rel	Release
S	Solvent
sol	Solvent phase
ss	Steady state
T	True
t	tip
upper	Upper plate
W	Corresponding to the width dimension of a gel particle
y	Yield
z	

Abbreviations

AA	Acrylic acid
APS	Ammonium persulfate
BIS	*N*,*N*′-methylenebisacrylamide
HPC	Hydroxypropylcellulose

PAMPS	Poly(2-acrylamido-2-methyl-1-propane sulphonic acid)
PDMS	Polydimethylsiloxane
PNIPAAm	Poly(*N*-isopropylacrylamide)
PVA	Poly(vinyl acetate)
PVCL	Poly(*N*-vinyl caprolactam)
SAP	Super absorbent polymer
TEMED	*N*,*N*,*N'*,*N'*-tetramethylenediamine

Résumé francophone

1. Contexte et objectif de l'étude

Les hydrogels sont des réseaux qui peuvent absorber de l'eau ou des solutions aqueuses. Leur capacité d'absorption est beaucoup plus prononcée pour les hydrogels chargés, qui forment le sujet de cette étude. De tels types de gels, appelés gels polyélectrolytiques, peuvent absorber plusieurs centaines de fois leur propre poids en solvant. C'est pour cela que ces gels sont utilisés en tant que superabsorbant dans des domaines variés, tel que l'hygiène, les applications médicales, les fertilisants de sol ou encore les produits anti-inondation. Toutes ces applications font appel à l'absorbance du matériau.

Cependant, les hydrogels polyélectrolytiques ne sont pas que des absorbants. Ils peuvent gonfler ou se contracter de façon réversible en réaction à un stimulus externe, tel qu'un champ magnétique ou électrique, une interaction chimique, la température, la lumière ou une force mécanique. A cause de cette sensibilité, les gels polyélectrolytiques sont appelés 'gels intelligents'. Ils forment une classe de matériaux prometteurs pour des applications au-delà de l'absorption. Depuis une vingtaine d'années, des équipes de chercheurs académiques et industriels évaluent l'utilisation potentielle de tels gels comme senseur, comme actionneur mécanique ou comme porteur d'agent actif dans des applications de relargage contrôlé. C'est dans ce dernier domaine que se situe notre travail.

La vectorisation et la biodisponibilité d'un ingrédient actif est un axe de recherche important pour les industries cosmétiques et pharmaceutiques. Les polymères et les gels polymériques en particulier offrent de nombreuses possibilités dans ce domaine d'applications. Si l'encapsulation est plutôt simple à réaliser, la libération avec ou sans cible précise est un sujet de recherche permanent. Un réseau polymère peut servir comme réservoir de stockage et de transport pour le composant actif. Il est alors nécessaire de trouver le stimulus approprié qui provoque la sortie du composant actif en quantités adéquates quand la cible est atteinte. La littérature sur les gels sensibles aux stimuli physico-chimiques (pH, température, environnement) est abondante. Les gels sensibles au pH qui protègent leur contenu contre l'acidité de l'estomac et qui le libèrent dans l'intestin en forment un exemple classique.
Or, de tels systèmes ne peuvent pas être implémentés dans des produits à application cutanée (émulsions cosmétiques, crèmes, pommades et lotions), où il est difficile de manipuler la composition environnementale afin d'initier le relargage. Cependant, une crème est fortement comprimée et cisaillée lors de son application. Un tel produit requiert alors des gels qui libèrent leur solvant sous une sollicitation mécanique. C'est pourquoi nous avons étudié le comportement de particules de gel contenant une solution de molécules polymères linéaires (modèle pour le composant actif) sous action mécanique. Nous avons cherché à comprendre pourquoi et comment un gel gonflé délivre son

contenu lorsqu'il est cisaillé ou comprimé. Des travaux antérieurement effectués aux Cemef ont montré qu'un gel gonflé d'eau libère de l'eau à faible contrainte de cisaillement (Zanina et al., 2002). Une question importante que nous avons cherchée à répondre est pourquoi et comment la présence d'un polymère linéaire dans le gel peut changer ce comportement. Est-ce que le polymère linéaire sera éjecté ou restera-t-il enfermé dans le réseau?

Une crème n'est pas seulement soumise à des forces lors de son application, mais aussi durant la production. A ce stade, le gel doit protéger son contenu. Clairement, les gels-récipient subissent des actions mécaniques multiples durant leur cycle de vie. Les effets de ces actions doivent être compris et maîtrisés afin de pouvoir implémenter ces gels avec succès dans des applications nouvelles. A notre connaissance, il n'a jamais été étudié si le procédé de fabrication ou l'application par cisaillement peut provoquer la libération d'une substance active. Les questions principales dans ce contexte sont:

- Quel est l'effet d'une action mécanique (cisaillement, compression) sur un gel gonflé?
- Est-il possible de libérer un composant actif d'un gel en suspension sous cisaillement et comment est-ce que cela va se passer?
- Quelles sont les conditions qui initialisent la sortie du composant actif?

Cette étude a aussi un intérêt plus fondamental. Les hydrogels utilisés peuvent subir des déformations très importantes qui sont loin des régimes décrits par les théories classiques d'élasticité utilisées pour décrire les gels sous compression dans la littérature. Nos observations pourraient donc également contribuer à une meilleure compréhension du comportement de gel. Les questions considérées sont alors les suivantes:

- Comment est-ce qu'un gel se déforme et se relaxe de manière qualitative?
- Quelles sont les paramètres influençant la déformation et la relaxation?
- Est-ce qu'on peut modéliser les déformations observées?

En bref, l'objectif de cette étude est d'obtenir une meilleure compréhension du comportement d'un gel polyélectrolytique qui gonfle ou qui se contracte lorsqu'il est soumis à l'action d'un cisaillement ou d'une compression afin d'ouvrir la voie vers des applications dans des formulations cosmétiques.

Ce résumé est organisé selon le même plan que le texte du mémoire. Pour commencer, nous ferons brièvement le point sur la littérature concernant le gonflement et la rétraction de gels plongés dans différents milieux. Une attention particulière sera donnée aux gels immergés dans une solution de polymère linéaire. Ensuite, une description des dispositifs expérimentaux est donnée et les échantillons sont caractérisés. Deux chapitres sont dédiés au comportement d'une particule de gel suspendue dans une huile sous cisaillement. Enfin, le dernier chapitre traite du comportement de disques de gel sous compression.

2. Littérature : définitions, gonflement et propriétés de gels gonflés

Le terme 'gel' peut désigner des matériaux très divers, mais nous limiterons son usage pour indiquer des gels dits 'chimiques'. Un gel dans son sens général est constitué de deux composants.

Premièrement un réseau, c'est-à-dire, un ensemble de chaînes polymères reliées les unes aux autres par des points de réticulation qui sont des liaisons covalentes dans le cas auquel nous nous intéressons. Ce réseau constitue le squelette du gel. Deuxièmement il faut un composant qui fait gonfler ce réseau: le solvant. D'autres éléments peuvent aussi être ajoutés, comme un deuxième solvant, des ions ou des polymères. Le terme 'solvant' est utilisé dans son sens le plus large tout au long de ce manuscrit, c'est-à-dire, le fluide qui pénètre le gel, que ce soit un fluide pur (p. ex. de l'eau), un mélange de fluides ou une solution de sel ou de polymère.

Un polyélectrolyte est une molécule polymère qui contient de nombreuses unités à caractère électrolytique. Dans un solvant, ces unités peuvent se dissocier, formant un macro-ion et un grand nombre de petits ions de charge opposée, les contre-ions. Par conséquent, des forces électrostatiques locales se manifestent autour de la molécule, les chaînes se repoussent entre elles et ceci d'autant plus que leur charge augmente. Les chaînes en solution dans un électrolyte sont donc fortement étirées, puisque chargées d'un même signe.

Lorsque l'on superpose le caractère 'gel' et le caractère 'polyélectrolyte' dans un matériau, on obtient un gel polyélectrolytique. Un gel polyélectrolytique est donc formé d'un réseau de macromolécules ionisables. Des contre-ions se dissocient des chaînes en contact avec le solvant et il en résulte un réseau chargé. Suite à une forte répulsion entre les chaînes et par la pression osmotique des contre-ions, ce type de gel a des capacités de gonflement beaucoup plus élevées qu'un gel neutre.

Le gonflement est une des propriétés les plus intrigantes d'un gel. Un réseau immergé dans un bon solvant aura tendance à se disperser le plus loin possible afin de réduire son énergie libre, comme font les molécules non-réticulées. Or, les réseaux sont limités dans leur possibilité de se disperser à cause des liaisons permanentes entre les chaînes. Il va s'en suivre une compétition entre les forces tentant à disperser les chaînes et les forces tendant à ramener la conformation moyenne des chaînes dans leur état d'équilibre, c'est à dire sans étirage. Premièrement, nous nous sommes intéressés au gonflement dans des solvants purs. Le degré de gonflement à l'équilibre dépend de l'architecture du réseau et de l'affinité du réseau pour le solvant. Les théories de Flory et de de Gennes sont deux approches différentes pour l'analyse théorique du gonflement. Ces théories ont inspiré les travaux plus récents à ce sujet. Bien que les théories ne soient pas toutes capables de prédire les effets observés sur le plan quantitatif, nous en retiendrons qu'un gel dans un solvant gonfle ou ne gonfle pas, selon la qualité du solvant. Toutes choses égales par ailleurs, à l'équilibre, un gel ionisé (polyélectrolytique) gonfle beaucoup plus qu'un gel neutre.

Dans un deuxième temps, nous avons focalisé notre attention sur les transitions provoquées par une solution de polymère en vue de notre étude expérimentale. Le système devient plus complexe et le nombre d'états possibles augmente quand le gel se trouve dans une telle solution. Nous avons résumé les effets rapportés dans la littérature de la concentration de cette solution de polymère sur le degré de gonflement du gel dans différentes circonstances. Le plus étonnant est que dans une solution de polymère, le degré de gonflement ne change pas forcément de façon continue avec la concentration du polymère dans la solution; deux types de transitions brutales ont été distingués en présence d'un mauvais solvant. Premièrement, le passage d'un état gonflé à un état entièrement effondré peut se manifester à une concentration critique de la solution pour un gel ionisé; dans le cas d'un gel neutre, le

gel dégonfle progressivement avec la concentration de polymère. Une deuxième transition de premier ordre peut avoir lieu à une concentration critique élevée: de larges quantités de polymère pénètrent alors dans le gel et son degré de gonflement augmente par saut. Cette transition est appelée transition de ré-entrance et elle peut se manifester pour tous les types de gels.

3. Matériaux et méthodes expérimentales

Pour imiter un vecteur superabsorbant avec une substance active à l'intérieur, un gel polyélectrolytique d'acide polyacrylique partiellement neutralisé (Aqua Keep 10SH-NF) a été choisi et gonflé avec une solution aqueuse d'un polymère linéaire, l'hydroxypropylcellulose (HPC). Il n'y pas d'interactions particulières connues pour cette combinaison de polymère et réseau et des changements de volume abrupts n'ont jamais été observés.

Afin de pouvoir étudier le comportement d'un gel sous une sollicitation mécanique, nous avons travaillé avec des outils rhéo-optiques. Ces outils combinent l'essai mécanique avec l'observation visuelle. Le geste d'étaler une crème peut être décomposé en une compression (réduction d'une noisette d'un centimètre en une couche de quelques micromètres) et un cisaillement (étalement sur une surface étendue). Pour l'étude en cisaillement, nous avons utilisé un rhéomètre transparent contra-rotatif (Figure 2.10). Cet outil permet d'immobiliser dans le repère du laboratoire un objet soumis à un cisaillement. Il est donc possible d'en observer le comportement pendant des temps très longs. Les essais de compression ont été effectués avec un rhéomètre de type RMS 800 en mode de compression (Figure 2.12). L'évolution du diamètre du disque de gel est enregistrée par une caméra placée devant le rhéomètre.

L'étude expérimentale se focalise sur la réaction d'un gel gonflé avec des solutions de polymère à ces deux types de contrainte. L'étude en cisaillement est effectuée avec une particule gonflée immergée dans une huile silicone (polydimethylsiloxane, PDMS, de deux viscosités différentes), afin de créer une émulsion modèle. Les effets de la concentration du polymère linéaire dans le solvant, de la tension interfaciale solvant/matrice, du degré de gonflement et de la taille de la particule ont été étudiés. Pour l'étude en compression, nous avons synthétisé des disques de gel ayant une composition proche de celle des particules étudiées en cisaillement. Ces disques sont gonflés à l'équilibre avec de l'eau ou avec une solution d'HPC. L'ensemble des échantillons étudiés est résumé dans le Tableau 1.

Tableau 1: Résumé des systèmes matériels expérimentaux

Solvant	**Degré de gonflement (g/g)**	**Matrice**	$\eta_{solvant}$ **(Pa.s)**	$\Gamma_{solvant/matrice}$ **(mN/m)**
Expériences en cisaillement – particules de gel Aqua Keep 10SH-NF				
1 % HPC	80	PDMS 200, PDMS 1000	2.10^{-3}	12,5
5 % HPC	80, 160, 210 ($Q_{éq}$)	PDMS 200	7.10^{-3}	12,5
10 % HPC	80	PDMS 200, PDMS 1000	2.10^{-1}	12,5
		PDMS 200 + 3 % émulsifiant		3
Expériences en compression – disques de poly(NaA-*co*-AA) synthétisés				
Eau	200 ($Q_{éq}$)	Air	1.10^{-3}	-
5 % HPC	130 ($Q_{éq}$)	Air	7.10^{-3}	-

4. Identification du comportement induit par cisaillement d'un gel gonflé et analyse de sa déformation et de sa relaxation

Dans les domaines de la cosmétique, de la pharmacie ou encore de l'alimentaire, les produits sont soumis à des forces de cisaillement lors de la production et de l'application. On peut penser à l'écoulement du produit dans des réacteurs, des pompes ou des tubes jusqu'au remplissage de l'emballage. Du côté de l'application, les produits rencontrent des cisaillements forts entre la langue et le palais dans le cas de la nourriture ou des médicaments et pendant l'étalement sur la peau pour les pommades et les crèmes. Le cisaillement est donc une sollicitation évidente que vont rencontrer des gels porteurs de substances actives dans de tels produits. Nous avons étudié les effets d'un cisaillement simple sur une particule gonflée d'une solution de polymère suspendue dans une huile. Il a été observé qu'un gel ne réagit pas seulement par une déformation, mais aussi par une rotation et par le relargage partiel de son solvant. Les phénomènes identifiés sont les suivants (Figure 3.1):

- des particules de gel sous cisaillement tournent autour de l'axe de vorticité. La période de rotation correspond à la période de rotation prédite par Jefferey (1922) pour des sphères non-déformables quand la matrice est newtonienne;
- soumise à une contrainte de cisaillement, une particule de gel se déforme en une ellipsoïde à trois axes différents. La longueur relative augmente de façon linéaire avec la contrainte avant relargage de solvant. La proportionnalité est la même pour tous les solvants utilisés à degré de gonflement égal;
- lorsque la contrainte appliquée est plus élevée qu'une première contrainte critique, la contrainte de relargage, mais inférieure à une deuxième contrainte critique, on observe que du solvant es libéré. Ce solvant reste attaché aux extrémités de la particule et forme une unité avec la particule. Si ces bouts restent petits comparés à la taille de la particule, la particule continue à se déformer, mais la déformation sature à des valeurs plutôt basses si des grandes quantités d'un solvant de faible viscosité restent attachées à la particule. Ce solvant libéré est réabsorbé quand la particule se relaxe. Ce phénomène de relargage est donc réversible;
- au-delà d'une deuxième contrainte critique, la contrainte d'éjection, des gouttelettes se détachent des bouts de liquide attachés au gel et se dispersent dans la matrice. Ce phénomène est irréversible et se manifeste d'autant plus facilement pour des rapports de viscosité solvant-matrice plus élevés;
- les particules de gel s'élargissent aussi dans la direction de la vorticité et du solvant peut être relargué des pôles de la particule lorsque le module complexe de la matrice dépasse le module élastique du gel.

La déformation dépend du degré de gonflement, mais pas de la taille initiale de la particule. Nous n'avons pas non plus pu distinguer d'effet de la viscosité du solvant sur la déformation avant relargage.

La déformation est comparée à la déformation de particules de gel gonflées dans de l'eau d'une part et d'autre part à la déformation de gouttes de solvant. Si on compare les gels aux gouttes de solvant en utilisant le rapport des viscosités solvant/matrice, toutes nos particules se seraient rompues.

Cependant, le gel réticulé est resté intact. Les modèles décrivant la déformation de gouttes dans des systèmes newtoniens ne sont pas capables de décrire la déformation d'un gel. Nous avons alors modifié le modèle de Cox en y ajoutant un terme représentant la résistance élastique du réseau à la déformation. L'accord entre les prédictions de ce 'modèle de Cox modifié' et les données expérimentales est satisfaisant pour des petites déformations.

Nous avons également étudié la relaxation du gel. Quand le cisaillement est arrêté, la particule déformée se rétracte et recouvre sa forme sphérique initiale. Les temps de relaxation augmentent avec la déformation du gel avant arrêt du cisaillement. A déformation équivalente, la relaxation dépend seulement de la viscosité de la matrice, mais pas de la taille de la particule. Les courbes de relaxation de la longueur se superposent si celles-ci sont représentées relativement à la longueur à l'arrêt de l'écoulement.
Les particules ayant des bouts de liquide se relaxent en deux étapes. D'abord, les bouts sont réabsorbés, suivi d'une recouvrance rapide de la forme sphérique initiale.

5. Libération de solvant par une particule de gel induite par cisaillement

Les phénomènes de libération sont d'une grande importance pour les applications des gels en tant que vecteur d'agent actif. Ainsi, nous nous sommes consacrés à l'analyse de la libération du solvant d'un gel induite par cisaillement. Les conditions critiques et les paramètres influençants sont identifiés. D'abord, le relargage sans détachement de gouttes est étudié et ensuite, l'éjection du solvant dans la matrice est analysée.

Dans des conditions appropriées, les contraintes de cisaillement causent le relargage et l'éjection de solvant d'une particule de gel dans la matrice. La particule libère une quantité de solvant à ses extrémités dés qu'elle dépasse une déformation critique. Le solvant reste attaché à la particule dans des 'bouts'. A contrainte plus élevée, des gouttelettes se détachent des bouts et se dispersent dans la matrice.
Les particules de gel s'élargissent dans la direction de la vorticité et du solvant peut être relargué des pôles de la particule aussitôt que le module complexe de la matrice devient plus grand que le module élastique du gel.

La concentration du polymère dans le solvant influence les phénomènes de libération. Une faible concentration de polymère (solvant de faible viscosité) favorise le relargage des bouts de solvant. La concentration joue aussi sur le détachement de gouttes via le rapport des viscosités solvant/matrice: plus ce rapport est élevé, plus le détachement de gouttes est facile. Une faible tension interfaciale promeut également le détachement de gouttelettes des bouts et la dispersion dans la matrice. Des réductions importantes du volume du gel gonflé peuvent ainsi être réalisées.

Les phénomènes de relargage et d'éjection ont également été observés sur des gels physiques et des capsules avec une peau gélifiée. Les phénomènes que nous avons identifiés et décrits peuvent alors être considérées comme des phénomènes généraux. Ceci rend les gels prometteurs pour des

applications en tant que porteur d'actifs. Cependant, les conditions critiques initialisant le relargage et l'éjection doivent être considérées au moment de la conception du procédé de fabrication.

6. Libération de solvant sous compression

La compression est un autre type de sollicitation mécanique que pourra rencontrer un gel lors de son application. Des disques de gel gonflé à l'équilibre dans de l'eau ou dans une solution d'hydroxypropylcellulose ont étés soumis à une compression uniaxiale. La force normale exercée par le gel sur le piston est mesurée et les dimensions du gel sont enregistrées en temps réel. La contrainte réelle est donc connue à tout moment.

Nos expériences ont montré qu'un gel gonflé à l'équilibre libère une partie de son solvant dès qu'une contrainte de compression est exercée sur l'échantillon. Initialement, le volume du gel diminue rapidement. Cette éjection ralentit d'à peu près un facteur 10 par la suite. La vitesse de libération est limitée par la cinétique de diffusion du solvant dans le réseau.
Si le solvant est une solution de polymère, le degré de gonflement à l'équilibre est modifié et il en est de même pour les propriétés mécaniques.

L'analyse du solvant libéré par le gel gonflé d'une solution d'hydroxypropylcellulose a montré que la concentration du polymère linéaire dans le solvant libéré est la même que dans la solution initiale absorbée par le gel.

La diminution du volume induite par compression est également prédite par une analyse thermodynamique de la compression de gels neutres et faiblement polyélectrolytiques. Les pertes de volume sont petites pour des gels neutres, mais augmentent quand le nombre de groupes chargés sur le réseau augmente. A pression égale, le gel polyélectrolytique perd relativement plus de solvant que le gel neutre. Néanmoins, il faut considérer que le gel neutre est initialement moins gonflé.
La forme de la courbe perte de volume en fonction de la pression mesurée expérimentalement sur un gel fortement chargé est similaire à la forme de la courbe théorique pour les gels peu chargés.

Introduction

Hydrogels are polymer networks that can absorb water or aqueous solutions. The absorption capacity is more pronounced for charged hydrogels, which are the subject of the present study. Those types of gels, which are called polyelectrolyte hydrogels, may absorb up to several hundred times their own weight of solvent. That is why they are applied as a superabsorbent in various fields (Kulicke and Nottelmann, 1989; Kazanskii and Dubrovskii, 1992; Li and Tanaka, 1992; Hoffman, 1995). They are mainly encountered in human hygiene products (baby diapers, sanitary towels, adult incontinence etc.), in medical applications (keeping wounds dry, soft contact lenses, …), as soil moisturisers, as flood control mats or as thickeners in foodstuff and personal care products. All these applications only make an appeal to the absorbency of the material.

Yet, polyelectrolyte hydrogels are not simply 'absorbers'. They can swell and shrink in a reversible way as a reaction to external stimuli, including electric or magnetic fields, chemical interactions (pH, solvent, solutes, …), temperature, light or mechanical forces. Because of this sensitivity, polyelectrolyte hydrogels are called 'smart' and they have been found promising materials for other applications than absorption. For the last twenty years, both industrial and academic teams have been examining the possibilities of using hydrogels as intelligent sensors, as mechanical actuators or as controlled delivery devices. The latter is the field wherein our work must be situated.

Motivation

The vectorisation or bioavailability of an active substance is a highly important field of research in cosmetic and pharmaceutic industries. Polymers and especially polymer gels offer many possibilities in this field of applications. If encapsulation is a rather easy thing to realise, liberation with or without a specific target is a permanent subject of research in these industries. A polymer network may serve as a reservoir for storage and transport of the active compound, so it is necessary to find the proper stimulus that liberates a desired amount of active substance when the gel reaches its target. Literature on gels sensitive to physico-chemical stimuli (pH, temperature, environmental composition) is abundantly available. The pH-sensitive gels that protect their contents to the stomach acidity and free it in the colon are an example of such gels.
However, such systems cannot be implemented in skin care products (cosmetic emulsions, salves, creams and lotions), where it is difficult to control the environmental composition to trigger release. Yet, a cream is highly compressed and sheared at application. Such products will require gels that release their contents when submitted to a mechanical action. That is why we studied the behaviour of gel particles containing linear polymer molecules in solution under mechanical action. To our knowledge, no systematic work has been performed on this topic. We investigated if and how the gel

delivers its content when being submitted to mechanical action. Previous work performed in our laboratory showed that a gel swollen with water already releases water at very low shear stresses (Zanina, 2001). An important question to be raised is whether the presence of a linear polymer in the gel changes this behaviour and how. Is the linear polymer itself released under shear or does it stay entrapped in the network?

However, shear is not only encountered at application, but also during production. At this stage, the gel should protect its content. It is thus obvious that gel containers in cosmetic emulsions will undergo multiple mechanical actions during their life cycle. The effects of such action have to be understood and mastered before novel applications can be developed. To our knowledge, it has never been studied whether rubbing could drive release of an active substance. The main questions to be answered in this context are:

- What is the effect of mechanical action (compression, shear) on swollen gels in suspension?
- Is it possible to liberate active compounds from a gel under shear and how will this happen?
- Under which conditions can the active compound be liberated and under which conditions will it remain inside the gel?

This study has also a more fundamental interest. The hydrogels used can undergo large deformations that are far from the regimes described by the classic elasticity theories generally used to describe gel compression experiments. Our observations might as well contribute to a better understanding of gel behaviour. The questions we will address are the following.

- How will a gel deform and relax in a qualitative way?
- Which parameters affect deformation?
- Can we model the observed deformations?

Summarising, the objective of this study is to understand how and why a polyelectrolyte gel swells or shrinks when it is submitted to the action of shear or compression and to open the way towards the application of such gels in cosmetic creams.

Approach

In order to answer the questions raised, model gels swollen with model linear polymer solutions where studied with rheo-optical tools. The tools combine mechanical testing and visual observations. The action of spreading out a cream was decomposed in compression (reduction of a 1 cm drop to a few µm layer) and shear (spreading over a large skin surface). Our study focussed on the reaction of gel particles swollen in polymer solutions to these two types of stress. To mimic a gel container with an active substance inside, a commercially available partially neutralised polyacrylic acid gel was selected and swollen with aqueous solutions of the linear polymer hydroxypropylcellulose. No particular interactions between network and linear polymer are known. The swollen gel particles were immersed in silicone oil, in order to create a model emulsion.

This manuscript is organised in the following way. The first chapter is an introduction to the wonderful world of gels. A short first paragraph explains what gels and polyelectrolyte gels are. The term 'gel' is used in many ways, but we will restrict its use to swollen chemically crosslinked networks. The rest of Chapter 1 is devoted to the swelling behaviour of gels. Thermodynamics of swelling will be briefly reviewed for neutral and polyelectrolyte gels in pure solvents and in solutions of linear polymers. Let it be clear from here on that the term 'solvent' will be used in its most general sense throughout this manuscript, i.e. as the fluid that penetrates into the gel, whether this solvent is a pure fluid (e.g. water), a mixture of fluids or a salt or polymer solution. The properties of swollen gels are highly related to the state of swelling but also to the architecture of the network. Some attention will be paid to the dependence of gel properties on degree of swelling and to methods to measure these gel properties. Despite its importance for gel applications in dampers and creams, e.g., no systematic studies on solvent release due to a mechanical action have been conducted. Literature on gel suspensions is rather rare. This lack of knowledge has lead to our experimental plan.

In the second chapter, the materials and experimental methods used in this work are presented. In order to study the fundamentals of mechanical impact on polyelectrolyte hydrogels containing an active substance, a system of model materials was selected. The system is composed of a poly(sodium acrylate-*co*-acrylic acid) gel network and a solution of hydroxypropylcellulose. The used materials are presented and interactions are determined. Two types of mechanical action were applied to the gels: shear and compression. Shear tests were performed with a homemade transparent counter-rotating rheometer. This set-up enables in-situ monitoring of the behaviour of a spherical swollen gel particle suspended in oil. Compression tests on the other hand, were executed on gel disks in open air. They were realised with an RMS 800 rheometer in compressive mode. A camera placed in front of the rheometer allowed observation of disk deformation and solvent release. Both mechanical testing machines are also described in Chapter 2.

The results of the shear tests are described in Chapters 3 and 4. The sample studied is an isolated swollen gel particle in oil. Chapter 3 starts with a description of the observed phenomena. A gel particle submitted to low shear stress rotates around the vorticity axis and deforms into an ellipsoid with three different axes. At higher stresses, the particle partially releases its solvent that remains attached to the edges as solvent tips. At stresses above a certain threshold, detachment of droplets from the solvent tips was observed. The remainder of Chapter 3 systematically treats the rotation of the particle, deformation and shape relaxation. The observations are compared to existing models for diluted suspensions or diluted emulsions. None of the models is able to fully describe the behaviour of suspended gel particles. Yet, an adaptation of Cox' model with an elastic term fitted our experimental deformation data well.

Because of its relevance for vectoring applications, a complete chapter is devoted to phenomena of solvent release from a gel under shear (Chapter 4). Two typical stress values could be determined above which solvent release and solvent droplet detachment were observed and the effect of polymer solution concentration and particle size was investigated. The volume of solvent ejected under shear was measured in time. We also related low deformation saturation to the release of low viscosity solvent tips.

Chapter 5 treats the compression of gels. Poly(sodium acrylate-*co*-acrylic acid) gel disks were synthesised for this purpose. The disks were submitted to uniaxial deformation and their dimensions were monitored. Our data show clearly that the gel is not able to maintain its volume when being compressed. Solvent release is measured and the released solvent is also recovered for analysis. The system was also treated analytically using thermodynamic arguments. The analysis predicts loss of solvent for neutral and weakly charged gels. Volume loss tendencies are qualitatively the same as those observed experimentally on highly charged polyelectrolyte gels.

Our findings are summarised and related in the Conclusions. We will also make some suggestions for further research in this field.

This work has been performed within the framework of the RNMP (Réseau de Recherche et d'Innovation Technologiques Matériaux et Procédés) project 'Gels polyélectrolytiques adaptatifs'.

Part of the work covered in this thesis has been published in scientific journals and was presented at international conferences (see Appendix B).

Résumé du Chapitre 1

Littérature : définitions, gonflement de gel et propriétés de gels gonflés

Les gels polyélectrolytiques forment le sujet de cette thèse. Ces matériaux sont composés d'un réseau polymère tridimensionnel dont les segments sont connectés dans des points de réticulation par des liaisons covalentes. Quand ce réseau est gonflé d'un solvant, on peut parler d'un gel. Si des groupes ionogènes sont incorporés dans le réseau, le gel est 'polyélectrolytique'. Ces groupes peuvent se dissocier en présence d'un solvant approprié, ce qui résulte en un réseau chargé et la présence de contre-ions.

Le gonflement est une des caractéristiques les plus intrigantes d'un gel. Non seulement ils peuvent absorber des quantités énormes de solvant, mais ils peuvent également changer leur volume de façon contrôlée, selon les propriétés physico-chimiques du gel et de son environnement. Le comportement d'un gel est gouverné par le bilan des forces de gonflement (forces de mélange et forces électrostatiques) et de contraction (forces élastiques et tension interfaciale). Quand le gel est soumis à une force extérieure (par exemple, dans le cas de cette étude, une force mécanique), leurs actions doivent être ajoutées au bilan de forces.

Ce chapitre a pour but de faire le point sur le gonflement et la rétraction des gels plongés dans différents milieux. La théorie des 'champs moyens' de Flory et l'approche des lois d'échelle de de Gennes sont les plus importantes. Ces théories ont inspiré les travaux plus récents qui sont principalement des raffinements et des extensions de ces théories fondamentales.

En général, le gonflement d'un gel est déterminé par les caractéristiques topologiques du réseau et par l'affinité du réseau pour son solvant. L'aptitude de gonfler est fortement augmentée lorsque des ions sont incorporés dans le réseau (gel polyélectrolytique). Selon les interactions réseau – solvant, le gel peut subir des transitions gonflement/contraction, qui peuvent être continues ou discontinues. Ces transitions seront examinées pour différents types de solvant. Une attention particulière est donnée au cas d'un solvant qui est une solution de polymère linéaire car c'est le sujet de notre étude expérimentale.

Les propriétés élastiques d'un gel sont aussi considérées. Ceux-ci dépendent fortement du degré d'étirement de la chaîne et donc du degré de gonflement. A faible degré de gonflement, le module élastique diminue avec le degré de gonflement suivant une loi d'échelle. La puissance de cette loi dépend de la nature du système. A degré de gonflement élevé, on s'approche des limites d'étirement de la chaîne. Le module augmente alors rapidement avec le degré de gonflement.
Enfin, des méthodes de mesure des propriétés élastiques d'un gel sont évoquées.

Chapter 1

Literature review: gel swelling and properties of swollen gels

The ability to swell is one of the most striking characteristics of a gel. They absorb or release solvent as a response to stimuli of various kinds in order to reach an equilibrium state. Equilibrium of a freely swelling gel is determined by the interaction between the network and the solvent. This interaction is highly sensitive to external conditions such as pH, temperature and presence of ions. External fields, like electric, magnetic or pressure fields also affect the maximum degree of swelling. Gels do not only swell in pure solvents. Dissolved substances can enter the gel together with the solvent. This property is at the origin of the potential use of gels as a drug carrier or as a vector of active compounds in e.g. cosmetic emulsions. Besides the swelling ability, the mechanical properties of swollen gels are of great importance for practical applications like shock damping and product structuring.

All these potential applications need good understanding of the fundamentals of gel swelling and deswelling. The present chapter aims to review the thermodynamics of swelling and to describe the effect of swelling on the properties of a swollen gel. A first introduction paragraph (1.1) gives some definitions necessary for a clear understanding of the text. In paragraphs 1.2 to 1.4 of this chapter the theory of swelling is presented for different cases: neutral or polyelectrolyte gel in pure solvent or in a linear polymer solution. Special attention is given to the latter case since this is the case we will study in the experimental section. Paragraph 1.5 considers the effect of interfacial tension on swelling. The last but one paragraph is dedicated to the elastic properties of gels from a theoretical and an experimental point of view. In conclusion, we will show how our work contributes to the study of gels.

For a clear understanding of this chapter and the whole manuscript, one should note to that the term 'solvent' is used in the most general sense of the word, namely the fluid penetrating into the gel. This solvent can consist of one component (pure solvent) or more (mixture of solvents, salt solution, linear polymer solution…).

1.1 What's in a name: definitions

Before diving into general theories of swelling, it is necessary to give some definitions. First, the term gel needs to be defined. This word has been given a very broad meaning in literature, but we will

specify in which sense it is used in this text. Second, the polyelectrolyte character will be explained and as a conclusion, it will be described what happens when these two intriguing features are joined within one material.

1.1.1 Gel

Most authors agree on the fact that at least two components are needed for a gel: a network and a solvent (see e.g. Almdal et al., 1993; Kavanagh and Ross-Murphy, 1998; Yamauchi, 2001). The network is an ensemble of polymer chains connected to a 3D structure in crosslinking points. In fact, it is a giant macromolecule with infinite nominal molar mass. It constitutes the skeleton of the gel.
A polymer is only suitable as a gel network if it has affinity for a solvent. If so, the polymer network strands can surround themselves with solvent molecules, thereby pushing neighbour chains away. This way, the network will occupy a larger volume, or, in other words, the solvent makes the network swell. The polymer network absorbs solvent without being dissolved. Such a swollen network is referred to as 'gel'.
Gels based on some very current solvents have been given specific denominations: hydrogels have water as a medium and lipogels are swollen with oil. The generic solvent is not necessarily a pure product; other elements may be added optionally like a second solvent, ions or polymer molecules. The mixture is still called 'solvent'.

One may easily understand that the network is an important element determining the character of the gel. Hence, it deserves to be considered more properly.
The network at the base of a gel is tridimensional and composed of polymer chains that can be neutral or charged. The chains are connected to the network in crosslinking points. Three different types of networks are generally distinguished by the nature of their crosslinks (de Gennes, 1979; Kavanagh and Ross-Murphy, 1998) (Figure 1.1).

- Entanglement networks: these are temporary networks, formed when two independent chains interpenetrate (Figure 1.1a). Polymer melts and highly concentrated polymer solutions belong to this category;
- Physical networks (Figure 1.1b), formed by rather weak bonds of finite lifetime or finite energy. These networks are reversible and their bonds may be easily ruptured; the number and the force of their bonds depend on mechanical, physical or chemical circumstances. This class contains networks formed by e.g. hydrogen bonds, van der Waals bonds or hydrophobic bonds, but also biopolymer gels formed by complex mechanisms as multiple helices.
- Chemical networks are formed by covalent bonds between atoms on the chains (Figure 1.1c); the network is in fact one giant macromolecule with infinite nominal molar mass. A chemical network is permanent: the number of reticulation points will not change with external conditions, supposing no degradation occurs. Only chemically crosslinked gels will be considered in this study.

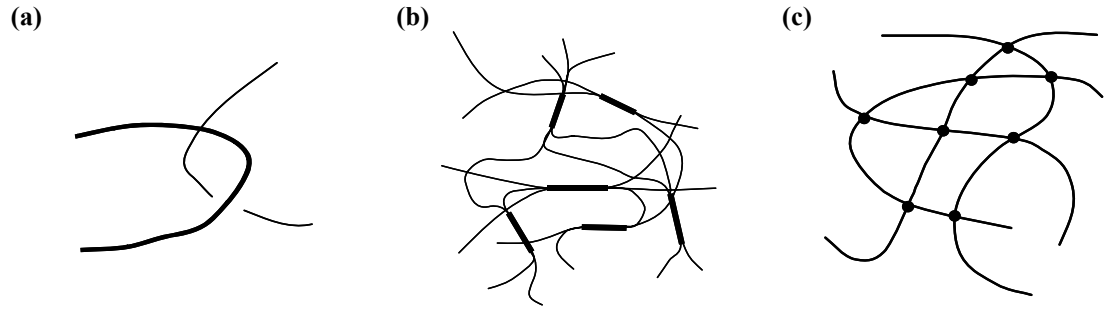

Figure 1.1: Classification of networks according to type of bonds: (a) entanglement; (b) physical network with junction zones; (c) chemical network [From Ross-Murphy, 1998].

The general structure of a chemical network is shown in Figure 1.2. A chemical network is characterised by the functionality of the crosslink points, f, which is the number of strands connected to one crosslink, and by the average weight of the strands between two neighbouring crosslinks, M_c. An alternative way to express M_c is the number of monomers in a strand, N. M_c and N are related through the mass of one monomer. Ideally both parameters are constant throughout the sample and chains are only linked by chemical bonds (Candau et al., 1982). Moreover, all chain ends are connected to a reticulation point and every chain will contribute equally to the network elasticity (Treloar, 1975).

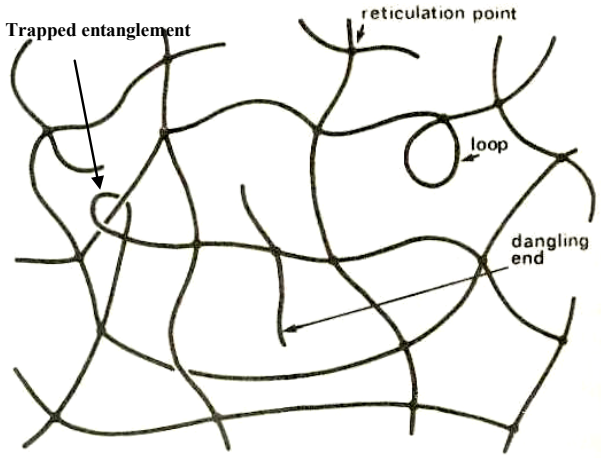

Figure 1.2: General structure of a chemical network [From de Gennes, 1979]

In reality however, lots of difficulties are met during gel synthesis (Candau et al., 1982; Bastide et al., 1989), which makes the existence of a perfectly ideal network very rare. Aside of strand length polydispersity, different types of defects – also presented in Figure 1.2 - may be introduced into the network. Most frequent defects are the following.

- Trapped entanglements, physical knots or slip-links: at short times, they behave as supplementary crosslinks and so increase the elastic modulus, but at a longer time scale, these knots may slip over the chain and even disappear;
- Pendent or dangling chains: a chain that is connected to the network by one end only; these chains do not contribute to the elasticity of the network. On the contrary, if there are many of

them, the network will be weaker than expected relative to its mass. Swelling is not really affected by this type of flaw (Bastide et al., 1979).

- Loops: two ends of one segment are connected to the same junction. Loops are in general inactive, except when another segment is entrapped in the loop.

The presence of different types of flaws as well as the broadness of strand mass distribution is related to the polymerisation process (Candau et al., 1982).

Macroscopically, a gel is soft, wet and able to maintain its shape under the stress of its own weight. The Young's modulus E is low, so it may undergo large and non-linear deformations at rather low stresses. A gel is also resilient: after deformation, it recovers its initial shape. Mechanically, gels are mostly treated as elastic solids. However, from a thermodynamical point of view, they are considered as a solution of a polymer in a solvent (see paragraph 1.4). Tanaka (1981) stated that a gel is an intermediate state of matter between solid and liquid.

1.1.2 Polyelectrolyte

The substances obtained when ionic groups are incorporated in a polymer chain, combine the properties of electrolytes and of polymers. The ionic groups on the chain dissociate when the molecule is dissolved in a polar solvent, generating a long charged chain (macro-ion) and a large amount of small ions of opposite charge that are named counter-ions. Since the chain units, covered with like charges, repel each other, the chain stretches out.

The counter-ions can be in two different states: some of them are localised on the molecule by ionic bond (condensed counter-ion) and others are not linked to the polymer (mobile counter-ions). However, they remain in the zone of influence of the macro-ion for electro-neutrality reasons. Figure 1.3 illustrates both categories. The distribution over both categories depends on the strength of the electrolyte and on the environmental circumstances.

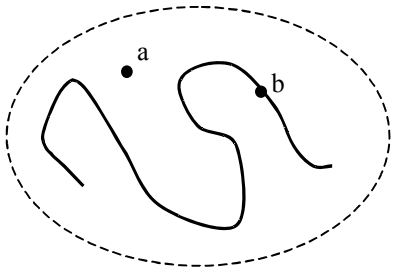

Figure 1.3: Different states for counter ions (•) around a polyelectrolyte macromolecule (—). The dashed line indicates the zone of influence of the charged macromolecule. Counter-ion 'a' is in the zone of influence but mobile, counter-ion 'b' is linked to the macromolecule (condensed).

Increasing the number of charges on the chain will reinforce the field around the macro-ion and the counter-ions will be more attracted. Once a critical degree of ionisation exceeded, the number of free charges saturates and the rest of the counter-ions condense on the chain. They form pairs with the charges on the macromolecule and reduce the electrostatic force. The mutual repulsion forces between chain segments decrease (Katchalsky and Lifson, 1951; Manning, 1969; Oosawa, 1977).

1.1.3 Polyelectrolyte + gel = polyelectrolyte gel

In the previous paragraphs, a gel and a polyelectrolyte have been defined:

- A gel is composed of a tridimensional network of chemically crosslinked chains swollen with a solvent.
- A polyelectrolyte is a macromolecule with ionogenic groups on the chain.

A swollen network made of polyelectrolyte chains combines both characters and is therefore called a polyelectrolyte gel. In this case, a fraction of the network monomers can dissociate into ions. The charged macromolecular network (Figure 1.4) is generally characterised by the number of monomers between charged groups, A. The number of charged groups on a strand is then N/A if A >> 1. In case of monovalent groups, this is also the number of (monovalent) counter-ions. For reasons of electrical neutrality, the counter-ions are confined to the volume of the gel. The degree of ionisation 'i' is defined as the number of charged monomers divided by the total number of monomers. For low degrees of ionisation (A >> 1), 'i' equals 1/A.

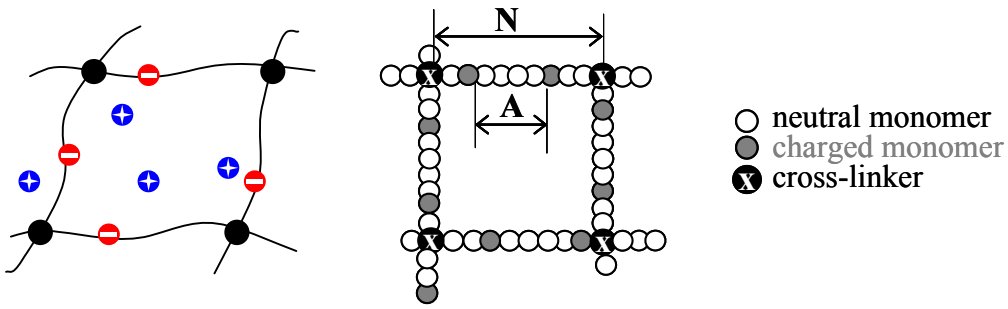

Figure 1.4: Polyelectrolyte network; definition of N and A.

It should be noticed that the degree of ionisation is not always equal to the fraction of ionogenic groups in the network. For high levels of ionogenic groups, 'i' will be lower due to counter-ion dissociation (Manning, 1969).

The ionic nature of the network chains raises unique properties (Schröder and Opperman, 1996). The swelling capacities of polyelectrolyte gels are many times higher than of a neutral gel; they are able to absorb up to several hundred times their own weight of solvent, while retaining coherence and elasticity. Therefore, these gels are widely used as superabsorbent polymers (SAP's) e.g. in diapers or as superabsorbent mats to remove residual water from flood (Degussa, 2003).
Two important effects are reported to be responsible for the increased swelling capacity: chain repulsion and osmotic pressure of counter-ions. First, the chains of an ionised network carry charges of the same sign, so electrostatic repulsion will cause the chains to drift apart. Second, the free counter-ions in the gel create an 'ionic' osmotic pressure between solvent and gel, which makes the solvent diffuse into the network.

1.2 Swelling pressure

1.2.1 Neutral networks

Gel swelling is often introduced in terms of swelling pressure, π, that is composed of an osmotic part, π_{osm}, and an elastic part, π_{el} (Flory, 1969; Li and Tanaka, 1992; Rubinstein et al., 1996).

$$\pi = \pi_{osm} + \pi_{el} \quad \textbf{[1.1]}$$

When a linear polymer is immersed in a solvent, the chains tend to disperse and form a solution, depending on the affinity of the components. This is the same for crosslinked polymers such as gels. Because of the initially high polymer concentration in the network, an osmotic pressure between the solvent outside and inside the gel is generated. This osmotic pressure drives solvent molecules into the network, which goes entails an increase of the network volume (Figure 1.5). This results in a dilution of the polymer concentration in the gel, entailing a decrease of the osmotic pressure. The osmotic pressure that causes network swelling is often called mixing pressure, π_{mix}, referring to the mixing of the network polymer with solvent molecules.

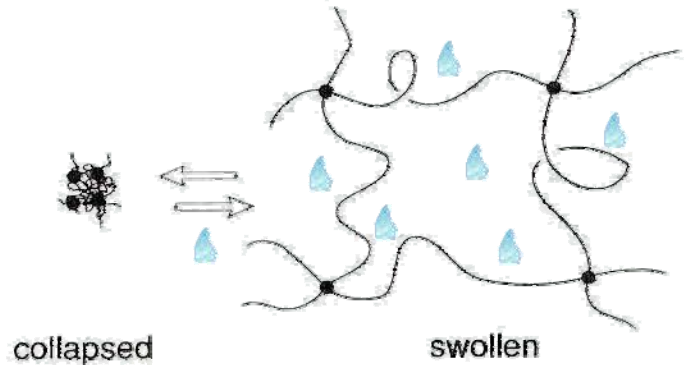

Figure 1.5: Reversible network swelling and shrinking with solvent [adapted from Li and Tanaka, 1992]

The major difference between a swollen network and a solution of a linear polymer is that networks are restricted in their ability to disperse because of permanent bonds between the chains, as illustrated in Figure 1.5. Nevertheless, the network will try to spread out as far as possible by absorbing appropriate quantities of solvent. This dilation entails deformation of the network chains, which calls in the chain elasticity. The elastic reaction is expressed as π_{el} and acts against swelling.

The total swelling pressure can simply be written as the sum of the mixing term and the elastic term:

$$\pi = \pi_{mix} + \pi_{el} \quad \textbf{[1.2]}$$

The mixing pressure represents the osmotic part here.
As long as π is positive, the network will swell but it will shrink for negative values of π (Tanaka, 1981). If $\pi = 0$, equilibrium swelling is reached, characterised by an equilibrium degree of swelling, Q_{eq}.

Initially the mixing contribution dominates the swelling pressure, as the polymer concentration in the gel is still high. As swelling proceeds, the polymer concentration decreases so its contribution gets less important and meanwhile, the elastic part will increase progressively due to further stretching of the chains. In excess of solvent, the gel will continue to absorb solvent until the elastic forces in the chains balance the mixing pressure out.

1.2.2 Polyelectrolyte networks

A polyelectrolyte network in a solvent will dissociate into free counter ions and a charged polymer network. Both components induce extra swelling compared with a neutral network. First, the swelling pressure of a polyelectrolyte network additionally includes a term reflecting the osmotic pressure of the counter-ions in the gel, π_{ion}. The free ions in the gel cause an ion concentration difference between the surrounding solvent and the network. This difference is the origin of a supplementary osmotic pressure, which causes more solvent molecules to enter the network. Second, electric charges on the backbone of the network repel each other. To reduce the internal repulsion, the chains will stretch in order to increase the distance between opposite charges (Katchalsky and Michaeli, 1955; Ilavsky et al., 1999). This is the Coulomb pressure or electrostatic pressure, π_{Coul}. The presence of charges on the network is thus favourable for network swelling.
Because of these two arguments, polyelectrolyte networks can absorb much more solvent than their neutral homologues. The swelling pressure of a polyelectrolyte gel is expressed as the sum of four terms (Flory, 1969; Katchalsky et al., 1951, 1952 and 1955):

$$\pi = \pi_{mix} + \pi_{ion} + \pi_{Coul} + \pi_{el} \qquad \textbf{[1.3]}$$

The total osmotic pressure is now caused by the network and the counter-ions in the network. For weakly charged networks, the electrostatic contribution is of minor importance compared to the ionic osmotic pressure and is therefore often neglected (Schröder and Opperman, 1996; Lagutina and Dubrovskii, 1996).

1.3 Degree of swelling

The state of swelling is generally characterised by the degree of swelling, Q. Q is defined as the quotient of the final (swollen) volume V_f and the initial (dry) volume V_i and may equally be given as the quotient of the volume fractions of the network in the initial and final gel, $\phi_{n,i}$ and $\phi_{n,f}$, respectively.

$$Q = \frac{V_f}{V_i} = \frac{\phi_{n,i}}{\phi_{n,f}} \qquad \textbf{[1.4]}$$

The degree of swelling logically increases as more solvent is absorbed by the gel. However, absorption is limited to a maximum, named equilibrium degree of swelling Q_{eq}. For free swelling, Q_{eq} is reached when the swelling pressure equals zero and depends on network characteristics and the interplay between solvent and network. In the 1940's, Flory was the first to establish a theory

predicting the equilibrium degree of swelling as a function of these parameters (Flory, 1969). His theory and some more recent findings are presented in the next paragraph.

1.4 Thermodynamics of swelling

In this section, the possibilities for a gel to swell in different solvents will be evaluated, both for neutral and polyelectrolyte networks. Only equilibrium of swelling will be considered. However, swelling/deswelling kinetics is an important factor determining the success of failure of some applications, especially slow kinetics has been a limiting factor. Kinetics is strongly dependent on network architecture but also on gel design (geometry and size).

Swelling equilibrium is often approached from a thermodynamical point of view. We will start this theoretical paragraph with the treatment of a neutral network in pure solvent as described by the Flory-Huggins theory. This was the first treatment of the problem, but more recent theories are still based on the same principles. Other, more complex, cases can be considered as an extension of the theory for a pure solvent. We only treat the special case of a gel swollen in a linear polymer solution since this will be the subject of our experimental investigation.

1.4.1 Swelling equilibrium of neutral networks

1.4.1.1 Flory-Huggins mean field lattice theory

From a thermodynamical point of view, gel swelling can be seen as the mixing of a network with a solvent. Flory's theory for network swelling is based on this postulate. He adapted general thermodynamics of polymer solutions to networks by adding a term akin to elastic free energy of rubbers to account for reticulation effects.
Alike any spontaneous process in nature, a network and a solvent only mix freely if this entails a decrease of the Gibbs free energy G of the system. In other words, the free energy change ΔG_{mix}, composed of an enthalpic part ΔH_{mix} and an entropic part ΔS_{mix} (equation [1.5]), has to be negative.

$$\Delta G_{mix} = \Delta H_{mix} - T\Delta S_{mix} \qquad \textbf{[1.5]}$$

Common expressions for both terms are the following:

$$\Delta H_{mix} = k_B T \chi_{sn} n_s \phi_n \qquad \textbf{[1.6]}$$

$$\Delta S_{mix} = -k_B \left[n_s \ln(1 - \phi_n) + n_n \ln \phi_n \right] \qquad \textbf{[1.7]}$$

k_B is the Boltzmann constant, T the absolute temperature, χ_{sn} the Flory-Huggins parameter for interactions between solvent and network, n_s and n_n the number of solvent and polymer molecules and ϕ_n the network volume fraction.

n and ϕ are related through:

$$\phi_s = \frac{n_s v_s}{n_s v_s + n_n v_n} \quad \textbf{[1.8]}$$

$$\phi_n = \frac{n_n v_n}{n_s v_s + n_n v_n} \quad \textbf{[1.9]}$$

where v_s and v_n represent the molar volumes of solvent and network monomers, respectively.
In the case of a polymer network, $n_n = 1$ (the network structure may be seen as one giant molecule). The second term ($n_n \ln \phi_n$) in equation [1.7] becomes then negligible compared to the first term and will therefore be neglected in the following consideration of networks.

Entropy always increases by swelling ($\Delta S_{mix} > 0$) as can be seen in [1.7]. This can be understood physically as follows: the volume occupied by a network grows during swelling and both network and solvent reach a state of greater disorder by spreading out into each other.
The heat of mixing on the other hand may be positive or negative depending on the affinity of the components. The sum of both terms determines the sign of ΔG_{mix} and thus whether the network will mix with the solvent or not. Negative ΔG_{mix} promotes swelling of the gel in the solvent. The result is an increase of the configurational entropy. In the particular case where $\Delta G_{mix} = 0$, the system is at equilibrium, so network and solvent will not further diffuse into each other.

The motion of chains in a network is limited due to the presence of crosslinks. As the network swells, chains are extended between the network junctions, causing an elastic retraction force. This new configuration entails an entropy change ΔS_{el}, which has to be considered in the free energy change of a swelling network. Assuming a Gaussian chain distribution and affine chain deformation during swelling, the free energy change due to chain stretching, ΔG_{el}, may be expressed as (Flory, 1969):

$$\Delta G_{el} = -T\Delta S_{el} = \frac{k_B T \nu_e}{2}\left(3\alpha^2 - 3 + \ln \alpha^3\right) \quad \textbf{[1.10]}$$

with ν_e the effective number of chains in the network and α an expansion factor relative to the reference state of the network, which is the relaxed unswollen state (V_o) in Flory's theory, $\alpha^3 = V/V_o$. Obukhov et al. (1994) cite experimental evidence that justifies the hypothesis of affine deformation during swelling in a good solvent. Other manners have been proposed to express the elastic free energy. Yet, the proportionality with α is fairly the same for all models.

The rest of this paragraph will deal with possibilities to swell in different solvents for neutral or charged networks. Only free swelling is considered. Flory's result will be given first. Some more recent results are also discussed in the following paragraphs.
As said above, the total change of free energy due to swelling of a neutral polymer network is caused by two effects: on the one hand the free energy of mixing and on the other hand the elastic free energy due to stretching of the network chains. Assuming additivity of these contributions, the total free energy change of a network due to swelling can be written as:

$$\Delta G = \Delta G_{mix} + \Delta G_{el} \quad \textbf{[1.11]}$$

The reader will notice the analogy between [1.11] and [1.2]. The relation between both equations is

$$\pi = -\frac{N_{Av}}{v_s}\left.\frac{\partial(\Delta G)}{\partial n_s}\right|_{P,T,n_n} \quad \textbf{[1.12]}$$

N_{Av} is Avogadro's number (6,023 10^{23}).

Application of [1.12] on [1.5] and [1.10] gives the expressions for π_{mix} [1.13] and π_{el} [1.14].

$$\pi_{mix} = -(RT/v_s)\left[\ln(1-\phi_n) + \phi_n + \chi_{sn}\phi_n^2\right] \quad \textbf{[1.13]}$$

$$\pi_{el} = -\left(\frac{RT\nu_e}{V_o}\right)\left[\left(\frac{\phi_n}{\phi_o}\right)^{1/3} - \frac{1}{2}\left(\frac{\phi_n}{\phi_o}\right)\right] \quad \textbf{[1.14]}$$

where R is the ideal gas constant (8,314 $J.mol^{-1}.K^{-1}$), ν_e the effective number of chains expressed in mol. The prefactor (ν_e/V_o) can also be written as $(v^*M_c)^{-1}(1\text{-}2M_c/M)$ and accounts for network imperfections due to dangling chain ends. v^* is the specific volume of the polymer, M_c the average molecular weight of a strand and M the primary molecular weight. One can see that for an ideal network, M tends to infinity and the second factor becomes 1. All chains are then effectively implied in the network structure.

A remark should be made on the notion of 'reference state'. The reference is defined as that state where no forces are exerted on the crosslinks. This does not necessarily mean that all chains have unperturbed configurations. In the network case, the junction points may affect the chain dimensions (Dušek and Prins, 1969). Different authors have tried to describe this reference state in the best way possible.

Flory (1969) took the non-swollen state as reference: $\phi_{n,o} = 1$. In this hypothesis, the gel is coiled up at maximum and the only thing it can do is swell. Dušek and Prins (1969) relate the reference state to the state of the network under formation conditions. After Khokhlov (1980), the gel reference state should be taken near θ-conditions for the linear constituting molecule. He takes $\phi_{n,o} \sim N^{-1/2}$ for a gel prepared in a large quantity of a good solvent. In this case $\phi_{n,o} << 1$ and the network is close to its non-perturbed state.

Some critical remarks have been formulated on the Flory model.

- First, solvent and monomer molecules occupy the same volume in Flory's lattice theory; molar and volume fractions are thus equal. This hypothesis is only acceptable for networks constituted of small monomers. Long or charged monomers occupy a larger space than the solvent monomer.
- Second, expression **[1.14]** is based on linear chain deformation and does not take into account the limited extensibility of the segments. This expression is only correct for chains not extended more than half of their fully stretched length, thus for moderate degrees of swelling or in poor solvents.
- The swelling mechanism is not only governed by affine stretching of the network strands. It appears that the swelling of a network arises from three different contributions: strand unfolding, isotropic swelling of the coils and extension of the strands less than affine with the

macroscopic dimensions (Bastide et al., 1981b). Shenoy's (1998) modified version of the Flory model supports this idea. His predictions correlate very well with experimental data. Dušek et al. (2001) proposed expressions for the free energy terms in the swelling equation that account for chain folding/unfolding.

- Real networks have many defects and are highly non-ideal. Only dangling chain end defects are taken into account via ν_e. Other defects and network inhomogeneity do not appear in the theory. Therefore, the elasticity of a real network will differ from the elasticity forecasted for an ideal network.
- The model can be refined by introducing a concentration dependence of the Flory-Huggins affinity parameter (Erman and Flory, 1980). Moreover, the presence of crosslinks may modify χ so that the interaction parameter in a network and the interaction parameter in a solution of the same polymer will differ (Dušek and Prins, 1969; Horkay et al., 1989).

The equilibrium degree of swelling can be derived from the thermodynamic equilibrium that is defined by ΔG minimal or equivalently by $\pi = 0$. At this point, the swelling forces are balanced by the elastic retraction force and the network will not be diluted further. Equilibrium defines the minimum polymer concentration in the gel, $\phi_{n,min}$. If $\phi_{n,i}$ in equation [1.4] is set equal to 1 (dry gel), $Q = \phi_{n,f}^{-1}$. The equilibrium degree of swelling may be calculated as a function of system parameters and is given in [1.15] (Flory, 1969). Practically speaking, equilibrium can only be reached in presence of an excess of solvent (Tanaka, 1981).

$$Q_{eq}^{5/3} \cong \frac{\left(M_c v^*\right)}{v_s}\left(1/2 - \chi_{sn}\right)\left(1 - 2M_c/M\right)^{-1} \qquad \textbf{[1.15]}$$

This expression has been determined for weakly crosslinked networks in a good solvent. Flory (1969) cites experimental results that confirm his theory.
Taking Khokhlov's reference state, one finds following expression for free swelling:

$$Q_{eq} \sim M_c^{4/5} \qquad \textbf{[1.16]}$$

Predicted degrees of swelling are higher than Flory's where $Q_{eq} \sim M_c^{3/5}$ for an ideal network.

1.4.1.2 Scaling theories

The problem of network swelling was analysed in a different way by de Gennes (1979). The gel network is visualised as a collection of adjacent blobs as shown in Figure 1.6, each blob being associated with one network chain (composed of N monomers) and having properties very similar to those of a single chain. The blobs in a network are not Gaussian because of the elastic contact points imposed by the crosslinks.

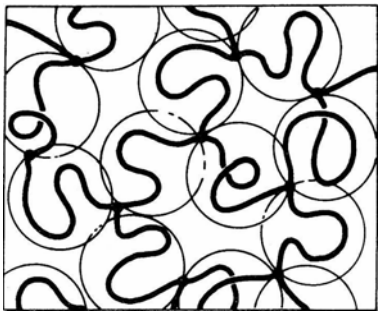

Figure 1.6: Blob network [From de Gennes, 1979]

de Gennes states that many properties of a neutral polymer gel are identical to those of a polymer solution in which the chains are just about to overlap. This gives following scaling law for the mixing pressure at and above θ-temperature:

$$\pi_{mix} = B\phi_n^{9/4} + C\phi_n^3 \qquad \textbf{[1.17]}$$

B and C are the second and third virial coeffcient, respectively. $B = RT\upsilon\tau/v_s$ with υ the excluded volume parameter, $\upsilon = a^3(1-2\chi)$ and 'a' represents the monomer length. τ is the reduced temperature $(T-\theta)/\theta$. This gives following scaling law for the equilibrium degree of swelling in a good solvent:

$$Q_{eq} \cong N^{4/5}(1-2\chi)^{3/5} \qquad \textbf{[1.18]}$$

This is coherent with Flory's result apart from the exponent of N, which is slightly higher in the result of de Gennes. Flory found a correct scaling expression by overestimating both elastic and osmotic parts of the free energy (de Gennes, 1979).

Obukhov et al. (1994) followed the same reasoning as Flory, but using scaling expressions for osmotic and elastic pressure. They take the gel preparation conditions as reference state. For a good solvent, the same scaling with N as in the Flory theory is found:

$$Q_{eq} \sim \begin{cases} N^{3/5} & \text{Good solvent} \\ N^{3/8} & \theta\text{-solvent} \end{cases} \qquad \textbf{[1.19]}$$

Obukhov also points out a dependence on the polymer concentration in preparation state. He precised that [1.19] was developed for tightly crosslinked networks that are supposed to be free of trapped entanglements. Loose networks would contain a considerable amount of trapped entanglements that have to be taken into account when predicting the degree of swelling for such networks.

1.4.2 Swelling equilibrium of polyelectrolyte networks

Despite numerous applications as superabsorbents and the perspective of using them as mechanical actuators, swelling of polyelectrolyte gels is not well understood yet because of its complexity. Most studies treat neutral gels and if polyelectrolyte gels are considered, they are usually immersed in salt solutions. In this paragraph, only the case of a polyelectrolyte gel in salt-free solvent (without supplementary ions) is considered. Many parameters, including network dimensions and solvent

quality enter the system. Discussing the role of each one of them would lead us too far. Only the relation between degree of swelling and degree of ionisation is discussed.

1.4.2.1 Flory's approach

As stated in the first paragraph, swelling is induced by osmotic pressure. In the case of a neutral network, the osmotic pressure originates from configurational entropy of the polymer. This factor also contributes to the osmotic pressure in the case of a polyelectrolyte gel, but it is dominated by the osmotic pressure due to translational entropy of the free ions in the network π_{ion} (Rubinstein et al., 1996). This term has to be added to the osmotic pressure. The simplest theories express ionic pressure as an osmotic pressure difference between ions in the surrounding medium and in the gel (equation [1.20]) (Flory, 1969; Lagutina et Dubrovskii, 1996).

$$\pi_{ion} = RT\sum_{ion}\left(C_{ion}^{gel} - C_{ion}^{sol}\right) \qquad \textbf{[1.20]}$$

In this expression, C_{ion}^{gel} and C_{ion}^{sol} represent the concentrations of mobile ions in gel and external solvent, respectively. The latter will be zero since the case of salt solutions is not considered here and electrical neutrality inside the gel has to be conserved. If N/A denotes the number of counter-ions per segment, π_{ion} for a polyelectrolyte gel in a salt-free solvent can as well be expressed as:

$$\pi_{ion} = RT\frac{\nu.(N/A)}{N_{Av}V_o}\frac{\phi}{\phi_o} \qquad \textbf{[1.21]}$$

According to the Flory theory, the equilibrium degree of swelling becomes:

$$Q_{eq}^{2/3} \cong \left(\frac{N/A}{v_c}\right)(M_c/\rho)(1-2M_c/M)^{-1} \qquad \textbf{[1.22]}$$

v_c denotes de molar volume of a segment between cross-links and ρ is the density of the polymer. This expression is valid for a gel in good solvent with monovalent counter-ions and ionised more than 10 %.

Comparison of the quotient of Q and M_c for a neutral and a polyelectrolyte gel shows that a higher equilibrium degree of swelling is forecasted for the polyelectrolyte gel. Equation [1.22] describes that Q will continuously increase with the degree of ionisation. However, experiments showed that Q goes to a plateau when i (= 1/A) is increased. The discordance between theory and experiment is due to the fact that the elastic term has been derived assuming a Gaussian chain length distribution. This is only acceptable for extensions not exceeding about half the fully extended length, which is clearly not the case for freely swelling highly charged polyelectrolyte gels. Other chain length distributions have to be used. Katchalsky and Michaeli (1955) took along the electrostatic chain repulsion in their analysis. The derived expression predicts the levelling off of the degree of swelling at high degree of ionisation in an excellent way.

A second reason for the existence of the plateau is counter-ion condensation. Due to this phenomenon, the actual degree of ionisation of a polyelectrolyte is lower than what could be expected from its composition (Manning, 1969).

For swelling of a polyelectrolyte gel in a θ-solvent without added salt, where only Coulomb interactions are encountered, swelling is induced only by the osmotic pressure of the counter ions inside the gel. The stress induced in this way is transmitted to the elastic chains by the reticulation points. The network strands deform like an isolated chain would do when a force is tearing at its extremes (Barrat et al., 1992). The degree of swelling becomes:

$$Q_{eq} \sim N^2 i^{3/2} \qquad \textbf{[1.23]}$$

Since N is proportional to M_c, Q is proportional to $M_c^2 i^{3/2}$. The considered reference state to derive this equation is the same as chosen by Khokhlov. One observes that this gives a higher power of M_c than found by Flory. The predicted degree of swelling is thus higher. Yet, both authors estimate the effect of the ions in the same way.

In the late 1970's, Tanaka observed a particular phenomenon on polyelectrolyte gels (Tanaka, 1978, 1979). He reports a discrete change in the degree of swelling, alike a phase transition, when the solvent quality is continuously changed from poor to good. A critical solvent quality could be defined. Sharper transitions were observed on gels with higher degree of ionisation (Tanaka et al., 1980). Dušek and Prins (1969) had predicted this transition. Such a sudden transition as a reaction to a small environmental change near the critical condition makes polyelectrolyte gels suitable materials for intelligent sensors and actuators.

1.4.2.2 Scaling approach

Rubinstein et al. (1996) theoretically derived expressions for the degree of swelling at equilibrium as a function of solvent quality, degree of ionisation and network characteristics:

$$Q \cong B\frac{N^{3/2}}{a^{3/4}}\begin{cases} A^{-6}\tau^{-9} & \text{bad solvent} \\ A^{-3/2} & \theta\text{-solvent} \\ A^{-6/5} & \text{good solvent} \end{cases} \qquad \textbf{[1.24]}$$

Parameter B groups preparation conditions and A represents the number of monomers between two effective charges. The prediction for a θ-solvent corresponds to [1.23].

1.4.2.3 Empirical results

Experimental data published by Melekeslan and Okay (2000) and given in Figure 1.7 show that Q does not increase continuously with the number of ionic groups in the network. The degree of swelling increases rapidly with the number of ionogenic groups as long as their number is low. For high i, Q hardly depends on i but tends to an asymptotic value. Comparison of the dotted line with the experimental points clearly shows that Flory's theory ($Q \sim i^{3/2}$) overestimates the degree of swelling. Melekeslan and Okay fitted following experimental law with their data:

$$Q \sim i^{0,66} \qquad \textbf{[1.25]}$$

The exponent 0,66 is much smaller than 3/2 given by Flory. Two explanations are possible. Since chains are extremely stretched, length distribution is not Gaussian anymore (as supposed in Flory's

theory) and π_{el} will increase with a higher power of the elongation factor. Another explanation is given by counter ion condensation: as a result of this effect, a part of the ions do not actively contribute to the swelling process.

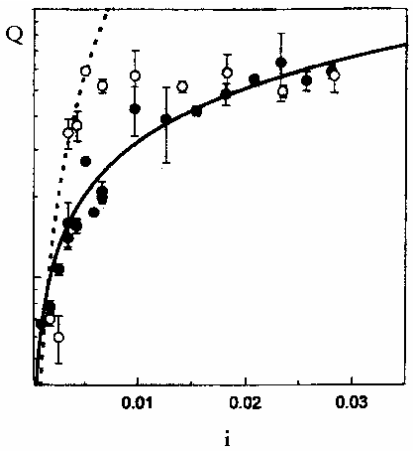

Figure 1.7 : Effect of ionisation i on the degree of swelling Q for two different types of ionogenic monomers; the dotted line represents the Flory-Huggins prediction [1.22]. The full line is the best fit with experimental points. [From Melekeslan and Okay, 2000]

1.4.3 Swelling in a linear polymer solution

The swelling of a network in a polymer solution is of great interest for pharmaceutical and cosmetic industries, in continuous pursuit of new means to store and release active components in a controlled way. A gel swollen in a good solvent that is immersed in a polymer solution with the same solvent, deswells (Boyer, 1945; Brochard, 1981; Bastide et al, 1981; Vasilevskaya and Khokhlov, 1992; Shenoy, 1998). The two opposing phenomena causing this result are extraction of the solvent from the gel to the solution and penetration of polymer chains into the network (Bastide et al., 1981; Shenoy, 1998). Parameters determining how far the gel deswells, are the degree of crosslinking, interactions between the different components, molar mass of the linear polymer and its concentration in the solution.
Because of the large number of parameters involved and because of the fact that not all authors specify them all, it is not evident to compare their results. Nevertheless, we will try to give a global qualitative overview of different phenomena occurring when a gel comes in contact with a polymer solution and to show in which circumstances it is possible to introduce polymer chains into the gel by diffusion.

Thermodynamical equilibrium between gel and polymer solution is considered. The free energy of a polymer solution has been described by Flory and Huggins (1969).

$$\Delta G^{sol} = RT\left[\phi_s^{sol} \ln \phi_s^{sol} + \phi_p^{sol} \ln \phi_p^{sol} + \chi_{sp}\phi_s^{sol}\phi_p^{sol}\right] \qquad \textbf{[1.26]}$$

where ϕ_p^{sol} represents the polymer volume fraction in the solution and χ_{sp} the polymer-solvent interaction parameter. The phases are indicated by the superscripts 'gel' and 'sol' respectively. The compounds (solvent, linear polymer and network) are referred to by indices s, p and n, respectively.

The free energy of the gel is expressed in equation [1.11] but expressions for polymer-network interactions ($\chi_{pn}\phi_p\phi_n$) and solvent-polymer interactions ($\chi_{sp}\phi_s\phi_p$) have to be added to the free energy of the gel.

Two conditions have to be met to reach equilibrium between gel and solution phase:

- Equality of solvent chemical potential in both phases:

$$\frac{\partial G^{gel}\left(\phi_s^{gel}, \phi_p^{gel}\right)}{\partial \phi_p^{gel}} = \frac{\partial G^{sol}\left(\phi_p^{Sol}\right)}{\partial \phi_p^{Sol}} \qquad \textbf{[1.27]}$$

- Equality of polymer chemical potential in both phases:

$$-G^{gel} + \frac{\partial G^{gel}\left(\phi_n^{gel}, \phi_p^{gel}\right)}{\partial \phi_n^{gel}}\phi_n^{gel} + \frac{\partial G_s\left(\phi_n^{gel}, \phi_p^{gel}\right)}{\partial \phi_p^{gel}}\phi_p^{gel} = \frac{\partial G^{Sol}\left(\phi_p^{Sol}\right)}{\partial \phi_p^{Sol}} - G^{sol} \qquad \textbf{[1.28]}$$

These two equations allow calculating the equilibrium degree of swelling and the linear polymer concentration inside the gel.

1.4.3.1 Swelling equilibrium of a neutral network in a linear polymer solution

When a gel is immersed in a solution of a linear polymer, the linear polymer may be similar to or different from the network polymer. Both cases will be treated separately. Two results are important: how the degree of swelling of the gel is affected and how the linear polymer is distributed among gel and solution phase. The latter is expressed as a partition coefficient $\phi_p^{gel} / \phi_p^{sol}$.

Complex cases of multiple polymer solutions will not be discussed. One should also note that the verb 'to deswell' is used with respect to swelling in pure solvent in the next of this paragraph.

1.4.3.1.1 Network and polymer are of the same chemical nature

The simplest case to solve is when interaction parameters are zero. Hence, the only variables affecting the swelling ratio Q and the partition coefficient K are the degree of polymerisation of the polymer chains, DP, and the polymer concentration in the solution. Numerous authors have considered this problem theoretically (Brochard, 1981; Bastide et al., 1981; Shenoy, 1998) and experimentally (Bastide et al., 1981; Kayaman et al., 1998). Qualitatively speaking, they all obtained the same result. Implicit expressions for the equilibrium degree of swelling and for the distribution coefficient are given by Bastide et al. (1981) and Horkay and Zrinyi (1986).

Effect of polymer chain length and solution concentration

Figure 1.8a shows that a polymer network is impermeable for very long chains in a diluted solution. The longer the chains, the closer the gel approaches its equilibrium state in pure solvent. This is confirmed by observations of Kayaman et al. (1998) for a polyacrylamide gel in a polyacrylamide solution. Brochard (1981) qualified this regime as 'Swollen unmixed'. When a dry network is immersed in a polymer solution, the system tries to equilibrate by migration of solvent molecules into the network in order to approach the diluted state of the external solution.

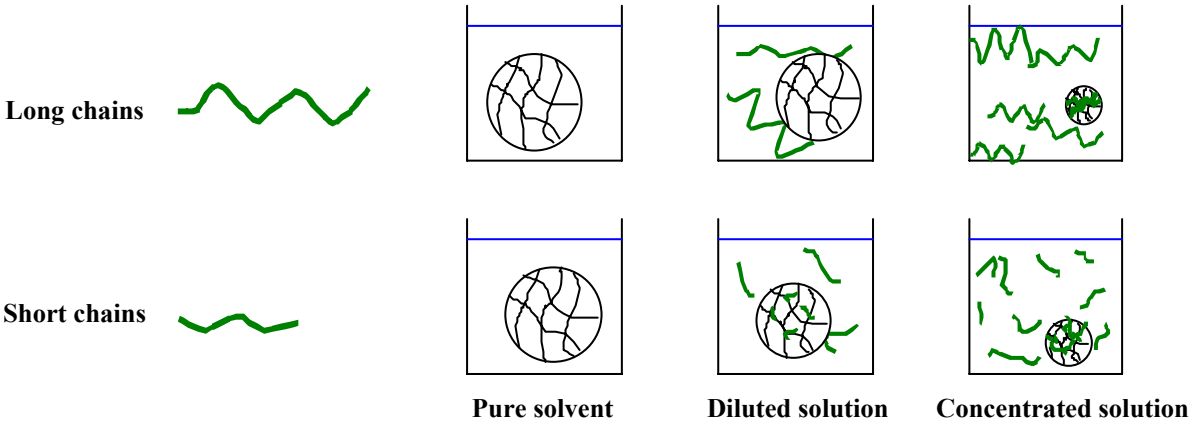

Figure 1.8: Schematic overview of the effect of polymer chain length and polymer solution concentration on degree of swelling and repartition of the linear polymer chains.

Above a given concentration, a small fraction of the linear polymer penetrates into the gel. This fraction increases with increasing external concentration. At the same time, the network is then less swollen than in pure solvent or low concentration polymer solutions. This effect is more pronounced for long chains. A reason for shrinking is the osmotic pressure of the external solution, which increases with increasing linear polymer concentration.

For long macromolecules (high M_w), Shenoy (1998) describes a linear relation between the degree of deswelling $\phi_n^{gel}/\phi_{n,min}^{gel}$ and $\phi_p^{sol}/\phi_{n,min}^{gel}$ where $\phi_{n,min}^{gel}$ is the minimum concentration of the network polymer in the gel, corresponding to maximum swelling (in a good solvent). His experimental observations confirm this prediction as shows Figure 1.9.

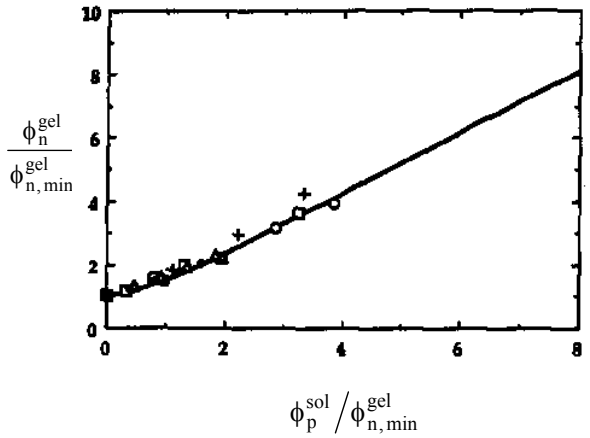

Figure 1.9: Comparison of the degree of swelling calculated by Shenoy (—) and measured experimentally on different types of gels [From Shenoy, 1998].

A critical chain length value $M_{w,crit}$ exists below which chains can easily diffuse into the network. This value depends on the length of the network strands. In diluted solutions, the degree of swelling reaches a minimum value when linear chains have length $M_{w,crit}$ (Bastide et al., 1981; Shenoy, 1998). Short chains (and monomer or solvent molecules in the limiting case) penetrate the gel even at low concentration solutions (Figure 1.8). The partition coefficient increases with solution concentration and Vasilevskaya and Khokhlov (1992) showed that this coefficient tends to unity rather rapidly. The

network deswells because of the polymer present in the network, but this effect is less marked than for chains longer than $M_{w,crit}$. At constant M_w, the transition from swollen to unswollen state takes place in a small interval of the external solution concentration.

Effect of solvent-network interactions

The effect of the solvent quality for the network on the degree of swelling in a polymer solution is given in Figure 1.10. One supposes the chains are short enough to penetrate the network. The analysis was made by Vasilevskaya and Khokhlov (1992). They based themselves on equations [1.27] and [1.28] to describe the swelling of a gel in a polymer solution. The presented case where $\chi_{pn} = \chi_{sp} = 0$, but χ_{sn} varying between 0 and 1 is a rather theoretical-one, but still interesting since it allows isolating the effect of χ_{sn}.

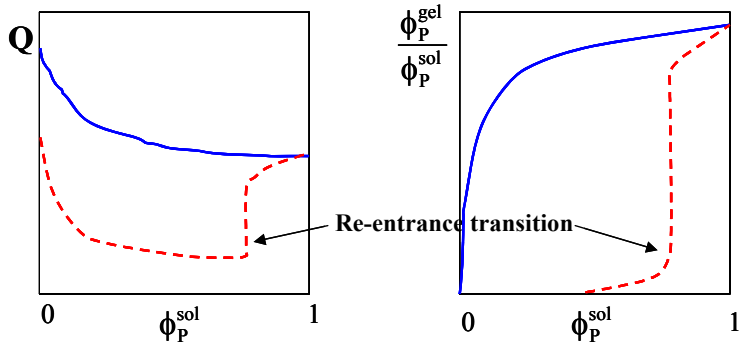

Figure 1.10: Gel swelling in a linear polymer solution: effect of solvent quality on the equilibrium degree of swelling (left graph) and on the partition coefficient (right graph) with linear polymer concentration in the outer solution for a good solvent (full line) and a poor solvent (dashed line). Conditions for the polymer are a-thermal ($\chi_{pn} = \chi_{sp} = 0$). [adapted from Vasilevskaya and Khokhlov, 1992]

For a good solvent, the repartition coefficient $\phi_p^{gel}/\phi_p^{sol}$ increases monotonously while the gel shrinks due to screening of excluded volume effects.

The swelling changes drastically when the gel is immersed in a polymer solution of a moderate to bad solvent for the network. At low ϕ_p^{sol}, the polymer does not enter the network at all. The gel contracts progressively as the concentration increases. A gel in a non-solvent is in shrunken state (dashed line in Figure 1.10). At a critical concentration, a remarkable transition takes place: the polymer penetrates in the network, making the network swell. This transition is called reentrant transition and is a first order transition showing a drastic jump of the degree of swelling and of the linear polymer partition coefficient. The resulting gel is swollen with the polymer since polymer-network contact is more favourable than solvent-network interactions. This transition is more drastic for longer polymer chains and shifts to higher solution concentrations. It does not exist for short polymer chains.

One should note that an 'abrupt' transition indicates a discontinuity in the curve 'degree of swelling as a function of solution concentration'. It is under no condition a sudden collapse of the gel in terms of time. Swelling and deswelling are diffusion processes that are slow for long molecules like polymers.

1.4.3.1.2 Gel swelling in a polymer solution different from the network polymer

If the dissolved polymer is different from the network polymer, χ_{pn} differs from zero, so polymer-network interactions enter the field. At low concentrations, a gel in contact with a solution of a poor or non compatible polymer, deswells. The lesser the polymer is compatible with the network (χ_{pn} increases), the more the surrounding solution has to be concentrated before the polymer may enter in the network and a re-entrance transition is observed. If polymer and network are completely incompatible, the polymer does not enter the network at all and the network deswells continuously with increasing polymer solution concentration. This continuous evolution has been observed experimentally by Momii and Nose (1989) for a gel in a solution of incompatible polymer. They do not mention the re-entrance transition, but it is possible that the polymers used in their study were not long enough (see 1.4.3.1.1 effect of M_w).

For completely compatible polymer and network ($\chi_{pn} < 0$), large amounts of polymer penetrate into the gel, even at low ϕ_p^{sol}. The presence of the polymer effectively improves the quality of the mixture in which the gel is placed. Hence, the latter may reach even higher degrees of swelling than in pure solvent. A particular case of strong polymer-network attractions is the formation of polymer-network complexes. This case will be treated briefly in 1.4.3.3.

1.4.3.2 Swelling equilibrium of a polyelectrolyte network in a polymer solution

Like a neutral gel, a polyelectrolyte gel strongly deswells when immersed in a polymer solution. This behaviour is forecasted theoretically and observed experimentally by different groups (Vasilevskaya and Khokhlov, 1992; Kayaman et al., 1998; Melekeslan and Okay, 2000). The transition swollen-collapsed may be continuous or discontinuous. At constant concentration, a charged network is always more swollen than a neutral-one. Nevertheless, for ϕ_p^{sol} approaching unity, both charged and neutral networks go to the same degree of swelling. The remainder of this part deals with the effect of charges on the transitions discussed in the previous section.

Melekeslan and Okay (2000) studied the behaviour of polyacrylamide hydrogels with different number of ionic groups on the network in a solution of polyethylene glycol. Weakly and very strongly ionised gels deswell continuously with increasing external polymer concentration, as was also seen for neutral gels. Intermediately ionised gels collapse abruptly at a critical solution concentration, as a first order transition. The critical concentration for the transition increases with increasing number of ionic groups and so does the magnitude of the jump-wise transition. This deswelling is correctly described by Flory's theory if taking into account the decrease of effective charges due to interactions with the linear polymer (Kayaman et al., 1998; Melekeslan and Okay, 2000). The calculations of Vasilevskaya and Khokhlov (1992) also foresee this drastic transition. They also concluded that the volume is conserved at any concentration ϕ_p^{sol} if the gel is highly ionised, but this differs from Melekeslan and Okay's experimental observations.

The re-entrance transition observed for networks incompatible with the solvent also exists for polyelectrolyte networks, but takes place at lower ϕ_p^{sol}.

1.4.3.3 Swelling equilibrium of a complexated network

A particular case of a gel in a polymer solution is encountered when the polymer network forms complexes with the linear polymer in the solution. This reaction is accompanied by a free energy change that may lead to the collapse of the swollen network (Osada and Sato, 1980; Philippova and Starodubtsev, 1995). Osada and Sato (1980) used this transition to mechanically levitate a heavy mass. The complexes may be formed by ionic bonds (Bekturov et al, 1998) or by hydrogen bonds (Philippova and Starodubtsev, 1995; Karybiants et al, 1996; Bekturov et al, 1999).

A theoretical treatment of deswelling as a consequence of intermolecular complex formation has been given by Khokhlov and Kramarenko (1993). The difference with all the previous cases is that the linear polymer chains entrapped in the network can now be in two different states: free chains (ϕ_p^{gel}) and chains participating in a complex (ϕ_c^{gel}). The same goes up for the network monomers: part of them participates in the complexes (ϕ_c^{gel}) whereas the rest of the monomers remain free ($\phi_n^{gel} - \phi_c^{gel}$). Figure 1.11 gives a schematic representation of this concept.

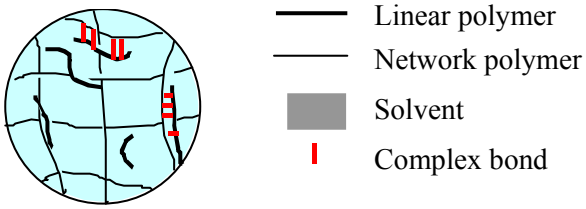

Figure 1.11: Schematic representation of a gel swollen in a linear polymer solution with intermolecular complexation.

Five extra terms enter the free energy of the gel expression:

- three interaction terms (complex-solvent, complex-linear polymer and complex-network),
- a free energy term, expressing the energy gain due to complex formation, and
- a migration term, expressing the possibility of complexated polymers to move along the network chains.

A new equilibrium condition has to be fulfilled as well: complex formation must be favourable from an energetic point of view.

$$\left.\frac{\partial(\Delta F)}{\partial \phi_c^{gel}}\right|_{\phi_c^{gel}+\phi_p^{gel}=cte} = 0 \qquad \textbf{[1.29]}$$

Together with conditions [1.27] and [1.28], one obtains a three-equation system allowing to calculate the degree of (de-)swelling, the linear polymer concentration inside the gel and the complex concentration.

This case will not be treated further here since it is beyond the scope of this work. Interested readers are referred to the papers of Osada and Sato (1980), Khokhlov and Kramarenko (1993), Budtova et al. (1994), Philippova and Starodubtsev (1995), Karbiants et al., (1996), Bekturov et al., (1998, 1999).

1.4.4 Conclusions on swelling

The state of the art of gel swelling studies has been reviewed in a nutshell. First, thermodynamics of a network immersed in a solvent have been described. Although theoretical results are not unanimous from a quantitative point of view, one should remind that a gel in a solvent can swell or not depending on the solvent quality. All other parameters being equal, an ionised network (polyelectrolyte) will occupy a larger volume at equilibrium than a neutral one.
Second, in view of the experimental work presented later in this document, we focussed on the transitions caused by a polymer solution surrounding the gel. The system gets more complex and the number of states possible increases when a gel is placed in a polymer solution. The most striking observation is that the degree of swelling does not change in a monotonous continuous way with solution concentration. Two sudden transitions have been distinguished in a bad solvent. First, a transition from a swollen state to a fully collapsed state can happen at a critical concentration for an ionised gel or for a network that forms complexes with the linear polymer; in all other cases, the gel will deswell progressively with increasing solution concentration. A second jump-wise transition may happen at a high critical concentration: large amounts of polymer enter the gel, which makes its degree of swelling increase abruptly. This transition has been named re-entrance transition and can be observed on all types of gels.

1.5 Interfacial tension acting against swelling

In the previous paragraph, gel swelling has been studied in a fluid that is the gel solvent. It is supposed that no interfacial tension effects take place. Because solvent and (solvent + small fraction of network) may be very similar, this is justified in most cases. However, in cases where interfacial tension cannot be ignored, an extra term has to be added to the swelling pressure balance.

The contact between two immiscible fluids causes stresses at the interface σ_{int} that can be quantified as (Macosko, 1996).

$$\sigma_{int} = \frac{\Gamma}{R_1} + \frac{\Gamma}{R_2} \qquad \textbf{[1.30]}$$

Γ is the interfacial tension between the two fluids in contact and R_1 and R_2 are the principal radii of the inclusion expressed in mm.
Since σ_{int} has pressure units, it can be incorporated in the swelling pressure balance without modification. A minus sign has to be added because interfacial tension opposes to swelling.
Using this approach, Fernández-Nieves and co-workers (2000) predicted in a satisfying way the volume phase transition of a spherical polyelectrolyte microgel particle. When a polyelectrolyte gel is immersed in a solvent, counter–ions dissociate and they may polarise the gel surface. The presence of a surface charge density induces an interfacial tension in this case.

Interfacial stresses also appear when a gel is extracted from its solvent and immersed in another fluid. The gel can e.g. be surrounded by air or immersed in a second fluid. The second fluid may interact with the gel, like another solvent would, or be inert, e.g. oils in the case of hydrogels. In the latter

case, an interface, involving interfacial tension, may be distinguished between gel and medium. This is the case we will face in our shear experiments (Chapter 3 and 4). A closer look will be given to the effect of interfacial tension in paragraph **3.3** where deformation models for droplets in blends of immiscible polymers are treated.

1.6 Elastic properties of swollen gels

The aim of this work is to investigate the reaction of a swollen gel to externally applied mechanical forces. The state of the art on that topic is reviewed in this paragraph. Gels can undergo large deformations without failing – reminding liquid-like behaviour, but unlike a liquid, a gel spontaneously recovers its initial shape after cessation of stress.

Deformation of swollen gels is a complex matter to study. From a chain point of view (molecular level), deformation of a swollen gel sample is the result of two subsequent deformations:

- chain stretching due to swelling (limited or strong, dependent on the degree of swelling);
- chain deformation induced by macroscopic deformation of the gel at constant degree of swelling.

Analysis of gel deformation and determination of the elastic properties of a swollen material is therefore a difficult task. A small deformation has not the same effect on a highly swollen gel as on a gel with a low degree of swelling.
The theoretical study of gel deformation is derived from rubber elasticity theories. Like a rubber, a gel is composed of a polymer network with the important difference that a gel also contains a considerable fraction of liquid. It will be shown in the following that the swelling of a network has a marked effect on its mechanical properties. The situation becomes even more complex when charges are added to the network, as is the case for polyelectrolyte gels. The complexity of the material system and the possible diversity makes it difficult to describe gel deformation with one universal relationship. A number of theoretical treatments and models that describe the relation between degree of swelling and elastic modulus can be found in recent literature. Most are only valid for a well-defined case.
Since it is difficult to theoretically predict gel modulus, the mechanical properties of hydrogels (the material of interest for our study) have also been intensively studied in an experimental way over the last 20 years. Deviations from the classic rubber-elasticity laws were observed. One of the reasons put forward is the polyelectrolyte character of hydrogels: because of the charges on the network and the osmotic pressure of counter-ions, the chains between the cross-links are highly extended and thus far from the Gaussian coil state that is assumed in the classical theory. Part of the deviations are described by recent theoretical models.

This paragraph is composed of two parts. First, some relevant theoretical relations between degree of swelling and gel modulus are reviewed. Second, experimental methods to measure the modulus are described.

1.6.1 Elastic modulus

Most hydrogels in their swollen state satisfy the criteria to be a rubber (Anseth et al., 1996). The highly extendible chains need rather low mechanical stress to reach large deformations. The network responds to the external stress with rapid rearrangement of the polymer segments and deformation is completely recovered after omitting the stress.
Swelling and mechanical properties of gels depend on factors as network structure and nature of the swelling agent. Their effect will be discussed in this paragraph.

Useful microscopic characteristics are the bulk compressional modulus, K (also called osmotic modulus), the shear modulus, μ, and the longitudinal modulus, E. They are related via

$$E = K + \frac{4}{3}\mu \qquad \textbf{[1.31]}$$

Since theoretical and experimental studies in literature mostly deal with shear modulus, we will limit this overview to the shear modulus, keeping in mind that similar scaling laws hold for all three moduli in the weak stretching regime (de Gennes, 1979; Candau et al., 1982).

1.6.1.1 Classic theory of rubber elasticity

The statistical theory of rubber elasticity predicts the bulk rigidity modulus of a dry network as given in [1.32] (Flory, 1969; Treloar, 1975). The hypotheses made to obtain this equation are Gaussian chain statistics, affine deformation of the network chains and constant volume.

$$\mu = \frac{\rho_n RT}{M_c}\left(1 - \frac{2M_c}{M}\right) \qquad \textbf{[1.32]}$$

Besides one material parameter (network polymer density ρ_n), this expression contains only structural characteristics of the network. The factor between brackets accounts for non-elastically effective loose ends in the network and reduces to unity for a perfect network. If the degree of crosslinking is increased (M_c decreased) the elastic modulus will increase as well.

1.6.1.2 Elastic modulus of swollen networks

Free swelling involves an isotropic expansion of the network and will therefore engender a reduction of the network entropy, as was seen in 1.4. Hence, it is interesting to evaluate how the elastic modulus of a network changes with changing degree of swelling.
The classic result, based on the same hypothesis as for [1.32], was established in 1943 by Flory and Rehner and by James and Guth (Flory, 1969).

$$\mu = \frac{\rho_n RT}{M_c}\left(1 - \frac{2M_c}{M}\right)Q^{-1/3} = \mu_{dry}Q^{-1/3} \qquad \textbf{[1.33]}$$

The prefactor may be recognised as the elastic modulus for a rubber network given in equation [1.32]. This relation is only valid for a network swollen in a θ-solvent and as long as chain behaviour can be

described by Gaussian statistics; this is at small chain deformations (low degrees of swelling). Equation [1.33] indicates that the shear modulus will decrease with increasing degree of swelling.
Zrinyi and Horkay (Horkay and Zrinyi, 1986; Zrinyi and Horkay, 1987) proposed a phenomenological model [1.34] that gives a relation between the modulus and the degree of swelling relative to the equilibrium degree of swelling.

$$\mu(Q) = \mu_{eq}\left(\frac{Q}{Q_{eq}}\right)^{-1/3} \qquad \textbf{[1.34]}$$

One recognises the same proportionality with Q as in the classic theory. For μ_{eq}, a phenomenological temperature-dependent equation was given (Zrinyi and Horkay, 1987). At constant temperature or solvent quality, μ_{eq} obeys de Gennes' scaling relations (eq. [1.36]). Experimental confirmation for the model is given in the same paper. Experimental data from Dubrovskii and Rakova (1997) for neutral polyacrylamide gels confirm the exponent –1/3 in a satisfying way at low degrees of swelling (Figure 1.12) and also Horkay et al (1988, 2000) provide experimental evidence for a poly(vinyl acetate) gel at the θ temperature and for polyisoprene gels in solvent close to θ. Up to this point, the discussion was limited to the weak stretching regime, corresponding to low and moderate degrees of swelling.

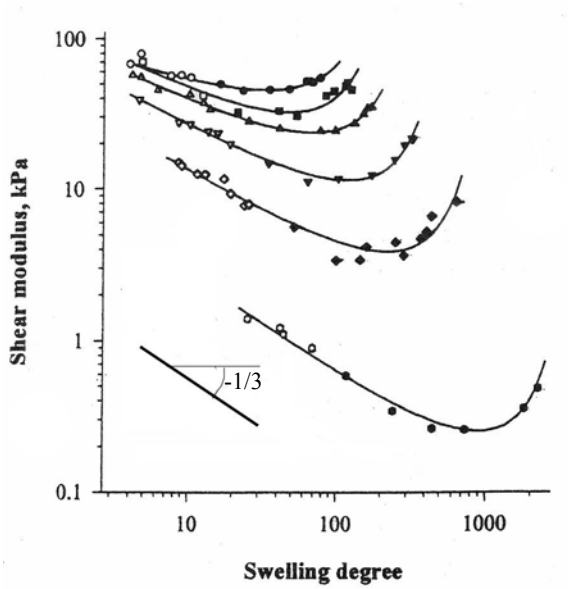

Figure 1.12: Elastic modulus as a function of degree of swelling. A decrease of the curve is followed by flattening and a steep upturn at the highest degrees of swelling. [From Dubrovskii and Rakova, 1997]. Data for polyacrylamide gels with different crosslink densities and in solvents of different quality.

The expression for μ in [1.33] is exactly the same as the expression for the elastic pressure given in [1.14]. The elastic pressure is essentially μ, when both are power laws of the network concentration with exponent 1/3 (Treloar, 1975; Rubinstein et al. 1996). This holds true for gels with Gaussian elastic behaviour (Horkay et al., 1996).
If at equilibrium swelling π_{el} counterbalances swelling π_{mix}, the equilibrium modulus is equal to $-\pi_{mix}$ (both as strong, but opposite sign). As a result, μ_{eq} will scale with ϕ in the same way as $-\pi_{mix}$.

When the gel reaches high degrees of swelling, the modulus does not decrease as a function of degree of swelling anymore, but flattens and then shows a steep increase. A typical plot is shown in Figure 1.12. Opperman and Schroder (1996) gave a theoretical description of this behaviour. The increase of the shear modulus with increasing degree of swelling is due to the finite extensibility of the network chains. The statistics of such strongly extended chains are not Gaussian anymore, and can better be described by the inverse Langevin function. The degree of swelling at which the upturn is initiated depends on the network properties. Numerous experimental observations of this phenomenon have been reported by a.o. Nisato et al., 1996 (neutralised polyacrylic acid); Lagutina and Dubrovskii, 1996 (polyacrylamide); Dubrovskii and Rakova, 1997 (polyacrylamide); Ilavsky et al., 1999 (poly(*N*-vinylcaprolactam)); Horkay et al., 2000 (polyacrylate hydrogels); Gundogan et al., 2002 (poly(*N*-isopropylacrylamide)). The scaling theory of Obukhov et al. (1994) predicts [1.35] for high degrees of swelling where the strands are strongly stretched

$$\mu \sim Q^{-1/6} \qquad \textbf{[1.35]}$$

Comparing the exponent to Figure 1.12, it is most probable that [1.35] describes the flattening part of the curve instead of the real upturn of the curve. One author (Gundogan et al., 2002) measured the slope of the upturn to be +1/3.

1.6.1.3 Modulus at equilibrium swelling

A special case of swelling degree is Q_{eq}, the maximal degree of swelling a particular gel can reach under given circumstances. In gels swollen at equilibrium, the elastic modules are closely related to the osmotic pressure. de Gennes (1979) and Candau et al. (1982) proposed that elastic modulus and osmotic pressure should scale to the degree of swelling in an identical way.

$$\mu_{eq} \sim \begin{cases} Q_{eq}^{-9/4} & \text{Good solvent} \\ Q_{eq}^{-3} & \theta\text{-solvent} \end{cases} \qquad \textbf{[1.36]}$$

This form accounts for pair correlations between monomers and does not assume Gaussian chain statistics. Experimental results confirm the validity of equation [1.36] (Candau et al., 1982). Zrinyi and Horkay (1984, 1987) found exponent –3 for a θ solvent and –2,3 for a good solvent, which is close enough to the theoretical value –9/4 (= 2,25). Obukhov et al. (1994) obtained the same scaling law for strongly crosslinked networks (without trapped entanglements). Exponent –2 was predicted and measured by Skouri et al. (1995) for polyelectrolyte gels in presence of salt.

1.6.1.4 Some scaling laws describing the elastic modulus in specific cases

The dependence of the shear modulus of a hydrogel on its degree of swelling is often represented as a power law:

$$\mu \sim Q^{-m} \qquad \textbf{[1.37]}$$

The exponent m depends on the physico-chemical nature of the system. The value of m is -1/3 in the classic case. Several authors analysed different kinds of systems both via a theoretical as via an experimental approach. The variety of systems and hypothesis resulted in different power law exponents. Some power laws for different cases are given in Table 1.1.

Obukhov et al. (1994) used Panyukov's (1990) ideas on network strand configuration to refine the scaling picture. For the case of neutral weakly cross-linked networks in a good solvent, where the modulus is dominated by entrapped entanglements, equation [1.38] was proposed

$$\mu \sim Q^{-7/12} \qquad \textbf{[1.38]}$$

The result for a θ-solvent coincides with the classic result. A dependence on the preparation concentration is also included in their model.
Rubinstein and co-workers (1996) used the same ideas to tackle the specific case of flexible, strongly cross-linked polyelectrolyte networks. They give for low salt concentrations and at low degrees of swelling:

$$\mu \sim Q^{-5/6} \qquad \textbf{[1.39]}$$

Data of Whiting and Voice (2002) for poly(2-acrylamido-2-methyl-1-propane sulphonic acid) gels give experimental evidence of this scaling law. The model also predicts that the modulus decreases as more charges are added to the network. Experimental data of Skouri et al. (1995) confirm this prediction; they observed a decrease of the modulus as a function of ionisation degree, followed by rather quick flattening due to counter-ion condensation, to reach a plateau value at high ionisation degrees. The case of a polyelectrolyte swollen gel remains a complex one, which can not be fully described by only one scaling relation with the degree of swelling. The picture gets more complete if a scaling relation with the ionisation degree is included. The qualitative results of Nisato et al. (1995) show that the μ(Q)-curve decreases steeper in the downward part of the curve as the degree of ionisation increases.

Table 1.1: Scaling exponents m for shear modulus as a function of degree of swelling

Reference	m	Application
Flory	-1/3	θ-solvent, Gaussian chains, strongly cross-linked network
Obukhov et al. (1994)	-7/12	Good solvent, trapped entanglements dominate, at low Q
Rubinstein et al. (1996)	-5/6	Flexible polyelectrolyte network at low Q

1.6.1.5 Large deformation experiments

Despite its importance, gels have not been thoroughly studied at very large deformations. At large strains, the finite extensibility of the constituent chains will play a role. Some papers can be found on compression experiments with biopolymer gels that were compressed up to rupture. See e.g. the works of Bot et al. (1996) on gelatine gels and of Mancini et al. (1999) on alginate gels. Stammen et al. (2001) performed compression experiments on poly(vinyl alcohol) hydrogels (PVA). The compressive modulus of PVA gels was found to increase with increasing strain and increasing degree of swelling. The highest failure strain was measured on the gel with the lowest degree of swelling. Matzelle et al. (2003) also observed behaviour similar to strain hardening on poly(*N*-isopropylacrylamide) gels. They due this behaviour to increasing physical interactions between pendant groups. Groot et al. (1996 a and b) developed a molecular theory of the strain hardening and the yield behaviour of a polymer gel and found good agreement with gelatine behaviour.

None of these studies mention any solvent release. Yet, it must be emphasised that the degree of swelling of the gels in the cited experiments was not higher than 15 g/g. We used polyelectrolyte hydrogels swollen with 80 g/g solvent or more in our experiments. It is obvious that other aspects may play a role in such system.

1.6.2 Measurement of elastic properties

The previous paragraph has shown that most theoretical models for the shear modulus are only valid for a well-defined case and the quantitative prediction of the modulus needs a detailed knowledge of the sample structure and preparation conditions. Most of the time, these data are not available. Hence, experimental methods for the determination of the modulus are necessary. The most common-ones are uniaxial compression (see for example the works of Zrinyi, Horkay and coworkers, Geissler's team and Gundogan and team) and the penetration technique (Dubrovskii and Rakova, 1997; Matzelle, 2003). Some other methods are described in literature like diaphragm deflection (Dubrovskii et al., 1994). Most studies are restricted to small deformations and assuming either no solvent is leaving the gel or the gel is immersed in excess solvent to ensure permanent swelling equilibrium.

1.6.2.1 Uniaxial compression

The modulus of a gel is most often measured by uniaxial compression tests because it is one of the simplest methods to install: one dimension of the sample is decreased with ratio λ while the other two dimensions are correspondingly increased. This gives in the case of constant volume compression along the Z-axis:

$$\lambda_z = \lambda; \qquad \lambda_x = \lambda_y = \lambda^{-1/2} \tag{1.40}$$

The compressional strain is defined as λ. One should note that λ is smaller than unity in the case of uniaxial compression. The gel reacts to the compression by exerting a force F_N in the direction of compression but in opposite sense. The elastic reaction of real networks is usually described by the empirical Mooney-Rivlin equation (Dušek and Prins, 1969; Treloar, 1975; Zrinyi and Horkay, 1984; Mark and Erman, 1988):

$$\sigma_E = \frac{F_N}{\Omega_0} = 2C_1\left(\lambda - \lambda^{-2}\right) + 2C_2\left(1 - \lambda^{-3}\right) \tag{1.41}$$

Ω_0 is the cross-section of the undeformed sample. The subscript E indicates that stresses are nominal (engineering stress), meaning force per unit initial cross section. The true stress is calculated by multiplying the nominal stress value with λ.

$$\sigma_T = \frac{F_N}{\Omega_0}\lambda = 2C_1\left(\lambda^2 - \lambda^{-1}\right) + 2C_2\left(\lambda - \lambda^{-2}\right) \tag{1.42}$$

C_2 is often thought to describe the deviation from Gaussian behaviour. According to Treloar (1975), the case of uniaxial compression requires $C_2 = 0$ at small deformations and C_1 is accepted to be half of the shear modulus. Therefore, for analysis of uniaxial compression, the Mooney-Rivlin equation is used in the simplified form [1.43].

$$\sigma_{comp} = \mu\left(\lambda^2 - \lambda^{-1}\right) \quad \textbf{[1.43]}$$

The shear modulus may thus be determined experimentally by plotting true stress as a function of (λ^2 - λ^{-1}). The slope of a straight line fitting the data points gives the modulus. Different teams used this method with success for small deformation compression (e.g. Bastide et al., 1981; Zrinyi and Horkay 1984, 1987; Gundogan et al. 2002). Deformations are usually limited to 20 % compression.
Since this analysis relies on the constant volume hypothesis, experiments have to be executed at strain rates faster than the rate at which solvent would be expelled (Nissato et al., 1996, Muniz and Geuskens, 2001). Furthermore, the deformation in the directions perpendicular to the compression direction are supposed to be homogeneous all over the sample height (the sample is cylindrical during the whole experiment). Therefore, absence of barrelling should always be verified.
However, if deformation leads to a change in the volume of the sample, the expression for the overall stress becomes (Hasa et al., 1975):

$$\sigma_{comp} = \mu\left(\lambda - \frac{V}{V_o}\lambda^{-2}\right) \quad \textbf{[1.44]}$$

When a gel looses solvent during testing, one has to bear in mind that diffusion of solvent out of the gel takes time (Milimouk et al., 2001). This diffusion time has to be taken into account when determining the equilibrium modulus. Another issue is that the degree of swelling changes continuously if the gel is loosing solvent.

1.6.2.2 Osmotic pressure

Swelling pressure is a key parameter for gels that may be measured experimentally by mechanical deswelling tests. One should remember from paragraph 1.2 that the swelling pressure is the result of the interplay between osmotic pressure and elastic retraction force. In section 1.6.1.2, we saw that the elastic pressure equals the elastic modulus:

$$\pi_{el} = -\mu \quad \textbf{[1.45]}$$

Substitution of π_{el} by -μ in equation [1.3] results in

$$\pi = \pi_{mix} + \pi_{ion} - \mu \quad \textbf{[1.46]}$$

Equilibrium swelling is reached when elastic and osmotic parts balance each other out, so the swelling pressure is equal to zero. The modulus is thus a measure for the osmotic pressure and inversely.

Deformation due to an external stress F will be accompanied by a decrease of the entropy, as described in the first paragraph. It will therefore limit the degree of swelling, but it provides a way to measure the swelling pressure as a function of the degree of swelling. With an external force, [1.46] becomes:

$$\pi = \pi_{mix} + \pi_{ion} - \mu = F \quad \textbf{[1.47]}$$

Bell and Peppas (1996) describe how osmotic pressure may be measured mechanically. A dry sample of known volume is placed in a vessel with excess solvent. In general the sample is confined in a tube to guide the swelling. At contact with the bath, the osmotic pressure is high and the dry sample will start absorbing the solvent. In absence of any load (free swelling) the gel will swell until it reaches its equilibrium degree of swelling. If a load F is placed on top of the sample, it will only swell as long as the sample is able to push up the load, meaning as long as the swelling pressure is higher than the pressure exerted by the load. As the degree of swelling increases, the swelling pressure decreases until it equilibrates the external load. The gel cannot push the load further upward neither may the load fall down. The swollen volume is measured at this stage and the relations between swelling pressure and degree of swelling may be established. As the load becomes heavier, the degree of swelling is limited to the one that corresponds to swelling pressures equal to the external load.
Experiments of this type have been described by various authors (e.g. teams in Moscow (e.g. Lagutina and Dubrovskii, 1996) and in Grenoble (Geissler et al., 1988)). Typical results are shown in Figure 1.13. The expected result of increasing swelling pressure with decreasing degree of swelling is observed. The inverse of this curve $\pi(Q)$ should give the effect of an external load on the degree of swelling.

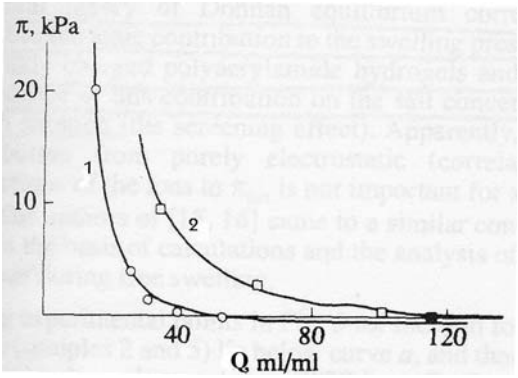

Figure 1.13: The swelling pressure as a function of degree of swelling for (1) uncharged polyacrylamide hydrogel and (2) an ionic polyacrylamide gel prepared by hydrolysis in a NaCl solution. Filled symbols correspond to free swelling. Full lines are calculated with a Flory approach. [From Lagutina and Dubrovskii, 1996].

An absolute requirement for a good swelling/deswelling experiment is the presence of a large excess of solvent. The second remark to be made is that swelling confined in a tube might not be completely isotropic.

1.7 Conclusions

Polyelectrolyte gels form the subject of this thesis. These materials are composed of a polymeric three-dimensional network of which the strands are connected in cross-linking points by covalent bonds. In order to speak of a gel, the network has to be swollen with a solvent. If ionogenic groups are incorporated in the network, we are dealing with a polyelectrolyte gel. These groups can

dissociate in presence of a suitable solvent, resulting in a charged network and a number of counter-ions.

One of the most remarkable features of gels and specifically of polyelectrolyte gels is their swelling capacity. Not only they can absorb enormous amounts of solvent, they also can change their volume in a controlled way, depending on the physico-chemical properties of the gel and its environment.
The balance of the forces acting on the sample, including mixing forces, elastic forces, interfacial tension and mechanic loads, governs the behaviour of a gel.

$$F_{mix} + F_{el} + F_{int} + F_{mech} = 0 \qquad \textbf{[1.48]}$$

A variety of expressions for each of these forces can be found in literature. The most frequently used have been reviewed in this chapter. Flory's mean field lattice theory and de Gennes' scaling approach have the most merit. They also inspired the more recent work that mainly consists in refinement and extension of the fundamental theories.

Generally, gel swelling is determined by the topological characteristics of the network and by the affinity between gel and solvent. The ability to swell is strongly improved when ions are incorporated in the network (polyelectrolyte gel). Special attention was given to the case of a gel in a linear polymer solution. Depending on the interactions between network and solvent, gels undergo swell/shrink transitions that may be continuous or discontinuous, as was discussed for some particular cases.
The elastic properties were discussed as well. They strongly depend on the extent of chain stretching, and thus on the degree of swelling. At low degree of swelling, the elastic modulus decreases with increasing degree of swelling. The slope of the decreasing curve depends on the nature of the system. At higher degrees of swelling, the limits of chain extensibility are reached and the modulus increases steeply with increasing degree of swelling. Finally, methods to measure the discussed gel properties have been evaluated.

It has become clear from this chapter that a variety of components can be incorporated in a gel. This makes them prosperous for vectoring applications. Yet, mechanical ways to trigger release of active compounds have not been explored in literature. This is a missing link for the implementation of gels in cosmetic or pharmaceutic formulations to be applied on the skin. Such products are mainly compressed and sheared by the user. Would it be possible to liberate active substances from a gel by mechanical action? Moreover, the deformations induced by rubbing are large whereas most studies on gel deformation are restricted to small deformations. What will happen when a highly swollen gel is largely deformed? Finally, a gel in a practical formulation will be in contact with other components, mostly oil in cosmetic formulations, or with open air when applied, and not with its own solvent, as is often the case in available literature. How will the contact with a foreign medium affect gel behaviour?
All the practical factors summed up here need to be considered seriously if aiming to implement hydrogels in product formulations. The purpose of our investigation is to provide some answers to the question raised above.

Therefore, following systems will be studied:

- gel particles swollen with a linear polymer solution immersed in silicone oil and submitted to simple shear flow (Chapter 3 and Chapter 4);
- gel disks swollen with water or with a linear polymer solution under compression in open air (Chapter 5).

All aspects of the systems will be studied, but release phenomena will be emphasised because of their practical interest.

The choice of the materials and a description of the experimental methods used for this purpose make up the subject of the next chapter.

Résumé du Chapitre 2

Matériaux et méthodes expérimentales

Ce chapitre décrit les produits, les dispositifs et les méthodes expérimentales utilisés pour ce travail. Un ensemble d'ingrédients modèles a été conçu afin d'étudier les possibilités d'application des hydrogels comme porteur d'agent actif dans des formulations cosmétiques. Le système est composé d'un gel polyélectrolytique de poly(acrylate de Na-*co*-acide acrylique) gonflé avec une solution d'un polymère linéaire (l'hydroxypropylcellulose) à différentes concentrations. Il n'y a pas d'interactions spécifiques entre le polymère linéaire et le polymère formant le réseau du gel qui pourraient influencer les propriétés de relargage. Les gels gonflés ont été étudiés sous forme de microparticules suspendues dans de l'huile silicone ou sous forme de disque exposé à l'air libre. Les particules étaient de type Aqua Keep 10 SH-NF de Kobo Products Inc. Les disques ont été synthétisés dans notre laboratoire.

Deux types de tests mécaniques ont été utilisés: le cisaillement simple et la compression uniaxiale. Les dispositifs expérimentaux pour ces deux types de sollicitation combinent l'essai mécanique avec une observation visuelle. Cette combinaison permet de visualiser le comportement d'un échantillon lorsque celui-ci est soumis à un effort mécanique. Les observations sont enregistrées en temps réel.
Les essais en cisaillement ont été effectués avec un rhéomètre contrarotatif transparent (Figure 2.10). Cet outil est composé de deux plateaux transparents qui tournent en sens opposé et à des vitesses indépendantes. A une certaine hauteur entre les deux plateaux, la vitesse relative par rapport au repère du laboratoire est nulle (Figure 2.11). Un objet se trouvant à cette hauteur est donc immobile, tout en étant cisaillé, et son comportement peut alors être observé en temps réel et sans interruption.
Pour les essais en compression, nous avons utilisé un rhéomètre de type RMS 800 en mode compressif (Figure 2.12). Un disque de gel placé sur le plateau inférieur est comprimé lorsque le plateau supérieur descend. La force normale exercée sur le piston est enregistrée et la déformation du gel et le relargage du solvant sont enregistrés par une caméra placée devant le dispositif.

Le degré de gonflement des différents gels dans les solvants utilisés et la tension interfaciale entre les solvants et la matrice ont été déterminés.

Chapter 2

Materials, experimental methods and sample characterisation

This chapter is devoted to the presentation of the materials used in this study on the one hand, and the experimental methods on the other hand. Highly swollen gels were submitted to the mechanical actions of shear and compression. The nature of the experiments requires some specific properties of the used materials. The needs will be identified and it will be shown how the selected materials meet these requirements.

2.1 Materials

Since the aim of this thesis was to study the behaviour of highly swollen gels containing linear polymer solutions submitted to mechanical stress, the samples will contain at least two components: a swelling network and a polymer solution. Shear experiments were performed with spherical gel beads in suspension, which introduces a third component into the experimental system: the suspending oil. Compression experiments were done with homemade gels in open air. Diagrams representing how the samples are organised in both types of experiments are given in Figure 2.1.

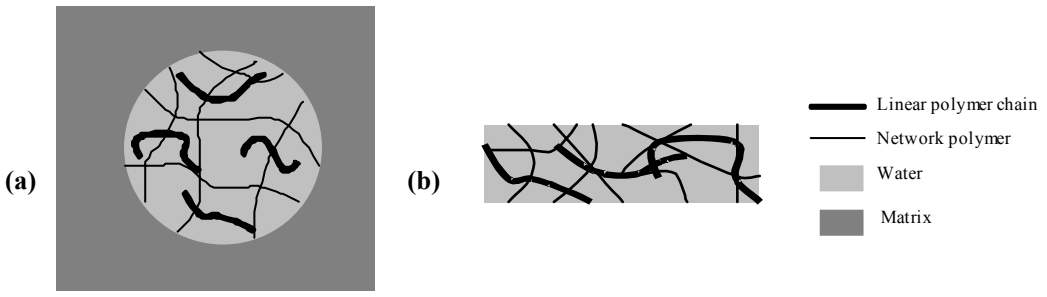

Figure 2.1: Schematic representation of the material system used in both types of experiments. (a) particles suspended in oil for shear experiments; (b) disks for compression experiments.

All constituents of the samples used in this thesis will be presented as well as relevant physico-chemical interactions.

2.1.1 Hydrogels

For the shear experiments, commercially available spherical beads of a chemically crosslinked polyelectrolyte network with high swelling capacity were used. These beads were unpractical to use in the compression experiments because of their small size and round shape. Therefore, we synthesised cylindrical gels of approximately the same composition.

2.1.1.1 Commercial gels: Aqua Keep 10SH-NF

Commercial grade gel particles of type Aqua Keep 10SH-NF from Kobo products Inc. were used. They are supplied as dry white particles that are mostly spherical. Their initial diameter ranges between 5 µm and ~ 60 µm.
Each bead is composed of a tri-dimensional copolymer network of poly(sodium acrylate) (NaPA) and poly(acrylic acid) (PAA) as schematised in Figure 2.2. The strands are chemically crosslinked with *N*,*N'*-methylene bisacrylamide (BIS). Supplier's data specify '75 % neutralised', meaning this network has a considerable amount of ionisable groups giving it a high affinity for polar solvents. When it makes contact with, e.g., water, the beads trap the water and will not release it spontaneously. Its applications as superabsorbent include hygiene products and horticulture (Aqua Keep, supplier's data).

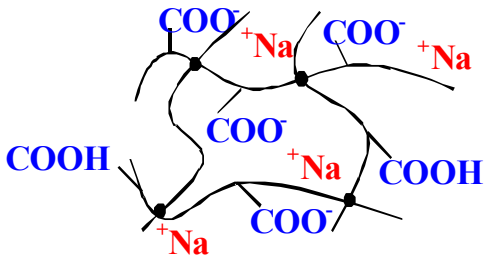

Figure 2.2: Schematic drawing of chemically crosslinked poly(sodium acrylate-*co*-acrylic acid)

2.1.1.1.1 Chemical composition and characterisation

As mentioned before, compression experiments were performed on home-synthesised cylindrical gels. It was attempted to synthesise gels that are physico-chemically identical to Aqua Keep. Most precise knowledge of the composition of Aqua Keep, in particular of the cross-link density, is therefore necessary. Element analysis (Service Central d'Analyse, CNRS, Vernaison, France; Institute of Macromolecular Compounds, St. Petersburg, Russia) and NMR analysis (Université du Maine), did not manage to fully characterise the powder because of the low amount of cross-linking agent. The (incomplete) results of element analysis were used to estimate the degree of crosslinking.

Table 2.1 gives the results of the element analysis of Aqua Keep 10SH-NF powder by the Service Central d'Analyse of the CNRS. Three components can be distinguished in the network: acrylic acid segments (-C_2H_3COOH-), sodium acrylate segments (-C_2H_3COONa-) and cross-linker molecules *N*,*N'*-methylene bisacrylamide ($C_7H_{10}N_2O_2$). The element composition of the network components is detailed in Table 2.2. Resolution of a system of elementary mass balances should now enable complete characterisation of the network. The goal is to determine the concentration of the cross-linking agent BIS.

Table 2.1: Results of element analysis of Aqua Keep 10SH-NF

	[C]	[Na]	[N]
wt%	35,22	18,03	<0,10

$\Rightarrow \Sigma \leq 53{,}35\ \%$ $\Rightarrow [O] + [H] = 46{,}65\ \%$ **[2.1]**

Table 2.2: Element composition of Aqua Keep 10SH-NF network components. The molecular weight of each element is shown between brackets.

Number of atoms:	C (12,01)	O (15,999)	H (1,01)	Na (22,99)	N (14,01)	M_w (g/mol)
AA-segment	3	2	4	-	-	72,07
NaA-segment	3	2	3	1	-	94,05
BIS	7	2	10	-	2	154,19

The mass concentration (wt%) of a product P or element E is symbolised by square brackets. $M_w(P)$ indicates the molar mass of product P. Element balances are written according to [2.2].

$$[\mathrm{E}] = \text{wt\% of element E} = \frac{\text{mass of E}}{\text{total mass}} = \sum_i \frac{\text{wt\% of E in } P_i \times \text{ mass of } P_i}{\text{total mass}} \qquad \textbf{[2.2]}$$

The unknowns of the system are [AA], [NaA], [BIS], [O] and [H].
Many equations may be written out (Table 2.3), but only three of the unknowns are interesting ([AA], [NaA] and [BIS]). A system of three equations with these three unknowns has thus to be selected.

Table 2.3: Mass balances for Aqua Keep 10SH-NF

(a)	$100 = [AA] + [NaA] + [BIS]$	→ total product balance
(b)	$100 = [C] + [H] + [O] + [N] + [Na]$	→ total element balance
(c)	$[N] = M_w(N)\frac{2}{M_w(BIS)}[BIS]$	→ balance for N
(d)	$[Na] = \frac{M_w(Na)}{M_w(NaA)}[NaA]$	→ balance for Na
(e)	$[O] = M_w(O)\left[\frac{2}{M_w(AA)}[AA] + \frac{2}{M_w(NaA)}[NaA] + \frac{2}{M_w(BIS)}[BIS]\right]$	→ balance for O
(f)	$[H] = M_w(H)\left[\frac{4}{M_w(AA)}[AA] + \frac{3}{M_w(NaA)}[NaA] + \frac{10}{M_w(BIS)}[BIS]\right]$	→ balance for H
(g)	$[C] = M_w(C)\left[\frac{3}{M_w(AA)}[AA] + \frac{3}{M_w(NaA)}[NaA] + \frac{7}{M_w(BIS)}[BIS]\right]$	→ balance for C

Method 1:
Equation (c) should better not be used, since it is based on the knowledge of [N], which is only described by an inequality (Table 2.1). Equations (e) and (f) should also be avoided, since they introduce a supplementary unknown [O] or [H], respectively. The best system to use consists of equations (a), (d) and (g).

Setting [AA] = x, [NaA] = y and [BIS] = z gives following system:

$$\begin{cases} 100 = x + y + z & \text{(a)} \\ 18{,}03 = 0{,}24y & \text{(d)} \\ 35{,}22 = 12{,}01\left[\frac{3}{72{,}07}x + \frac{3}{94{,}05}y + \frac{7}{154{,}19}z\right] & \text{(g)} \end{cases}$$

from (d) follows : **y = 73, 76 = [NaA]** $\Rightarrow$ [AA] + [BIS] = 26,24

The calculated degree of neutralisation is close to the 75 % specified by the supplier. This is a good result. However, a negative value for z is found: z = -176,67, meaning there would be phantom material in the system. This is not possible and thus we cannot continue our calculations with these results. Consequently, the BIS concentration cannot be deduced from the system of equations chosen.

Method 2:
Another method consists in using the badly defined [N] and solving the system (a), (c), (d). For the resolution of this system [N] is taken 0,10.

This gives:
(d) => y = 73,76 (a) => x + z = 26,24 **[2.3]**

(c) => $z = \frac{[N]*M(\text{crosslinker})}{2M(N)} = \frac{0{,}10*154{,}19}{2*14{,}01}$ => z = 0,55

Note that in reality [N] < 0,10 and thus z < 0,55

(a) => x = 100 – y – z x = 25,69

Note that in reality this equation should give rise to an inequality: x > 25,69
combined with the fact that z > 0, we can also write : 100 – y > x,
which gives x < 26,24 $\Rightarrow$ 25,69 < x < 26,24

Solution: **25,69 < [AA] < 26,24**

[NaA] = 73,76 **[2.4]**

[BIS] < 0,55

For more precise determination of the concentrations of crosslinker and polyacrylic acid, the values of [AA] and [BIS] were varied between their minimum and maximum values, always keeping in mind that the sum must fulfil => x + z = 26,24 **[2.3]**. Using [NaA] = 73,76, the sum ([O] + [H]) is calculated for each combination of [AA] and [BIS]. The last column in the table indicates whether this sum fulfils **[2.1]** in Table 2.1. The calculations are summarised in Table 2.4.

Table 2.4: Variation of [AA] and [BIS] and calculated O- and H-concentrations

[AA]	[BIS] = 26,24 – [AA]	[O]	[H]	Σ ([O] + [H])	= 46, 65 ?
26,14	0,10	36,72	3,84	40,56	No
26,0	0,24	36,69	3,84	40,53	No
25,94	0,30	36,68	3,85	40,53	No
25,69	0,55	36,62	3,85	40,47	No

From this table, it has become clear that no correct solution can be found by varying [NaA] and [BIS]. There is always 6 wt% of material missing. This might be due to some absorbed air humidity present in the sample that interfered with the element analysis. The deficit should then only consider H and O molecules.

Conclusion:
The results of element analysis do not enable better determination of the composition of Aqua Keep 10SH-NF than by the specification '75% neutralised'. A positive point is that [NaA] and thus the degree of neutralisation is defined exactly by [Na], but the crosslinking degree, following directly from [N], is not determined.
We will consider the degree of cross-linking intermediate between the extremes of solution **[2.4]**, i.e. 0,33 mol% of the amount of monomer. This means the number of monomers per strand is about 150. This value will be used in the recipe for gel synthesis.

2.1.1.2 Synthesised gels

To enable a certain degree of comparison between shear and compression experiments, the compressed samples should be of similar physico-chemical composition as Aqua Keep. We aimed to prepare cylindrical poly(sodium acrylate-*co*-acrylic acid) gels that are completely transparent (sign of homogeneity) and with an equilibrium degree of swelling in water close to that of Aqua Keep. The results of the calculations made in 2.1.1.1.1 were used to determine the formulation.

2.1.1.2.1 Synthesis procedure

The gels were synthesised following the procedure described by Horkay et al. (2000). Poly (sodium acrylate-*co*-acrylic acid) gels were synthesised by free-radical copolymerisation of partially neutralised acrylic acid (AA) crosslinked with *N*,*N*′-methylenebisacrylamide (BIS) in a ratio of 300 mol to 1. 75 % of the monomers were neutralised by sodium hydroxide (NaOH). The monomer concentration in the initial mixture was 25 % (w/w). The formulation is given in Table 2.5.

Table 2.5: Composition of the reaction mixture for gel synthesis

Component	Mass (g)	# moles (mol)	mol % of monomer amount
Acrylic acid monomer	5,000	$6{,}939.10^{-2}$	100,0
N,*N*′-methylenebisacrylamide	0,0357	$2{,}316.10^{-4}$	0,3338
Sodium hydroxide	2,0800	$5{,}200.10^{-2}$	74,94
N,*N*,*N*′,*N*′-tetramethylenediamine	0,0081	$6{,}971.10^{-5}$	0,1005
Ammonium persulfate	0,0158	$6{,}924.10^{-5}$	0,09978
Demineralised water	15,000	$8{,}324.10^{-1}$	300,0

Figure 2.3 shows how the free radical polymerisation reaction proceeds. As shows the figure, the initiator molecule is incorporated in the reaction product and will therefore affect end properties.
In our case, the propagation step consists of linking a monomer molecule to the reacting chain (chain polymerisation) or linking a crosslinker molecule to the chain (crosslinking). Both take place at the same time with a probability (initially) of $n_{monomer}/(n_{monomer}+ n_{crosslinker})$ to link a monomer and $n_{crosslinker}/(n_{monomer}+ n_{crosslinker})$ to incorporate a crosslinker molecule. This supposes similar reactivity of both types of molecules (ideally equal reactivity), otherwise the resulting network will not be uniform.

However, the reactivity of a chain changes continuously as chains of different length are formed (Osada, 2001; Okuzaki, 2001).

(a) Initiation: formation of free radicals ($R^{\bullet}$) out of initiator molecules (I) and activation of monomers by interaction with free radicals

$I \rightarrow 2R^{\bullet}$

$M + R^{\bullet} \rightarrow RM^{\bullet}$

(b) Propagation: chain polymerisation

$RM^{\bullet} + nM \rightarrow RM_{n+1}^{\bullet}$

(c) Chain termination: two activated chains combine to form a polymer chain P

$RM_{n+1}^{\bullet} + RM_{n}^{\bullet} \rightarrow P$

(d) Removal of free radicals

$R^{\bullet}$ + poison, … $\rightarrow$ S

Figure 2.3: Free radical polymerisation: reaction scheme

The preparation went as follows: 5 g of chain monomer was diluted in 10 g of water and mixed with an appropriate amount of NaOH to neutralise 75 % of the monomer. The neutralisation is carried out before the crosslinking reaction because of the better solubility characteristics of polymerised sodium acrylate compared to polymerised acrylic acid. Good dissolution of the polymer favours the formation of a more homogeneous gel. Because of the slow dissolution of BIS in an acrylic monomer solution, the crosslinker monomer was entirely diluted in another 5 g of water before being added to the network monomer solution. Note that crosslinking and polymerisation reactions take place at the same time. Dissolution and mixing are optimised using a magnetic stirrer to obtain homogeneous mixtures. All the water is demineralised and has been boiled prior to use in order to limit its oxygen content (oxygen is poison for free radicals (Okuzaki, 2001)). *N,N,N',N'*-tetramethylenediamine (TEMED) was added as a conditioner, pH was 5,22. The solution was degassed by bubbling nitrogen through it. At the very end, ammonium persulfate (APS) was added to initiate the reaction.
The reacting mixture was then gently poured into cylindrical glass vessels (0,7 cm diameter) with a syringe to avoid entrapment of air bubbles. However, this transfusing has to be done quickly since the reaction initiates immediately after addition of APS to the mixture. The vessels were put in a stove at 40 °C and in inert (nitrogen) atmosphere for 1h. The gels were allowed to set at room temperature for another 24h. Gel cylinders were removed from the moulds and washed in excess of demineralised water during 2 weeks while refreshing the water daily, in order to remove unreacted monomer. The gels were stored in demineralised water at room temperature prior to use.

2.1.1.2.2 Characterisation of synthesised gels

The resulting cylinders were completely transparent, indicating a homogeneous composition (Figure 2.4). They show some surface defects, which do not cause problems since disks will be cut out of the cylinders from the smooth sections.
Supposing the network is homogeneous, one can calculate the crosslinking density and the strand length straightforward from the composition of the reaction mixture. An average strand is composed

of 150 monomers and the crosslink density is $3{,}3.10^{-3}$ (one crosslinker molecule for 300 chain monomers).

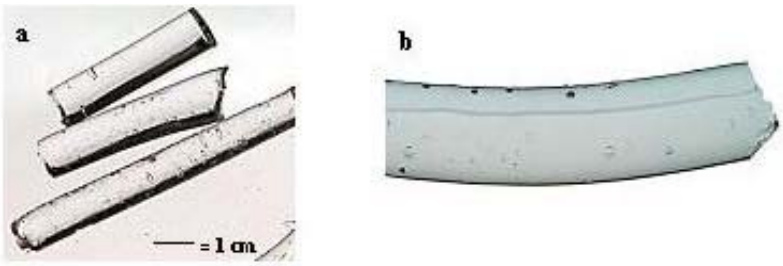

Figure 2.4: Results of gel synthesis: a) after preparation; b) fully swollen in water.

This gel has an equilibrium degree of swelling in demineralised water of 200 ± 20 g/g (see section 2.4.1.4). Gels with higher degrees of swelling, closer to that of Aqua Keep were also prepared, yet they were very inhomogeneous and the mechanical properties varied too much within the sample. Since optimising the gel synthesis procedure goes beyond the aim of this thesis, the described gel (with lower Q_{eq} than Aqua Keep) was chosen as a compromise.

2.1.2 Linear polymer solutions: hydroxypropylcellulose in water

The practical aim of this work is to study whether a gel could serve as a container for active compounds in cosmetic formulations. The active compound is represented by a linear polymer. The gels are thus swollen with a solution of this linear polymer. The main requirement for the model polymer is that it has to be soluble in water and compatible with the network polymer. The linear polymer chosen was hydroxypropylcellulose (HPC). Aqueous solutions of this polymer can penetrate into an Aqua Keep network without any chemical reaction taking place. Budtova and Navard (1995) showed that hydroxypropylcellulose does not form complexes with a Na-PAA network, neither does one component destroy the other. Its applications cover food, personal care and pharmacological products as a thickener or as a matrix for tablets. All this makes HPC a suitable polymer for this study.

2.1.2.1 General information

The HPC (Figure 2.5) used in this work was KLUCEL grade E provided by Aqualon. The molecular weight is 60 000. Hydroxypropylcellulose is soluble in water at temperatures below 45 °C. Because of its amphiphilic character, it also has an affinity for organic liquids. It is a hydrophilic-lipophilic material (Aqualon). This implies that its presence lowers the interfacial tension between water and oil.

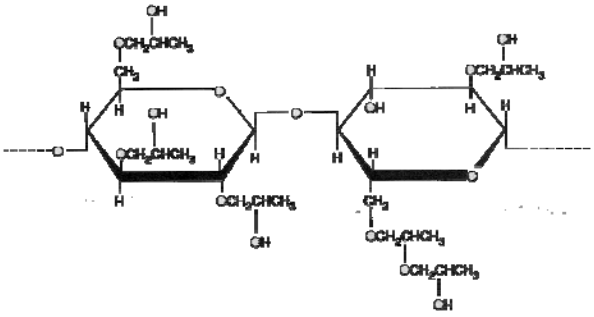

Figure 2.5: Theoretical structure of hydroxypropylcellulose [From Aqualon, Klucel]

2.1.2.2 Preparation of aqueous HPC-solutions

First, HPC-powder was dried during 24 hours in a vacuum oven at 80 °C. This was necessary because HPC powder absorbs atmospheric humidity, which would falsify solution concentrations. To prepare the solutions, demineralised water and HPC powder were mixed gently with a spatula for almost 10 minutes and were then stored in a refrigerator. They were mixed another time to homogenise and were then set to rest during 5 days. Finally, the solutions were centrifuged to eliminate entrapped air bubbles. The fluids were stored in a refrigerator in air-tight containers to avoid water evaporation.
Solutions of 1 %, 5 % and 10 % by weight were used in this study.

2.1.2.3 Physical characterisation

A calibration curve for the refractive index n_D as a function of HPC concentration is given in Figure 2.6a. The refractive indices were measured with an ausJENA Abbe refractometer. n_D increases linearly with concentration and can be fitted by a straight line with slope 0,0016. This calibration will be used to verify the concentrations of the solutions after preparation and storage or to identify a released solution.
Figure 2.6b shows the density for the used solutions measured with a standard picnometer.

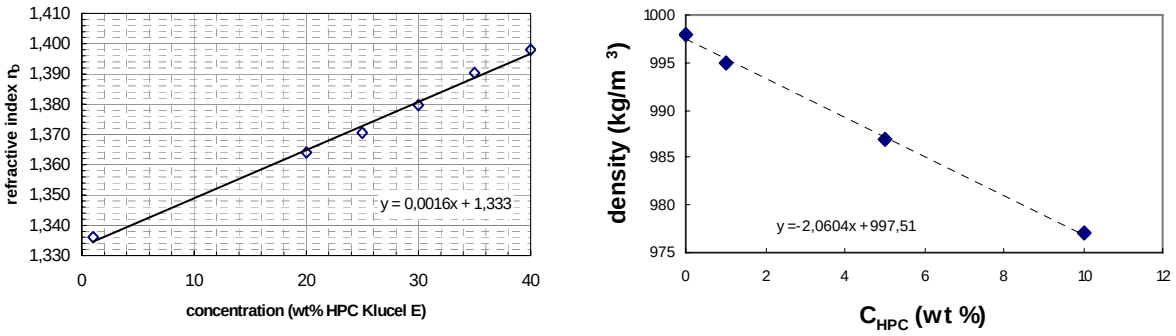

Figure 2.6: Properties of HPC type E solutions (a) Refractive index; (b) Density

2.1.2.4 Rheological characterisation

The HPC solutions were characterised rheologically with a Stresstech rheometer from Rheologica Instruments under continuous and dynamic regime at 21 °C. The 10 % solution was measured with plate-plate geometry while a double wall cylinder was used for the 1 % and 5 % solutions. Figure 2.7 shows the viscosity η of the HPC solutions in the range of shear rates used in our experiments with the counter rotating apparatus. All selected solutions are Newtonian in this range of shear rates.
The dynamic moduli are also shown for as far as they could be measured.

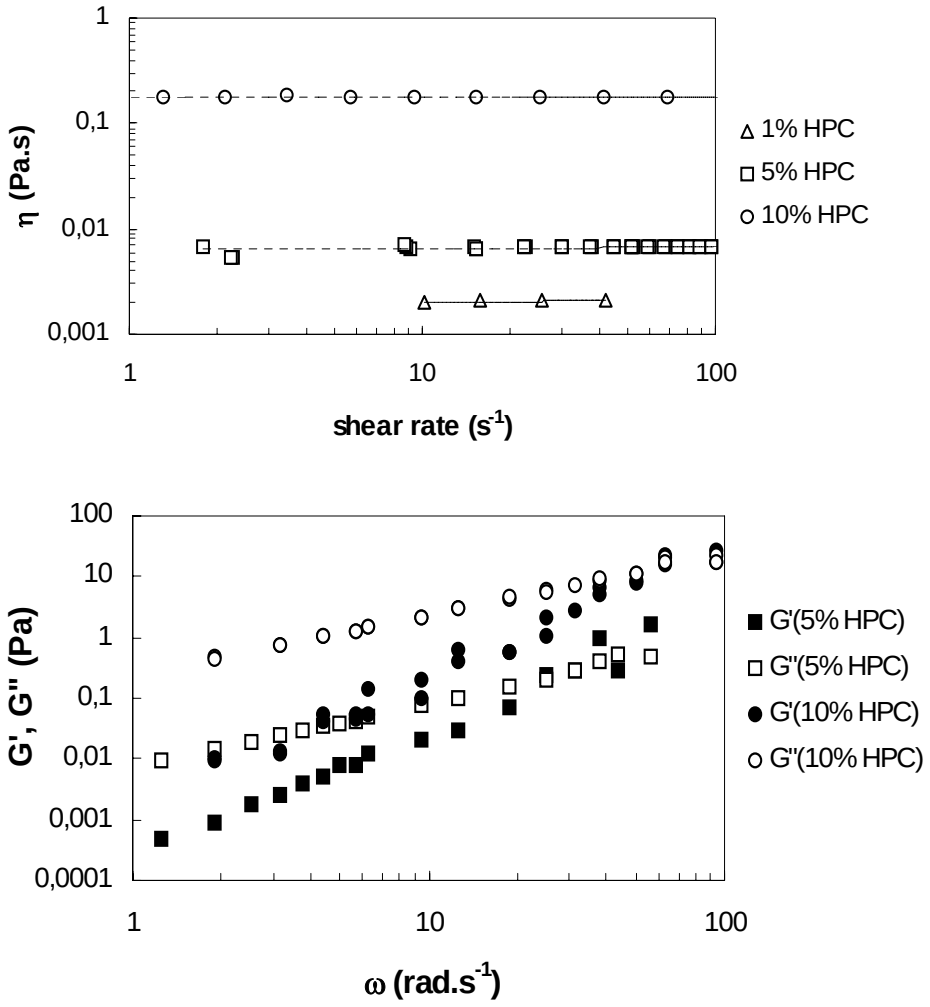

Figure 2.7: Rheological characterisation of HPC solutions of different concentration at 21 °C. Lines in the viscosity graph indicate Newtonian fits.

2.1.3 Preparation of swollen gels

In order to prepare gels swollen to a desired degree of swelling and to quantify the linear polymer concentration inside the gel, the following procedure was followed. A known amount of dry gel powder M_{dry}, was mixed with an amount of solvent $M_{solvent}$. The quantity of solvent was taken such that the gel reaches the desired degree of swelling by complete absorption of the added solvent. Powder and solvent were mixed gently with a spatula to distribute the powder homogeneously in the solution. The mixture was then set to rest to allow complete penetration of the polymer solution into

the gel. All swollen gels were prepared at least 24h prior to use. The degrees of swelling chosen were lower than the equilibrium degree of swelling. The gel will absorb everything and one can thus be sure that no solvent is left freely around the particles. For one solvent, also gel particles swollen at equilibrium were used. They were also prepared following the procedure described above. The equilibrium degree of swelling was determined in a separate experiment (2.4.1).

This preparation method has two advantages. First, the degree of swelling is well defined and second, the linear polymer concentration inside the gel corresponds to the concentration in the solution added to the gel. The composition of a swollen gel particle is thus completely defined.

The swollen particles are spherical with diameters varying from 80 μm to 200 μm. Only particles smaller than 150 μm were selected for the shear experiments to avoid wall effects.

The homemade cylindrical gels were used at $Q_{eq.}$ Gels swollen with water could be used as they came out of the washing procedure. To swell the gels with another solvent, the water has to be evacuated first. Pieces of gel were dried until they reached a constant weight. The drying must be done in two steps to avoid high stresses between the already dry surface and the still swollen core, which would cause cracks in the surface. Hence, the gel was first dried in open air at room temperature. To evaporate the very last humidity, the gels were put in an oven at 40 °C and weighed regularly until mass stabilisation. A dried disk of known mass was immersed in excess solvent and was allowed to swell for at least 24h. The disk was taken out of the solution just before use. Excess solution was gently wiped off with absorbing tissue and the weight of the disk was determined. Knowing the mass of the dry disk, the degree of swelling could easily be calculated.

2.1.4 Matrix fluids: Silicone oil

An absolute requirement for rheo-optical observations is the transparency of the suspending fluid. A good contrast with the suspended particles and released solvent is also needed. Further, the matrix should be inert with respect to the swollen gel particles: it should not be absorbed by the gel neither extract nor mix with its solvent. In the present case, this means the matrix has to be hydrophobic. It has to be liquid at ambient conditions. Densities should be similar to prevent buoyancy. Finally, it has to be sufficiently viscous to cause shear stresses high enough to deform the gel particles.
Two supplementary requirements are imposed by the disposition of the experimental apparatus: non-volatility and non-toxicity.

It was decided upon silicone oils, polydimethylsiloxane (PDMS). These are flexible macromolecules composed of silicium, carbon and oxygen, whose formula is shown in Figure 2.8. We used commercial silicone oils of brand Rhodorsil from Rhône-Poulenc. Three grades differing by their viscosity were used: 47 V 100 000, 47 V 200 000 and 47 V 1 000 000. They are referred to as PDMS 100, PDMS 200 and PDMS 1000, respectively.

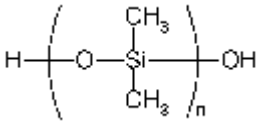

Figure 2.8: Polydimethylsiloxane

These oils meet all requirements (Carette and Pouchol, 1996; Rhodorsil, 1996). The density at 25 °C is about 973 kg/m^3, the refractive index is 1,404 and the surface tension 21,1 mN/m (Rhodorsil technical data, 1996).

2.1.4.1 Rheological characterisation

The oils were characterised with a Stresstech rheometer using cone and plate geometry at continuous and dynamic regimes in the range of shear rates used in the counter-rotating experiments. PDMS 100 and PDMS 200 show a constant viscosity plateau for shear rates up to ~10 s^{-1}. PDMS 1000 is shear thinning at shear rates above 0,3 s^{-1}. The viscosities can be fitted with an Ellis law (equation [2.5]).

$$\eta = \frac{A}{1 + K\dot{\gamma}^n} \qquad \textbf{[2.5]}$$

with A, K and n adjustable parameters. Table 2.6 gives the fitted parameter values for the different PDMS's used. This equation will be used to calculate the viscosity at the shear rates used during our experiments.

Table 2.6: Ellis law parameters for different PDMS's at 21 °C

Rhodorsil type	A (Pa.s)	K (s^n)	n (-)
47 V 100 000	106	2.35.10^{-3}	1,70
47 V 200 000	217	2,58.10^{-4}	2,52
47 V 1 000 000	963	0,198	1,18

The first normal stress difference N_1 is weak for PDMS 100 and for PDMS 200 in the experimental range of shear rates [0,5 – 20 s^{-1}], but is more pronounced for PDMS 1000.
The dynamic modulus plot shows that G" is always higher than G' for shear rates below 100 s^{-1}.

2.1.4.2 PDMS with emulsifier

The interfacial tension oil-gel solvent (or released fluid) was modified by adding 3 % by weight of ABIL® EM 90 to the silicone oil. ABIL® EM 90 is a commercially available emulsifier produced by Goldschmidt AG, a Degussa company, that is used for the formulation of cosmetic water-in-oil creams and lotions. It is composed of modified polyether-polysiloxane chains.

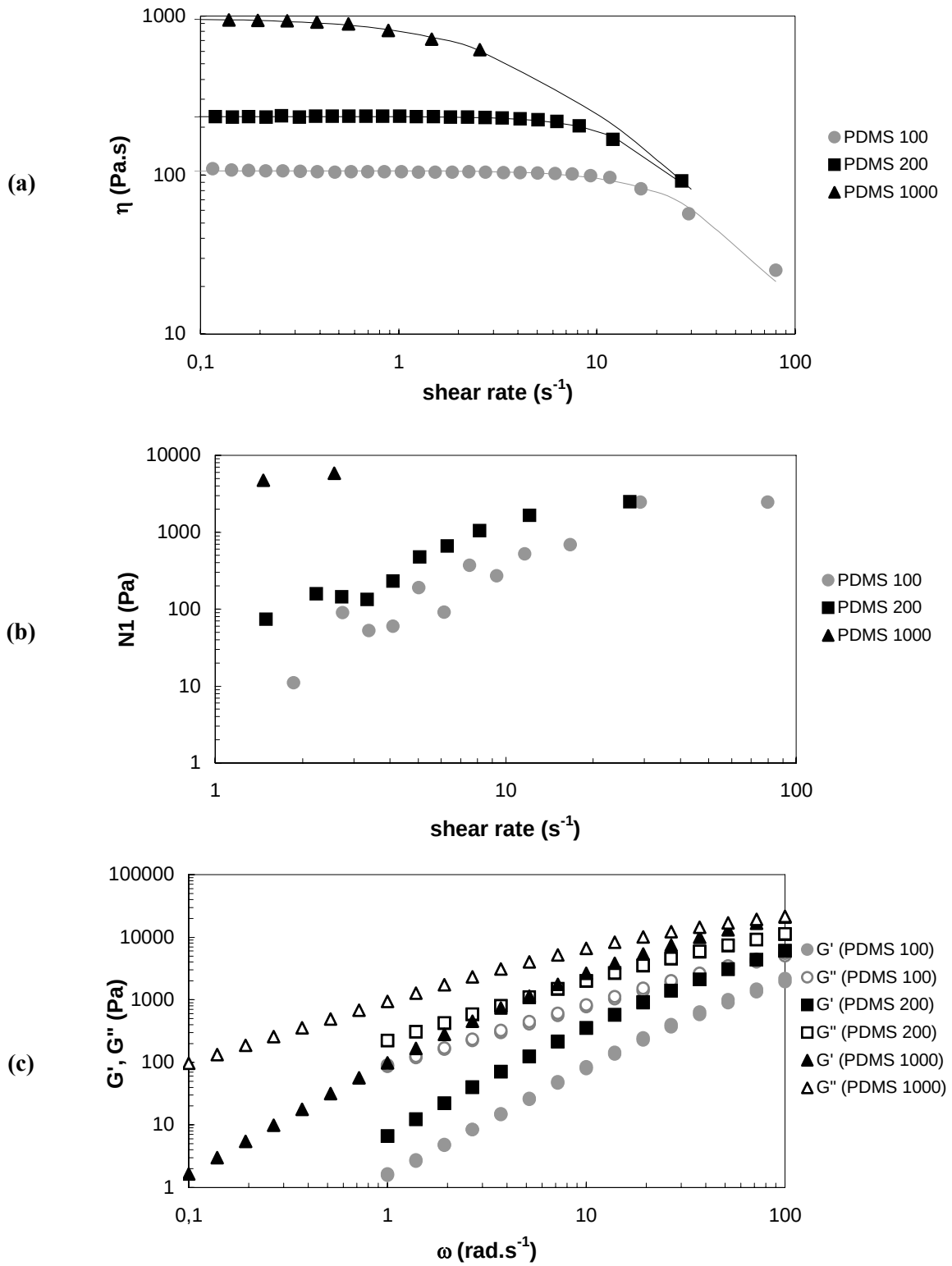

Figure 2.9: Rheological characterisation of different PDMS's at 21 °C. (a) viscosity; (b) first normal stress difference; (c) dynamic moduli. Dots represent measured data; full lines in viscosity plot are Ellis-law fits.

2.1.5 Total experimental material system

Since one of the purposes of this study is to investigate the possibility of using hydrogels as containers for active compounds, the samples are clearly multi-component. For each component, a model substance was selected and described in this paragraph. The requirements for the components and the selected substances are summarised in Table 2.7. The hydrogel was used in two different forms adapted to the mechanical tests: beads suspended in oil for shear experiments and disks for compression experiments. The gel beads were used at different degrees of swelling and the particles selected for experiments had initial diameters between 90 and 150 µm. The disks were used at equilibrium degree of swelling. Monitoring the diameter of a swollen gel particle suspended in oil at rest for several hours confirmed that the linear polymer solution did not drain out of the particle into the oil spontaneously within the duration of an experiment. Table 2.8 gives an overview of all gel-solvent combinations and degrees of swelling selected for the experiments.

Table 2.7: Requirements and material choices

Product	Requirements	Choice	Remarks
Network polymer	Superabsorbent	75-25 poly(NaA-*co*-AA)	Polyelectrolyte
Linear polymer solution	Soluble in water Compatible with network No interactions	Hydroxypropylcellulose 1 %, 5 % and 10 % solutions	Hydrophilic–lipophilic
Suspending fluid	Transparent Inert Viscous Contrast with other components	Silicone oils with various viscosities	Hydrophobic

Table 2.8: Overview of gel –solvent combinations used in shear and compression experiments.

Solvent	Q_{eq} (g/g)	Q (g/g) used
	Aqua Keep gel beads:	
1 % HPC	320	80
5 % HPC	210	80, 160, 210
10 % HPC	200	80
:	*Homemade gel disk*	
Water	200	200
5 % HPC	130	130

2.2 Experimental devices

The effect of a mechanical action on hydrogels was studied in this work. The applied actions were shear and compression. The devices used to realise these actions are described in this paragraph. In each type of experiment, visual observations were combined with mechanical testing.

2.2.1 Transparent counter-rotating shear cell

Rheo-optical systems consist of a means of observation (visible light, laser light,…) and a flow-inducing device. The combination of both adds the great advantage that flow-induced structural and morphology changes can be visualised. The counter-rotating device used in this work combines simple shear flow with optical microscopy.

2.2.1.1 Description

The counter rotating rheo-optical apparatus, shown in Figure 2.10 was developed in CEMEF (Seyvet, 1999; Astruc, 2001). Its geometry consists of two parallel transparent plates which rotation can be controlled independently. The diameter of the upper plate is 40 mm but the lower one is much larger. The gap between the plates has to be set manually after loading the sample. The gap width varied between 400 and 600 µm in all the experiments described in chapters 3 and 4.

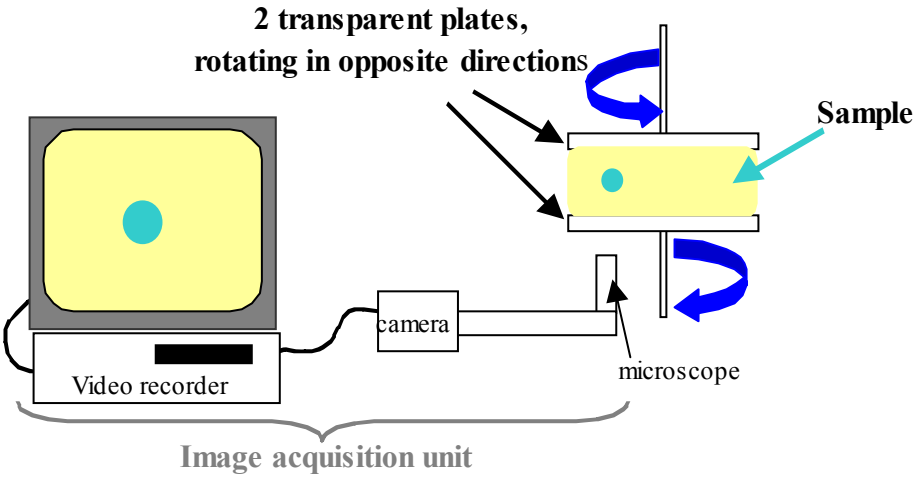

Figure 2.10: Schematic representation of the transparent counter rotating device.

Independent motors drive top and bottom plates. The angular velocities of the plates are adjusted by imposing a voltage x to the driving motor. The motors are calibrated as follows:

$$\text{Lower plate (revolutions.s}^{-1}\text{):} \quad \omega_l = 1{,}4168x + 0{,}0016$$
$$\text{Upper plate (revolutions.s}^{-1}\text{):} \quad \omega_u = 1{,}4917x \qquad \textbf{[2.6]}$$

If x is positive for ω_l and negative for ω_u, both plates turn in opposite directions. An optical microscope (from Zeiss) equipped with a camera (Sony DXC 107 AP) is placed under the shearing unit. The camera is linked to a video recorder with a monitor, in order to record the experiments. A time code is superimposed to each of the recorded images. The system takes 25 images per second.

2.2.1.2 Principle

In a counter rotating system, shear flow is generated by two plates rotating in opposite directions. With a Newtonian fluid between the plates, the resulting unperturbed flow velocity varies linearly with height between ω_l and ω_u as shown in Figure 2.11b.

The shear rate $\dot{\gamma}$ is then calculated as:

$$\dot{\gamma} = \frac{(\omega_u - \omega_l) * r}{h} \qquad [2.7]$$

with r the radial position of the particle in the flow-vorticity plane and h the gap width. Shear rates in the experiments varied between 0,5 s^{-1} and 20 s^{-1}. The exerted shear stress σ is estimated as the shear stress in unperturbed Newtonian flow:

$$\sigma = \eta(\dot{\gamma}) * \dot{\gamma} \qquad [2.8]$$

At a certain height h_0, given in equation [2.9], the velocity is zero with respect to an observer in the fixed laboratory framework. This enables to keep a particle in the field of view, although it is submitted to shear flow, and observe it for extended times.

$$h_0 = \frac{h * |\omega_l|}{(\omega_u - \omega_l)} \qquad [2.9]$$

It is important that upper and lower velocities are nearly equal during an experiment, to ensure the plane of observation at h_0 is approximately in the middle between both plates. This is to avoid the particle being too close to one of the plates and consequently, subject to wall effects.

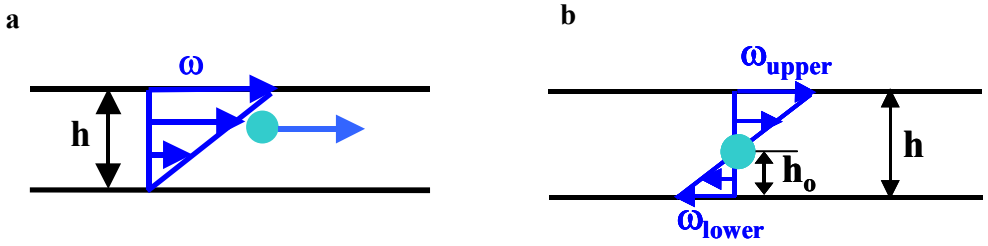

(a) set-up with 1 rotating plate **(b) counter rotating set-up**

Figure 2.11: Flow profiles in unperturbed Newtonian flow. Comparison between systems with 1 and 2 rotating plates.

Comparison of Figure 2.11a and b shows the major advantage of this system. In a system with one rotating plate, objects move with a certain speed relative to a fixed observer and can thus not be followed continuously.

2.2.1.3 Sample loading

First, an appropriate volume of the matrix fluid is applied to the bottom plate with a syringe. A small amount of swollen gel particles is dispersed in it with a needle and the whole system is let to rest for about 20' until entrapped air bubbles escaped. The plates are then approached slowly to set the desired gap and the excess of fluid, squeezed out of the system, is removed in order to proceed with clean borders.

For the experiments with droplets in a matrix, an identical procedure is followed: a small volume of dispersed phase is gently mixed with the layer of matrix fluid in order to obtain a dispersion of small droplets.

2.2.1.4 Pros and contras

The main advantage of a counter rotating system is that it enables to fix a particle under shear in the laboratory framework. This allows in-situ observations of its behaviour.
An important drawback of the present system however, is that it induces a rather large error on the calculation of the applied shear rate, especially at low velocities, as demonstrates the calculation below.

Following factors induce errors on the calculated shear rate:

- small variations of 0,01 on the voltage setting cannot be avoided. They entail errors in the velocity measurement of $\Delta\omega_l = 0{,}014168$ and $\Delta\omega_u = 0{,}01497$ rad.s^{-1};
- the radial position of the particle is determined by displacement of the microscope from the outer edge of the top plate to the location of the particle. The location is obtained by focussing the microscope on the particle and the displacement is measured on a micrometer screw. However, the observed particle does not necessarily stay in the same position. This may be due to small system defects like imperfect parallelism or concentricity. The maximum mistake Δr that can be made on the radius is estimated as the half-height of the observation window, namely 350 µm;
- the gap setting is done manually and thus susceptible to human and mechanical inaccuracy. Δh is taken 20 µm.

The square of the relative error on the applied shear rate is calculated as the sum of the squared relative errors on the different factors:

$$(\delta\dot{\gamma})^2 = \left(\frac{\Delta\dot{\gamma}}{\dot{\gamma}}\right)^2 = \frac{(\Delta\omega_l)^2 + (\Delta\omega_u)^2}{(\omega_l + \omega_u)^2} + \left(\frac{\Delta r}{r}\right)^2 + \left(\frac{\Delta h}{h}\right)^2 \qquad \textbf{[2.10]}$$

The error varies with the applied shear rate and is more important for smaller shear rates as can be seen in Table 2.9. However, a given shear rate can result from different combinations of ω_l, ω_u, r and h. Therefore, the relative error is not constant for a given shear rate.

Table 2.9: Example of errors on the calculated shear rate of the counter-rotating device for h = 400 µm.

$\dot{\gamma}\left(s^{-1}\right)$	$\omega_l + \omega_u$ (rad.s^{-1})	r (mm)	$\Delta\dot{\gamma}\left(s^{-1}\right)$	$\delta\dot{\gamma}$ (%)
1,15	0,0255	18	0,9	81
1,13	0,0566	8	0,4	37
4,22	0,0844	20	1,1	25
4,22	0,1405	12	0,7	17
10,10	0,202	20	1,2	11
10,14	0,4056	10	1,0	8

Taking the absolute average error on the matrix viscosity as $\Delta\eta = 10$ Pa.s gives a relative average error on the shear stress $\delta\sigma$ of the same order of magnitude as $\delta\dot{\gamma}$.

2.2.1.5 Conclusions

A transparent counter-rotating shear cell was presented. The main asset of such system is that objects submitted to shear can be observed in-situ. The shear stress is transferred to a microparticle by a continuous medium that is silicone oil in the present case. The presented system has one important drawback, which is the rather high error on the applied shear rate.
The counter-rotating apparatus was used for different purposes:

- study of the behaviour of swollen isolated gel particles immersed in oil,
- measurement of interfacial tension between solvent droplets and oil.

2.2.2 Compression set-up

2.2.2.1 Description

The compression device is schematically represented in Figure 2.12.

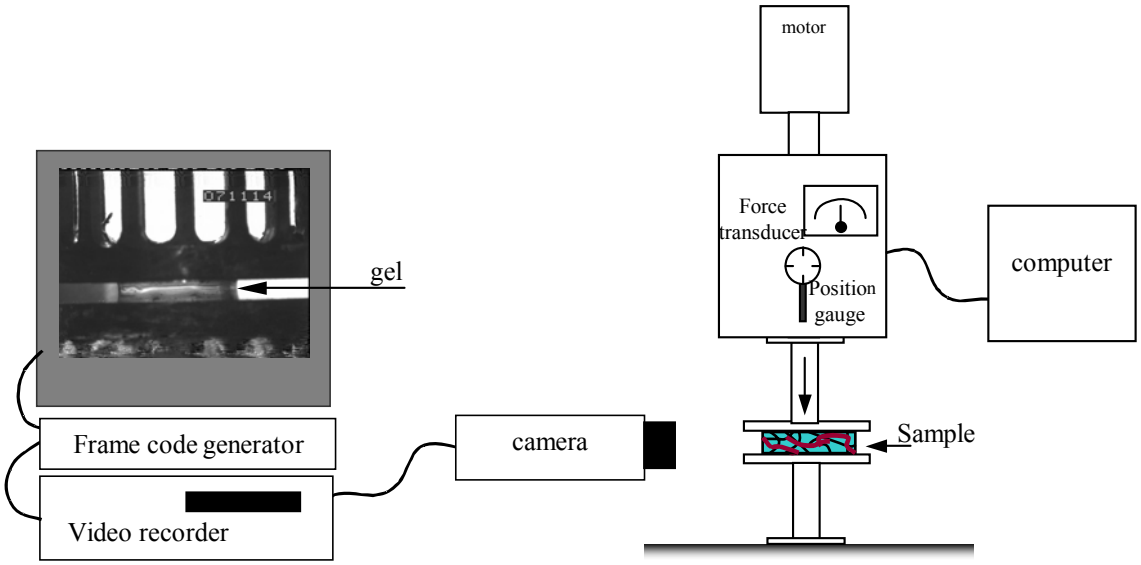

Figure 2.12: Compression set-up with RMS 800 rheometer

The gels were compressed with an RMS 800 rheometer manufactured by Rheologica. The RMS is a mechanical test system for evaluating viscoelastic properties. The system was used with horizontal parallel plate geometry where the lower plate is fixed and the upper plate moving. Both plates have smooth surfaces. This experiment is velocity-controlled: the upper plate is lowered at constant speed v during a programmed time. The cylindrical sample is placed on the lower plate.
The initial gap G_o is set manually by lowering the piston until it almost touches the cylinder surface, in a way that no normal force is recorded yet. The gap h at every moment is determined by [2.11].

$$h = G_o - v \cdot t \qquad \textbf{[2.11]}$$

A transducer continuously records the normal reaction force F_N exerted by the compressed sample. Meanwhile, a COHU black and white high performance CCD camera equipped with a macro objective

(AF micro Nikkor 105 mm from Nikkon) records the deformation of the gel disk under the piston in real time. Optical fibres placed near the sample guarantee sufficient illumination. Systematic analysis of the video frames allows quantifying the evolution of the sample diameter. Data from the rheometer and from the images are synchronised by a frame code superimposed on the images.
The error on the gap is estimated at 0,02 mm and the error on the normal force at 5.10^{-5} N. The error on the sample diameter is taken 0,2 mm.

One should note that the response of a gel to compression is often dominated by friction between the sample surface and the compressing plates (Kavanagh and Ross-Murphy, 1998). If the sample is completely incompressible (which is probably different from our case (Whiting and Voice, 2002)), uniaxial compression in the z-direction entails biaxial extension in the x-y plane. However, if the condition of good lubrication is not satisfied, friction with the plates makes the sample bulge (Figure 2.13a). Because of the wetness of the gel samples, it is considered that the lubrication condition is satisfied in our experiments. Observations of the sample during the experiments confirmed this hypothesis. The observations are schematically represented in Figure 2.13b.

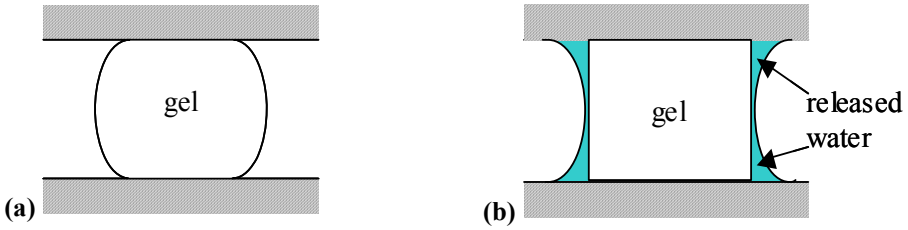

Figure 2.13: (a) Bulging due to surface friction; (b) Sliding contact

2.2.2.2 Sample preparation

Flat and homogeneous disks are required to perform a correct compression experiment. Therefore, slices were cut from a fully swollen gel cylinder and a smaller disk was cut out of it with a sharpened circular cutter, to eliminate the surface defects mentioned earlier. Each disk was characterised by its initial height, h_o, and diameter, D_o. From these two dimensions, the initial volume, V_o, was calculated. The samples were also weighed before testing. Typical initial sample dimensions were about 10 mm x 1,5 mm. The samples were conserved in excess of water to guaranty equilibrium swelling state. They were transported to the rheometer in a closed container.

2.2.2.3 Experimental conditions

Continuous compression experiments were performed in open air until rupture of the sample occurred. The sample was compressed at constant speed v = 0,001mm/s and the duration of an experiment was chosen as to compress the disk to about half of its initial height. The force exerted on the piston was recorded as a function of piston position and can be associated to a gel diameter via the time code on the images. The force increased monotonously with increasing displacement of the piston until it shut down abruptly at the rupture point. Deformation and stress at this point are defined as yield strain ε_y and yield stress σ_y.

The true normal stress σ_N is calculated as the quotient of the measured normal force and the circular disk surface that was known thanks to diameter measurements on the recorded images.

$$\sigma_N = \frac{4F_N}{\pi D^2} \quad \textbf{[2.12]}$$

The engineering strain ε_E is defined as the quotient of displacement and initial disk height.

$$\varepsilon_E = \frac{\Delta h}{h_o} \quad \textbf{[2.13]}$$

Knowledge of height and diameter at each moment also allows calculation of disk volume and volume loss at each moment.

2.3 Experiment analysis

In order to determine the dimensions of the deformed gels or droplets, the video-images were analysed with help of image analysis software VISILOG® from Noesis. The dimensions of interest were measured. For the compression experiments, these are disk height and diameter. For the shear experiments, these are length, L, and height, H, of the particle or droplet, height at the base of the released solvent tips, H_t, and total length of the particle with tips, L'. These dimensions are defined in Figure 2.14. The third dimension of the ellipsoid, width, W, cannot be seen in the used set-up.

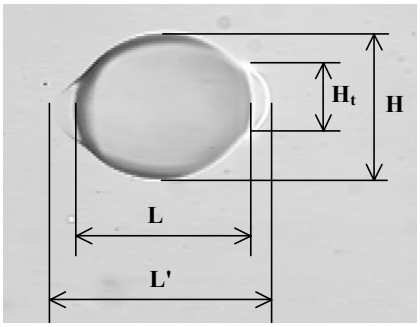

Figure 2.14: Definition of dimensions of deformed gels in shear experiments.

2.3.1 Shear experiments: note on orientation

During the experiments with the counter-rotating device, it was observed that the gel particle was not aligned to the flow direction: differences in the microscope focus of both edges indicated that a gel particle is slightly oriented under flow. This can also be seen in Figure 2.14. The deformed gel particle adopts a certain orientation ϑ with respect to the flow direction, as illustrates the scheme in Figure 2.15. Hence, the length measured on the monitor (parallel to the flow direction) is a projection L_p and the real length L is thus given by $L_p/\cos\vartheta$.

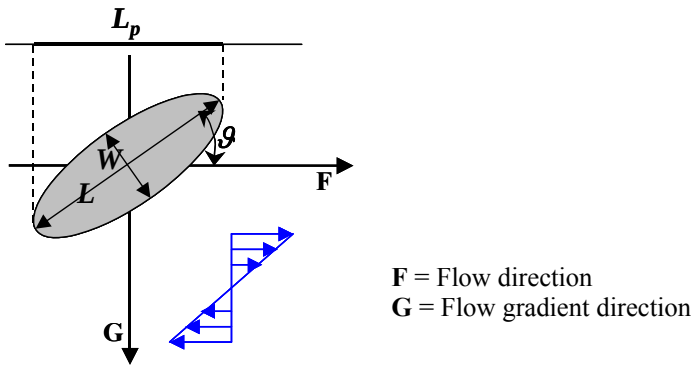

Figure 2.15: Gel particle orientation under simple shear flow in a plane perpendicular to the vorticity axis.

The orientation angle was estimated using a counter-rotating rheo-optical set-up from the Research Centre Paul Pascal (CRPP) in Bordeaux, equipped to measure distances along the shear gradient direction. Gel particles swollen with 10 % HPC suspended in PDMS 200 were placed in the system. The difference in focus for both edges of the particle was measured and divided by the projection of the length on the flow direction. This value gave the tangent of the orientation angle. High experimental errors (the focus position is determined by the eye) made it difficult to determine an exact dependence of the angle on the shear rate and the results were rather scattered. Therefore, the data sets were averaged within reasonably small shear rate intervals (maximum 1 s^{-1}). These averaged results are plotted in Figure 2.16.

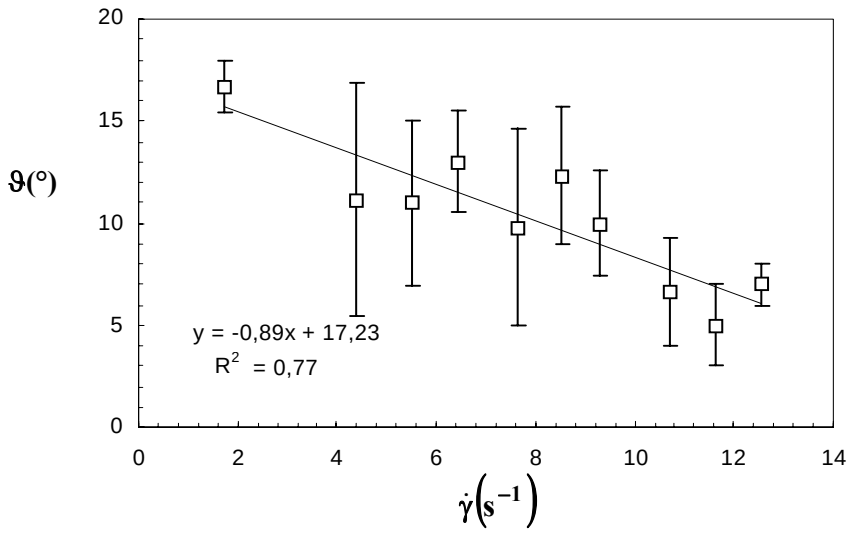

Figure 2.16: Averaged orientation angle of swollen gel particles as a function of applied shear rate. Gel particle swollen with 10 % HPC to 80 g/g suspended in PDMS 200.

It can be seen that all orientation angles measured were smaller than 20° and the orientation decreased with increasing shear rate, demonstrating the tendency to orient the particle along the flow direction. This tendency of particles to drift towards an orientation parallel to the flow direction was observed earlier for droplets as well as for rods or other slender objects when the viscoelastic character of the suspending matrix increases (Iso et al., 1996; Astruc et al., 2003; Guido et al., 2003). Increasing normal stresses start to develop in the PDMS used for the orientation tests above shear rates around 5 s^{-1} (Figure 2.9), which is probably causing the orientation drift of the swollen gel particles.

Because of the large scatter on the data and consequently the important error on the angle estimation, it was chosen not to correct measured length values for orientation. As far as $\cos(\vartheta<20°) > 0{,}94$, the particle length L will be approximated by its projection L_p in the rest of this text. The maximum error entailed by this simplification is 6 %. Because of the tendency to align with the flow direction with increasing shear rate, the error induced by this approximation will decrease with increasing shear rate. Errors will be taken into account in the error estimation of L. Since only projected L-values will be used in this text, the subscript 'p' is omitted.

2.4 Methods of characterisation

Some properties of the used materials or interactions between different materials that were used together were not available. They had to be determined experimentally. The methods used for this purpose are described in this section.

2.4.1 Equilibrium degree of swelling

Although defined as a ratio of volumes, in practice, the degree of swelling is often determined as the mass ratio of swollen and dry gel, supposing that the density of solvent and swollen gel are the same. Relation [2.14] allows calculating the degree of swelling Q in terms of weight.

$$Q = \frac{M_{swollen} - M_{dry}}{M_{dry}} = \frac{M_{solvent}}{M_{powder}} \qquad \textbf{[2.14]}$$

M_{dry} and $M_{swollen}$ represent the mass of the dry and swollen gel, respectively. The degree of swelling is expressed in [g/g] meaning grams of *solvent* per gram of dry polymer.

The equilibrium degree of swelling was determined by adding small amounts of a solvent to a given amount of dry gel in a transparent plastic tube. The results were validated by microscope observations.

2.4.1.1 Determination of the equilibrium degree of swelling of fine gel beads

In order to determine the equilibrium degree of swelling of a gel in demineralised water or another low viscosity solvent, a known amount of dry gel is immersed in excess of solvent. The network starts absorbing the solvent immediately. The gel was let at rest for 1 h to reach equilibrium swelling. The excess of water was then separated from the swollen gel by paper filtration and the swollen gel was weighed. We found that one gram of Aqua Keep 10SH-NF absorbs 400 ± 20 g of water to reach equilibrium.

The excess of solvent cannot be properly separated from the swollen gel if the solvent is viscous or sticky. The amount of solvent that remains attached to the gel remains too important and entails an overestimation of the equilibrium degree of swelling. The HPC solutions used in this work were actually too viscous. Therefore, the following method was developed to determine the equilibrium degree of swelling in these solutions.

A transparent plastic tube was taken for each gel/solvent combination. The empty tube was first weighed and a defined amount of dry gel was placed inside. Some solvent was than added and the tube was weighed again. The tube was well covered and set to rest until all the solvent was absorbed by the gel. Next, another quantity of solvent was added, the tube was weighed again and set to rest until all the solvent was absorbed. The content of the tubes was never stirred, since there would always be a small, undetermined, quantity of product that sticks to the spatula and gets lost for the mixture. This set of actions was repeated until the gel did not absorb the last added liquid anymore. Therefore, each time before adding solvent, one has to ensure that the previously added solvent has been entirely absorbed. This can be done by the 'flow test'. If the mixture in the tube flows, the swollen gel particles are in suspension in solvent, meaning that there is enough solvent *around* the particles to allow them to move among each other. Not all the solvent has been absorbed and no more has to be added: the gel passed its saturation swelling point. This experiment was repeated five times for each gel-solvent combination.

The degree of swelling is calculated with equation [2.14] at last measurement before the suspension started to flow and the first observation of the flowing suspension. The two values give a lower and an upper limit for the equilibrium degree of swelling.

The long duration is a drawback of this method. One experiment may last a few days during which the liquid is subject to evaporation. Airtight coverage of the tubes is necessary to avoid this problem.
Another point of attention is that the gel cannot swell homogeneously. The liquid is always added on top of the sample, so the liquid is absorbed immediately by the upper particles, while the particles below remain in a less swollen state for a longer time. This inhomogeneous swelling can be observed easily by differences in opacity just after solvent addition.

The results of the tube test should therefore be validated and refined by a second experiment. The tube experiments only indicate the order of magnitude of Q_{eq}. To determine Q_{eq} in a more precise manner, a number of possible Q_{eq}'s are chosen around the limits defined by the tube experiments and the corresponding quantity of liquid is added to the dry powder at once. The whole is mixed with a spatula until a homogeneous bulk of swollen particles was obtained. The recipients were put to rest for at least 24 h.
A first test consisted then in observing the upper surface of the swollen bulk: if it was not horizontal and flat, all the liquid was supposed to be absorbed. If on the other hand, the surface was horizontal and the sample flowed, the whole was considered as a suspension of soft particles in free liquid.
Microscopy observations completed this study. A sample was taken from the bulk and observed between microscope slide and cover glass. One could easily observe eventual interstitial liquid.
Complementary microscopy observations showed densely packed particles with polygonal contours for a gel swollen less than at equilibrium (Figure 2.17a). One could hardly observe liquid flow between the particles and if one did, it was only in the first minute after deposit of the cover glass.
If more liquid had been added than needed for equilibrium swelling, spherical particles (Figure 2.17c) were observed in a liquid medium and liquid flowed between the particles. Figure 2.17b shows a densely packed amount of almost spherical gel particles. No interstitial liquid is observed, but the particles are nearly spherical. This is the absorption limit.

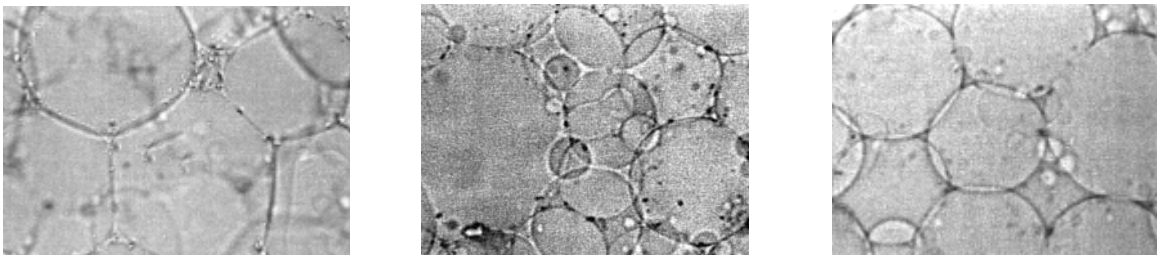

(a) 80 g/g **(b) 210 g/g** **(c) 220 g/g**

Figure 2.17: Microscope observations of swollen gels with different amounts of solvent added (here: Aqua Keep with 5 % HPC). Q_{eq} can be determined from the shape of the particles in the samples.

2.4.1.2 Results

Figure 2.18 shows the maximum degree of swelling of Aqua Keep 10SH-NF in water and aqueous HPC solutions as a function of the linear polymer concentration in the solution as found by the combination of the methods described in the previous paragraph. Q_{eq} decreases with increasing linear polymer concentration and seems to reach an asymptotic minimum. The same tendency was described in the literature review (part **1.4.3**).

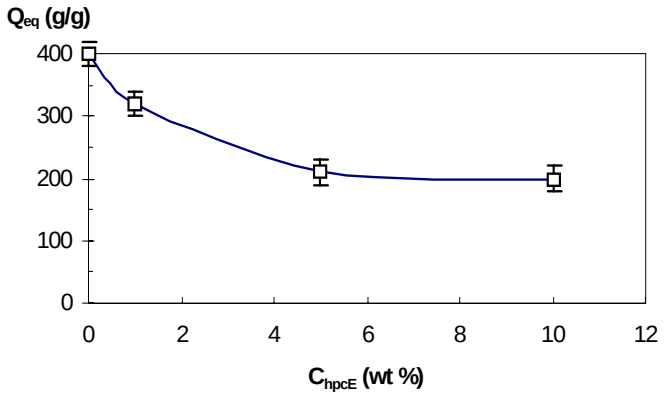

Figure 2.18: Equilibrium degree of swelling of Aqua Keep 10SH-NF in aqueous HPC solutions

The measured equilibrium degrees of swelling correspond quite well to the values in Figure 1 in Evmenenko and Budtova (2000).

2.4.1.3 Swelling kinetics: validation of equilibrating time

Swelling kinetics of Aqua Keep particles was monitored by following the diameter of a swelling particle in time under a microscope. Swelling in water and in 1 % HPC solution was so fast that no change in diameter was observed after 1 min contact time between the dry gel bead and the solvent. Swelling in 10 % HPC was slower and is shown in Figure 2.8 for different particle sizes. The time needed to reach swelling equilibrium in this solvent is about 600 s.
It can be concluded from this experiment that 1 h equilibration time is sufficient for Aqua Keep gels.

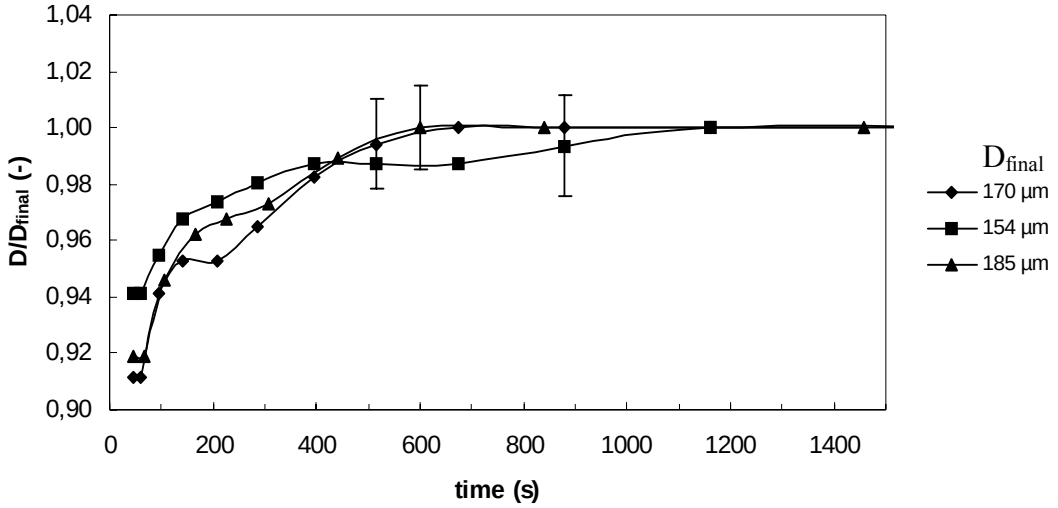

Figure 2.19: Swelling kinetics of Aqua Keep particles in 10 % HPC.

2.4.1.4 Determination of equilibrium degree of swelling of synthesised gel disks

The equilibrium degree of swelling in water was determined by immersing a dry disk of weight, M_{dry}, in excess solvent in a closed container. It was taken out of the beaker after one day. Surface water was gently wiped off the disk and the weight of the completely swollen disk, W_{eq}, was determined. The equilibrium degree of swelling of the gel disks was $Q_{eq} = 200 \pm 20$ g/g in water and 130 g/g in the 5 % HPC solution.

2.4.2 Interfacial tension HPC-solution/PDMS

Interfacial tension reflects an interaction between the components of a liquid multiphase system. The solvent of the gel is supposed to play a major role in the interfacial tension between a swollen gel particle and the suspending oil. The method used to determine the interfacial tension between the gel solvents (water and aqueous HPC-solutions) and silicone oil is presented in this paragraph and the determined values are given.

2.4.2.1 Method

The determination of the interfacial tension Γ is based on droplet deformation measurements and Cox's equation for small droplet deformations (Cox, 1969). Knowing the steady state dimensions of the droplet, the interfacial tension can be calculated via Cox' deformation model. First, two dimensionless numbers have to be defined: the capillary number Ca and the viscosity ratio p.

$$p = \frac{\eta_d}{\eta_m} \qquad \textbf{[2.15]}$$

$$Ca = \frac{\eta_m \dot{\gamma} R_o}{\Gamma} \qquad \textbf{[2.16]}$$

η_d and η_m are the viscosities of droplet and matrix phase respectively. The deformation is described as a function of these two numbers:

$$D_{Taylor} = \frac{L - W}{L + W} = \frac{5(19p + 16)}{4(1 + p)\sqrt{(20/Ca)^2 + (19p)^2}} \quad \textbf{[2.17]}$$

where L represents the real length of the deformed particle (in the flow direction) and W is the width (particle dimension in the flow gradient direction).

A deformed droplet under flow also adopts a certain orientation ϑ, which cannot be measured with the counter-rotating rheometer. It has to be estimated in order to know the real length of the deformed droplet. Cerf's equation [2.18] (Cerf, 1951) corrected by Rumsheid and Mason (1961) seems the most suitable to calculate the orientation in our case. Rumsheid and Mason found good agreement between measurements at small viscosity ratios, which is our case, and the equation of Cerf.

$$\vartheta = \frac{\pi}{4} - D_{Taylor}\left(\frac{2p + 3}{5}\right) \quad \textbf{[2.18]}$$

This equation involves the unknown deformation. Hence, the orientation has to be calculated by iteration. The algorithm followed for this calculation is shown in Figure 2.20. The inputs of the procedure are the measured length L_m and height H_m and the viscosity ratio. One also has to give an estimate for the orientation angle, ϑ_e. The first estimate was always taken 0 rad. It was verified that changing the first estimate of the orientation angle did not alter the result. The real length is calculated from the orientation and the width can then be deduced from the volume. The corresponding Taylor deformation is calculated and put into the corrected Cerf equation to obtain the corresponding calculated orientation angle ϑ_c. This angle is compared to the estimated angle. If they differ, the calculated angle becomes the new estimate and the loop is executed another time. If estimated and calculated angle are equal, the correct orientation has been found and the iterative procedure can be ended. The angle varied between 25° and 35° depending on deformation for all solvents tested. True length, width and deformation are also result of this iterative procedure.

To determine the interfacial tension Γ from deformation measurements D_{Taylor} is plotted as a function of $\dot{\gamma} * R_o$ and a straight line through the origin is fitted with the data points. Since $D_{Taylor} \approx Ca$ for small p and small deformations (Taylor, 1934; Cox, 1969), the slope corresponds to η_m/Γ, so $\Gamma = \eta/\text{slope}$. Data treatment with this method is shown in Figure 2.21.
Alternatively, Γ could be calculated separately for each data point and averaged over the data series.

Practically, the interfacial tension was measured using the counter-rotating device. Some droplets of solvent were suspended in PDMS 100. For each measurement, one droplet is selected at rest and then submitted to a low shear rate in order to induce a small deformation. The deforming droplet is recorded until it reaches the steady state corresponding to the applied shear rate. The least viscous grade of PDMS was chosen for these experiments since it enables to apply the lowest stresses. It is recalled that Cox' model is only valid for small deformations. Since Wu (1999) states that the effect of molecular weight on interfacial tension may be neglected for polymers, the results obtained in PDMS 100 will be transposed to the other PDMS's. Relevant parameters for the different solvents investigated are listed in Table 2.10.

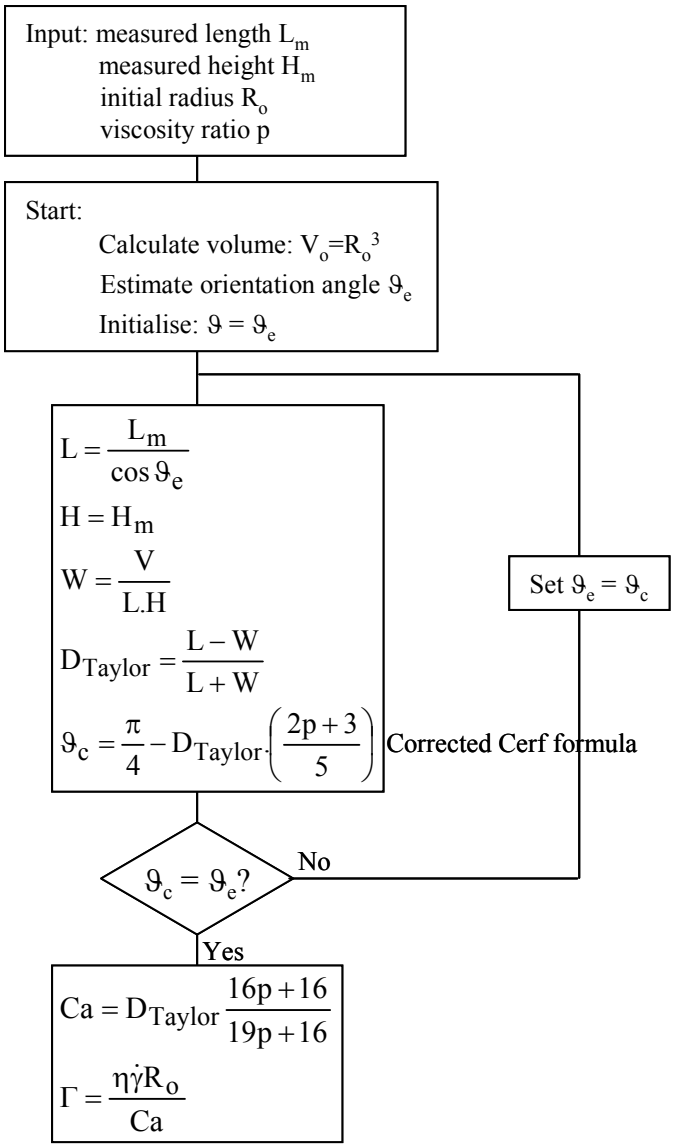

Figure 2.20: Algorithm used for the calculation of the interfacial tension

Experiment analysis consists in measuring the initial droplet radius R_o and the steady state height and projected length, which are the entries for the algorithm in Figure 2.20. The error on the interfacial tension determined in this way is estimated ± 1 mN/m.

Table 2.10: Rheological data used for interfacial tension determination. p is relative to PDMS 100.

	Water	1 % HPC	5 % HPC	10 % HPC
η (Pa.s)	$1*10^{-3}$	$2*10^{-3}$	$7*10^{-3}$	$2*10^{-1}$
p	$1*10^{-5}$	$2*10^{-5}$	$7*10^{-5}$	$2*10^{-3}$

2.4.2.2 Application: Interfacial tension HPC solution – PDMS

The method described above was applied to all solvents used in this study. Figure 2.21 shows the data treatment for the HPC solutions.

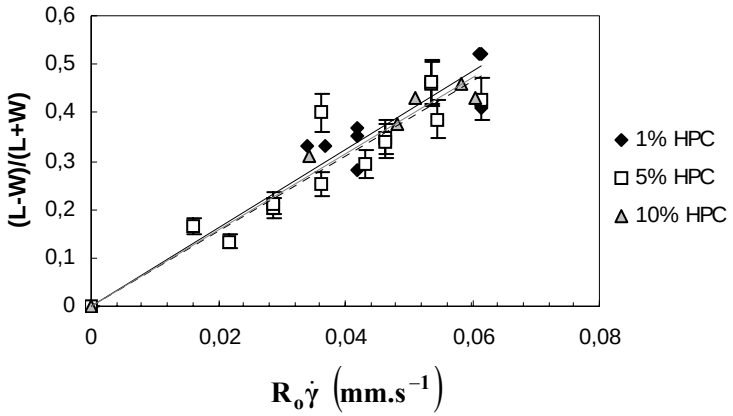

Figure 2.21: Taylor deformation as a function of $R_o\dot{\gamma}$ for droplets of HPC solutions of different concentrations in PDMS 100. Straight lines are linear fits whose slopes determine interfacial tension: full black line: 1 % HPC; dashed black line: 5 % HPC; full grey line: 10 % HPC. Error bars are only shown for one series to avoid overloading the graph.

The slopes of the linear fits through the measurements are 8,1 for 1 % HPC, 7,7 for 5 % HPC and 7,8 for 10 % HPC. The quotient of the matrix viscosity and the slope gives the interfacial tension. The values of the interfacial tension between silicone oil and the solvents used in this study are given in Table 2.11. The interfacial tension between 0,1 % HPC and a mineral oil given by the supplier and the interfacial tension between water and PDMS are added to table for reasons of comparison.

Table 2.11: Interfacial tension between gel solvents and PDMS

Solvent	$\Gamma_{solvent\ -\ PDMS}$ (mN/m)
Water[†]	18 ± 1 mN/m
0,1 % HPC[‡]	12,5 (supplier)
1 % HPC	12,4 ± 1 mN/m
5 % HPC	13,1 ± 1 mN/m
10 % HPC	12,7 ± 1 mN/m

[†] Zanina et al., 2002
[‡] Aqualon, Klucel.

2.4.2.3 Conclusions

The interfacial tension between aqueous HPC solutions and PDMS is definitely lower than between water and PDMS. The interfacial tension values between the different HPC solutions and PDMS are not different considering the experimental error. The concentrations all happened to be larger than the critical micelle concentration of HPC in water as given by the producer (0,1%), which explains that the concentration did not affect the interfacial tension. The interfacial tension between a 0,1 %

solution and refined mineral oil is 12,5 mN/m according to supplier's data. The experimental values also coincide with this figure, so Γ = 12,5 mN/m will be used as the interfacial tension for all combinations of aqueous HPC solutions and silicone oil.

In the further analysis, we will use the hypothesis that the interfacial tension between a swollen gel and silicone oil is the same as the interfacial tension between the gel solvent and the oil. This is a simplification of the reality. We are dealing with highly charged polyelectrolyte gels of which ionic groups are dissociated in a polar solvent. Counter ions located at the surface induce an interfacial tension (Fernández-Nieves et al., 2000). Unfortunately, we cannot estimate the surface charge density of the used microgels.

2.4.3 Measurement of solvent evaporation from gel disks

During measurements in open air, water evaporates from the sample surface. It is important to know at which rate water is lost in this way. Therefore, gel disks similar to the ones used in the experiments were placed between microscope slide and cover glass to simulate the experimental geometry. The system was weighed every minute during 40 min. The amount of dry polymer can be calculated from the initial weight of the disk and the degree of swelling at equilibrium. This allows converting the mass to the instantaneous degree of swelling at every moment. Figure 2.22 shows the evolution of the degree of swelling of different gel disks. Data series for different samples coincide. They show that the degree of swelling decreases at the constant rate of 0,008 g/g.s^{-1}. Its mass decreases at constant rate 0,4 % per second. Weight loss due to evaporation of solvent goes to about 7 % in 2000 s, which is longer than the duration of a typical compression experiment. As it will be shown later, this effect is significantly less important than the loss of weight caused by compression of the gel.

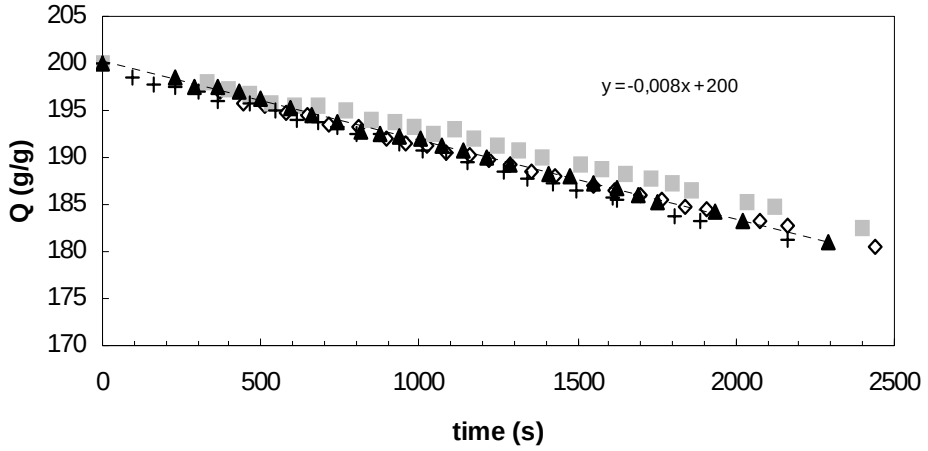

Figure 2.22: Change of gel disk degree of swelling in time due to solvent evaporation

2.5 Conclusions

A material system composed of model ingredients was designed in order to study the possibilities to apply hydrogels as a carrier of active compounds in cosmetic formulations. The system is composed of a polyelectrolyte hydrogel swollen with a linear polymer solution. The swollen gels are studied in the form of microscopic beads immersed in silicone oil or as disks in open air. Table 2.12 gives an overview of material systems used. Data from Zanina et al. (2002) for gel particles swollen with water suspended in silicone oil are added since we will often compare our findings to theirs.

Table 2.12: Overview of material systems and properties

Solvent	**Degree of swelling (g/g)**	**Medium**	**$\eta_{solvent}$ (Pa.s)**	**$\Gamma_{solvent/matrix}$ (mN/m)**
Shear experiments – Aqua Keep 10SH-NF gel beads				
Water	50, 10, 280, 400 (Q_{eq})	PDMS 100, PDMS 200	1.10^{-3}	18
1 % HPC	80	PDMS 200, PDMS 1000	2.10^{-3}	12,5
5 % HPC	80, 160, 210 (Q_{eq})	PDMS 200	7.10^{-3}	12,5
10 % HPC	80	PDMS 200, PDMS 1000	2.10^{-1}	12,5
		PDMS 200 + 3 % emulsifier		3
Compression experiments – synthesised poly(NaA-*co*-AA) disks				
Water	200	Air	1.10^{-3}	-
5 % HPC	130	Air	7.10^{-3}	-

Two experimental methods that combine visual observation and mechanical testing were presented. These methods enable to study the effect of deformation on highly swollen polyelectrolyte gels. The common asset of both methods is the possibility to observe the samples while they are undergoing the mechanical test. Phenomena can easily be spotted in this way. The high errors induced are the main drawback.

Résumé du Chapitre 3

Identification du comportement induit par cisaillement d'un gel gonflé et analyse de la déformation et de la relaxation

Dans les domaines de la cosmétique, la pharmacie ou encore l'alimentaire, les produits sont soumis à des forces de cisaillement lors de la production et de l'application. On peut penser à l'écoulement du produit dans des réacteurs, pompes et tubes jusqu'au remplissage de l'emballage. Du côté de l'application, les produits rencontrent des forts cisaillements entre la langue et le palais dans le cas de la nourriture ou des médicaments et pendant l'étalage sur la peau pour les pommades et les crèmes. Le cisaillement est donc une sollicitation évidente que vont rencontrer des gels porteurs d'actifs dans de tels produits. Dans ce chapitre, nous étudions à l'aide du dispositif contrarotatif les effets d'un cisaillement simple sur une particule de gel gonflée d'une solution de polymère suspendue dans une huile de silicone. Il a été observé qu'un gel ne réagit au cisaillement non seulement par une déformation, mais aussi par une rotation et par le relargage partiel de son solvant. Plusieurs régimes ont été identifiés:

- soumis à une contrainte de cisaillement, une particule de gel se déforme en une ellipse à trois axes différents;
- lorsque la contrainte appliquée est plus élevée qu'une première contrainte seuil, mais inférieure à une deuxième contrainte critique, le gel relargue un peu de son solvant. Ce solvant reste attaché aux extrémités de la particule. La déformation du gel et la libération de solvant sont réversibles : dès que le cisaillement est arrêté, le gel réabsorbe son solvant et revient à sa forme initiale;
- au-dessus d'un deuxième seuil de contrainte, des gouttelettes de solvant se détachent des bouts de liquide attaché aux extrémités du gel et se dispersent dans la matrice. Ce phénomène est irréversible;
- les particules de gel s'élargissent aussi dans la direction de la vorticité et du solvant peut être relargué des pôles de la particule et dispersé dans la matrice.

Ce chapitre traite particulièrement du comportement de la particule elle-même (rotation, déformation et relaxation après arrêt de l'écoulement).
Les particules de gels soumises au cisaillement tournent autour de l'axe de la vorticité. Quand la matrice est newtonienne, la période de rotation correspond à la période de rotation prédit par Jefferey (1922) pour des sphères non-déformables. Dès que le comportement de la matrice devient viscoélastique, la rotation de la particule est ralentie.

La déformation d'une particule de gel gonflée dans une solution d'hydroxypropylcellulose est comparée d'une part à la déformation de particules de gel gonflées dans de l'eau et d'autre part à la déformation de gouttes de solvant. Le rapport longueur sur diamètre initial de la particule augmente de façon linéaire avec la contrainte avant relargage de solvant. La dépendance entre la déformation et la contrainte ne dépend pas du solvant utilisé. Au-delà d'une déformation critique, des poches de solvant sont libérées dans la direction de l'écoulement. Si des grands bouts d'un solvant de faible viscosité restent attachés à la particule, la déformation sature à des valeurs basses. Si le solvant se détache facilement, les poches restent petites et affectent moins la déformation du gel. Les limites de la déformation sont alors plus élevées pour des particules de gels ayant des petits bouts. La déformation du gel dépend du degré de gonflement, mais pas de la taille initiale de la particule.

Si nous comparons les gels aux gouttes de solvant, toutes nos particules auraient du se rompre en considérant le rapport des viscosités solvant-matrice. Cependant, le gel réticulé reste intact. Les modèles décrivant la déformation de gouttes dans des systèmes newtoniens ne sont pas capables de prédire la déformation d'un gel. Nous avons alors modifié le modèle de Cox en y ajoutant un terme représentant la résistance élastique du réseau à la déformation. L'accord entre les prédictions de ce 'modèle de Cox modifié' et les données expérimentales est satisfaisant pour les petites déformations.

Nous avons également étudié la relaxation du gel après arrêt de l'écoulement. Les temps de relaxation augmentent avec la déformation du gel avant arrêt du cisaillement. A déformation équivalente, la relaxation après arrêt de l'écoulement dépend seulement de la viscosité de la matrice, mais pas de la taille de la particule. Ceci est différent de la relaxation d'une goutte liquide.
Les particules ayant des bouts de liquide relargué se relaxent en deux étapes. Les bouts sont réabsorbés en premier, suivi par un recouvrement rapide de la forme sphérique.

Chapter 3

Identification of shear-induced behaviour of a swollen gel particle and analysis of shape deformation and relaxation

In the fields of cosmetics, pharmaceutics or foods, products are submitted to shear forces during production and application. One may think of product flow in reactors, pumps and pipes until final filling in an appropriate container. On the application side, the product meets strong shear fields between tongue and palate for food and oral medicines and during rubbing on the skin for creams and salves. Shear is thus an obvious type of stress that carrier particles in such products will encounter.
Only few publications exist on the study of suspensions of soft solids and most of them considered the bulk rheology of the suspension (e.g., Budtova et al., 1994; Frith and Lips, 1995). The in-situ study of diluted suspensions of gel particles under shear has been started some years ago at CEMEF (Zanina and Budtova, 2002; Zanina et al., 2002). In the present study, that work is extended to gels swollen with linear polymer solutions in order to explore possible applications for gels as excipients.

To study the effect of shear on swollen gels, particles were immersed in viscous oil that serves as a stress-transmitting medium from the moving geometry to the swollen particle. Different phenomena such as particle rotation and deformation, solvent release and solvent detachment, could be identified. We shall separate them into two categories according to whether the gel volume remains constant (no solvent release or detachment) or not. The behaviour of a swollen particle under shear will be described from a purely phenomenological point of view in the first paragraph. The following sections treat each of the phenomena separately in order to build basic understanding of the system. In the focus of the present chapter are the phenomena in which the gel conserves its degree of swelling, i.e. rotation and shape deformation and relaxation. Phenomena that change the gel volume, i.e. solvent release and detachment, will be studied in Chapter 4.

It was observed that highly swollen hydrogels undergo large deformations that are far from the linear elastic region. Most theories of linear elasticity that are currently used to describe compression experiments in literature do not cover the large deformations that we encountered in the present study. The second purpose of this study on gel particles under shear is thus of a more fundamental interest: to describe the deformation of elastic, chemically cross-linked particles under shear. As no theories exist to our knowledge that describe such system, predictions made by some basic models used to describe droplet deformation in a polymer blend were compared to our experimental results.

3.1 Identification of phenomena that take place when a suspended gel particle is submitted to shear flow

The counter rotating apparatus was used to study the effect of shear on swollen gel particles immersed in silicone oil. A few particles together with the PDMS were placed between the transparent plates. During each experiment, a constant shear rate was applied stepwise and the particle's evolution was followed until a steady state was reached. In subsequent runs, the particle was submitted to higher stresses by increasing the rotation velocity of the plates. Each experiment was recorded on videotape and analysed with help of image analysis software afterwards.

Several effects were observed when a gel particle was submitted to a shear field. They are schematically represented in Figure 3.1. All studied particles were spherical at rest characterised by their initial length L_o (Figure 3.1a). First, shear flow makes the particle rotate around the vorticity axis. Second, when submitted to small shear stresses, the particle deforms into an ellipsoid, which is more adapted to the stress field surrounding the particle. The shape of a deformed gel particle can be described by two parameters: length, L, and height, H, as defined in Figure 3.1b. These are the two dimensions observed in the counter-rotating shear system. The third dimension will be referred to as width, W. The length of the particle increases while the height remains practically unchanged. Assuming conservation of volume before solvent release, the instantaneous width may be calculated from the initial volume V_o and L and H. Since L increases and H remains unchanged, W has to decrease to ensure volume conservation. The deformed gel particle is an ellipsoid with three different axes. The higher the applied shear stress, the more the particle is deformed. After cessation of the flow, the particle relaxes and recovers its initial spherical shape.

Above a first stress threshold, referred to as release stress, σ_{rel}, release of a small amount of liquid is observed at the edges of the ellipsoid (Figure 3.1c). This liquid does not separate from the particle but stays attached to the edges, forming tips of a second phase. Particle and tips form a unit and flow together. At fixed shear stress ($> \sigma_{rel}$), the volume of solvent released increases in time until a steady state is reached. At this point, the gel and tips continue to flow together without further changes. Further increase of the shear stress leads to an increasing amount of solvent released in the tips. To each stress corresponds a different steady state. Solvent release is also reversible. After cessation of the flow, the gel, which adopts a spherical shape again, reabsorbs the released liquid. This phenomenon had been observed earlier on gels swollen in water. In that case, the tips became pointed as cones and grew very large up to containing 50 % of the initial volume of the gel (Zanina and Budtova, 2002; Zanina et al., 2002).

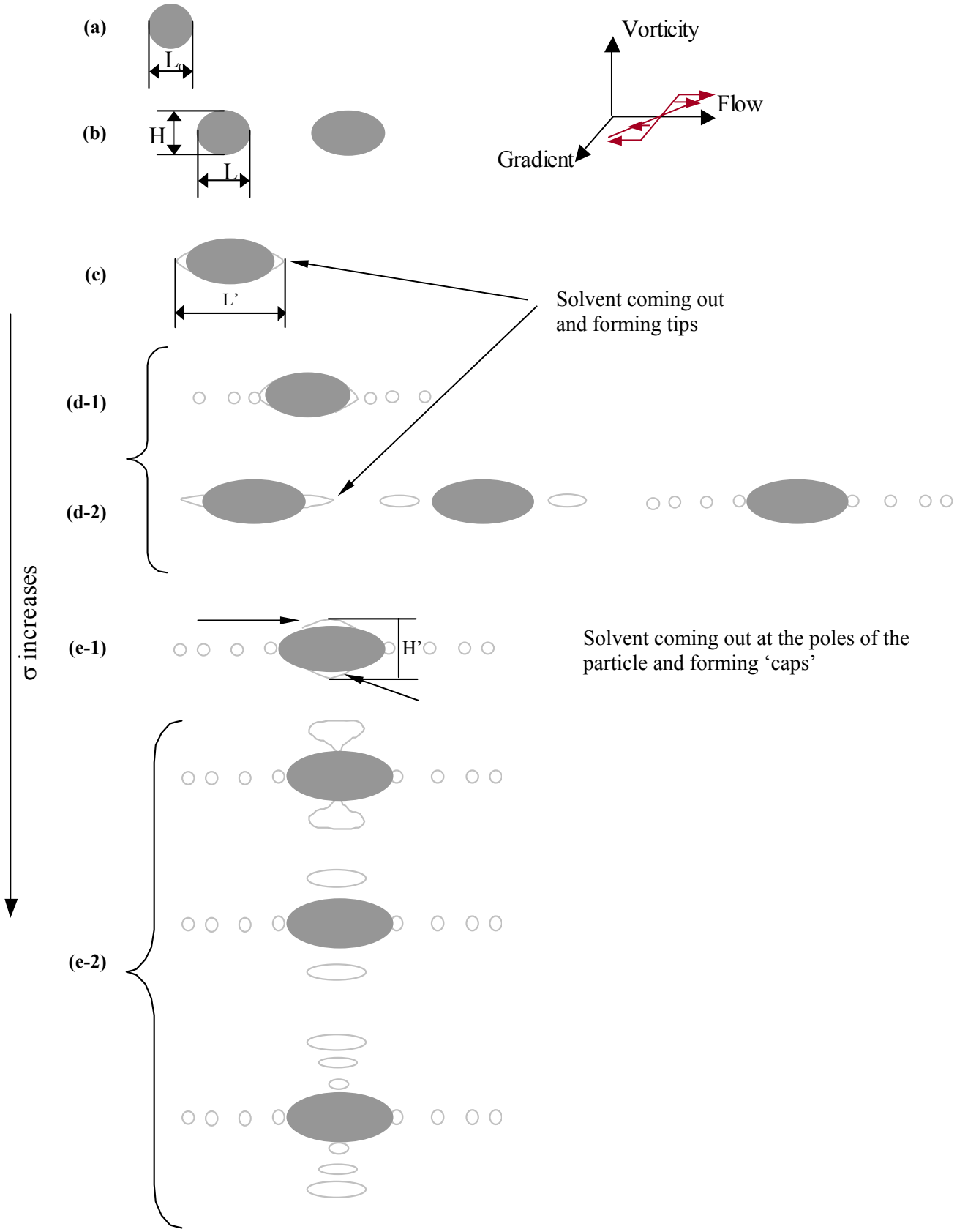

Figure 3.1: Behaviour of a swollen gel particle under simple shear flow as observed in the Flow-Vorticity plane. Shear stress increases from (a) to (e). (a) rest; (b) pure deformation; (c) release of tips; (d) lateral solvent ejection: (d-1): ejection of droplets, (d-2): expulsion of a filament; (e) transversal ejection: (e-1): height increase and "cap" formation, (e-2): detachment of" mushrooms".

Above a second stress threshold, named 'ejection stress' σ_{ej}, some liquid is detached definitively by the ejection of small droplets from the edges of the tips (Figure 3.1d-1). If the stress is applied abruptly, the first solvent is ejected as filaments (d-2). As long as the stress is fixed at a constant value, the gel expulses liquid droplets until equilibrium is established between the absorbing powers of the network, the interfacial tension matrix/released solvent and the external shear forces. The expulsion stops as soon as the stresses balance each other out. The result is a steady state for a less swollen deformed gel. As a reaction to further increasing stress, the gel releases more solvent in order to reach the steady state corresponding to the applied stress. It is evident that this process is irreversible since the expulsed droplets disperse into the matrix and will not flow back into the gel particle after cessation of the flow.

At even higher stresses, a third critical stress level σ_{cap} may be defined. Above this stress, the particle height, which did not vary in previous stages, increases slightly and liquid can be released at the poles of the particle (Figure 3.1e). First, a small amount of liquid comes out of the particle and forms some kind of 'caps' at the poles of the particle as drawn in Figure 3.1e-1. These caps are similar to the tips at the edges of the particle and they grow slowly in time towards deformation into cones and are finally distorted into a 'mushroom'. The stem of the mushroom then contracts until it ruptures, allowing the mushroom hats to flow away. They form ellipsoidal droplets that immediately flow away from the particle in the direction of the vorticity axis (Figure 3.1e-2). This transversal liquid ejection under shear flow has never been reported before, but it implicates that important quantities of liquid may be released from the gel particle. The solvent volumes in the detached hats are far larger than in the droplets detached from the sides of the particle.

The teams of Barthès-Biesel and Pozrikidis studied the behaviour of capsules composed of a liquid enclosed by a thin elastic membrane under flow. They do not report any release phenomenon. At low shear rates, initially spherical capsules reversibly deform into an ellipsoid. At higher shear rates, the capsules get very deformed and finally break up (Chang and Olbright, 1993; Lac et al., 2004). In this, capsule behaviour reminds of droplet behaviour, whereas our gel particles never ruptured under the experimental conditions applied.

This chapter and Chapter 4 are dedicated to the analysis of the identified phenomena. The remainder of this chapter discusses phenomena during which the degree of swelling of the gel remains unchanged. Release and ejection phenomena, which entail a decrease of the degree of swelling, will be discussed in Chapter 4. It was already stated in Chapter 1 that a gel is a state of matter intermediate between a solid and a liquid (Tanaka, 1981). We will consider our observations from both sides in the following. Gel particle rotation will be discussed in §3.2. The remainder of this chapter studies shape deformation (§3.3 - §3.5) and relaxation (§3.6).

As mentioned in the experimental part, only L and H can be observed in the used set-up. Assuming conservation of volume before solvent release, W may be calculated from the initial volume V_o and L and H [3.1]:

$$W = \frac{V_o}{L * H} \qquad \textbf{[3.1]}$$

Deformation of an inclusion is generally expressed with the measure defined by Taylor (1932), D_{Taylor}:

$$D_{Taylor} = \frac{L - W}{L + W} \qquad \textbf{[3.2]}$$

As soon as the solvent is partially released from the particle, the volume of the gel becomes undefined and consequently, W and D_{Taylor} cannot be calculated anymore. Therefore, in most of this work, particle deformation will be expressed as the deformed dimension relative to its initial value. This means deformation will be expressed as:

$$\begin{array}{c} L/L_o,\ H/H_o \text{ and } W/W_o \text{ in cases where W is known} \\ L'/L_o,\ H'/H_o \text{ to characterise particles with tips and caps} \end{array} \qquad \textbf{[3.3]}$$

This measure of deformation equals unity for undeformed dimensions. It is larger than unity for a stretched dimension and smaller than one for a compressed dimension.

3.2 Rotation

Objects that are submitted to shear flow get a rotational motion induced. A solid object will turn around the vorticity axis and internal circulation around this axis will be observed in liquid droplets. A highly swollen gel particle also rotates in a shear flow field. Since a gel is intermediate between a solid and a liquid, the measured rotation will be compared with theoretical predictions for solid particles and for liquid droplets.

3.2.1 Rotation of a solid sphere: Jeffery's law

The motion of a solid particle was first analysed by Jeffery (1922). He considered the case of a solid ellipsoid in a Newtonian matrix under simple shear flow, at low Reynolds' numbers and neglecting the inertia of particle and fluid. By considering a sphere as an ellipsoid with three equal axes, Jeffery's law predicts its rotation period T to be:

$$T = \frac{4\pi}{\dot{\gamma}} \qquad \textbf{[3.4]}$$

The plot of the inverse rotation period as a function of shear rate is a straight line with slope $1/4\pi$ (= 0,0795).

3.2.2 Viscous droplet under shear: circulation at the droplet surface

In the case of sheared diluted emulsions, viscous drag exerted by the matrix induces circulation of the fluid inside a droplet (Bartok and Mason, 1958). The mean period of circulation at the surface of a droplet should obey:

$$T = \frac{4\pi}{\dot{\gamma}} \frac{p + 1}{\sqrt{p(p + 2)}} \qquad \textbf{[3.5]}$$

The parameter p is the ratio of viscosity η_d/η_m, with η_d and η_m being droplet and matrix viscosity, respectively. Relation [3.5] is valid for any value of $p > 0$. This equation represents a linear relation between the inverse period of rotation and the shear rate. The slope only depends on the viscosity ratio and increases with increasing p. Setting $p = \infty$ in this equation gives Jeffery's equation [3.4] for suspended solid spheres.

3.2.3 Rotation of deformed swollen gel particles

During the counter rotating experiments, it was observed that a swollen gel particle turns around the vorticity axis. The period of rotation could be measured on particles with a small defect on the surface. The defect serves as a reference point. By following the defect on the otherwise perfectly smooth and transparent particle, the rotation speed could be determined; the time to execute a number of periods (at least 10) was measured with a stopwatch and divided by the number of periods executed during this lap of time in order to calculate the period of rotation. The particles were seen to rotate regularly for all shear rates applied.
At high shear rates when the particle is ejecting solvent, the rotation could not really be seen as a rotation; a 'pulsing particle' was observed. The pulses were counted and it is suggested that the time to pulse twice corresponded to one period of rotation. (This is logical if the observed pulses are in fact an effect of fast rotation: the rotation is so fast that the particle cannot adapt its contour to the stress field by internal circulation as fast as the flow demands). Another option is that the pulses would be related to the expelling of droplets. Undamped periodic oscillation was also predicted and observed for the case of droplets in a matrix with zero interfacial tension and high viscosity ratio (Cox, 1969; Bartram et al., 1975). The period of two pulses should equal the rotation period predicted by Jeffery. The pulsing measured by Bartram et al. (1975) however, was slower than predicted. Although the zero interfacial tension hypothesis was not fulfilled in the case of a suspended gel particle, we measured longer pulsation periods than the Jeffery period, like Bartram and co-workers.

Figure 3.2 shows the reciprocal of the period of rotation as a function of applied shear rate for gel particles swollen in two different solvents (5 % and 10 % solutions of HPC) and to different extents in the case of 5 % (80, 160 and 210 g/g). Data on dry Aqua Keep beads are also added as well as Jeffery's law.

The dry gel particles obey this law perfectly. That is not surprising since they can be considered as solid spheres. It was shown before that Jeffery's law describes the motion of filler particles in Newtonian fluids in a satisfying way (Astruc et al., 2003). It was also shown in the same paper that the rotation is slowed down as soon as the matrix becomes viscoelastic. The rotation of swollen gel particles is in good agreement with Jeffery's law at low shear rates, until about 5 s^{-1}. At higher shear rates, the particles turn slower around their axis than a solid sphere. This is when PDMS 200 starts showing some elasticity. One has to bear in mind too that at this higher shear rates, the particles become increasingly deformed, being more and more different from the spherical particle for which the straight line has been calculated. Besides that, the stresses generated at shear rates above 5 s^{-1} induce solvent release and eventually ejection. The tips are quite small and may probably be neglected for these solvents, but the ejection phenomenon may have a damping effect on the particle's

rotation. The longer period of rotation of ejecting particles suggests that part of the energy is absorbed every time a droplet is pinched off. This energy is lost for the particle, resulting in a slower rotation.

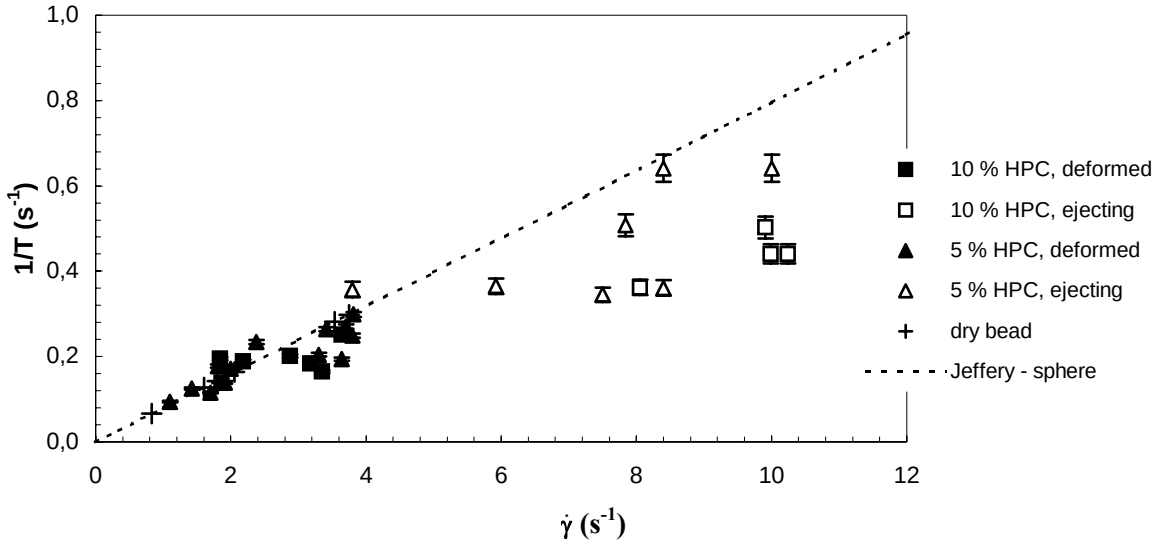

Figure 3.2: Rotation period as a function of shear rate for swollen Aqua Keep particles in PDMS 200. Particles were swollen with 5 % and 10 % HPC solutions. Dry Aqua Keep bead rotation was added for comparison. Dotted line represents Jeffery's law.

The swollen gel might as well be considered as a liquid droplet in another fluid. Shear flow induces internal circulation of the fluid in the droplet. The presented motion of the gel particles must then be compared to the flow on the surface of a deformed droplet. The flow speed depends on the viscosity ratio between droplet and matrix, which is undefined for a swollen gel particle. According to the model cited in equation [3.5], the reciprocal of the rotation period is a linearly increasing function of shear rate with the slope a function of the viscosity ratio. Figure 3.3 represents the data of Figure 3.2, this time compared with the theoretical model of Bartok and Mason (1958). The viscosity ratio in this figure is defined as the ratio between gel solvent viscosity and matrix viscosity (PDMS 200). The theoretical lines are clearly disparate from the linear best fits through data points of gels swollen with the corresponding solvent. A straight line is then fitted with the data, considering parameter 'p' as a variable. The correlation parameters for the optimal linear fits are rather poor: 0,80 for gels swollen with the 5 % solution and 0,78 for gels swollen with the 10 % solution.

Supposing the Bartok and Mason model describes the rotation of the swollen gel particles correctly, we can deduce an equivalent viscosity ratio from the slope of the straight-line '1/T as a function of shear rate'. The slope is 0,0634 for gel particles swollen with the 5 % HPC solution, which gives p = 0,65 and the slope becomes 0,0485 for particles containing the 10 % HPC solution, giving p = 0,59. Those p-values are completely different from the viscosity ratio between gel solvent and matrix. Again, this is not surprising, since a swollen, deformed and rotating particle is rather different from a droplet of its solvent. Considering the p-values calculated from the fitted lines, one may conclude that the rotational motion of a gel particle stays close to that of a solid sphere even though the particle is highly deformed and its elongated flat ellipsoidal shape is far from spherical.

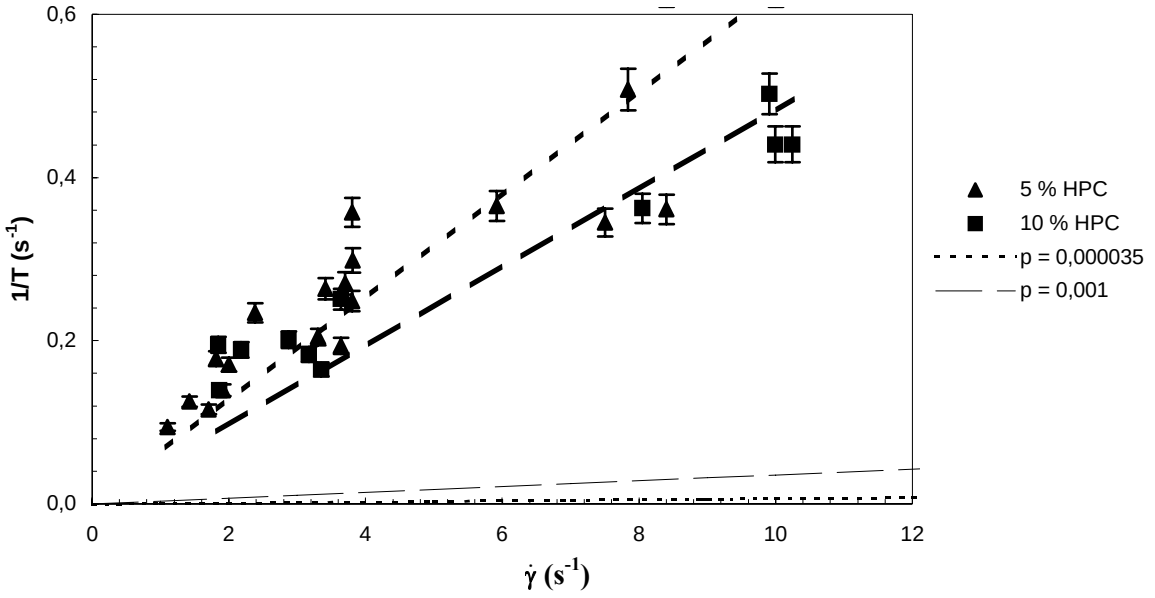

Figure 3.3: Period of rotation of swollen gel particles compared to predicted circulation at the surface of a droplet according to Bartok and Mason (1958). Viscosity ratio used in the predictions is chosen as the ratio between solvent viscosity and matrix viscosity (thin dashed and dotted lines) $p = 3{,}5.10^{-5}$ for 5 % HPC vs. PDMS 200 and $p = 1.10^{-3}$ for 10 % HPC. Thick lines are linear best fits through data points (R^2 = 0,80 for 5 % and R^2 = 0,78 for 10 % HPC).

3.2.4 Conclusions

Weakly deformed gel particles show a regular rotation that can be described in an accurate way by Jeffery's solid sphere theory as long as the matrix is Newtonian. As soon as the fluid becomes viscoelastic, the period of rotation slows down and deviates from the Jeffery model. Even though the ellipsoidal shapes and the solvent tips on the edges of the gel particles make them more resemble the case of a deformed droplet in a matrix, the period of internal circulation in a droplet as predicted by Bartok and Mason does not predict the gel rotation in a satisfying way.

3.3 Literature: main formulas describing droplet deformation in an emulsion

Gel particle suspensions are somewhere intermediate between suspensions of solid spheres and emulsions of viscous droplets in a viscous matrix. Solid spheres in a sheared suspension will rotate around the vorticity axis with a period that is inversely proportional to the macroscopic shear rate. Gels, even deformed, show the same rotation, as was shown in paragraph 3.2. One aspect that clearly distinguishes a gel from a solid undeformable particle is deformation: the spherical particles are deformed into ellipsoids under the influence of shear stress. This is a more liquid-like feature. Droplets in a sheared emulsion deform into ellipsoids at low shear rates (capillary number), while more complex phenomena as break-up, end-pinching and Rayleigh instabilities occur at higher capillary number. These phenomena were the subject of numerous experimental and theoretical publications. For a comprehensive overview of droplet behaviour, the reader is referred to reviews by e.g. Rallison (1984) or Tucker and Moldenaers (2002). We will only give some models that describe

ellipsoidal deformation, because of the similarity to gel behaviour. Some of the cited models will be used in the next paragraph to compare with our results on gel particle deformation.

3.3.1 Newtonian systems

Taylor (1932, 1934) was the first to tackle the issue of droplet deformation in an emulsion. He defined two dimensionless numbers, viscosity ratio p and Capillary number Ca that where defined in 2.4.2.1 (equations [2.15] and [2.16]). The capillary number represents the ratio of viscous stresses to interfacial tension. The viscous stresses tend to stretch the droplet in the flow direction while the interfacial tension tends to minimise the droplet surface, i.e. to maintain a spherical shape. Ca can thus be seen as the ratio between deforming forces and forces resisting to deformation.
Taylor's model **[3.6]** states that the deformation of an isolated droplet in the small deformation limit equals the capillary number.

$$D_{Taylor} = Ca \qquad \textbf{[3.6]}$$

D_{Taylor} is zero for spherical (undeformed) droplets and increases as soon as the droplet shape changes into an ellipsoid.

Cox (1969) developed a model that describes droplet deformation in terms of the dimensionless parameters p and Ca. The model has been developed for Newtonian droplets in a Newtonian matrix.

$$\frac{L-W}{L+W} = \frac{5(19p+16)}{4(1+p)\sqrt{(20/Ca)^2+(19p)^2}} \qquad \textbf{[3.7]}$$

This equation is valid if the resulting deformation is small. Practically, for deformation induced by shear flow, this means that either p must be large or Ca must be small or both conditions must be fulfilled. Cox' model coincides with Taylor's model for $p \to 0$.

More recently, Maffetone and Minale (1998) developed a phenomenological model (referred to as MM model) for the deformation of a Newtonian droplet immersed in a Newtonian matrix. They assumed that the deformed droplet is ellipsoidal at all times and that interfacial tension and drag forces are additive. The steady-state values of the three ellipsoid dimensions are:

$$L^2 = \frac{f_1^2 + Ca^2 + f_2 Ca\sqrt{f_1^2+Ca^2}}{\left(f_1^2+Ca^2\right)^{1/3}\left(f_1^2+Ca^2-f_2^2Ca^2\right)^{2/3}}$$
$$W^2 = \frac{f_1^2 + Ca^2 - f_2 Ca\sqrt{f_1^2+Ca^2}}{\left(f_1^2+Ca^2\right)^{1/3}\left(f_1^2+Ca^2-f_2^2Ca^2\right)^{2/3}} \qquad \textbf{[3.8]}$$
$$H^2 = \frac{f_1^2 + Ca^2 - f_2^2Ca^2}{\left(f_1^2+Ca^2\right)^{1/3}\left(f_1^2+Ca^2-f_2^2Ca^2\right)^{2/3}}$$

With

$$f_1 = \frac{40(p+1)}{(2p+3)(19p+16)}$$
$$f_2 = \frac{5}{2p+3} + \left(\frac{3Ca^2}{2+6Ca^2} \right) \qquad \textbf{[3.9]}$$

The term between brackets in the equation for f_2 was added to improve the predictions at high viscosity ratios and high capillary number.
The model breaks down when a droplet gets so much deformed that it will break up. It is assumed this will be when the solutions of **[3.8]** become complex. From this condition, a critical capillary number is obtained.

3.3.2 Non-Newtonian systems

Most practical systems do not consist of two perfectly Newtonian fluids; one or both fluids may have viscoelastic properties. The analytical description of such systems is more complicated. In general, higher matrix elasticity promotes droplet deformation whereas higher droplet elasticity acts against deformation. This is reflected in the qualitative stress balance written by Ghodgaonkar and Sundararaj (1996):

$$\eta_m \dot{\gamma} + 2G'_m = \Gamma/R + 2G'_d \qquad \textbf{[3.10]}$$

G'_m and G'_d are the elastic moduli of matrix and droplet phase, respectively. On the left hand side are the deforming forces and the right hand side groups the forces resisting deformation. A similar idea had been proposed by Vanoene (1992) who added a term for normal stress differences between droplet and matrix phase to the interfacial tension.

The MM-model described in the previous section was extended to non-Newtonian systems by Minale (2004). He used first and second normal stress differences of droplet and matrix to characterise the non-Newtonianness of the system. Unfortunately, such data are not available for our gel inclusions. Therefore, it is not straightforward to apply this model to predict the deformation of a suspended gel particle.

3.4 Deformation of gel particles

Particle deformation is a typical liquid feature, although the gels described here do not deform to the same extent as Newtonian droplets in a Newtonian medium do. That is because the strong elastic character of the gel limits deformation. The pure HPC solutions (gel solvent) in PDMS 200 fall in the category of Newtonian systems at low shear rates. Their deformation will be shown in section 3.4.4.

3.4.1 Kinetics of deformation

The behaviour of a gel particle submitted to constant shear stress was monitored from rest until a steady state had been reached. The purpose of this experiment was to study how a particle evolves to equilibrium dimensions.

Kinetics of deformation curves all have the same profile, independent of stress. Figure 3.4 shows a detailed example. They show a fast evolution towards a steady state length, L_{ss}, which is reached after a steady state time, t_{ss}. At a given moment, t_t, solvent tips come out of the particle at the edges and start to grow in order to reach a steady state value, L'_{ss}, reached at $t_{t,\,ss}$. The deformation of the gel particle itself levels off to the steady state length, as soon as the first solvent is released. The total steady state is established within 2 s. The final particle deformation is only slightly higher than what it was at the moment solvent release started. These typical times and dimensions are indicated in Figure 3.4. Images illustrate the key steps.

In order to study the effect of applied shear rate, the evolution of deformation with time was compared on particles with the same initial size and degree of swelling at different shear rates. Typical results are shown in Figure 3.5(a) to (c) for gel particles swollen with polymer solutions of different concentrations all immersed in the same matrix (PDMS 200). Kinetics of deformation curves all have the same profile, independent of applied shear rate, but they grow to higher values of deformation at higher stresses.

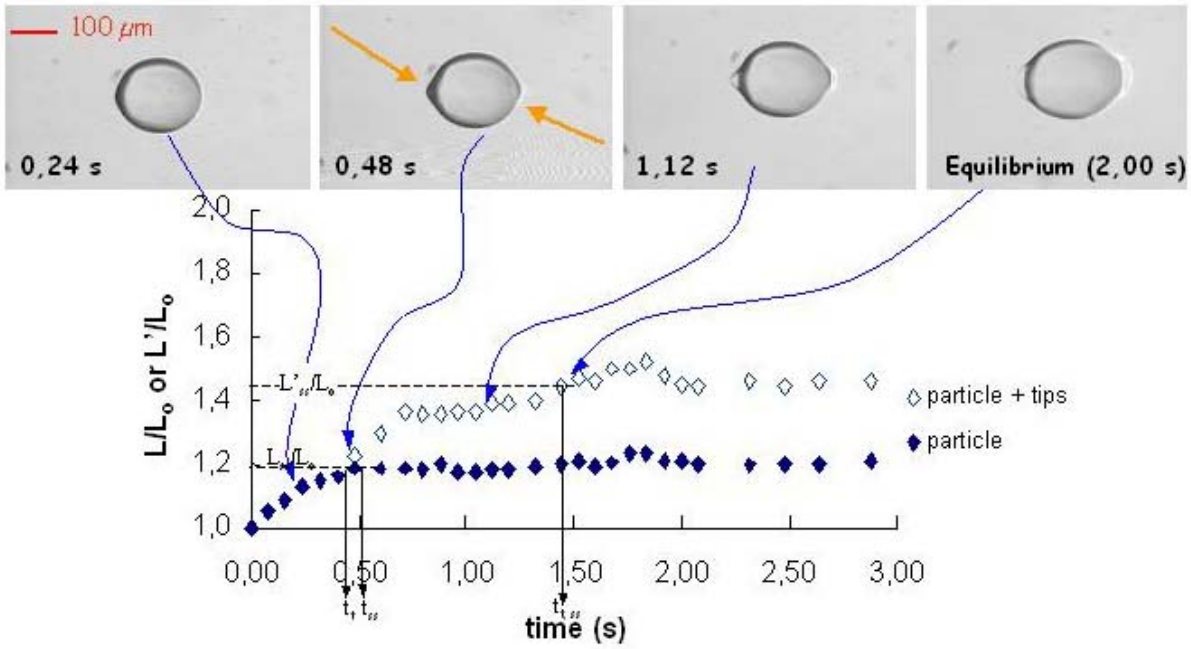

Figure 3.4: Deformation kinetics of a gel particle swollen with 1 % HPC, Q = 80 g/g, submitted to shear stress 1000 Pa ($\sigma_{rel} < \sigma < \sigma_{ej}$).

The time to reach the steady regime, t_{ss}, is not the same for the different shear rates. Moreover, the data do not show a clear tendency. One possible explanation for the lack of coherence between the different data series is the fact that the shear rate is imposed manually. This is not always done in the same way and consequently, the stable flow regime is not established in the same way neither.

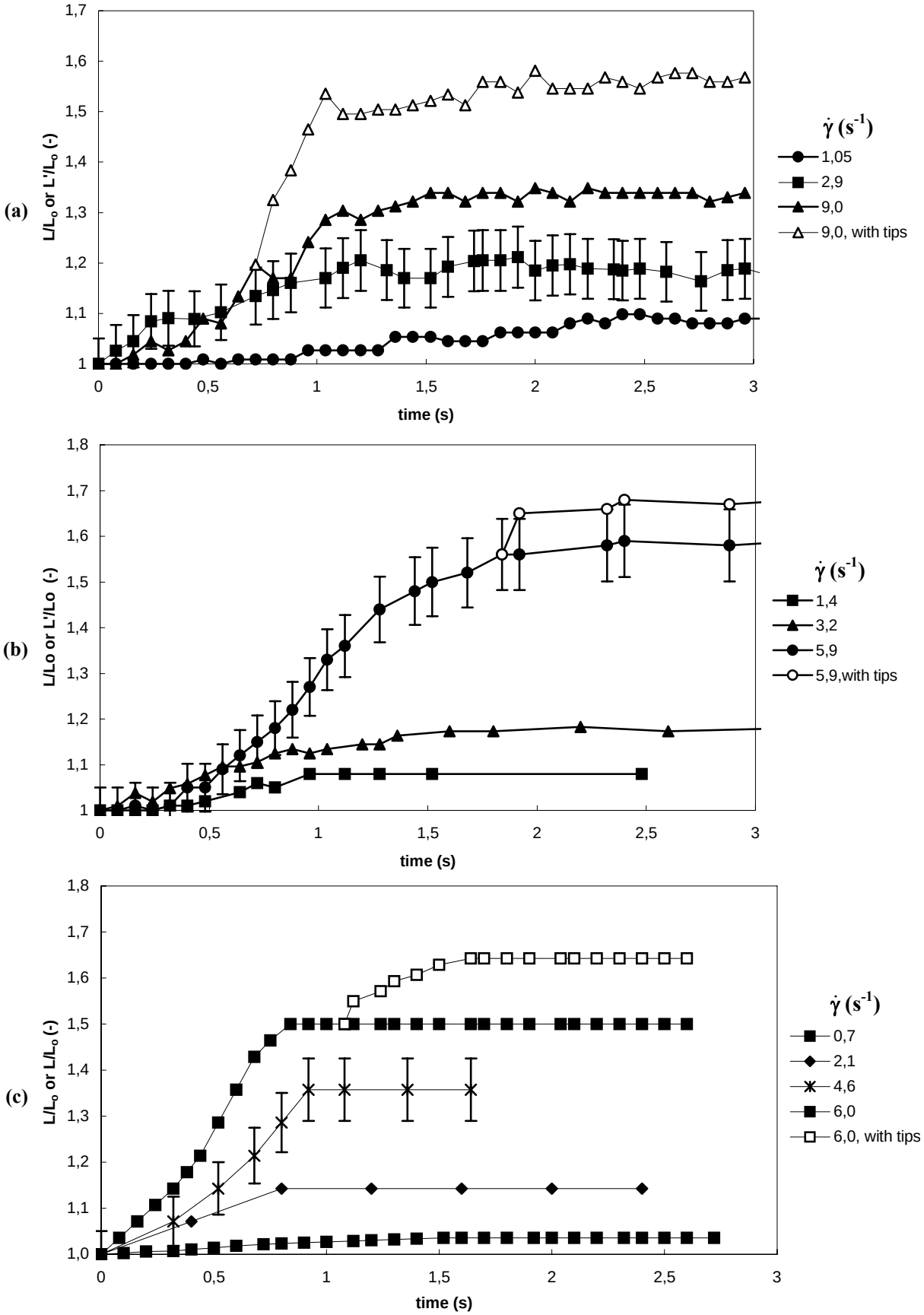

Figure 3.5: Deformation kinetics of gel particles swollen in different HPC solutions (Q = 80 g/g) at various shear rates. Matrix is PDMS 200. (a) 1 % HPC, D_o = 150 µm; (b) 5 % HPC, D_o = 100 µm; (c) 10 % HPC, D_o = 140 µm. Error bars are given for one series only to avoid overloading the graph.

Knowing that the particle deforms at the mere stress, it would be logic that its deformation is sensitive to the establishment of the flow field.
Nevertheless, t_{ss} is always lower than three seconds, which is two times smaller than the times measured on gels swollen with water. They reached steady state deformation in about 7,5 s (Zanina and Budtova, 2002).

One case with tip appearance was added to each of the Figure 3.5 (a) to (c). The kinetics of tip growth is represented by the series L'/L_o. L'/L_o also goes to a steady value that is reached soon after the tips appeared. In the case of gel swollen with the 1 % HPC solution, the steady value of L'/L_o is much larger than the steady state value of L/L_o and tips can still grow larger in the case of gels swollen with water (Zanina and Budtova, 2002). The difference between both deformation parameters is less important for the gels swollen with 5 % and 10 % HPC solutions. In the next chapter, we will take a closer look at what is expressed quantitatively here: tips of the 1 % HPC solution grow larger than tips of the other used solutions.

In order to know whether initial particle size has an effect on deformation kinetics, the times to reach the steady state deformation were compared at the same stress for particles having different initial sizes. This is depicted in Figure 3.6 for particles submitted to a shear stress of 1100 Pa. The steady state times for the different particles are close. This figure suggests that initial particle size does not affect deformation kinetics in the range of particle sizes studied.

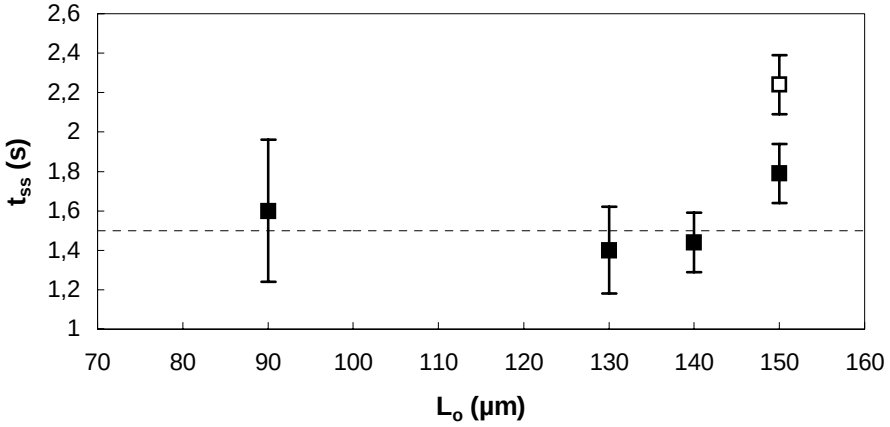

Figure 3.6: Effect of initial size on t_{ss}. Gel swollen with 10 % HPC solution, Q = 80 g/g immersed in PDMS 200. Shear rate ~5,5 s^{-1}. The open symbol represents steady state of tips.

Time-related data obtained from experiments with the counter rotating shear cell should be treated with great care, especially the first seconds of an experiment are very sensitive to errors. Because of the manual nature of shear application to the system 'gel particle in silicone oil', the shear acceleration differs from one experiment to another. As long as this acceleration is faster than the shape adaptation of the gel to the establishing stress field, observed kinetics are dominated by the gel particle. On the other hand, when the shear field is applied very slowly, the gel shape will permanently be in equilibrium with the present field. The observed kinetics are then governed by the shear acceleration and do not give any information about the gel particle. In the tests run for this study on, the shear field was stabilised as fast as possible, yet, always starting from zero to avoid too strong shocks to the

particle that might induce premature ejection of solvent. These tests showed that the scheme in Figure 3.4 gives a general representation of the order of appearance of the phenomena. Steady state deformation of the core particle is reached soon after the tips appear. In all cases, times are very short: a complete steady regime is established within three seconds. Off course, this cannot be observed when the application of the steady shear field lasts longer. The comparison of fast and slowly applied shear fields learned that it is extremely complicated to obtain correct information on such fast phenomena with the present counter-rotating set-up.

3.4.2 Stress-effect on steady state deformation

The steady state deformation is analysed in this part. Before proceeding to the results on gels swollen with linear polymer solutions, results obtained by Zanina and Budtova (2002) on gels swollen with water are recalled.

3.4.2.1 Former research: gel swollen with water (Zanina and Budtova, 2002)

Earlier work performed at CEMEF by Zanina and Budtova (2002) learned that gel particles swollen with water deform only to a small extent as shows Figure 3.7. The data published by Zanina et al. (2003) were calculated using the hypothesis that the droplet orientation was 45 ° with respect to the flow direction. Our orientation measurements (2.3.1) showed that this is somewhat exaggerated. Besides, no correction was made at low stresses, so that at zero stress, their graphs indicated deformation 1,4 for a non-deformed particle. Since neglecting any small orientation would not significantly change the estimated error, we recalculated their data in order to make comparison with the results in the rest of this chapter straightforward.

The figure shows that the particle height hardly varies for stresses up to 2000 Pa. At higher stresses, a slight height increase is monitored. The deformation of length saturates at 1,40, but cones (represented by L'/L_o) can grow very large as stress increases. Tips appeared at the very low stress of ~ 250 Pa. From that point on, W/W_o is not shown anymore. Because of the volume in the cones, the calculation of the particle width is not straightforward anymore.

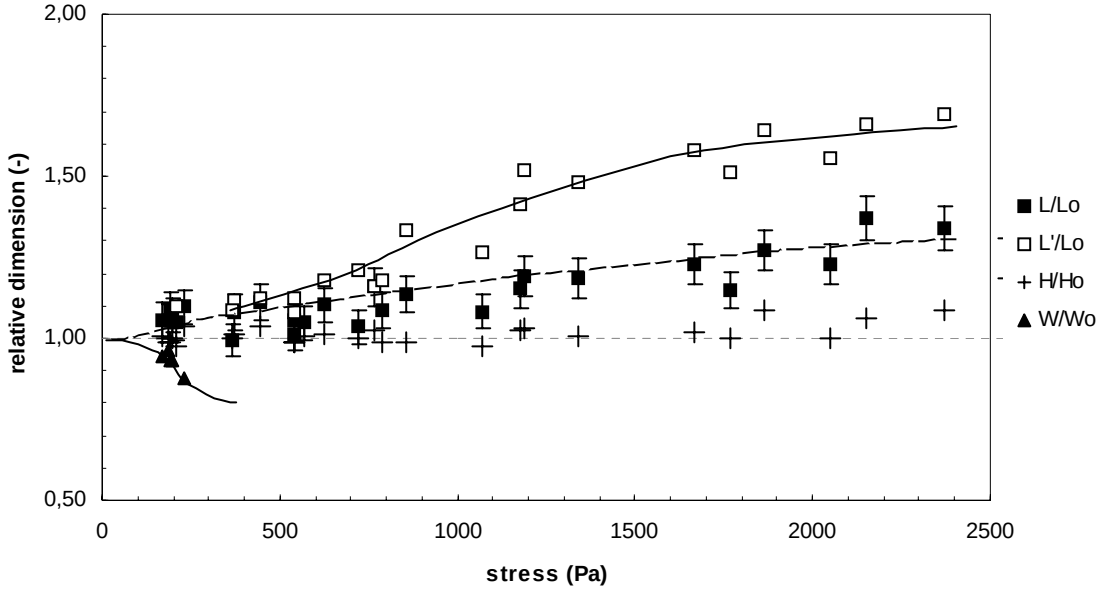

Figure 3.7: Stress-deformation curves for Aqua Keep particles swollen with water (Q = 50 g/g). Lines are added to guide the eye. (Data recalculated from Zanina and Budtova, 2002).

3.4.2.2 Gels swollen with 1 % HPC

The relative dimensions at steady state of gel particles swollen with a 1 % HPC solution are shown in Figure 3.8 and Figure 3.9. Tips attached to the particle – if present – are represented in the series L'/L_o. At stresses below 300 Pa, the gel keeps all the solvent inside and the deformation seems to increase linearly with increasing stress. The deformation continues to increase more slowly as solvent tips are released, and finally levels off at a relative length of 1,3.

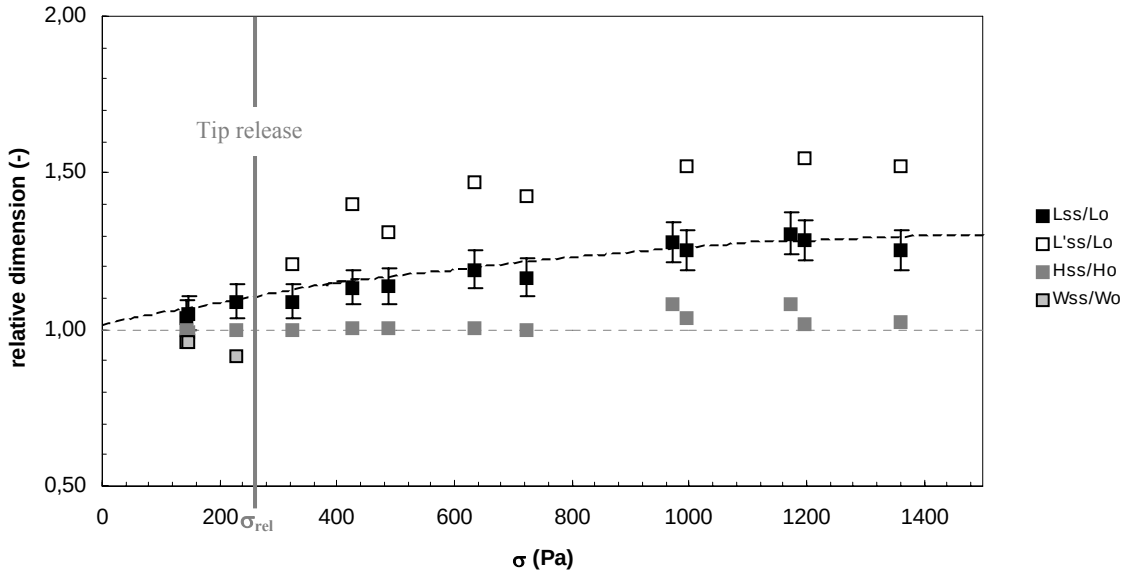

Figure 3.8: Deformation as a function of stress of Aqua Keep particles swollen with 1 % HPC-solution (Q = 80 g/g). Particles from which droplets were ejected are excluded. D_o= 110-160 µm. Dashed lines are drawn to guide the eye.

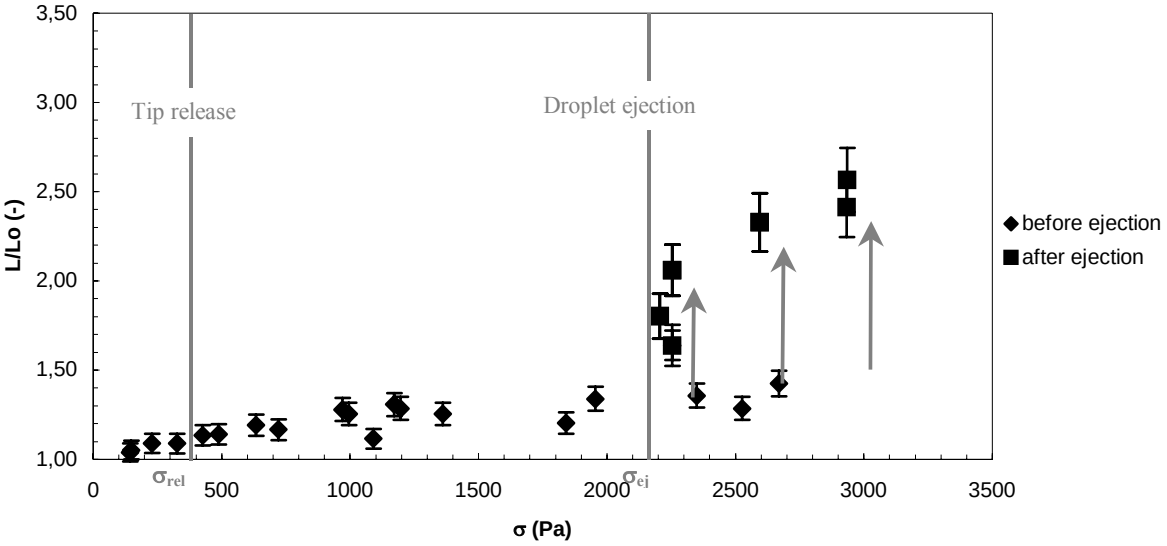

Figure 3.9: Pseudo-steady state stretching ratio as a function of stress (♦) for particles swollen with 1 % HPC (Q = 80 g/g). The stretching ratio increases to a second steady value (■) after tips have been ejected.

At stresses around 2500 and higher, droplets are pinched off the tips and dispersed in the matrix. As no more solvent is provided to the tips, the tip volume decreases irreversibly until they are entirely consumed. After the tips are gone, the particle is further stretched and larger deformations are observed. Arrows indicate this in Figure 3.9.

The height-ratio is one for stresses lower than 1000 Pa. At higher stresses, the relative height raises a few percentages above its initial value.

3.4.2.3 Gel swollen with 5 % HPC

Figure 3.10 shows the relative dimensions at steady state of gel particles swollen with a 5 % HPC solution. Tips appeared at stresses around 900 Pa, but were too tiny to be measured accurately. Therefore, they are not represented in the graph.

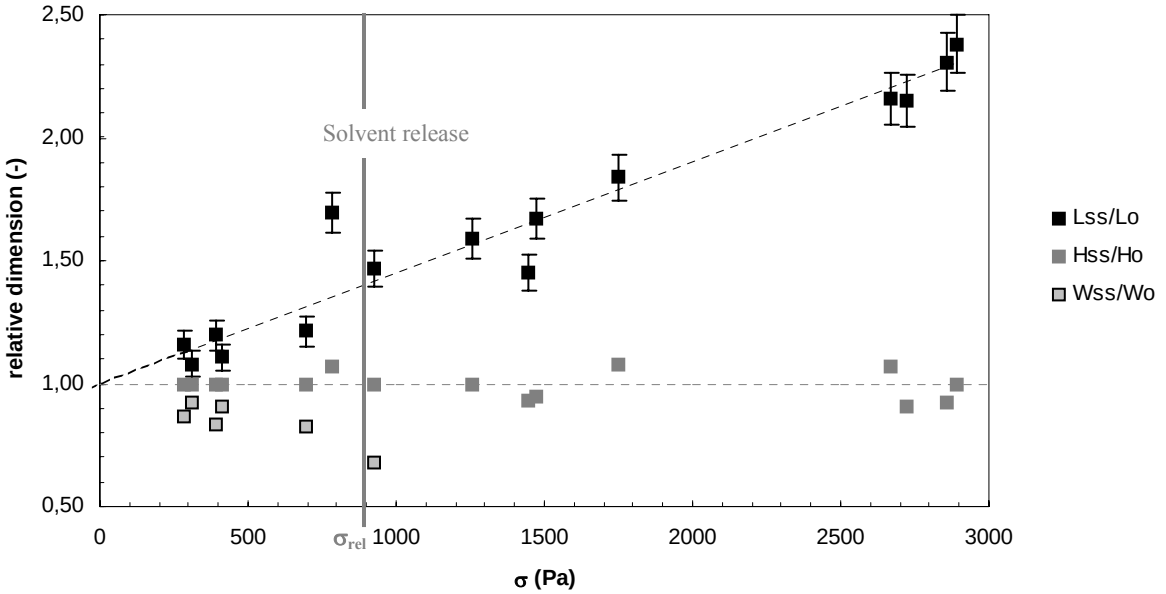

Figure 3.10: Stress-deformation data for particles swollen with 5 % HPC (Q=80 g/g). D_o= 110 µm.

Before tips appear, the relative length of the particle increases linearly with increasing stress, while the height remains practically unchanged and the width decreases. One can see in the graph that the linear increase continues invariably when tips are present: the slope of the linear fit through data points before release is 0,42 kPa^{-1} against 0,45 kPa^{-1} for the full data set (points before and after release). It must be noted that the tips always remain very small with respect to the gel particle for this combination of gel and solvent.

At first the particle height does not change under shear. Yet, at higher stresses, deviations of H/H_o from unity are observed. This height increase is discussed in **4.3**.

3.4.2.4 Gel swollen with 10 % HPC

Figure 3.11 shows a typical deformation-stress curve of a gel particle swollen with 10 %HPC.

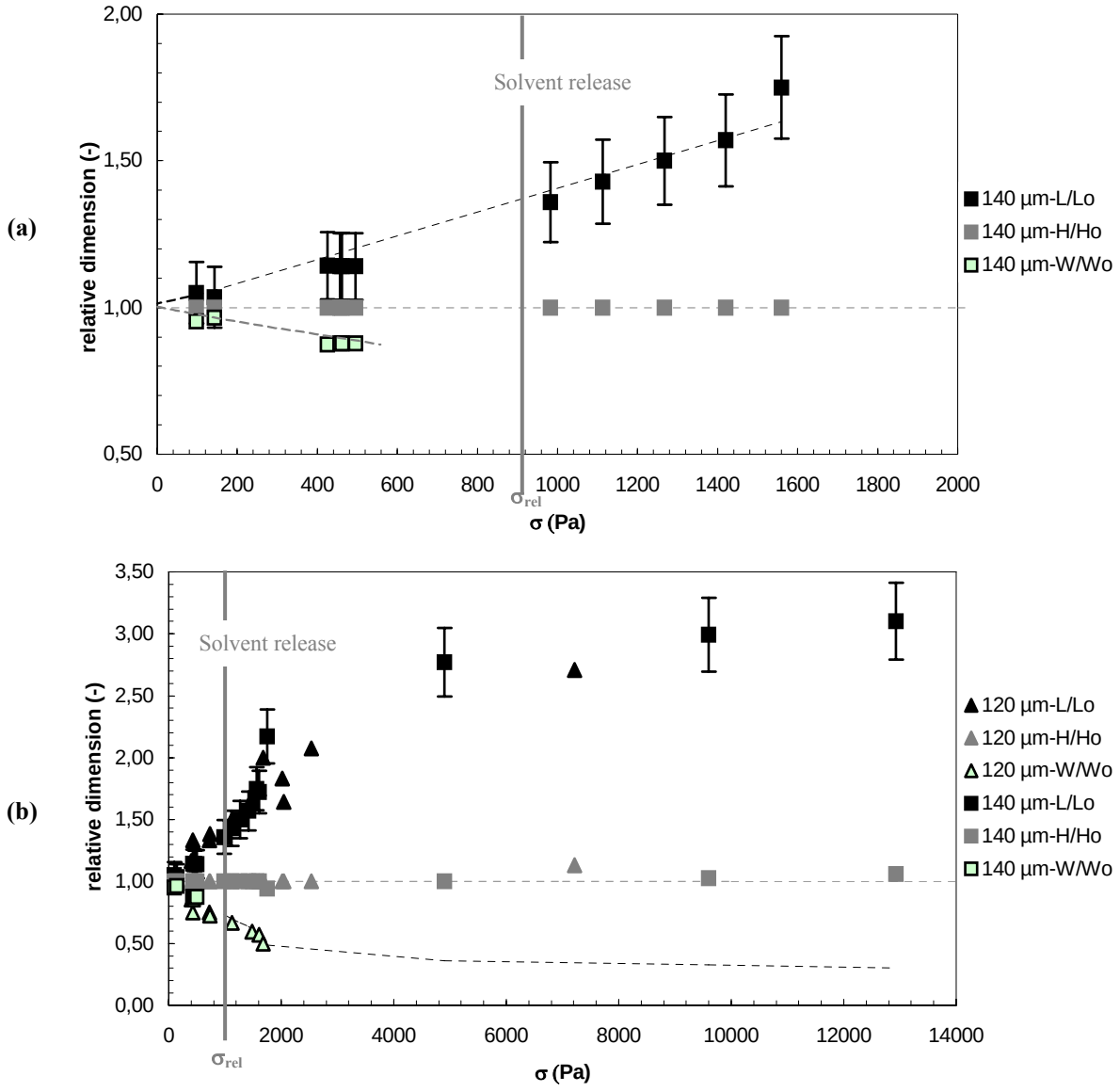

Figure 3.11: Pseudo-steady state deformation as a function of applied shear stress for particles swollen with 10 % HPC to 80 g/g, L_o= 140 (■) and 120 (▲). Upper graph is a close-up of the initial part.

The data in the figure are for particles of initial diameter 120 and 140 µm swollen to 80 g/g. The stress at which tips were first observed is around 900 Pa. Like in the case of gels swollen with 5 % HPC, this point is not characterised by a sudden change in the stress-deformation curve. The released tips are very small and can hardly be seen. The steady-state deformation of a gel particle continuously increases with increasing shear stress up to 10000 Pa. The increase is linear for stresses below 1500 Pa. At stresses above 2000 Pa, the dimensionless length saturates at about 3,3. Increasing stress above 10000 Pa does not lead to further increase of the steady-state deformation of the gel particle.

3.4.2.5 Discussion

Three main parameters were varied during the experiments described above: solvent concentration, initial particle size and degree of swelling. The effect of each of them on the steady state deformation is analysed in the following sections.

Effect of HPC solution concentration on gel deformation

The deformation data shown in sections 3.4.2.2 - 3.4.2.4 are compared in Figure 3.12. All gels are swollen with 80 g/g of different HPC solutions. Changing the HPC concentration actually implies two main changes:

- the amount of water absorbed by the gel is slightly different. It varies between 79 g/g and 70 g/g for the 1 % and the 10 % HPC solutions respectively;
- the solvent viscosity is different, as shown in the Materials section.

Only data at stresses below σ_{rel} are considered here. Under theses circumstances, W is known. The data can thus be represented in terms of Taylor deformation. The stress ranges covered by the series are not the same since σ_{rel} depends on the solution concentration.

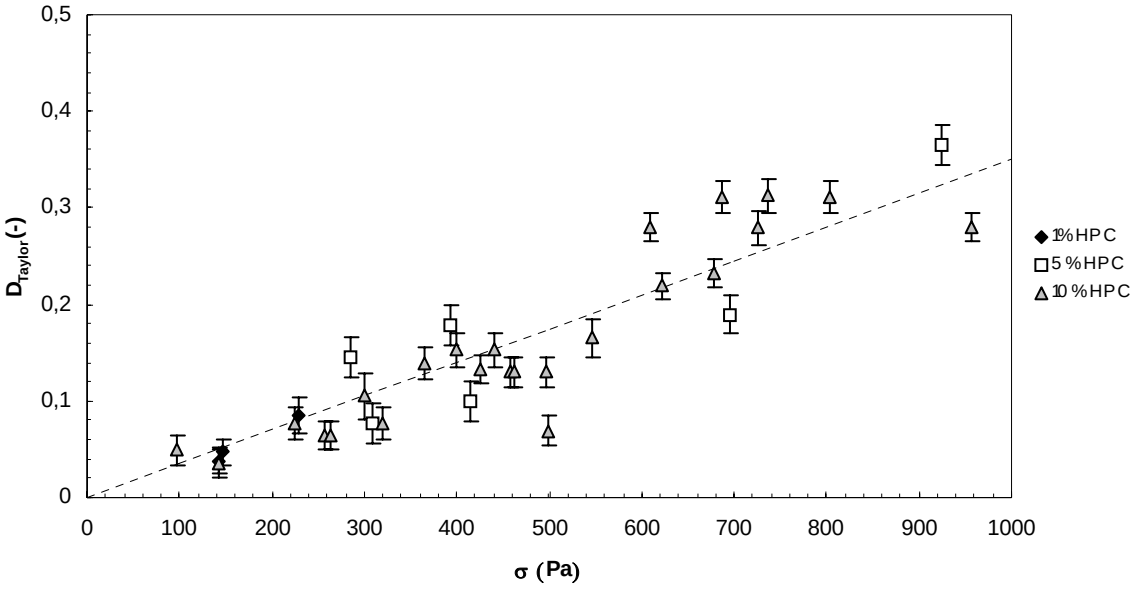

Figure 3.12: Steady state deformation before release as a function of applied shear stress for Aqua Keep particles swollen with different HPC-solutions at 80 g/g. Dotted line is the common linear fit through data points.

The three series are coincident in the respective ranges of stress before solvent release. At equal degree of swelling, the HPC concentration in the solution does not affect gel deformation in the range of concentrations tested. This means as well that gel deformation is independent of solvent viscosity as long as all the solvent is trapped in the gel. The tendency of the L_{ss}/L_o increase is linear in this range and so is D_{Taylor}:

→ Before solvent release, gel length and Taylor deformation increase linearly with applied shear stress: $L/L_o \propto \sigma$ and $D_{Taylor} \propto \sigma$ **[3.11]**

Comparison of Figure 3.7, Figure 3.8 and Figure 3.11 shows that the maximum steady state deformation of gels swollen with water and with 1 % HPC solution is much lower than the maximum deformation of gels swollen with the 10 % HPC solution. This difference could be related to the different sizes of the respective tips attached to the edges of the particles. Water as well as the solution with the lowest polymer concentration (1 %) were released at rather low stresses and large solvent tips were formed at the edges of the particle. L_{ss}/L_o levelled off at a saturation value from this point on. The two solutions with higher concentrations (5 and 10 %) were released at higher stresses and tips remained small because the released solvent is detached practically as soon as it is released. The gels swollen with 5 % en 10 % solutions deformed further even when tips were present and in the early stages of ejection. The explanation for this difference must be sought in the different viscosities and will be discussed in section 4.2.1. In all cases, the solvent viscosity is much lower than the matrix viscosity. The stress exerted at the particle's edges by the solvent is thus far lower than the stress exerted by the viscous matrix. This hypothesis is confirmed by the behaviour of gel particles swollen with 1 % HPC (Figure 3.9): when the solvent is detached at high stresses, the volume of the tips decreases and a sharp increase of the gel deformation can be observed. Such increase of deformation could not be observed on gels swollen with water since no droplets could be detached from the tips.

Summarising, deformation saturates at a given stress. Large tips, if present, initiate saturation of deformation. If tips are small compared to the particle size, deformation is limited by the limited extensibility of the network chains. Size and viscosity of the tips vary with solvent concentration. C_{HPC} has only an indirect effect on particle deformation via the release and ejection phenomena.

At stresses above 1000 Pa, increase of the particle height is observed. This phenomenon is discussed in **4.3**.

Effect of particle size on gel deformation

The effect of initial particle size on steady state deformation of gel particles is represented in Figure 3.13. Only particles that did not eject any solvent are considered. The particles in the figure are swollen with 10 % HPC. That means released tips are very tiny and do not entail significant solvent loss out of the core or the particle. Particles with tips are included to enlarge the data series. It should be noted that ejection started at lower stresses for larger particles (4.2.1). Therefore, the series do not all cover the same stress range.

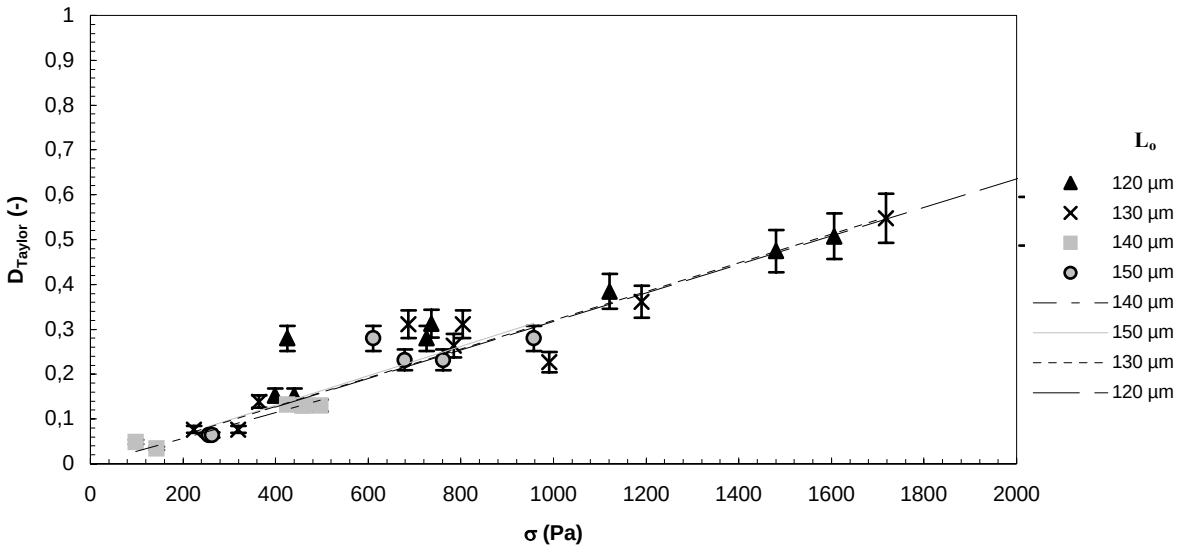

Figure 3.13: Steady state deformation (without tips) as a function of applied shear stress for different particle sizes. Particles are swollen with 10 % HPC, Q = 80 g/g. Lines are linear trends through the data series.

Linear trend lines were fitted through the data series for each particle size. The slopes were not significantly different for the different series (varying between 0,29 and 0,33 kPa^{-1}) and trend lines are coincident within the range of experimental precision. These observations show no effect of initial particle size in the presented range of sizes and stresses. This is characteristic for elastic materials. Following conclusion can be derived from Figure 3.13:

→ Gel deformation before solvent release or with only very small amounts released is independent of initial particle size: $L_{ss}/L_o \neq f(L_o)$ **[3.12]**

The initial size does affect the moment at which solvent ejection starts. In this way, it determines the validity range of rule [3.12]. Droplet deformation on the other hand, is dependent on particle size via the capillary number.

Effect of degree of swelling on gel deformation

In order to assess the effect of degree of swelling on gel deformation, gels swollen with a 5 % HPC solution were prepared at three different degrees of swelling: 80 g/g, 160 g/g and 210 g/g (= Q_{eq}). Particles were considered at stresses below release stress. Under theses circumstances, W is known and deformation is thus given in terms of Taylor deformation in Figure 3.14 and linear trend lines are fitted with the data. The slopes of linear trend lines appear to be inversely proportional to the degree of swelling of the gel in the investigated range of Q (inset Figure 3.14):

$$D_{Taylor} = k * \sigma \quad \text{with} \quad k \propto \frac{1}{Q} \qquad \textbf{[3.13]}$$

This observation can be understood by the fact that higher degrees of swelling imply higher stretching of the gel network. Dubrovskii and Rakova (1997) and Horkay et al. (2000), a.o., measured increasing shear moduli for highly swollen gels. Further stretching of the chains becomes more difficult as their initial stretching is higher. That is why at fixed stress D_{Taylor} decreases with increasing degree of swelling. This phenomenon alike strain-hardening may be the reason for the dependence of k on the

degree of swelling: the higher the degree of swelling, the lower k and the more effort it needs to reach a given deformation.

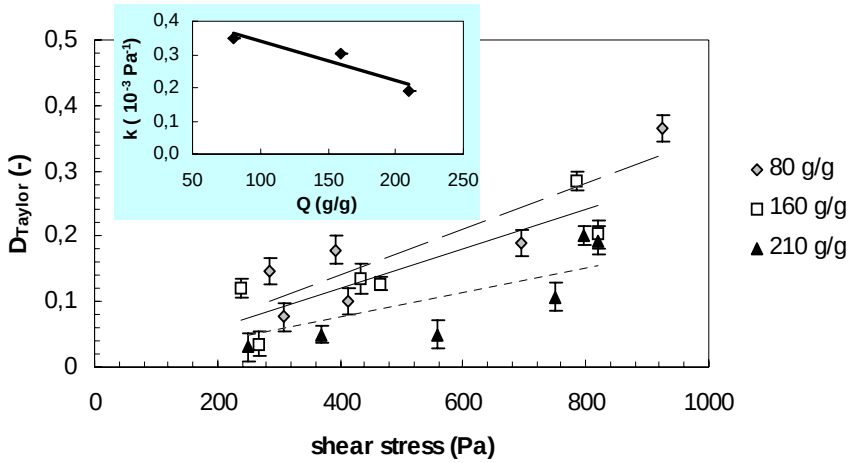

Figure 3.14: Effect of degree of swelling on steady state deformation (without tips) for gel particles swollen with 5 % HPC. Lines are linear fits through the series 80 g/g (dashed line), 160 g/g (full line), 210 g/g (dotted line). Inset shows the slopes k of the straight lines as a function of degree of swelling.

3.4.3 Determination of the shear modulus

In order to better understand and describe gel deformation under shear, the shear modulus has to be known. No information was available on the shear modulus of Aqua Keep particles swollen with either water or HPC solutions. Supplier's data specify μ around 1800 Pa for particles swollen with 60 g/g of a salt solution, but no data are available on the degrees of swelling or the solvents used in this study. The modulus of a single microgel particle was never measured using rheo-optics. Mechanical properties of gels are mostly determined using compression or penetration test (see 1.6.2). It is current practice in literature to analyse e.g. compression experiments with the simplified Mooney-Rivlin equation to determine the shear modulus of a gel. We used the rheo-optical deformation measurement to determine the shear modulus of the Aqua Keep microparticles swollen with water or with HPC solutions. Analogously to literature on other types of tests, the Mooney-Rivlin equation was used for data analysis. For shear deformation, this equation has the following form:

$$\sigma = \mu\left(\lambda - \frac{1}{\lambda}\right) \qquad \textbf{[3.14]}$$

where $\lambda = L/L_o$. Since we cannot determine the stress inside the gel particle, the average stress in the surrounding fluid is taken as a first simple estimate of this value. To determine the shear modulus, a graph was plotted with stress in the ordinate and $(\lambda - 1/\lambda)$ on the abscissa. Only data obtained before any release were used. The slope of the straight line trough the data points gives the shear modulus. This procedure was repeated for each solution and degree of swelling and the results are shown in Figure 3.15 and Figure 3.16.

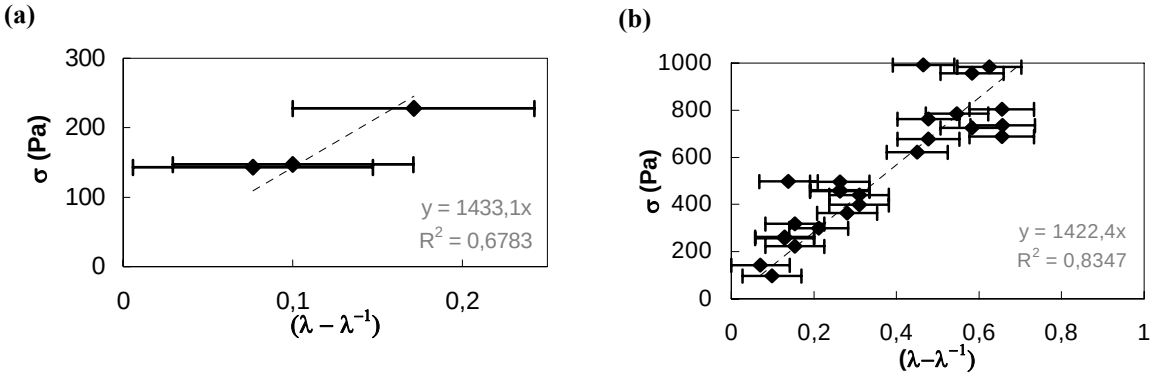

Figure 3.15: Determination of the shear modulus of gels swollen at Q = 80 g/g in different HPC solutions. (a) 1 %; (b) 10 %.

It was difficult to determine the shear modulus for the gel swollen with the 1 % HPC solution. Only data where no solvent was released should be considered. Since solvent is released at very low stresses with this solvent, the data set available for modulus determination was limited. The situation was more comfortable for the gels swollen with 5 % and 10 % solutions.

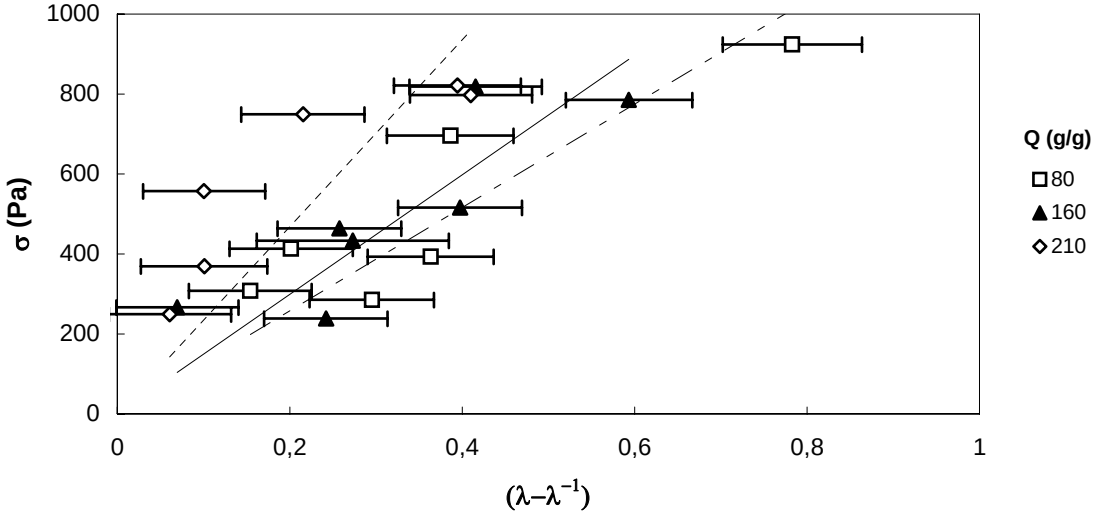

Figure 3.16: Determination of the shear modulus of gels swollen with 5 % HPC at different degrees of swelling.

For the gels swollen to 80 g/g in the different solutions, the moduli found differed not more than 100 Pa. Considering the 10 % error on the stress, one may say that the modulus is not dependent on the HPC concentration in the studied range. The moduli for the different degrees of swelling tested with the 5 % solution are clearly different, as can be seen in Figure 3.16. The modulus increases with increasing degree of swelling. Numerous studies on the dependence of shear modulus on degree of swelling have been published (see review in Chapter 1). The trend we obtained on our gels is shown in Figure 3.17 and compared to data from Horkay et al. (2002) on sodium polyacrylate gels. In the Gaussian region, the slope of the dependence of μ on Q should be –1/3; the slope becomes positive at degrees of swelling higher than a typical value (200 g/g in Figure 3.17b). The moduli we found are an increasing function of increasing Q. The gels used must thus be in the non-Gaussian regime. This is not surprising since we worked with highly swollen polyelectrolyte gels.

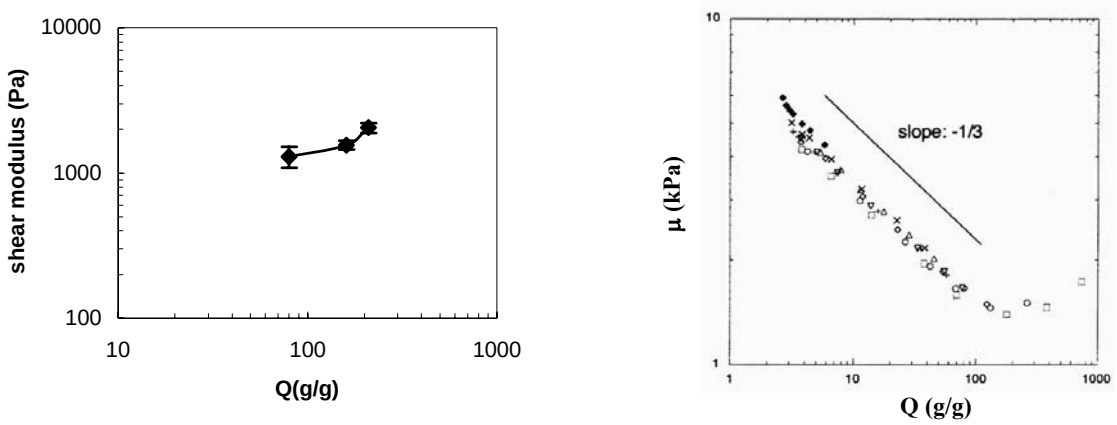

Figure 3.17: Gel swollen with 5 % HPC. (a)Effect of Q on μ. (b) Comparison with tendency from literature [From Horkay et al., 2000].

The moduli determined in this section will be used as characteristic parameter of the gels in §3.5.

3.4.4 Comparison of a swollen gel with a solvent droplet

Shear experiments were also performed on isolated droplets of the different HPC solutions immersed in silicone oil in order to evaluate the effect of entrapping a polymer solution in a chemical network. Figure 3.18 shows the deformation of a gel particle swollen with 10 % HPC and of a 10 % HPC droplet at similar stress levels. Two main differences can be distinguished. First, the droplet is stretched to far higher elongation ratios than the gel particle. Second, the gel particle reaches its steady state much faster than the droplet.

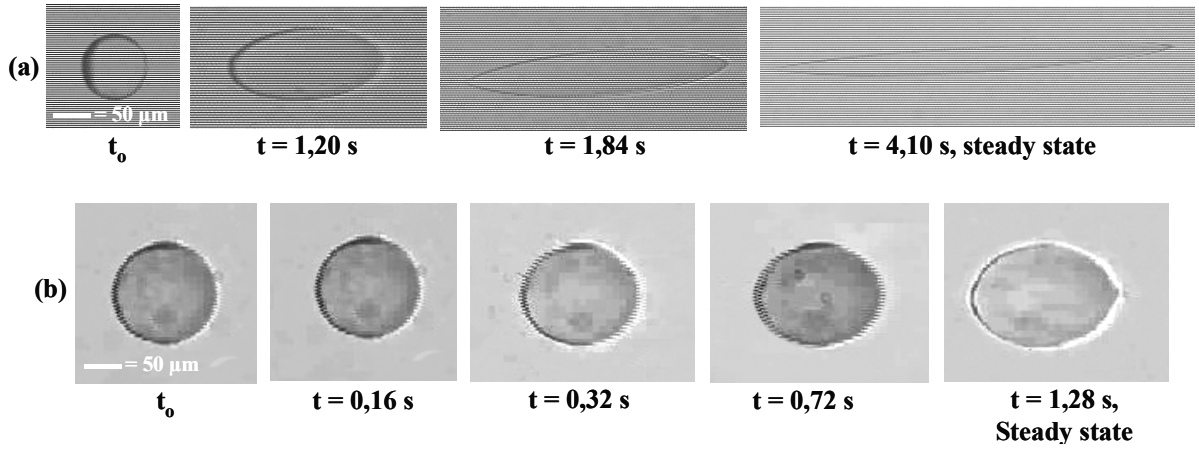

Figure 3.18: Deformation of a 10 % HPC droplet at 850 Pa (a) and of a gel particle swollen with 10 % HPC (Q = 80 g/g) at 910 Pa (b). Matrix is PDMS 200.

The dimensionless axes of deformed HPC droplets are shown as a function of Capillary number in Figure 3.19. The length of a 10 % HPC droplet increases rapidly with Ca while both height and width decrease. HPC droplets deform into an ellipsoid at low Ca. Their shape becomes cigar-like with pointed edges when Ca is increased (see also Figure 3.18a). Above a critical Ca, droplets are detached from the edges and dispersed in the matrix. For the present study, only droplets that remained intact were considered.

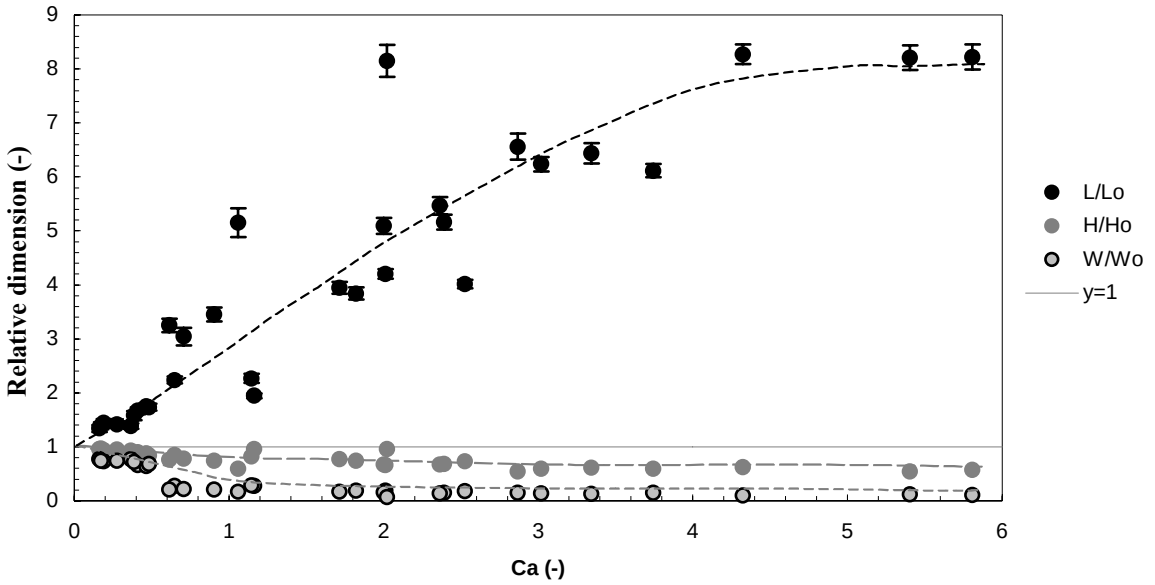

Figure 3.19: Relative dimensions at steady state of a 10 % HPC droplet immersed in PDMS 100 and 200.

Deformation kinetics of a droplet and a swollen gel particle are plotted together in Figure 3.20. The droplet and the particle compared here were both spherical at rest and had the same initial diameter. It may thus be considered that the volume of solvent is the same, since the polymer network occupies only a small volume fraction in the gel. The figure shows that in the same shear field, the gel is far less stretched than the polymer droplet. This is illustrated for a whole range of shear stresses in Figure 3.21.

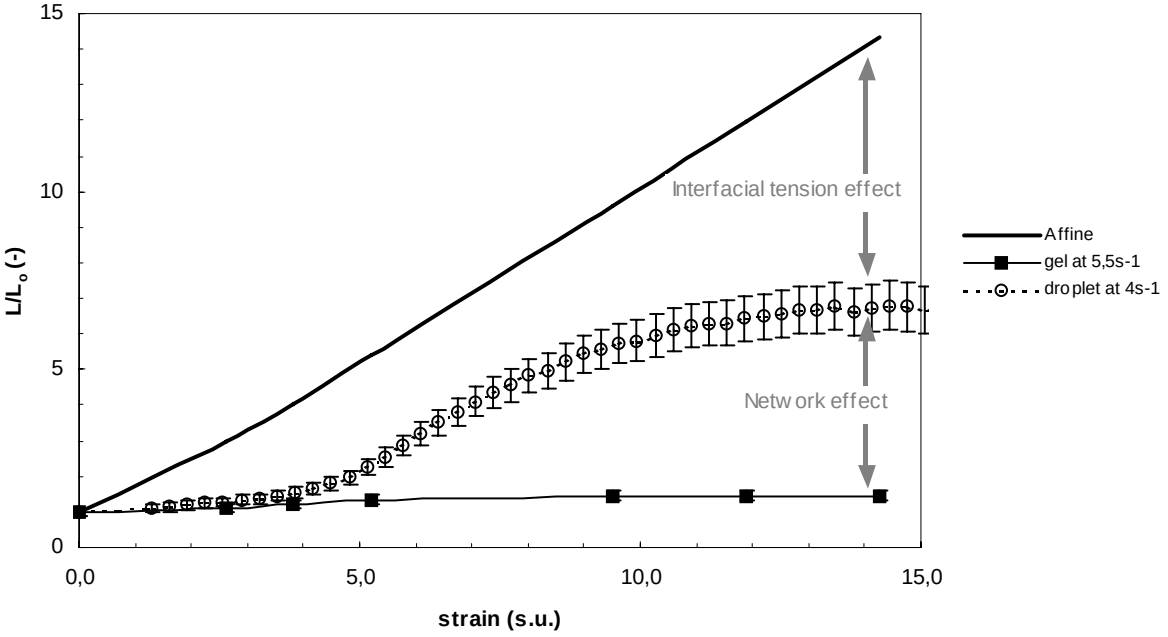

Figure 3.20: Deformation kinetics of a gel particle swollen with 10 % HPC (80 g/g) compared with affine deformation and with deformation of a 10 % HPC droplet.

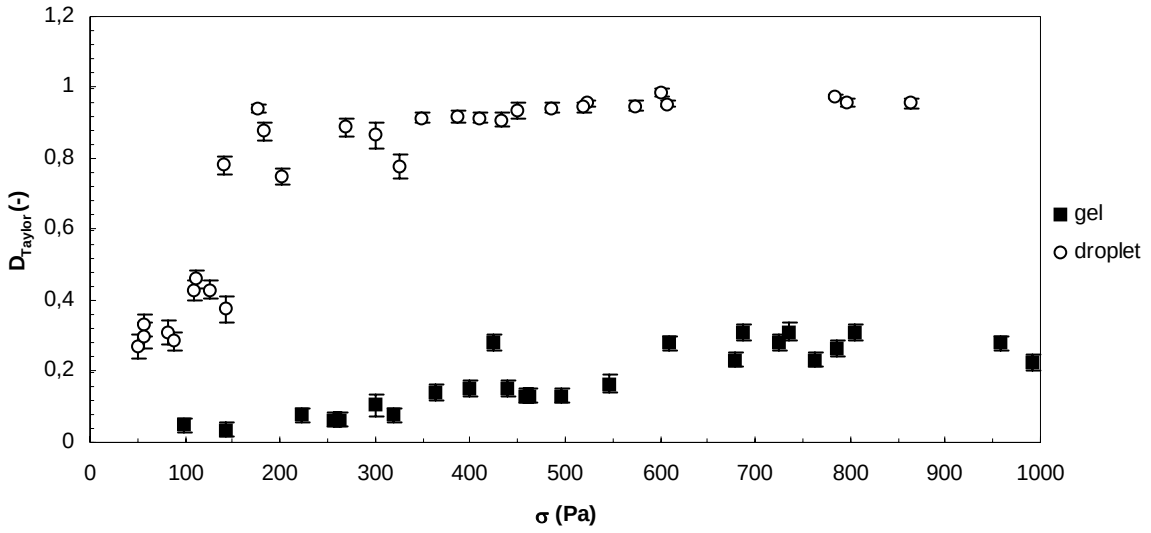

Figure 3.21: Steady state Taylor deformation of swollen gel particles, 80 g/g with 10 % HPC solution, and of droplets of the same solution. Dotted lines are added to guide the eye.

It is clear from Figure 3.11 and Figure 3.19 to Figure 3.21 that a droplet of the same solvent as incorporated in the gel, deforms to a much wider extent than the solvent captured in the crosslinked network. As shows Figure 3.21, the droplet deformation reaches values close to unity at low stresses already, whereas the deformation of the gel particle hardly reaches 0,2 at a stress of 1000 Pa.

Consider now the factors governing the deformation of an object. For a Newtonian droplet in a Newtonian matrix, only shear stress and interfacial tension play a role. Interfacial tension withholds the droplet from deforming in an affine way with the flow. In the case of a swollen gel particle, elastic forces due to the crosslinks in the network also resist to deformation. Because of the high fraction of solvent in the swollen gel, it is supposed that the interfacial tension droplet-matrix is the same as the interfacial tension swollen gel-matrix. Thus, the elastic forces must be held responsible for the differences between droplet and gel deformation.

3.5 Modelling of gel particle deformation under shear

The system studied in the previous paragraphs was never described in literature before and no theories exist that model the deformation of a chemically cross-linked sphere under shear.
Deformation models for isolated droplets were briefly summarised in paragraph 3.3. However, the case of a chemically cross-linked network forming the inclusion was never analysed. Therefore, the equilibrium deformation data were compared to models established for isolated droplets in this paragraph. Following analysis considers particles of which deformation is not affected (limited) by the presence of large tips.

3.5.1 Affine deformation model

The relative length of an inclusion that deforms in an affine way with the matrix is only dependent on shear strain and can be described as follows (Janssen, 1993):

$$\frac{L}{L_o} = \sqrt{1 + \frac{\gamma^2}{2} + \frac{\gamma}{2}\sqrt{4+\gamma^2}} \qquad [3.15]$$

γ denotes the shear strain and is the product of shear rate and time $\dot{\gamma} * t$. A droplet in an emulsion will only deform affinely if the shear forces are much more important than the interfacial forces.

The deformation of a gel particle and a solvent droplet are depicted in Figure 3.20 and compared with the affine prediction. Neither gel, nor droplet follows the affine deformation, not even at low strain. The reason why the droplet does not follow the affine deformation is that interfacial forces are too strong to be neglected before the shear forces. For the gel particle, network elasticity is a second force opposing to shear-induced deformation. The models for droplet deformation described earlier in this chapter take interfacial tension into account. We will consider the remainder of this paragraph to the comparison of those models to our gel deformation data.

3.5.2 Comparison with models for droplet deformation: modified Cox model

Cox (1969) described a model for droplet deformation only as a function of the dimensionless parameters p and Ca (equation [3.7]). The model is depicted for different values of p in Figure 3.22. Experimental data for swollen gel particles are added. The shape of the gel particle deformation curve is similar to the shape of the curve describing Cox' model, but the curve is shifted. The model is thus not ready-to-use on deformed gel particles.

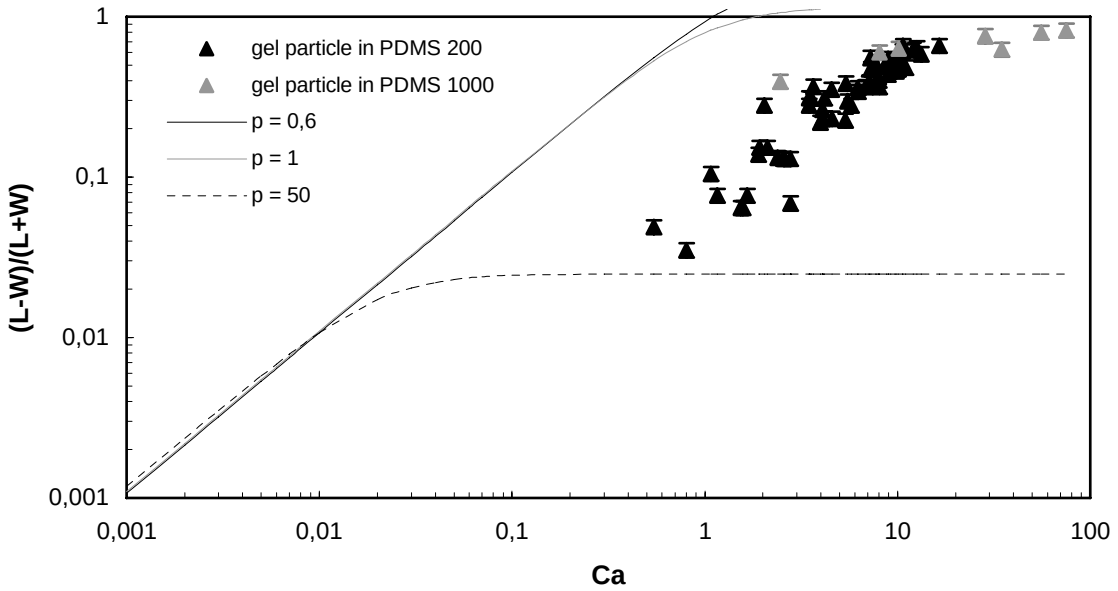

Figure 3.22: Experimental deformation data for gel particles swollen with 10 % HPC solution (Q = 80 g/g) compared to Cox' model for different values of p.

Models established for viscous droplets cannot be applied directly to gel particles. Two important questions arise due to the differences between a gel particle and a liquid droplet:

- How to define the viscosity ratio p for a gel?
- How should the capillary number be interpreted when the suspended object is a gel particle?

The answer to the first question: "What does viscosity ratio mean for a suspension of gel particles?" is not evident. Different options are:

- to set p as the ratio between the viscosities of gel solvent and matrix. This does not seem logic since the solvent is entrapped in the gel and is therefore not free to behave in the way it would behave if it were present as a solvent droplet; the absorbing gel network strongly constrains the solvent behaviour. This was illustrated in 3.4.4.
- the most logic option seems to replace the droplet viscosity by a 'gel viscosity'. Some authors defined gel viscosity as infinite (Kavanagh and Ross-Murphy, 1998). This would lead us back to the case of a suspended solid particle, which is clearly not representative for the discussed case. Opposite to a rigid particle, a gel particle deforms when it is submitted to shear stresses.
- parameter p could as well be derived from the rotation period, applying the equations for surface circulation in a sheared liquid droplet (section 3.2.2). Yet, the values found were unexpectedly low for a gel (p = 0,6 – 0,7).

Since none of these options is completely satisfying, p will remain an adjustable parameter in a first approach.

The second question is more straight-forward to tackle. One should remember that the capillary number was defined as the ratio of deforming to resisting forces (equation [2.16]). In the case of the described experiments, only viscous forces tend to deform the inclusion, but in the denominator, a term accounting for the elasticity of the network that resists to deformation should be added. It is chosen to express this elastic force as twice the elastic modulus as done by Ghodgaonkar and Sundararaj (1996). The accounting for elasticity results in a modified capillary number Ca*:

$$\frac{\text{deforming forces}}{\text{resisting forces}} = \frac{F_{viscous}}{F_{interfacial} + F_{elastic}} = \frac{\eta\dot{\gamma}}{\Gamma/R_o + 2\mu} = Ca^* \qquad \textbf{[3.16]}$$

The experimental range of modified capillary numbers Ca* is [0,03; 5] whereas the classic capillary number interval was [0,5; 100].

Comparing the forces in the denominator gives interfacial stress of ~200 Pa versus elastic stress of 3000 Pa for a particle with an initial diameter of 120 μm. Interfacial forces depend on initial particle size, contrary to elastic forces. F_{int} varies roughly between 100 and 300 Pa in the range of particle sizes used. The resistance against deformation is thus dominated by the elastic forces.

The modified Cox model is obtained by replacing the capillary number by the modified capillary number as expresses equation [3.17].

$$\frac{L-W}{L+W} = \frac{5(19p+16)}{4(1+p)\sqrt{(20/Ca^*)^2+(19p)^2}} \qquad \textbf{[3.17]}$$

This modified Cox model approaches the gel particle from a 'liquid' point of view using the same approach as Gadgoankar and Sundararaj. Yet it is true that for elastic materials, the elastic stress is generally expressed as G*γ. The model could be refined in this way and the resulting equation would then become implicit in gel particle dimensions.

The graph in Figure 3.23 shows the experimental deformation data together with plots of the modified Cox model for different values of p. The values chosen are the viscosity ratio between the solvent and PDMS 200 and the p-value derived from the rotation measurements. These values are not able to predict the deformation saturation at high Ca*. A fitting procedure based on least square differences with p as adjustable parameter gave 1,5 as optimal value for p. The model fits the experimental data points well when p is set 1,5. Gel deformation in PDMS 200 and in PDMS 1000 follow the same tendency, since gel deformation is a function of stress. It needs only one p-value to describe the full gel deformation curve.

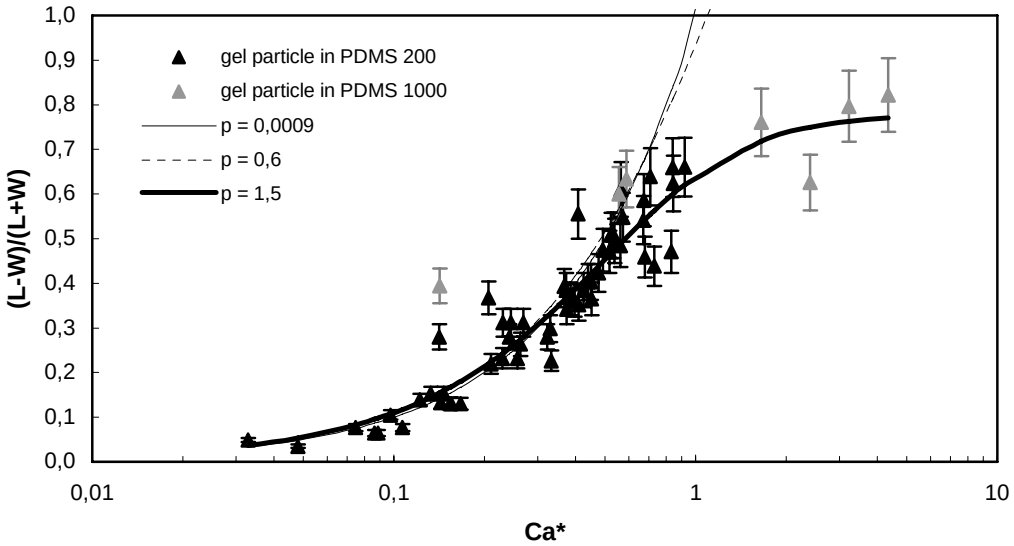

Figure 3.23: Experimental data compared to the modified Cox model with different values of p. Gel swollen with 10 % HPC before solvent ejection. Q = 80 g/g.

The modified Cox model gives good predictions of deformations of gels swollen with 10 % HPC to 80 g/g. Let us now verify whether the model remains valid for gels swollen with the other HPC solutions. This is shown in Figure 3.24 for 1% HPC and in Figure 3.25 for different degrees of swelling in 5 % HPC. For the particles swollen with 1 % HPC, only particles at stresses lower than the release stress are considered because of the important effect of the released tips on deformation (Figure 3.8).
Figure 3.24 and Figure 3.25 illustrate that the modified Cox model also describes the deformation data for gel particles swollen with other solvents and to different degrees of swelling.

Because of the limited number of data for gels swollen with 1 % HPC, no proper p-value could be fitted for this series. However, the points coincide with the curve with p = 1,5, the optimal p found for particles swollen with 10 % HPC.

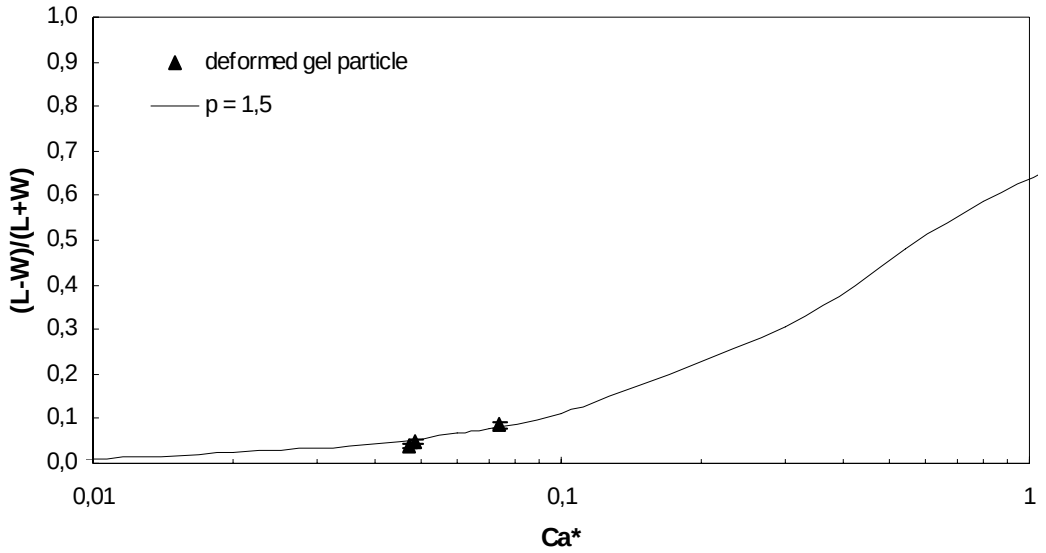

Figure 3.24: Experimental data compared to the modified Cox model for gels swollen with 1 % HPC solution (Q = 80 g/g) suspended in PDMS 200.

The particles swollen with 5 % HPC have only tiny tips that do not affect deformation, as was shown in Figure 3.10. Optimal p-values were found by the same fitting procedure as used for the particles swollen with 10 % HPC and they are shown in the graphs. The optimal p-value for the gel swollen to 80 g/g is 1,4, which is close to the 1,5 found for gels swollen in 10 % HPC. For the higher degrees of swelling, the optimal p-value is lower.

Summarising, the modified Cox model is a simple first approach directly derived from liquid droplet deformation theories to describe gel deformation under shear flow. The model uses a new capillary number that accounts for the elastic properties of the gel via its shear modulus. Yet, it remains unclear what physical meaning should be assigned to parameter p in this context.

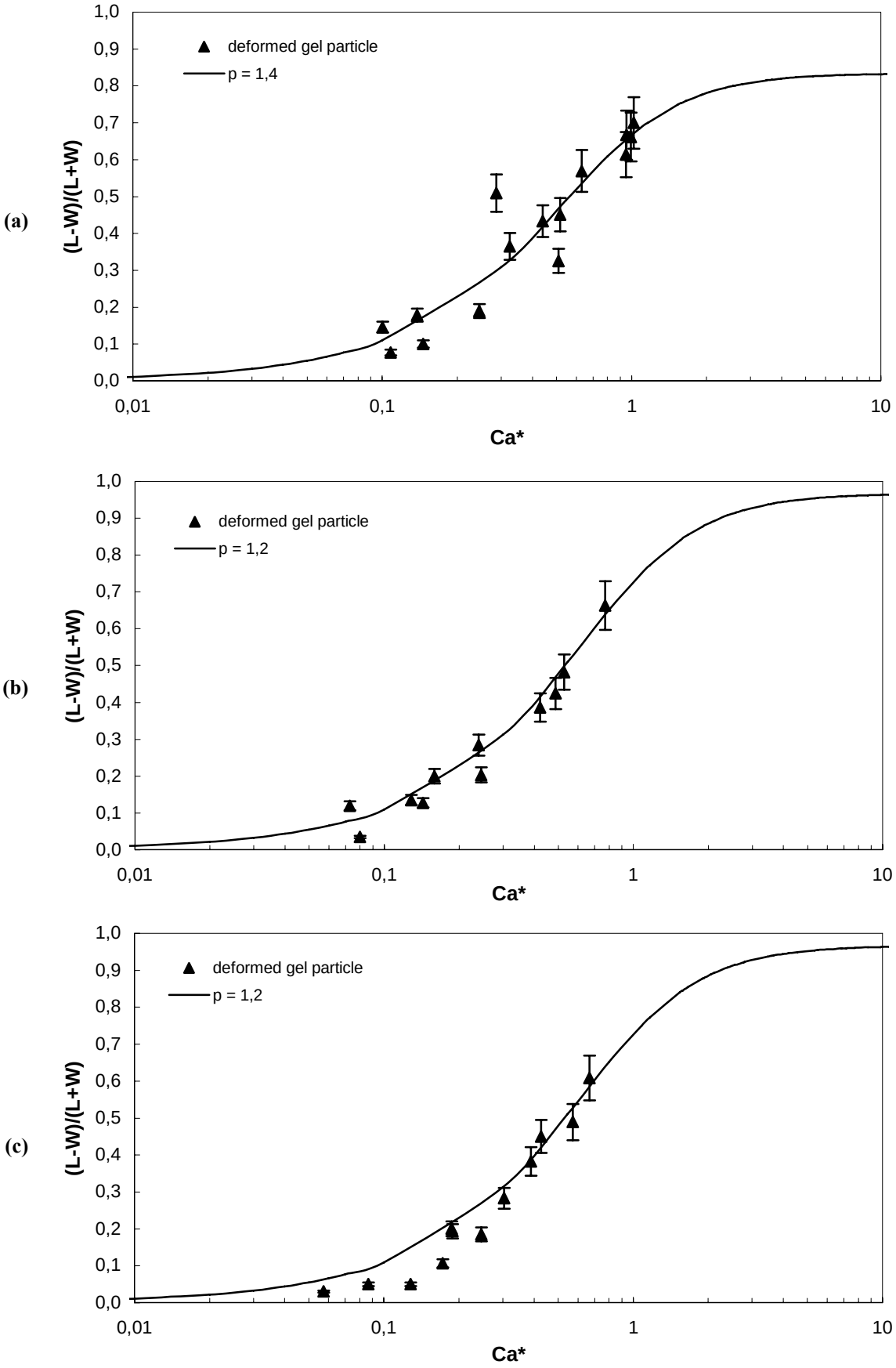

Figure 3.25: Experimental data compared to the modified Cox model with optimal p-values for gels swollen with 5 % HPC to different degrees of swelling. (a) Q = 80 g/g; (b) Q = 160 g/g; (c) Q = 210 g/g.

3.5.3 Maffetone-Minale model

None of our experimental systems fulfil the conditions to apply this model if taking the viscosity ratio as the solvent-matrix viscosity ratio (p varying from 2.10^{-6} for 1 % HPC in PDMS 1000 to 0,009 for 10 % HPC in PDMS 200). The capillary numbers applied are higher than the critical capillary number for this viscosity ratio. The deformation predicted by the model saturates above a certain Ca for p > 3,5 and no break-up is predicted for such high viscosity ratios.
Using the modified capillary number, the smallest deformations are in the same range as the predictions. However, the model predicts steeply increasing deformations for low p at Ca above 4 whereas the gel particle deformation saturates.

Minale (2004) modified the MM-model for non-Newtonian systems. First and second normal stress difference of both fluids are used to characterise the non-Newtonian behaviour of the fluids. Unfortunately, we do not know like parameters for a gel. Therefore, the model could not be applied to our system.

3.6 Relaxation at cessation of shear

Gel particles recover their initial spherical shape when the shear flow is arrested. Shape relaxation is studied in this paragraph. It is identified which factors affect gel shape relaxation and a comparison is made with solvent droplet relaxation.

3.6.1 Shape relaxation of a viscous droplet: literature

Retraction of a deformed viscous droplet is controlled by the balance between interfacial force, which tends to restore the spherical shape, and the viscous stress (Sigillo et al., 1997). This implies that interfacial tension and matrix viscosity affect shape relaxation. In the initial stage, the relaxation rate also depends on the shear history, namely on the amount of deformation γ before cessation of flow, yet in the final stage, shape recovery happens at a constant rate, independent of strain (Yamane et al., 1998; Hayashi et al., 2001). The total duration of relaxation is longer for droplets that were more deformed prior to cessation of flow. Droplet size has also an effect: Okamoto et al. (1999) found that small droplets recover the spherical shape more rapidly than larger droplets.
The effects of the system parameters are grouped in the 'surface tension time', τ, given in [3.18], which is used to make the time scale of a relaxation experiment dimensionless (Guido & Greco, 2001).

$$\tau = \frac{\eta_m R_o}{\Gamma} \qquad \textbf{[3.18]}$$

At equal deformation, droplet shape relaxation only depends on properties of the material system (matrix viscosity, initial droplet size and interfacial tension).

3.6.2 Relaxation of a deformed gel particle swollen with an HPC solution

The relaxation of the gel particles upon cessation of shear was monitored. First, the sample is sheared at a constant rate (constant stress applied) until steady state deformation has been reached. Next, the shear is stopped and the stress drops down to zero. The two observed dimensions of the particle L and H are monitored during some time after arresting the flow, until no change is noticed anymore. This experimental procedure and the reaction of the gel are represented schematically in Figure 3.26. Shape relaxation data were obtained for gels swollen in 1 % and 10 % HPC solutions. Some examples are shown in Figure 3.27 and Figure 3.29. Gels with released tips are also considered but gels that expelled some solvent are not considered at all. The latter volume has changed, so it is impossible for them to recover their initial diameter.
After the start of a relaxation experiment (arresting the flow), no human interference is necessary to conduct the experiment. Relaxation will thus only depend on the material properties and the deformation history.

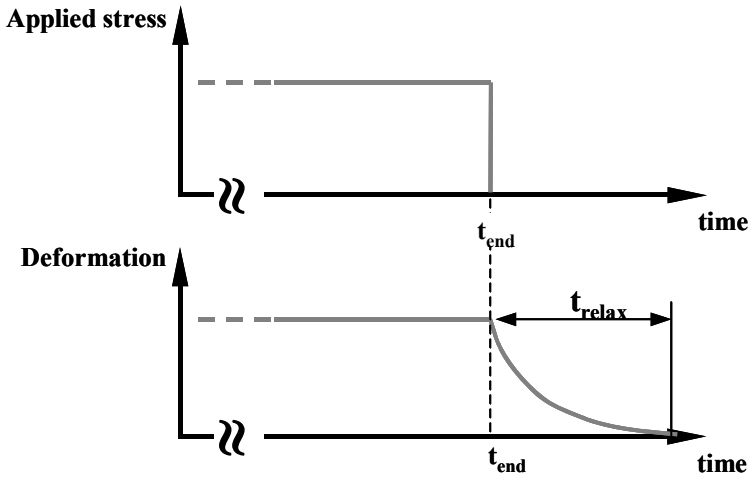

Figure 3.26: Schematic representation of a relaxation experiment.

A deformed gel particle completely recovers its initial spherical shape when it is not submitted to flow anymore. The time needed for L/L_o to become unity after cessation of shear is defined t_{relax}.

3.6.2.1 Kinetics of shape relaxation

Three examples of shape relaxation of gel particles swollen with a 1 % HPC solution and deformed at different shear rates are plotted in Figure 3.27. The range of deformations in which gels swollen with 1 % HPC solution do not release solvent is very small ($L/L_o < 1{,}06$). At higher deformations, tips are attached to the particle and affect relaxation. We shall treat relaxation of the gel particle and of its tips together. The gel reabsorbs the tips after the flow has been arrested. One could say that the deformation of the particle with tips, L'/L_o, relaxes too. This is shown by the open symbols in Figure 3.27. We can define relaxation of the tips separately from relaxation of the gel particle.

One can distinguish two stages in the relaxation kinetics of a particle with tips. The first stage is characterised by the steep decrease of L'/L_o while L/L_o hardly changes. The released liquid is reabsorbed by the particle, resulting in disappearance of the tips. The chains of the network are

contracting because the stress has been taken away, but at the same time, they are stretched again due to the re-swelling. Both processes balance each other out, resulting in slow change of L/L_o. As soon as all the liquid has been reabsorbed, the gel particle is only subject to elastic relaxation. L/L_o diminishes faster in this second part of the curve.

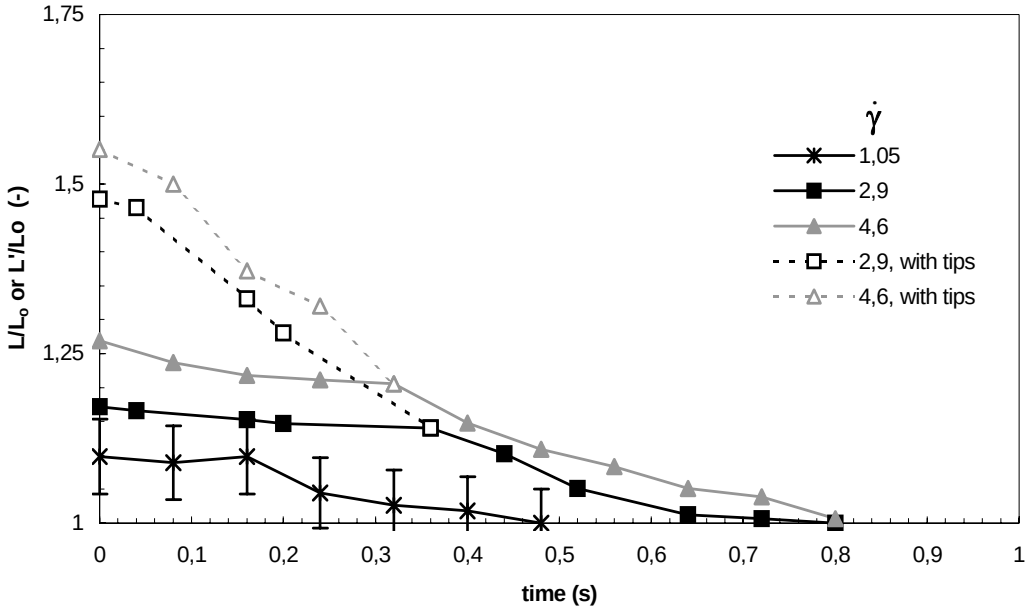

Figure 3.27: Shape relaxation of a gel particle swollen with 1 % HPC solution after having been submitted to different shear rates. Matrix fluid was PDMS 200, D_o = 150 µm.

The couple relaxation time – deformation prior to relaxation goes doubtlessly together. Hence, we introduce a new variable L_{max}, which indicates the length of the particle at the moment shear is stopped. Since deformation can be directly linked to shear stress via the relations from 3.4.2, these measures are equivalent. We chose to plot deformation prior to relaxation instead of shear rate or shear stress in order to minimise errors. Relaxation times could not be measured on particles with $L_{max}/L_o < 1{,}05$ prior to relaxation because they relaxed almost immediately.

The relaxation times derived from shape relaxation kinetics are represented in Figure 3.28. The figures indicate that total particle relaxation times increase with increasing deformation prior to relaxation. The tip relaxation times are somewhat shorter, but they also increase with increasing L'_{max}/L_o. It seems tip relaxation time also slightly increases with increasing tip size. Dashed lines in the graph indicate these tendencies. Nevertheless, because of the high experimental errors on the determined times and the limited data-interval ($L_{max}/L_o < 1{,}25$ for gels swollen with 1 % HPC), no solid conclusions could be drawn with respect to curve shape or slope.

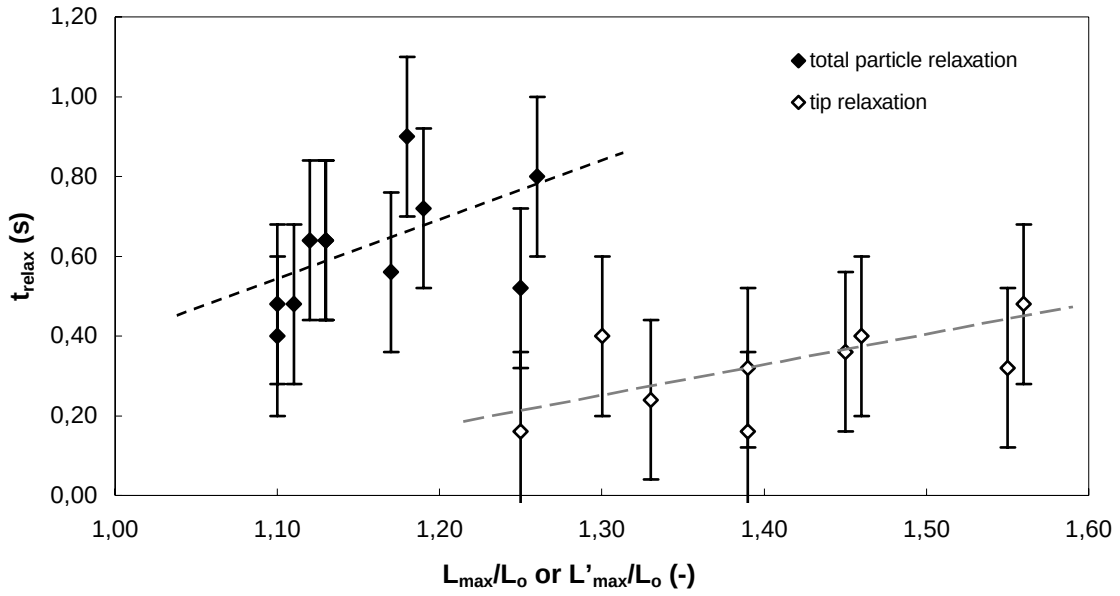

Figure 3.28: Relaxation times of gels swollen in 1 % HPC solution (80 g/g) suspended in PDMS 200. Dotted lines indicate tendencies.

The same exercise was performed for gels swollen in 10 % HPC. It was shown in section 3.4.2.4 that this solution forms only tiny tips and that the gel can deform to large extents. This system is more suitable to evaluate the relaxation behaviour of a swollen network after flow than a system that forms large tips, like a gel swollen with 1 % HPC discussed above. The relaxation times are shown in Figure 3.29. In order to extend the experimental interval, also particles that had ejected some droplets are considered. The duration the shear before relaxation was kept the shortest possible in order to limit volume reduction due to ejection before relaxation. This way, the lost volume was always too small to be measurable so that the gel had its initial diameter back after relaxation.
Figure 3.29 shows that the more a particle was deformed when shear was stopped, the longer time was needed to recover a spherical shape.

$$\rightarrow \; t_{relax} = f(L_{max}/L_o) \Rightarrow t_{relax} = f(\sigma \text{ before relaxation}) \qquad \textbf{[3.19]}$$

In Figure 3.30, the actual length during relaxation is plotted relative to the length when shear was stopped. This is a way to represent the progress of shape relaxation. The slope of this curve is a measure of the relative relaxation speed. Relaxation curves measured on particles of the same size, but deformed to a wider extent prior to relaxation fall on the same master plot. Thus, unlike droplet relaxation, the rate of gel shape relaxation does not change with deformation prior to relaxation in the studied range of deformations. The deformations considered here all fell in the linear part of the stress-deformation curve in Figure 3.11.

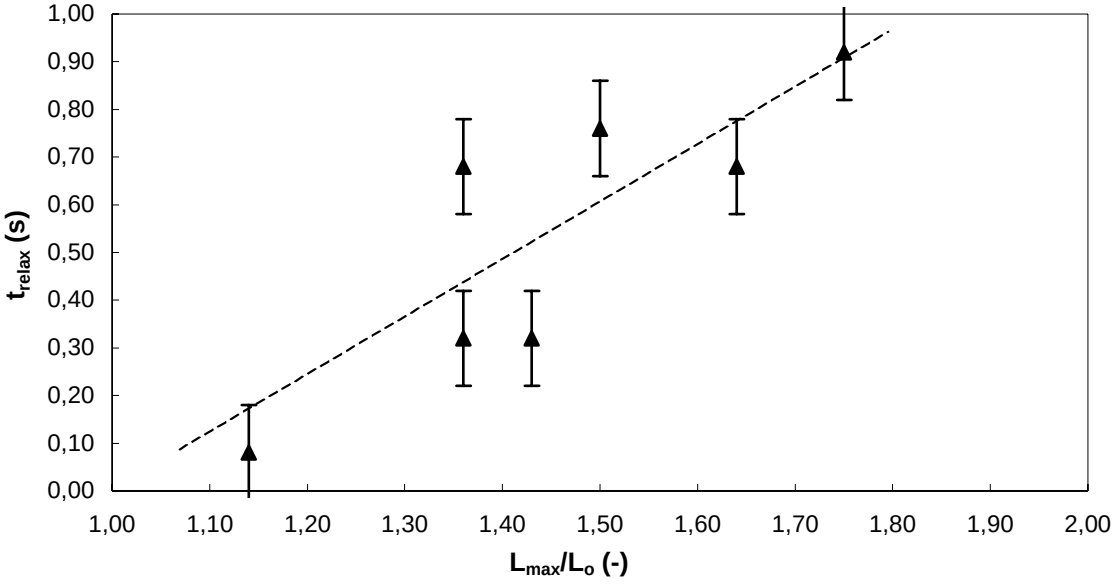

Figure 3.29: Relaxation times of gel particles swollen with 10 % HPC solution (Q = 80 g/g, D_o = 140 µm) in PDMS 200.

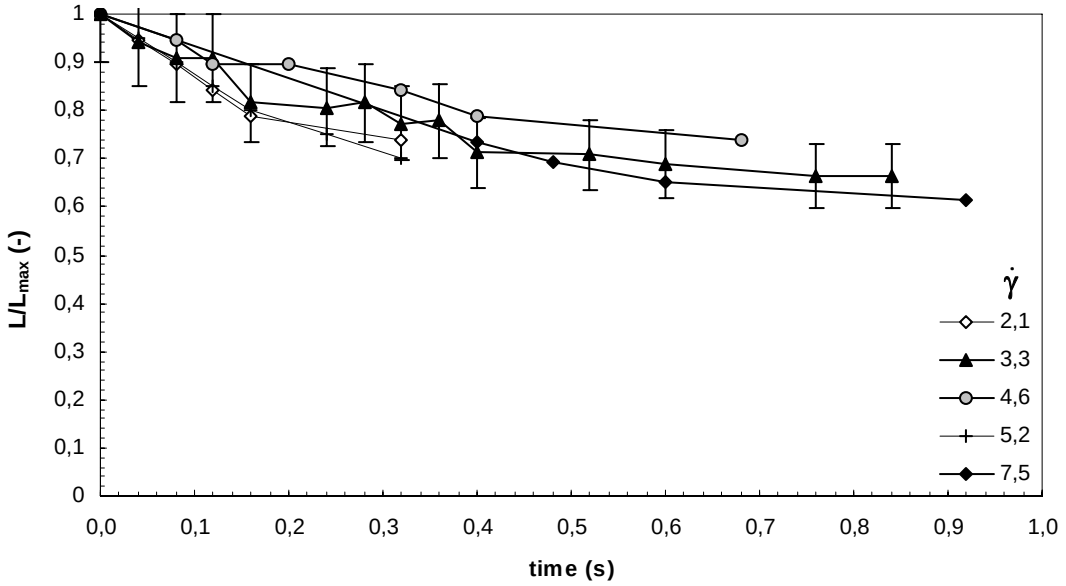

Figure 3.30: Actual length divided by length when shear was stopped as a function of time. Data for gels swollen with 10 % HPC (80 g/g) in PDMS 200. Shear rates are indicated in the legend.

L/L_o-relaxation of 10 % HPC droplets in PDMS 200 is shown in Figure 3.31. After having reached a steady deformation under shear, droplets are farther deformed than gel particles under similar conditions. We do not have droplet data on such small deformations as the gel deformations shown in Figure 3.29, but one can compare the highest gel deformation in the figure (L_{max}/L_o = 1,8) with the lowest droplet deformation (L_{max}/L_o = 2,2). From this comparison, it is clear that the gel recovers the spherical shape faster than the droplet. The restoring elastic forces in the gel are responsible for this difference.

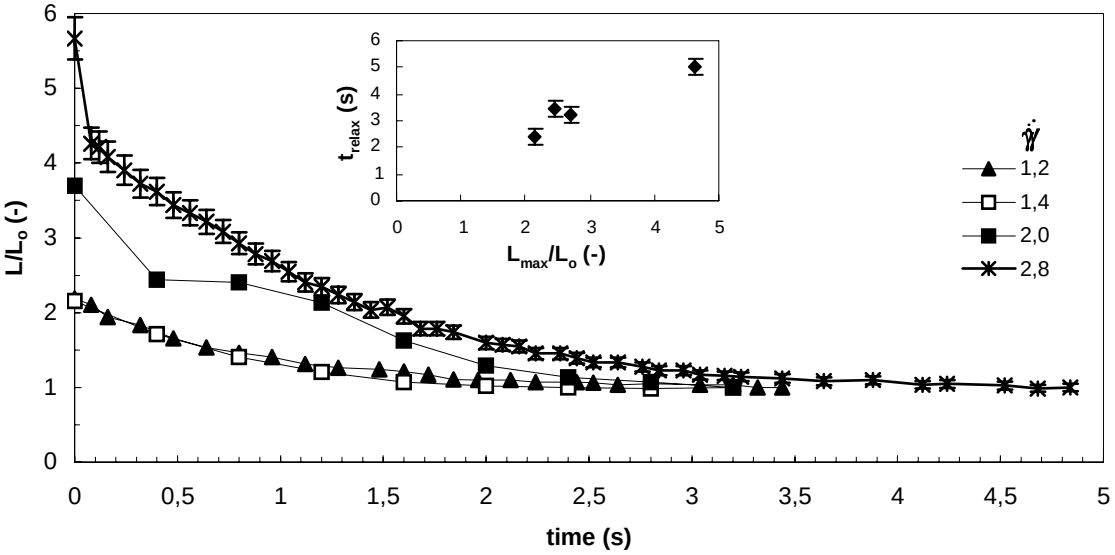

Figure 3.31: Relaxation of 10 % HPC droplets (L_o = 85 µm) in PDMS 200 after being sheared at different shear rates. Relaxation times are given in the inset.

3.6.2.2 Effect of system parameters on the gel relaxation time

In order to evaluate which factors affect relaxation of a gel particle, different system parameters, like initial particle size and viscosity of the suspending matrix were varied. The results are discussed in this section.

Effect of particle size

The relaxation time as a function of initial diameter for particles having the same stretching ratio just before cessation of the flow, $L_{max}/L_o \in [1{,}3;\ 1{,}4]$ is plotted in Figure 3.32a. Within the range of the experimental error, no difference could be distinguished for different particle sizes. This is different for liquid droplets, where the initial size enters the equation for the relaxation time. If surface tension is the main driving force for relaxation, which is the case for viscous droplets, particle size will show an effect. However, we observed size-independency, which is a typical elastic property.

In Figure 3.32b, relaxation time is plotted as a function of deformation before stopping the shear for particles of different size. All data series are found in the same cloud of points. The series cannot be distinguished.

$$\rightarrow \ t_{relax} \neq f(L_o) \qquad \textbf{[3.20]}$$

Effect of matrix fluid

According to the model for τ [3.18], the matrix fluid viscosity affects shape relaxation of a droplet. Figure 3.32c shows that this holds true for gel particles. Gel particle relaxation was studied in PDMS 200 and PDMS 1000. The relaxation times measured in PDMS 1000 are clearly higher than those measured in PDMS 200. In Figure 3.32d, the relaxation times are scaled with the matrix viscosity.

This caused the series for the two matrices to coincide. The relaxation time is thus proportional to the matrix viscosity.

$$\rightarrow \; t_{relax} \sim \eta_m \qquad \textbf{[3.21]}$$

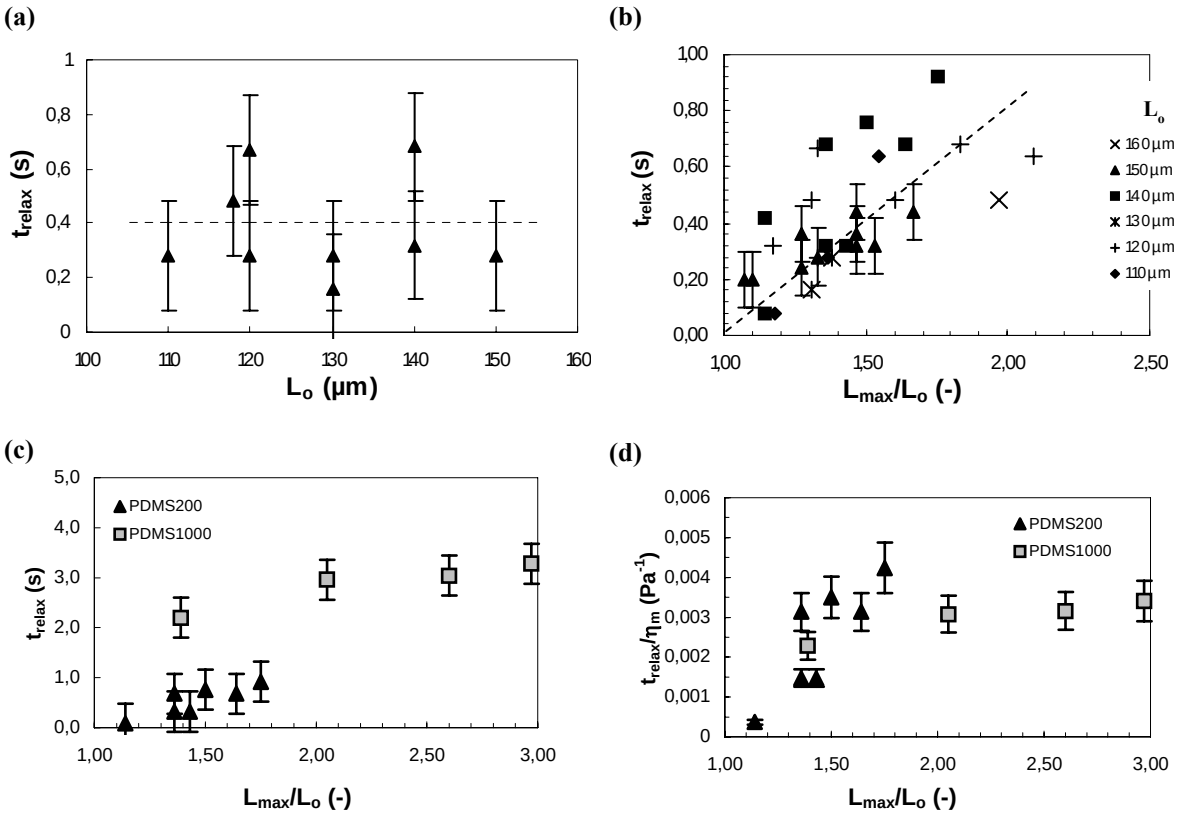

Figure 3.32: Effect of various parameters on relaxation times of gels swollen with 10 % HPC (80 g/g) in PDMS 200 except where precised differently. (a) Relaxation times for particles of different size with the same deformation before relaxation; (b) Relaxation time as a function of deformation before cessation of flow, sizes separated; (c, d) Effect of matrix viscosity on relaxation time for particles of the same size (L_o = 140 µm). Relaxation time is scaled with matrix viscosity in (d).

3.6.3 Conclusions on relaxation

Gel particle relaxation is mainly driven by the stretch of the particle at the moment the shear field is arrested. The relaxation time is proportional to the viscosity of the surrounding fluid, but does not depend on initial particle size in the studied range of parameters. The initial relaxation rate is independent of deformation prior to relaxation. At equal deformation, a gel particle relaxes faster than a droplet of its solvent due to restoring elastic forces in the network.

3.7 Conclusions

The behaviour of gel particles swollen with different linear polymer solutions was studied with a transparent counter-rotating shear cell. Isolated swollen gel particles were submitted to shear stress and observed in-situ. It was observed that a gel does not only react to stress by deforming, but also by the partial release of its solvent. Several shear-induced regimes were identified:

- if a stress is applied, a gel particle deforms into an ellipsoid with three different axes and it rotates around the vorticity axis;
- if the applied stress is higher than a first critical stress, but lower than a second critical stress, some fluid is released by the particle but stays attached to it. Particle with its released fluid remain united;
- above a second critical stress, droplets detach from the tips and are dispersed into the matrix. This phenomenon is irreversible;
- gel particles start to widen in the vorticity direction and solvent can be released from the poles of the particle.

The focus of this chapter was on the phenomena related to the gel particle itself. Solvent release and detachment phenomena will be the subject of the next chapter.

Deformed gel particles rotate around the vorticity axis in the same way as a solid sphere. The period of rotation corresponds to the Jeffery period as long as the matrix is a Newtonian fluid and no significant release has taken place. The rotation speed slows down as the matrix becomes viscoelastic. In the studied material system, this moment coincided with the initiation of solvent release, which might also affect rotation.

Gel deformation was first studied as a function of applied stress. The relative deformed length increases linearly with stress before any solvent is released. The dependence is the same for all solvents used, all other things being equal. Deformation depends on degree of swelling but not on initial particle size. After a critical deformation, release of small or large tips was observed. If large tips of a low viscosity solvent are attached to the particle, the deformation levels off at rather low values whereas the limit of deformation is much higher for gels with tiny tips.

Gel deformation was compared to the deformation of gels swollen with water on the one hand and to the deformation of solvent droplets on the other hand. Comparing gels to droplets and using the solvent-matrix viscosity ratio, most of the studied particles would have ruptured. However, the cross-linked gel remained intact. The models describing droplet deformation in Newtonian systems are not appropriate to predict gel deformation. The Cox model was therefore extended with an elastic term to represent the resistance of the gel network to deformation. The predictions by this "modified Cox model" were satisfactorily close to the experimental data as long as deformations remained small.

Gel relaxation was also studied. Relaxation times increase with increasing deformation prior to relaxation. Shape relaxation after cessation of the flow only depends on the viscosity of the surrounding matrix at equivalent deformation, but not on particle size. This is different from liquid

droplet behaviour. Length relaxation data of gel particles in the same matrix superimpose if they are represented relative to the length at the moment shear was stopped.
Particles with tips relax in two stages. The tips are reabsorbed first, followed by fast recovery of a spherical shape.

Résumé du Chapitre 4

Libération et éjection de solvant par une particule de gel induites par cisaillement

Les phénomènes de libération des produits inclus dans le gel sont d'une grande importance pour des applications de gels en tant que vecteur d'agent actif. Ainsi, ce chapitre est consacré à l'analyse de la libération et l'éjection du solvant d'un gel induites par cisaillement. Les conditions critiques et les paramètres influençant ces phénomènes sont identifiés. D'abord, le relargage sans détachement de gouttes est étudié et ensuite, l'éjection de solvant dans la matrice est analysée.

La particule de gel libère une quantité de solvant à ses extrémités dés qu'elle dépasse une déformation critique qui correspond à une contrainte critique. Le solvant reste attaché à la particule dans des 'poches'. A contrainte plus élevée, des gouttelettes se détachent des poches et se dispersent dans la matrice.
Aussitôt que le module complexe de la matrice devient plus grand que le module élastique du gel, les particules de gel s'élargissent dans le sens de la vorticité et du solvant peut être relargué aux pôles de la particule.

La concentration du polymère dans le solvant influence les phénomènes de libération. Une basse concentration de polymère (solvant de faible viscosité) favorise le relargage des bouts de solvant. La concentration joue aussi sur le détachement de gouttes via le rapport des viscosités solvant/matrice: plus ce rapport est élevé, plus le détachement de gouttes est facile. Une faible tension interfaciale promeut également le détachement de gouttelettes des bouts et leur dispersion dans la matrice. Des réductions importantes du volume du gel initial peuvent ainsi être réalisées.

Les phénomènes de relargage et d'éjection ont également été observés sur des gels physiques et des capsules avec une peau gélifiée. Les phénomènes que nous avons identifiés et décrits peuvent alors être considérés comme des phénomènes généraux. Ceci rend ces matériaux prometteurs pour des applications en tant que porteur d'actifs. Cependant, les conditions critiques initialisant le relargage et l'éjection doivent être prises en compte au moment de la conception du procédé.

Chapter 4

Shear-induced solvent release from a swollen gel particle

The first paragraph of the former chapter describes the general shear-induced behaviour of highly swollen gel particles. Since that chapter focussed on deformation of these elastic particles, the expelling of solvent out of the particle was only briefly mentioned. However, solvent release phenomena are of high importance for carrier and controlled release applications. Hence, this chapter is devoted to the analysis of shear-induced solvent release from a gel particle and its ejection into the suspending matrix. Critical conditions and influencing parameters are identified. First, solvent release without detachment is studied and second, solvent ejection into the matrix is analysed. At the end of the chapter, the relations between different phenomena will be discussed.

4.1 Solvent release

4.1.1 Conditions initiating solvent release

Solvent is only released from the gel swollen below equilibrium at stresses above a threshold value, named release stress, σ_{rel}. This threshold differs when the gel solvent changes. In the present work, the solvent was varied between solutions of 1 % to 10 % HPC. This modification implies variation of the rheology of the solvent and of the chemical potential of the bound water. As was shown in 2.4.2, the interfacial tension does not change within this range of concentration.

The lowest stress at which tips were observed at the edges of a deformed gel particle are summarised in Table 4.1 for all studied concentrations. Data concerning gels swollen with pure water are added for comparison. They are taken from Zanina et al. (2002). From Table 4.1 can be concluded that increasing the polymer concentration delays solvent release in terms of stress. The release stress increases with increasing polymer concentration in the solvent. The critical stresses can depend on the linear polymer concentration via interfacial tension, viscosity ratio between solvent and matrix and osmotic pressure. The interfacial tension is the same for all HPC concentrations used. This parameter can thus be excluded, leaving viscosity ratio and osmotic pressure as the only differences:

- Higher concentration leads to higher viscosity and thus higher stresses are needed to expel the solvent from the gel.
- Higher polymer concentration creates higher osmotic pressure for the water inside the gel (common solvent to network and linear polymer). The water is strongerly retained inside the gel, so higher stresses are required for release.

Table 4.1: Critical condition parameters for solvent release from Aqua Keep gels swollen with aqueous solutions (Q = 80 g/g) at 21 °C. L_o = 150 µm.

	Water*	1 % HPC	5 % HPC	10 % HPC
p	$4{,}3.10^{-6}$	$7{,}8.10^{-6}$	$3{,}4.10^{-5}$	$7{,}8.10^{-4}$
Γ (mN/m)	18	12,5	12,5	12,5
σ_{rel} (Pa)	[200 – 250]	[250 – 400]	[900 – 1200]	[900 – 1000]
L/L_o at release start	1,06	1,17 ± 0,02	1,48 ± 0,05	1,50 ± 0,04

* Data from Zanina et al. (2002), Q = 110 g/g.

At constant stress, deformation at initiation of tip release $L//L_o$ may also be an appropriate parameter. It appeared to be constant for a given couple gel-solvent (Table 4.1). They are calculated as the average of at least 10 data points. These values are the non-steady state deformation of the particle when the tips appear. In general, tips appeared just before the steady state deformation was reached. The tips also grow towards a steady value. This steady value depends on the applied shear stress and can only be reached as long as no solvent droplets are detached from tips. In the latter case, solvent detachment can last for a long time. Most of the time it was not possible to follow a particle until ejection stopped in order to determine the steady size of its tips after solvent detachment. However, the steady size of a particle that has lost some solvent cannot really be compared to a particle that did not loose any solvent since their degree of swelling is different.
Examination of the last row of Table 4.1 suggests that the deformation of the particle that triggers solvent release increased with increasing polymer concentration in the solvent. The increasing σ_{rel} with increasing C_{HPC} discussed before is coherent with this observation: higher stresses are needed to reach the higher deformations.

The time at which tips appear is given as a function of applied stress in Figure 4.1. The relative error is quite large and the data are rather scattered because of the reasons developed in paragraph 2.2.1.4. In spite of these errors, the charts allow us to conclude that tips appear faster when higher stresses are applied. This time eventually goes to ‘almost immediately’ as can be seen very clearly in graphs (a) and (c) of the figure. The decreasing trend can be understood through the fact that the deformation necessary to initiate tip release is reached faster at higher stresses.
The delay times for the gel containing the 1 % HPC solution are clearly shorter than for the other solutions (notice the different scales). The deformation needed to initiate tips from this type of gel is much smaller as well, and thus reached sooner.

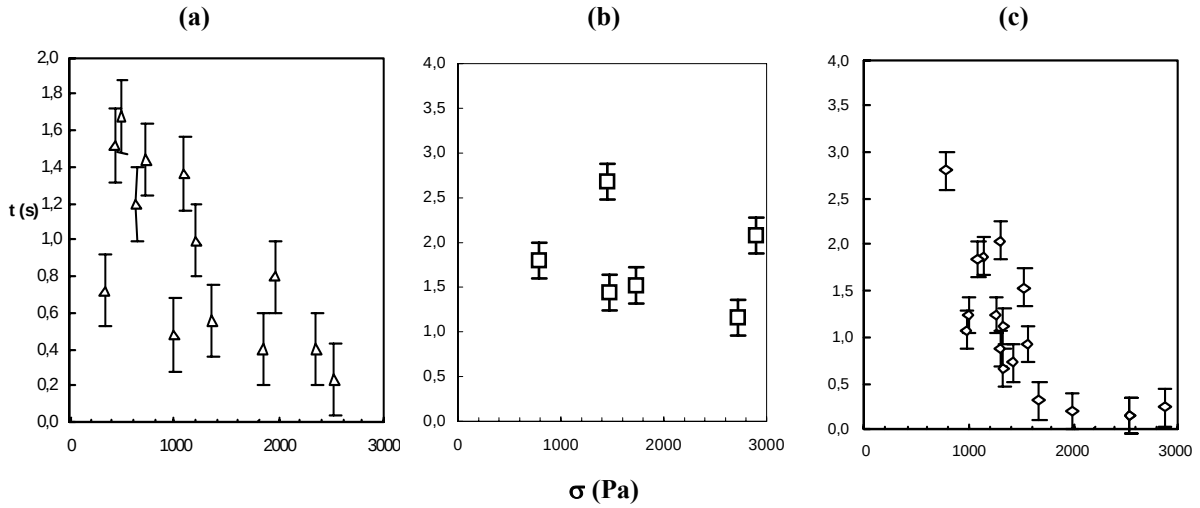

Figure 4.1: Time at which tips appear at the edges of a deformed gel particle (Q = 80 g/g). HPC concentration increases from left to right: (a) 1 %, (b) 5 %, (c) 10 %. L_o = 130 – 160 µm.

The data from Figure 7 in Zanina et al. (2002) show the same tendency of decreasing time with increasing stress for particles with L_o between 130 and 160 µm. The delay times themselves are initially longer than the delay times measured for the gels swollen with 1% HPC, yet the decrease as a function of stress is steeper, so they approach 'zero' at lower stresses.

After having considered the first appearance of tips from different points of view, it seems all conclusions coincide with the critical deformation argument. This points out that the critical parameter for solvent release is a certain deformation of the swollen particle. Deformation of the particle mainly means reorganisation followed by stretching of the network strands. However, stretching the length induces compression of the width dimension (not observed). Critical time and stress are derived parameters. Critical stress is the minimal stress needed to reach the critical deformation value.

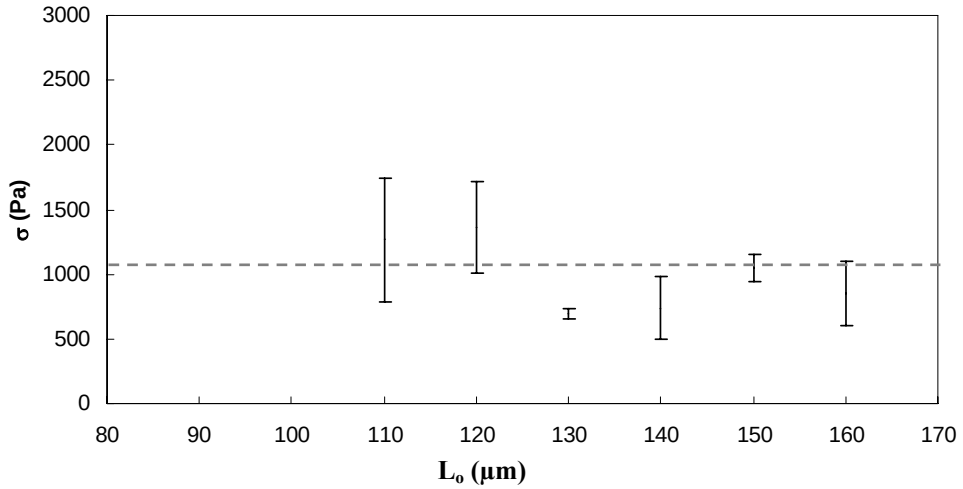

Figure 4.2: Critical interval for tip appearance. Aqua Keep swollen with 10 % HPC, Q = 80 g/g.

It was also determined whether the critical circumstances depended on the initial size of the swollen particle. Particle sizes were grouped in intervals of 10 μm (e.g. 140 ± 5 μm). In each group the highest shear stress at which no tips appeared at the edges of a deformed particle and the lowest shear stress at which tips were observed were determined. These intervals are shown in Figure 4.2. The critical stress triggering the actual release of these tips must be in this interval. The centre of the interval is taken as an estimate.

The critical stress is somewhat higher for the smaller particles (110 to 120 μm), but decreases slightly at larger initial diameters. The intervals for particles of 130 to 160 μm partially overlap. Since these stresses are the same for this range of sizes, it is correct to study the critical times all together. Zanina et al. (2002) did not find any effect of gel size on the release times in this range of particle sizes either. Considering the experimental error on the applied stress, there is probably no effect of gel size on the stress initiating solvent release, within the range of particle sizes investigated.

4.1.2 Effect of linear polymer concentration C_{HPC} on the solvent release phenomenon

Figure 4.3 shows how large tips can grow before droplets are pinched off and dispersed in the matrix for gels swollen with water and with HPC solutions at different concentrations. The particles shown in the picture had similar initial sizes and the degree of swelling was 80 g/g. Water tips can grow very large and become pointed. The tips on the particles containing an HPC solution are considerably smaller and rounded at the apex. Comparing Figure 4.3b to Figure 4.3c shows that higher C_{HPC} gives rise to smaller stable tips.

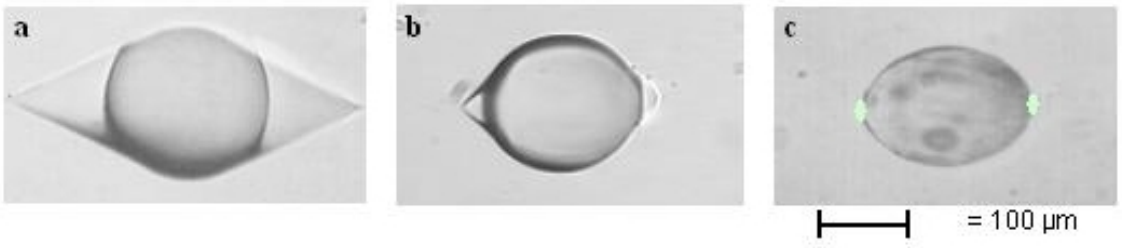

Figure 4.3: Stable tips before droplet ejection on an Aqua Keep particle for different C_{HPC}. L_o~140 μm. (a) water (Q = 110 g/g; from Zanina et al., 2002); (b) 1 %, Q = 80 g/g; (c) 10 %, Q = 80 g/g.

The first point may be understood by the different interfacial tensions for the couples water/PDMS and HPC-solution/PDMS. The lower interfacial tension of the pair HPC-solution/PDMS makes solvent break-up or droplet ejection easier, thereby limiting the growth of the tips. No ejection was observed from gels swollen with water for stresses up to 4000 Pa (Zanina et al., 2002). Further solvent release at higher stresses only leads to further growth of the tips.

The differences between figures b and c may be explained by the different critical stresses that initiate droplet ejection (Table 4.2). The largest difference between σ_{rel} and σ_{ej} is noted for the 1 % HPC solution. There is hardly any difference for the 10 % HPC solution. In the latter case, formation of small droplets is more advantageous than letting the tips grow larger. We will further focus on the reasons behind this fact in 4.2.1.

4.1.3 Released tip volume

Gel particles swollen with water release an important part of the initial volume as conical tips that stay attached to the particle. The volumes mentioned in Zanina et al. (2002) and Zanina and Budtova (2002) are somewhat overestimated since they ignored the flattening in the width direction in their calculation of the released volume. Still, the fact is that high fractions of the water absorbed by the gel may be released.

As could be seen in Figure 4.3, the tips on gel particles swollen in 10 % HPC solutions are very tiny. The same holds true for gels swollen in 5 % HPC (not shown). Both types of tips cannot be measured in an accurate way to estimate the volume. Only the tips on gels swollen with 1 % HPC solution were large enough to be measured. Since these tips were rounded at the apex instead of conical, it was more difficult to estimate the volume inside. We estimated this volume by using two different approaches to calculate it:

- Approach 1: suppose the tip is a true cone with H_t as diameter of the bottom surface and height (L'-L)/2. Because the tips are rounded instead of conical, an important part of their volume is ignored. Hence, approach 1 underestimates the volume in the tips.
- Approach 2: Calculate the volume of an ellipsoid with length L' that fits the contours of the tips. Deduct from this the volume of the inscribed ellipsoid with the same height but length L. The edges of the inner ellipsoid do not exactly coincide with the border between the particle and the tips. A part of the particle is accorded to the tips in this method. It overestimates the tip volume.

A schematic representation of the approaches is given in Figure 4.4 and the calculations are developed in Appendix A.

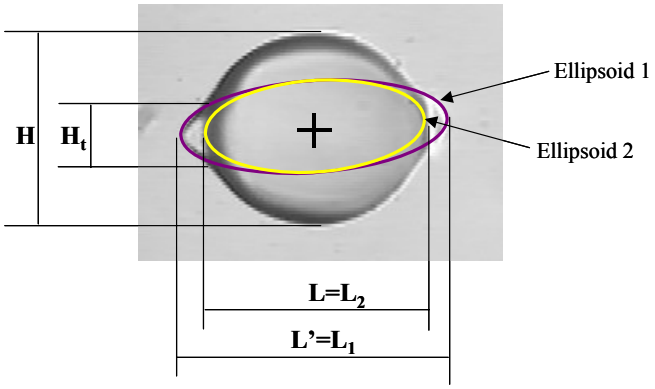

Figure 4.4: Scheme for understanding the methods used to calculate the volume of the tips.

The volume of the tips at steady state calculated by the two methods is represented in Figure 4.5. Approach 1 underestimates the released volume while approach 2 overestimates it. The results of both approaches indicate therefore the range in which the real released volume should fall. No measurable tips were present at stresses lower than 300 Pa. Above this threshold, the relative steady state tip volume increased with increasing stress. A maximum of 20 % of the 1 % HPC solution can be released into tips at stresses below 3000 Pa.

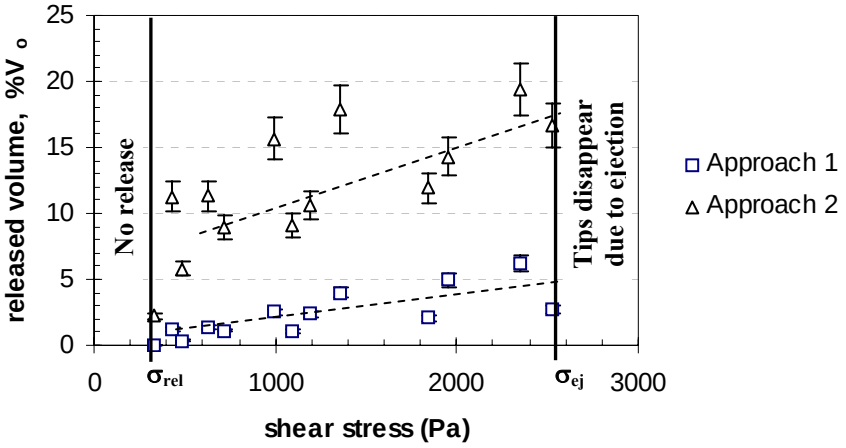

Figure 4.5: Released steady state tip volume with respect to initial volume for gels swollen in 1 % HPC calculated with two different methods. Method descriptions are given in Appendix A.

The degree of swelling of the particle decreases as the tips grow with increasing stress and becomes $Q_o \cdot V_{particle}/V_o$. The decreasing degree of swelling with increasing stress corresponds to the findings in literature about equilibrium deswelling under a load: the heavier the load on the gel, the less solvent it can hold (1.6.2). The same holds true under shear: the higher the shear stress, the more solvent the gel will release in order to re-establish the balance between inner and outer forces. At stresses above 2500 Pa, the 1 % HPC tips could not grow larger because solvent droplets were pinched off the edges and dispersed into the matrix. This process, which reduces the volume in the tips, is the subject of the next section.

4.1.4 Conclusion

Sheared swollen gel particles release part of their solvent as soon as a critical deformation (stress) is reached. The released solvent remains attached to the gel particle as liquid tips. The critical deformation increases with increasing polymer concentration in the solvent. The maximum steady state size of the tips decreases with increasing solvent viscosity.

4.2 Ejection of solvent droplets

A phenomenon that was not observed on gel particles swollen with pure water is solvent detachment. Above the ejection stress σ_{ej}, fine droplets are pinched off from the edges of the tips and dispersed in the PDMS matrix. The streams of tiny dots left and right from the particles in Figure 4.6 show this very clearly. The phenomenon of droplet ejection from the solvent tips was observed on gels swollen with all three studied HPC solutions and for all degrees of swelling. It was observed as well on gels swollen with water to which a small amount of surfactant was added (Hachani, 2000). This phenomenon is reminiscent of tip streaming, which is observed on droplets in an emulsion and related to the presence of surfactant by De Bruijn (1993).

During the experiments, it was observed that solvent ejection did not happen in identical ways for all solvents. Figure 4.6 shows two extreme cases. Tips grew rather large on gel particles swollen with

the 1 % HPC solution before droplets were pinched off (left picture in the figure). The droplets were therefore detached from a pocket of solvent fluid. This tip streaming is supposed to be governed by similar phenomena as tip streaming from droplets in a blend system.

This droplet ejection can consume the solvent pockets until they are completely finished. The tips do not grow large again. It seems tip growth is slower than droplet ejection. The system slowly reaches equilibrium in the following way: at a fixed stress, tip growth and solvent detachment take place. The tips become smaller and smaller until no droplets can be pinched off anymore. Further ejected droplets come directly out of the particle, in the same way as with 10 % HPC until the gel reaches equilibrium with the applied stress. It is obvious that as more solvent has been released, the gel becomes less swollen, so it becomes more difficult to extract more solvent from the gel. Observations also showed that as the tips reduce, the particle became more elongated. Gel deformation with and without tips was discussed in the previous chapter.

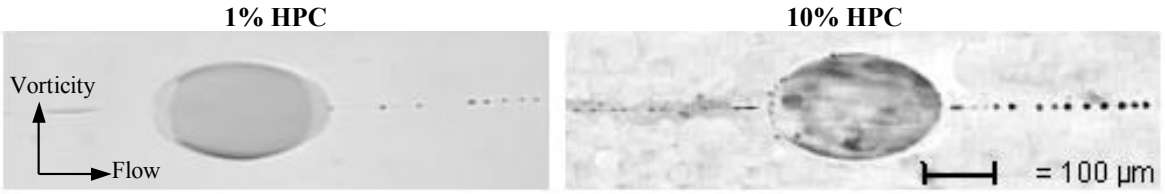

Figure 4.6: Ejection of droplets from an Aqua Keep particle swollen with HPC solutions of different C_{HPC}. L_o~140 µm, Q = 80 g/g.

In the case of particles swollen with the 10 % HPC solution, tips never grew large; droplets were detached soon after the appearance of the tips.

4.2.1 Critical conditions

The critical intervals for initiation of droplet detachment from particles with different initial size were determined following the method described in 4.1.1 and they are plotted in Figure 4.7. A clear effect of initial particle size can be noticed: the ejection stress decreases with increasing initial diameter. The effect of particle size flattens out for particles larger than 130 µm.

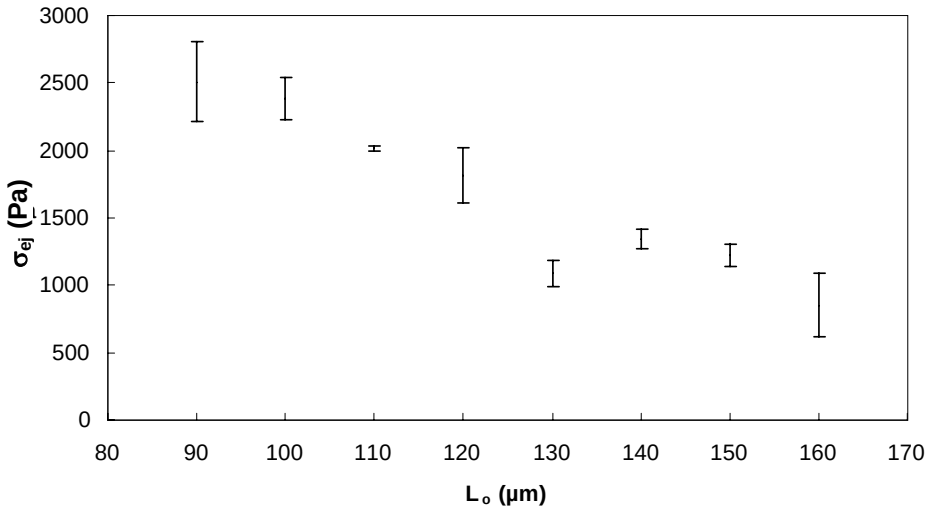

Figure 4.7: Critical interval for droplet detachment. Aqua Keep swollen with 10 % HPC, Q = 80 g/g.

All critical parameters characterising initiation of droplet ejection are summarised in Table 4.2.
The highest σ_{ej} is measured for 1 % HPC and the lowest for gels swollen with 10 % HPC solutions. For the 1% solution, σ_{rel} and σ_{ej} are very different: tips grow for a long time and in a wide zone of stresses without any possibility of forming droplets. This is different for the 5 % and 10 % solutions: the two critical stresses are closer, indicating that the moment when solvent is released by the gel is very close to the conditions to form droplets of these tips. Droplet forming is governed by the phenomena on the interface between two immiscible liquids, while solvent release is governed by the interplay between the stresses acting on a swollen gel particle.

Table 4.2:Critical condition parameters for ejection of droplets in PDMS 200. Q = 80 g/g, L_o = 140 µm.

	Water	1 % HPC	5 % HPC	10 % HPC
p	$4{,}3.10^{-6}$	$7{,}8.10^{-6}$	$3{,}4.10^{-5}$	$7{,}8.10^{-4}$
Γ (mN/m)	17	12,5	12,5	12,5
σ_{ej} (Pa)	No ejection	~ 2500	[900 – 1200]	[800 – 1200]
L/L_o at ejection start	-	No information	1,53 ± 0,07	1,53 ± 0,06

The critical stress for droplet detachment should depend on the linear polymer concentration via interfacial tension and viscosity ratio between solvent and matrix. Interfacial tension is high between water and silicone oil. No detachment of droplets was observed for this case. It is more favourable for the water to remain inside the cone than to create extra surface by forming a droplet. The interfacial tension is the same for all HPC concentrations used. This parameter can thus be excluded, leaving viscosity ratio as the only difference. The parameters of interest for droplet break-up under shear are grouped in the critical capillary number that was introduced by Grace (1982) and given in Figure 4.8. This curve was established for emulsions and describes the critical conditions where droplet break-up and coalescence balance each other out. A droplet in the area above the line will break up whereas a droplet below the curve is more prone to coalescence. The lower the viscosity ratio, the higher is the critical capillary number. The lines corresponding to different solvent-PDMS pairs used in this study are superimposed onto this figure.

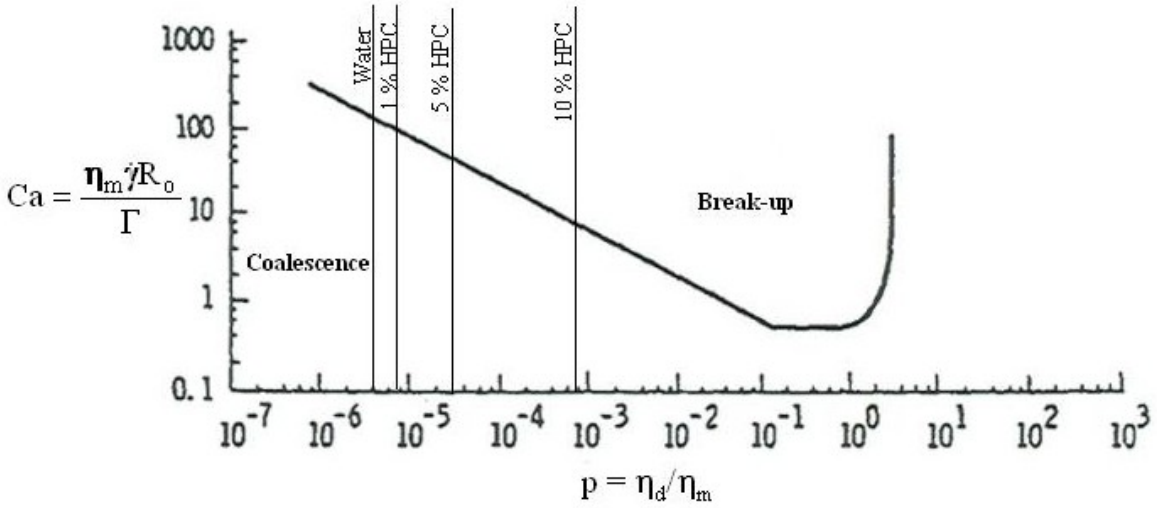

Figure 4.8: Critical capillary number as a function of viscosity ratio p for shear flow [After Grace, 1982].

Although we are dealing with suspended gel particles instead of emulsions, the observations made on the released fluid in the tips must be governed by the same parameters as those that determine the behaviour of a droplet in an emulsion. This is indeed the case: parameter p increases with increasing HPC concentration, meaning droplets are more keen to be formed for the 10 % HPC solution than for the 1 % HPC solution (Ca_{crit} is lower for 10 % HPC). Formation of small droplets is more advantageous than letting the tips grow larger in the case of higher polymer concentration. It is now clear that tips composed of 10 % HPC should break up at lower capillary numbers and thus that the ejection stress for gels swollen with 10 % HPC is lower than for tips composed of 1 % HPC.

Summarising, low interfacial tension, large size and high solvent/matrix viscosity ratio promote detachment of droplets from the tips.

4.2.2 Loss of volume

We have demonstrated the possibility of solvent ejection by a gel submitted to stress. If this ejection of droplets can be continued for extended times, it could be an interesting delivery mechanism. On the other hand, if a carrier would loose its contents due to stress before it has arrived at its target, this phenomenon is a real drawback of the system. In both cases, it is important to know to which extent solvent can be pressed out of a gel by shear stresses from the surrounding medium.

To determine the ability of a gel particle to loose volume by ejecting the solvent, a particle was submitted to constant shear rate and stress during a certain time Δt after which the shear was stopped abruptly and the particle was allowed to relax to a spherical shape again. The initial and final diameters were measured and the corresponding volumes calculated. One particle could be submitted to stress repeatedly, whereby we tried to apply the same stress. This was not always possible because of the manual operation of the system. Figure 4.9 illustrates the protocol.

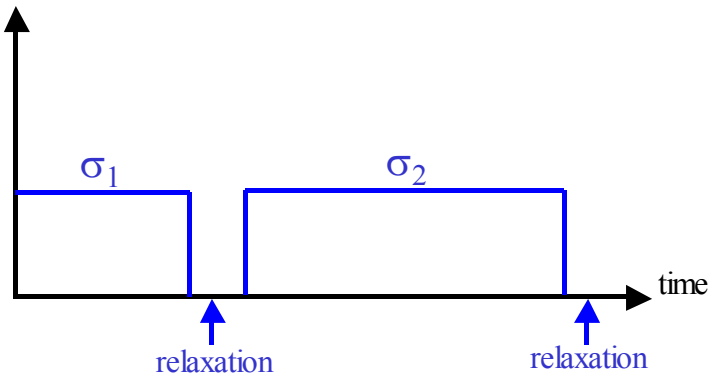

Figure 4.9: Experimental protocol to measure loss of solvent from a gel particle by droplet ejection. Time intervals between two measurements may be different and so may σ_1 and σ_2.

This type of experiment has been done on gels swollen with 1 % and 10 % HPC solutions suspended in silicone oil and on gels swollen with 10 % HPC suspended in silicone oil with 3 % surfactant ABIL® EM 90. The interfacial tension solvent/matrix is reduced from 12,5 mN/M to only 3 mN/m.

The loss of volume was calculated as the difference between the actual volume and the initial volume. This difference was divided by the initial volume, to exclude the effect of different initial sizes. Not all particles could be immobilised at exactly the same stresses. To counter the effect of different stresses, the relative loss of volume is represented as a function of strain ($\gamma = \dot{\gamma} * \Delta t$) in Figure 4.10. Curves of such shape are typical for negative exponential decay that can be described by the following equation (Zeo et al., 2005):

$$\frac{\Delta V}{V_o} = 1 - \exp(-k * \gamma) \qquad \textbf{[4.1]}$$

where k is a measure for the rate of deswelling. This model is fitted with the experimental data using a least squared differences procedure. The values for k are given in Table 4.3 and the quality of the fit is reflected by the average of the squared residues r_i.

Table 4.3: Rate of deswelling parameters for Aqua Keep particles swollen to 80 g/g, fitted with [4.1].

Solvent	$\Gamma_{solvent/matrix}$ (mN/m)	k (s.u. $^{-1}$)	$(\Sigma r_i^2)/n$
1 % HPC	12,5	3,6 10^{-5}	0,004
10 % HPC	12,5	1,6 10^{-5}	0,0004
10 % HPC	3	9,4 10^{-5}	0,004

4.2.2.1 Effect of solvent viscosity

To evaluate the effect of solvent viscosity, the data for gels swollen in 1 % and 10 % HPC solutions suspended in pure oil must be compared. The two series show that the volume loss initially increased linearly with strain. Losses up to 15 % were obtained within 10^4 s.u., which corresponds to about 15min. shearing at shear rates of about 11 s^{-1} applied by the counter-rotating device. It should be noted that solvent was expelled from the gel along both flow (Figure 3.1d) and vorticity direction (Figure 3.1e). At the same strain, the particles swollen with 1 % HPC have lost more solvent than the particles swollen with 10 % HPC. This is also reflected in the higher deswelling rate parameter for gel swollen with 1 % HPC. Lower solvent viscosity thus accelerates ejection kinetics.

4.2.2.2 Effect of interfacial tension

In order to assess the effect of interfacial tension on ejection kinetics, experiments were executed with a w/o emulsifier added to the silicone oil matrix. Gels swollen with 10 % HPC were used for these experiments and the results are added to Figure 4.10 (series 10 % HPC + emulsifier). The relative loss of volume kinetics in a matrix with emulsifier is much higher than in the pure matrix (series 10 % HPC) at the same strain. The gel immersed in oil with emulsifier could loose up to 70 % of its initial volume. This is promising for applications as a carrier even though the release is quite slow; it needs about 15 minutes to free these amounts of solvent.

The emulsifier clearly accelerates ejection. The rate of loss parameter is about six times higher for the system with the emulsifier added to the oil. Intuitively this is not surprising since droplet formation and detachment are expected to be favoured by lower interfacial tension.

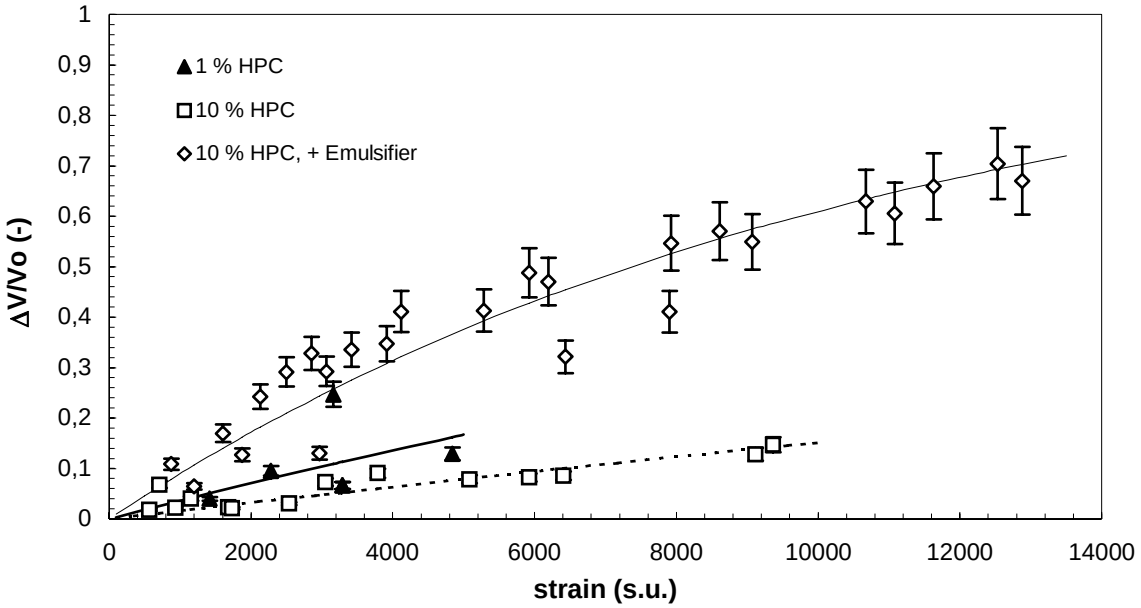

Figure 4.10: Relative loss of volume of gel particles due to ejection induced by simple shear flow. Aqua Keep with two different HPC solutions starting from Q = 80 g/g immersed in PDMS 200. Interfacial tension was changed by adding a w/o emulsifier to the matrix. Shear rates were near 12 s^{-1}.

Zeo et al. (2005) pursued this study of shear-induced deswelling kinetics. They systematically investigated the effects of interfacial tension, degree of swelling, solvent viscosity and solvent quality on loss of solvent under shear. Their findings confirm the here described enhanced ejection by lowering the interfacial tension and by lowering solvent viscosity.

4.2.3 Ejected substance

In view of possible applications as a delivery system, it is important to know the polymer concentration in the liquid that is ejected by a gel. The different behaviours observed on the tips (see 4.1.2) indicate that they are composed of a different substance, most probably proportional to the concentration of the linear polymer in the initial solvent of the gel. The ejected droplets should have the same composition as the tips. Therefore, increasing the concentration of the polymer solution in the gel entails the ejection of more concentrated droplets. The hypothesis put forward here was verified during the compression experiments described in Chapter 5. They confirmed that the liquid released by the gel was the same as the liquid absorbed.

4.2.4 Laboratory test conditions versus application conditions

Let us now have a look at the stresses encountered in cosmetic cream applications. Most oils used in cosmetic applications are less viscous (0,1 – 1 Pa.s) than the PDMS's used in our experiments. However, the shear rates that undergoes a tiny layer of cream may rise from 100 up to 10 000 s^{-1} (Macosko, 1994). A gel carrier particle in such a cream would then be submitted to stresses in a range of 10 to 10^4 Pa. This range coincides with the experimentally applied stresses and on may thus suppose that the observed phenomena are relevant for applications.

4.2.5 Conclusion

Droplets can be detached from the tips in a mechanism similar to end-pinching or tip streaming in emulsions. The critical stress for droplet ejection decreases with increasing polymer concentration because of the increase of the solvent/matrix viscosity ratio according to the mechanisms known for immiscible blends. Low interfacial tension also facilitates droplet formation. Substantial volumes of solvent can be ejected by this mechanism.

4.3 Gel widening and solvent release in the vorticity direction

4.3.1 Description of the phenomenon

In the former paragraphs it was described how a microgel particle strongly elongates in the flow direction and how it releases droplets of solvent when the particle is gently submitted to stresses higher than about 900 Pa. When the gel was held at high stress for a few seconds, some particular observations were made. The elongated gel particle became higher and solvent was also ejected along the vorticity direction. Different stages could be identified in this slow phenomenon. They are depicted in Figure 4.11. The particle height first increases (a) and solvent caps appear on both sides of the particle in the direction perpendicular to the flow direction (b). These caps grow in time and gradually transform into cones (c). While growing further, the cones retract their lumbar region – making them look like mushrooms (d) that are finally necked off from the gel particle and first flow away in the vorticity direction as several droplets of different sizes (e, f). The droplets adopt an ellipsoidal shape, elongated in the flow direction and flow away from the gel along the vorticity direction (f). Soon after that, they are further dragged away from the particle in the flow direction.

In (e) and (f) it can be seen that small solvent caps remain attached to the particle during the sequence of release/detachment in the vorticity direction. They start growing again after detachment and the whole phenomenon is repeated. The duration of one cycle is approximately one minute. It should be noted that this phenomenon is accompanied by the earlier described solvent release and detachment in the flow direction, as can be seen on the figure. After cessation of flow, the gel recovers its initial spherical shape, yet with reduced volume because of the solvent excretion.

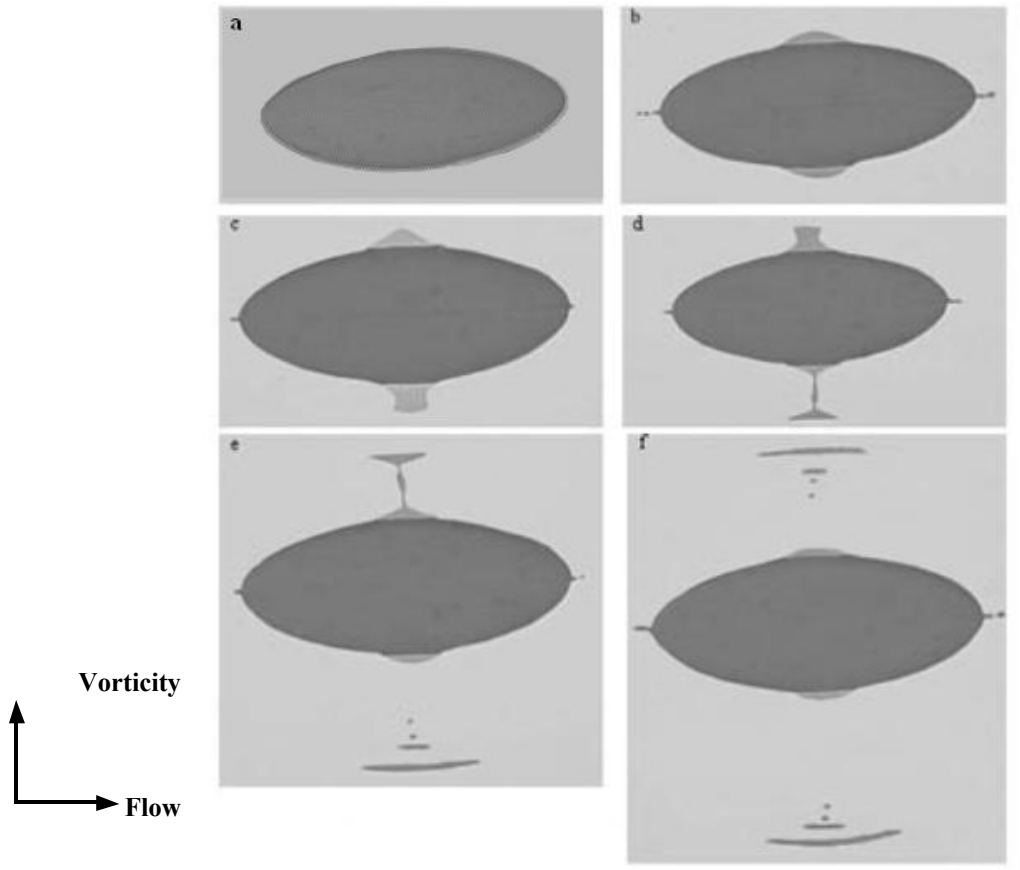

Figure 4.11: Cycle of gel widening, cap growth and detachment in the vorticity direction. (a) deformation (b) formation and growth of caps; (c) caps transform into cones while growing further; (d) cones retract their lumbar region; (e) drops are pinched off; (f) ellipsoidal drops initially flow away in the vorticity direction.

An example of the kinetics of change of the three particle dimensions is given in Figure 4.12 for a particle immersed in PDMS 200 at 2700 Pa. Although difficult to distinguish on this overall time scale, the graph represents four cycles of cap growth and detachment. This becomes clear when looking at the detail given in Figure 4.13. The dimension L becomes stable within a few seconds. The initially spherical particle becomes strongly elongated ($L/L_o > 1$) and later on slightly higher in the vorticity direction ($H/H_o > 1$). The particle becomes flattened in the flow gradient direction ($W/W_o < 1$). The width dimension cannot be observed in the used set-up and is therefore calculated assuming volume conservation. This is actually an overestimation since the gel looses some solvent during the experiment. The true values of W/W_o should be lower than the ones in the figure. In the figure, a distinction is made between the true values for W that could be calculated before any solvent was released, and the overestimated values. It is clear from this picture that the gel is transformed into an oval pancake. Similar shapes were observed in polymer blends (Levitt et al., 1996). However, the gels presented here are composed of a chemically crosslinked network that will never be able to elongate into fibre-shaped droplets as droplets do, since the 3D-network structure prohibits such anisotropic deformation.

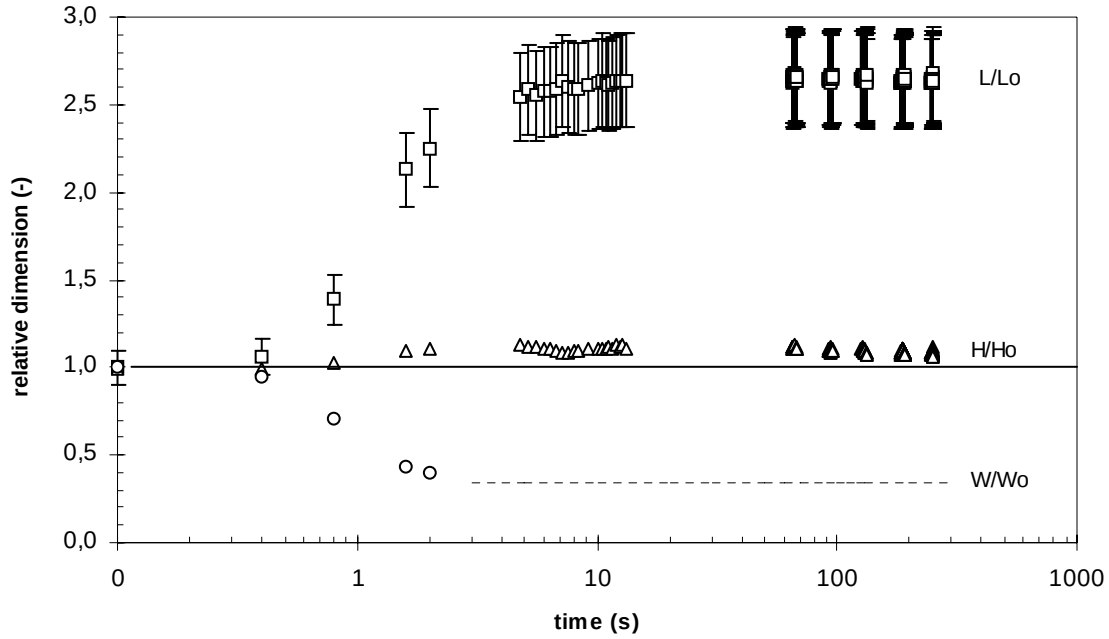

Figure 4.12: Kinetics of change of relative gel particle dimensions for a particle swollen to Q = 80 g/g in a 10 % HPC solution suspended in PDMS 200 at 2700 Pa. L is the dimension in the flow direction, H in the vorticity direction and W in the flow gradient direction. Dashed line indicates the upper limit for W/W_o as soon as solvent is released from the particle.

Detailed time-dependent deformation of gel dimensions in flow and vorticity direction and of the dimensions of the caps at the poles of the particle are shown in Figure 4.13. The dimensions of the gel itself stabilise in 10 s. The deformation of the caps is represented by H'/H_o. These caps appear only after 6 s and grow slowly to a first plateau. Their deformation remains stable for about 30 s and then continues its growth to very high deformations that finally lead to the ripping off of solvent. During this last part, H'/H is difficult to measure and is therefore not represented. The two mushrooms are not always ripped off at exactly the same moment. That is why we observe two tops in the H' evolution of cycles 3 and 4. After detachment, the caps relax again to the plateau value. Some 30 s later, they start growing again. Four such cycles are shown in the figure. The time between two detachments increases from cycle to cycle, as more solvent has been lost. This is probably due to the fact that the degree of swelling gradually decreases and that it becomes more difficult to release solvent as a consequence.

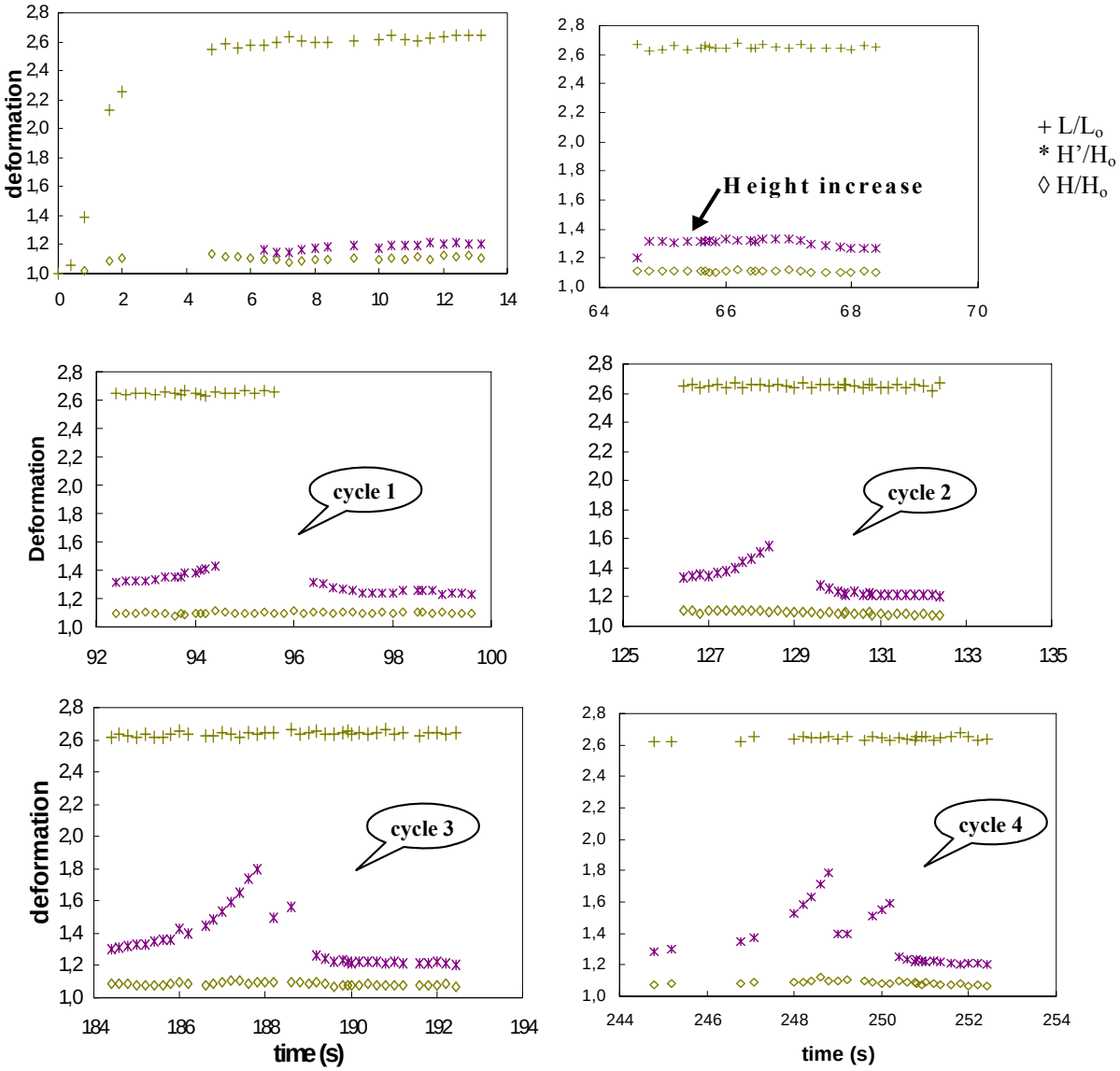

Figure 4.13: Kinetics of particle dimension stabilisation for a gel particle swollen with 10 % HPC in PDMS 200 at 2700 Pa. L adopts a steady value within the first 10 s. H and H' only start growing after a longer time. H' increases until the cap shape becomes impossible to measure, but H' can be measured again after mushroom detachment.

The relative gel height at steady state (here: when H has reached a final constant value) is represented as a function of applied shear stress in Figure 4.14. Each dot is the result of a separate experiment on a new gel particle. The figure shows results for gels swollen in different solvents: in water, in 1 %, 5 % and 10 % HPC solution. Two silicone oils with different viscosity were used: PDMS 200 and PDMS 1000. Points of interest for the present discussion are those at high shear stresses, but some points at low stresses are added to highlight the transition. The increase of the gel dimension in the vorticity direction is small and the ensemble of all experimental points shows just a general trend. Increasing height is not observed at low stresses. Noticeable enlargement, more than 5 % of the initial diameter, can be observed at stresses higher than 1000 Pa.

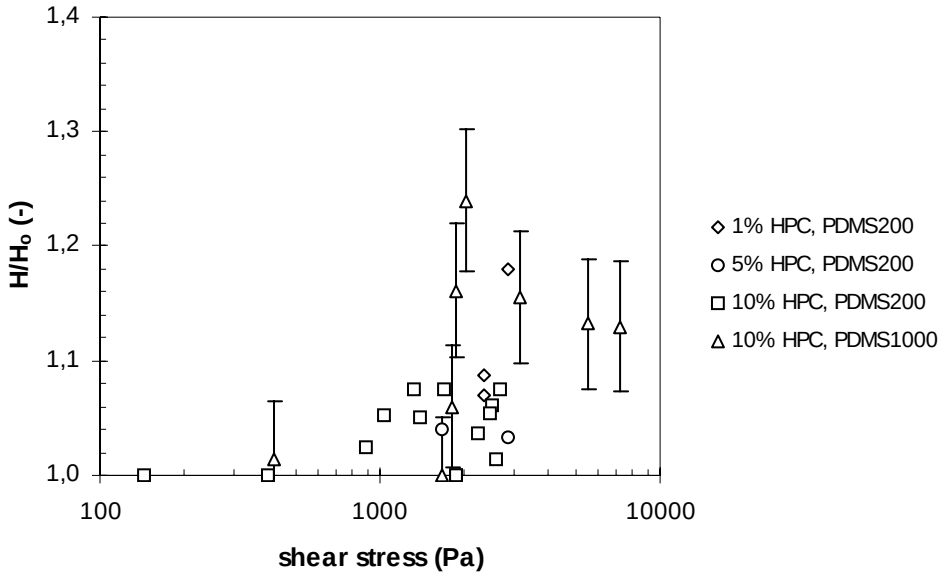

Figure 4.14: Relative height of gel particles as a function of applied shear stress. Gels were swollen in different solvents and suspended in two different silicone oils. Q = 80 g/g. Error bars are only shown for one series in order not to overload the graph.

The above described phenomena of increasing height, solvent release and detachment in the vorticity direction were observed for the gels swollen in all three mentioned HPC solutions immersed in both PDMS's as well as for gels swollen in a 5 % PVA solution (Zeo et al., 2005) immersed in PDMS 200 with and without surfactant added. The systems differ in growth-detachment kinetics. For a gel swollen in pure water, widening in the vorticity direction occurred, but no solvent release and detachment were observed in the studied range of stresses [0 - 5000 Pa]. Nor were water droplets pinched off in the flow direction (Zanina and Budtova, 2002; Zanina et al., 2002). The absence of detachment can be explained by the high interfacial tension between silicone oil and water. However, gel widening in the vorticity direction at high stresses seems to be a universal phenomenon that does not depend either on the type of solvent, nor on the suspending fluid.

4.3.2 Discussion

This paragraph treats three related phenomena that occur when a swollen gel particle is submitted to high shear stresses.
While solvent detachment from the released edges in the flow direction is governed by mechanisms described for immiscible blends (end-pinching in the present case), increasing height of an elastic cross-linked particle under shear is a far less explored domain.

4.3.2.1 Literature: Droplet widening and break-up in the vorticity direction: existing approaches and general comparison with a gel particle

Widening phenomena observed on polymer blends depend on system parameters such as droplet/matrix viscosity ratio, visco-elastic properties of the constituent fluids, capillary number, etc., and several approaches were developed to understand and model this droplet deformation in the vorticity direction.

Droplet widening in the vorticity direction was first observed by Macosko's team on a Newtonian droplet immersed in a visco-elastic matrix, but the authors did not mention any break-up (Levitt et al., 1996; Cristini et al., 2002). They observed widening as transitory phenomenon: the relative drop width increases in time, reaches a maximum and then decreases to finally become smaller than one. The phenomenon was attributed to different second normal stress differences in matrix and droplet, which is caused by a difference in elasticity of the fluids. Guido et al. (2003) related droplet widening to normal stresses in the matrix. Droplet widening was reported to occur in Newtonian systems as well and was described by Yu and Bousmina (2002) using an ellipsoidal droplet model. Shear widening of droplets in Newtonian systems is generally explained as a purely viscous effect (Wetzel and Tucker, 2001; Jackson and Tucker, 2003). Cristini et al. (2001) showed that widening occurs only above a critical capillary number. Widening and break-up in the vorticity direction was also reported for the case of a visco-elastic droplet in a Newtonian matrix (Hobbie and Migler, 1999; Migler, 2000; Migri and Huneault, 2001) and explained by the appearance of strangulating forces in the droplets due to the development of normal stresses inside (Migri and Huneault, 2001). Similar observations were reported for mixtures of Newtonian fluids at high viscosity ratios (Lin et al., 2003). The authors described their observations as an erosion phenomenon. Finally, widening was also observed in a blend composed of two viscoelastic fluids by Cherdhirankorn et al. (2004).

The case of an elastic swollen gel particle in a liquid matrix is an unexplored field. The parameters and approaches used for two-component immiscible blends cannot be transposed in a straightforward way. A major difference is that our system actually consists of three components: matrix fluid, network and solvent. Some examples of problems arising when dealing with a gel suspension are the following:

- The viscosity ratio is not defined for a gel-in-matrix system. If it is taken as solvent/matrix viscosity ratio, it will be very low (see Materials section), whereas it will tend to infinity if it is taken as the gel/matrix viscosity ratio;
- The stress distribution in a gel must obviously be different from the stress field in a sheared droplet;
- It is not clear if and how solvent circulates inside the gel or not and whether that may influence solvent release and detachment.

Because of these open questions, the interpretation of gel widening and solvent release in the vorticity direction can only be phenomenological at present.

4.3.2.2 Gel particle widening in the vorticity direction

Gel widening can be understood when considering the system (network + solvent) as one entity and applying the arguments given by Levitt et al. (1996) for liquid droplet widening in a visco-elastic fluid. Levitt and co-workers stated: the higher the matrix/droplet elasticity ratio, the more the droplet will be stretched in the vorticity direction. The elasticity is characterised by G' in the cited paper. We shall consider that the complete mechanical resistance of the gel is comprised in the shear modulus G (defined in section **3.4.3**). Because it is infeasible to apply the properties of a liquid to a chemical gel, only general material parameters were chosen as criterion. We will thus characterise the matrix fluid by G*, which expresses both viscous and elastic resistance against deformation, in order to compare

gel and matrix on the most general level. Both parameters are represented as a function of oscillation rate in Figure 4.15. The modulus of all the components involved are shown in this figure.

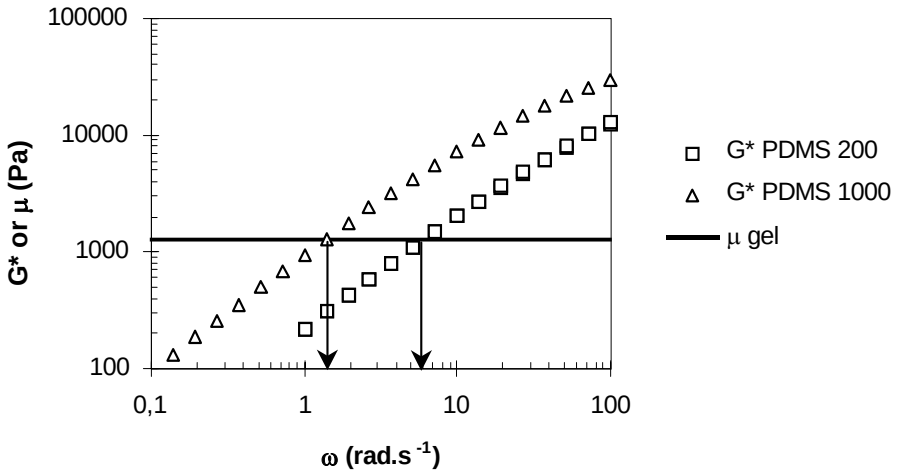

Figure 4.15: Elastic modulus vs. oscillation rate of all matrix fluids and gel particles swollen to Q = 80 g/g.

Figure 4.14 showed that the gel widens at stresses higher than 1000 Pa, which corresponds to a shear rate of 5 s^{-1} in PDMS 200 and 1 s^{-1} in PDMS 1000. It is at about these oscillation rates that the respective G* overcome the gel modulus (Figure 4.15). According to the paper of Levitt et al. (1996), N_2 is responsible for the observed widening. Unfortunately, this parameter is unknown for the used fluids. However, knowing that N_2 is proportional to the first normal stress difference, this parameter was measured instead (see Materials section). It is clear from the materials section that the first normal stress differences in the PDMS's used are not negligible and increase with increasing shear rate. All solvent moduli are smaller several orders of magnitude and should not play a decisive role. Since N_2 is proportional to N_1, yet smaller, second normal stresses rising in the PDMS matrix are probably not negligible in the studied case.

It has become clear that matrix elasticity is an important parameter causing a gel to widen. The presented data lead to the conclusion that the crossover $G^*_{matrix}/\mu_{gel} = 1$ triggers the widening of the swollen gel.

4.3.2.3 Solvent detachment in the vorticity direction

Figure 4.11 also showed that solvent could be released form a widened gel particle. This is more difficult to relate to the observations in immiscible blends described in literature. In the presented case, a Newtonian fluid (the HPC solution) is entrapped in a chemically crosslinked gel and immersed in silicone oil that displays viscoelastic properties. There is a difference between widening without breaking of a low viscosity Newtonian droplet and the present case of solvent detachment in the vorticity direction from a gel particle. Droplet widening is a transient phenomenon; the relative width passes through a maximum but gets smaller than unity afterwards due to dominating elongation forces (in the flow direction). If such a droplet would break, it would be in the flow direction. For example, a HPC-solution droplet becomes elongated very rapidly at large strains and disintegrates by tip-streaming, as was described in the previous chapter. When such low-viscosity fluid is captured in a

gel by swelling forces, it is preserved from these high elongations in the flow direction since it follows the deformation of the elastic gel. As soon as the solvent is released from the gel, it is immediately subjected to high stresses. So, it will adopt a large deformation (corresponding to the high stress) because of the large difference in viscosity between the matrix and the released solvent (p varying from $7{,}8\ 10^{-6}$ for 1 % HPC to $7{,}8\ 10^{-4}$ for 10 % HPC) and the rather low interfacial tension.

4.4 Some practical cases

Different shear-induced release phenomena were identified on swollen model gel particles. Similar experiments were performed on some none-model gel systems in order to verify whether the observations made on the model gels remain valid for other types of gel. Different types of systems were tested: capsules (gelly skin and liquid core) and physical gels. Unlike the model system, these practical gels do not have well-defined shapes and it is therefore complicated to characterise their deformation. Therefore, we will only focus on release phenomena.

The two types tested were:

- chitosan-alginate capsules, synthesised at DELSI (Delivery Systems International), St. Petersburg, Russia. They are core-shell capsules consisting of a gelled skin filled with liquid. The shell is composed of Na-alginate crosslinked with chitosan by $CaCl_2$. This gelly shell is swollen with water to a degree of swelling of 2 g/g. The capsule-core is filled with a 2 % Na-alginate solution. These particles were tested by A. Zanina (Zanina et al., 2002).
- κ-carrageenan physical gels, synthesised at ENITIAA (Ecole Nationale d'Ingénieurs des Techniques des Industries Agricoles et Alimentaires), Nantes, France. They are physical gels prepared by gelation of microdroplets in vegetable oil. The droplets consisted of an aqueous solution of 1,5 % κ-carrageenan with 0,01 M $CaCl_2$.

A schematic representation of the particles is given in Figure 4.16. The gels were used as they were supplied. This implies e.g. that no extra solvent was added to obtain a desired degree of swelling.

The capsules and the physical gels were submitted to increasing shear stress in subsequent runs and it was noted whether release and/or ejection was observed and under which conditions. PDMS 200 was used as suspending fluid for these experiments.

Solvent release and flowing with tips was observed on both types of practical gels, as illustrated in Figure 4.16. Release was initiated at different stresses, typical for the particle. The released solvent is probably the core content in case of the capsules and water in case of the physical gels.

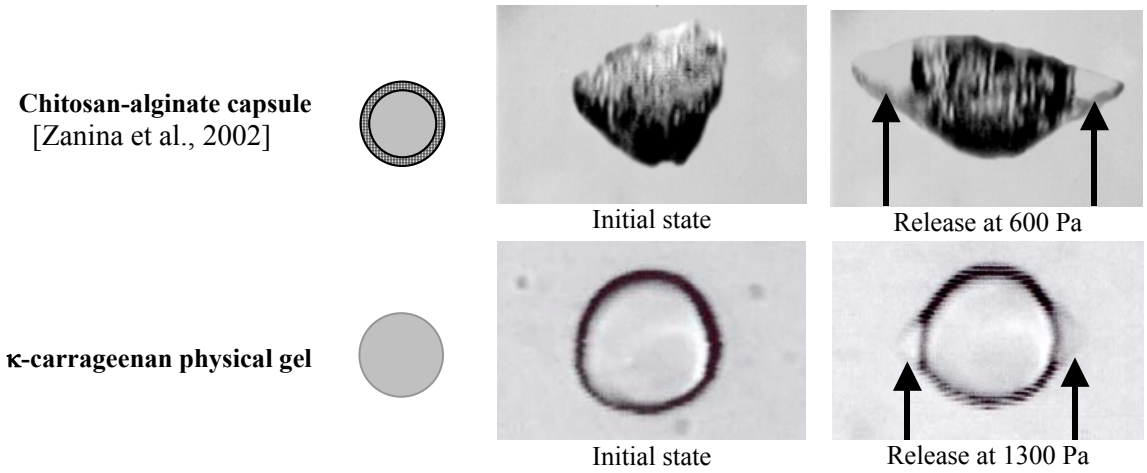

Figure 4.16: Shear-induced solvent release by non-model gels suspended in PDMS 200.

Droplet ejection was observed on the chitosan-alginate capsules. Droplets are pinched off the tips at the same stress as tip appearance, but delayed. This is only possible if the interfacial tension between the released solvent and the suspending oil is low enough to promote formation of droplets. No ejection was noticed on the κ-carrageenan gels. This is in line with the idea that the solvent released from the carrageenan gels would be water.

For the physical gels, it was also tested whether they could be fragmented by shear. However, this was not the case for shear rates below 50 s^{-1} in PDMS 200.

4.5 Discussion

4.5.1 Why does a gel particle release its solvent?

The force system that acts on the strands of a swollen gel submitted to shear flow is shown in Figure 4.17. Gel swelling is the result of the quest to reach minimal energy. Swelling forces tend to stretch the cross-linked chains while elastic forces counteract the stretching. A gel particle immersed in another medium, silicone oil in the present case, is also subjected to interfacial tension. If the system is sheared, extra forces are imposed onto this system. The shear forces cause the strands to stretch and the network to reorganise.

Solvent release from a gel particle under shear is easy to understand: the release is due to the mechanical stress. As soon as some stress is applied, the equilibrium is violated and the gel tends to reach another degree of swelling by releasing part of its solvent. The solvent is released in the direction of the applied forces. This is what was observed at low shear stress values (Zanina and Budtova, 2002; Zanina et al., 2002; Vervoort and Budtova, 2003). The gel is elongated in the flow direction; hence solvent could be released in the flow direction. At high stresses, normal forces are enlarging the gel's height. In that situation, solvent can also be released in the vorticity direction. A

threshold stress can be associated to both phenomena. This threshold should depend on the properties of the system.

Before starting to reason on the dependence of the release stress on system parameters, it should be emphasised that the 'release stress' was defined as the first *observation* of release. Yet, a thin layer of solvent of 1 µm or less thick cannot be distinguished from the contour of the particle and release will not be observed in that case. Such thin layer would represent about 6 % of the particle's volume. Even though this is not a large fraction, it could important for fundamental understanding of gels in suspension.

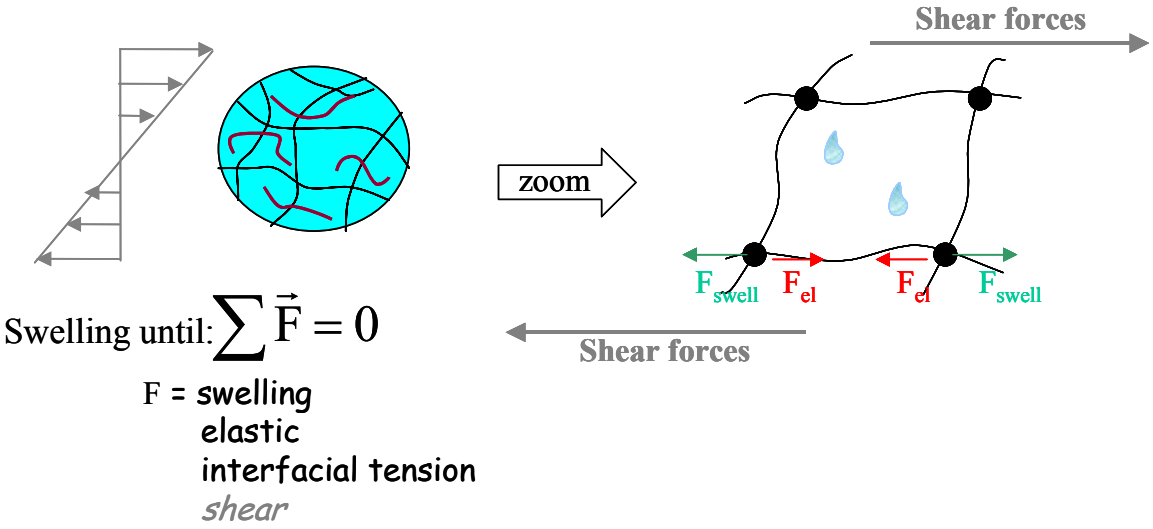

Figure 4.17: Schematic representation of stresses acting on a swollen gel under shear.

Consider now the role of the degree of swelling on solvent release. Based on thermodynamic arguments, one would think that gels swollen at equilibrium release some solvent as soon as they are submitted to stress. This is exactly what was observed on gels swollen at equilibrium under compression in open air (Chapter 5). However, this was not the case for gel particles swollen at equilibrium in water or in 5 % HPC and suspended in oil. In the latter case, release was only observed above a typical 'release stress'. This discrepancy between intuition and the behaviour of suspended gel particles may be due to the above-mentioned limited resolution of our observations. Another explanation we want to propose is that the interfacial tension is the factor responsible for delayed release by gels swollen at equilibrium.

In the case of the present study, the force system represented in Figure 4.17 includes elastic forces, swelling forces, interfacial tension and mechanical forces. A delay of solvent release must then be composed of a term accounting for the fact that most studied gels were not swollen at equilibrium, shortly referred to as the degree of 'underswelling', and of a factor accounting for interfacial tension. The release stress is thus composed of at least two terms. Eventual effects unidentified at present are grouped in the last term, σ_{other}. In the simplest approach, all these stresses are additional [4.2].

$$\sigma_{rel} = \sigma_{interfacial} + \sigma_{Q<Q_{eq}} + \sigma_{other} \qquad \textbf{[4.2]}$$

Let us now consider each of these stresses separately:

- Interfacial stress by definition holds

$$\sigma_{interfacial} = \Gamma / R_o \qquad [4.3]$$

The diameters of the studied particles are largely taken between 90 µm and 200 µm, meaning R_o varies between 45 and 100 µm. Using the Γ-values determined in Chapter 2, one can calculate the limiting interfacial stresses. These are given in Table 4.4.

Table 4.4: Interfacial stresses compared to release stress for different solvents.

Gel solvent	Q (g/g)	σ_{rel} (Pa)	Interfacial stress interval
Water:	80	[400 – 500]	$\sigma_{interfacial} \in$]150 Pa; 400 Pa[
	280	[200 – 300]	
	400 = Q_{eq}	[100 – 200]	
5 % HPC:	80	[700 – 800]	$\sigma_{interfacial} \in$]100 Pa; 300 Pa[
	160	[500 – 800]	
	210 = Q_{eq}	[350 - 800]	

- Stress due to an 'underswollen' state with respect to Q_{eq}, $\sigma_{Q<Qeq}$: this stress is related to the osmotic pressure of a swelling gel and should be an increasing function of (Q_{eq} – Q). We do not have quantitative data for osmotic pressure in Aqua Keep 10SH-NF particles when immersed in either water or one of the HPC solutions. This stress factor can thus only be considered in a qualitative way. As discussed in Chapter 1, the osmotic pressure decreases with increasing degree of swelling and reaches zero when the equilibrium degree of swelling is attained. Hence, the underswelling stress should fade away when the degree of swelling approaches the equilibrium degree of swelling.
- Other stresses affecting the release stress. We noticed an effect of solvent viscosity: the lower the solvent viscosity, the lower the release stress at equal degree of swelling. There might be a relation with the slower network diffusion in a more viscous solvent.

Based on osmotic pressure arguments, the third column of Table **4.4** should suggest a decreasing tendency in σ_{rel} with increasing degree of swelling: interfacial tension is always the same for all degrees of swelling, but the 'underswelling' stress decreases with increasing degree of swelling. It should also point out a relation between σ_{rel} at Q_{eq} and $\sigma_{interfacial}$: if no other effects affect solvent release, they would be the same since the osmotic pressure contribution will be zero for this degree of swelling. Unfortunately, the measured release stress intervals are not refined enough to be able to distinguish between different degrees of swelling for 5 % HPC, yet the data for water seem to confirm our hypothesis.

Concluding, there are arguments to say that the release stress threshold depends on the degree of swelling, yet our shear experiments did not provide full proof of it. The release stress should go to zero when the degree of swelling approaches the equilibrium value and when the gel is free from other forces that prevent the solvent from coming out of the gel. If one of these two conditions is not fulfilled, the release stress will have a non-zero positive value. In the case of a gel particle at $Q < Q_{eq}$

that is immersed in a fluid different from its solvent, the release stress will be governed by the degree of underswelling, by the interfacial tension between the solvent and the suspending medium and on some other factors like solvent viscosity.

Interfacial stress should also affect droplet deformation. Such effect would result in a dependency of deformation on particle size. Yet no such effect was observed (3.4.2.5). Comparing elastic stresses to interfacial stresses elucidates this observation. Elastic stresses are of the order of 3000 Pa and do not depend on particle size whereas the size-depending interfacial stresses are a factor 10 lower. Any size-effect on deformation due to interfacial tension is most probably masked by the dominant effect of the elastic forces on gel particle deformation.

Ejection and dispersion of solvent droplets in the matrix is a different phenomenon by nature. As soon as the solvent has been released into the tips, the elasticity of the gel cannot affect this liquid anymore. The formation of the droplets is mainly governed by the physics of contact between two liquids in a shear flow field. Important parameters for this phenomenon are interfacial tension and viscosity ratio between the two fluids.

4.5.2 Discussion: how release and deformation phenomena affect each other

All the phenomena described above are induced by shear stress. Especially deformation is directly determined by the stress transmitted to the particle. High and homogeneous stresses induce highly deformed ellipsoids. This is seen on particles swollen with 10 % HPC: they hardly show tips, so they are completely surrounded by PDMS, transferring the shear stress to the particle by constant medium viscosity. However, in case tips become large (water or 1 % HPC), the particle does not reach as high deformations (Figure 4.18). Besides, a discontinuity is observed in the contour of the particle right where the tips are attached to it. The matrix cannot transfer the shear to the particle at this spot, because they make no contact. The PDMS still acts on the central part of the particle, but at the edges the stresses have to be transferred via the intermediate of the released solvent. The solvent has much lower viscosity, exerting lower stresses. Consequently, the particle is less deformed.

The largest tips are observed when the solvent is water. The interfacial tension between water tips and silicone oil is high, so that no droplets can be detached from the tips. At constant stress, the tips remain stable and the small gel deformation does so too. If the interfacial tension between the solvent in the tips and the silicone oil is low enough to allow detachment of droplets, the tips can be detached from the particle. As the tips progressively disappear due to droplet ejection, the particle deformation increases to larger deformations of the same order as the deformations of particles having small tips from the beginning. This is schematised in Figure 4.18.

The solvent has thus a major effect on the deformation of swollen gels in suspension, but it also affects the phenomena of release and ejection. The higher the solvent viscosity, the higher the stress at which solvent release was first observed. On the other hand, the higher the solvent viscosity, the closer the viscosity ratio came to unity and the easier droplets are detached from the tips. Interfacial tension is the other important parameter for ejection. The higher the interfacial tension solvent-matrix, the more

difficult it is for droplets to detach. Table 4.5 summarises the effects of the different system parameters.

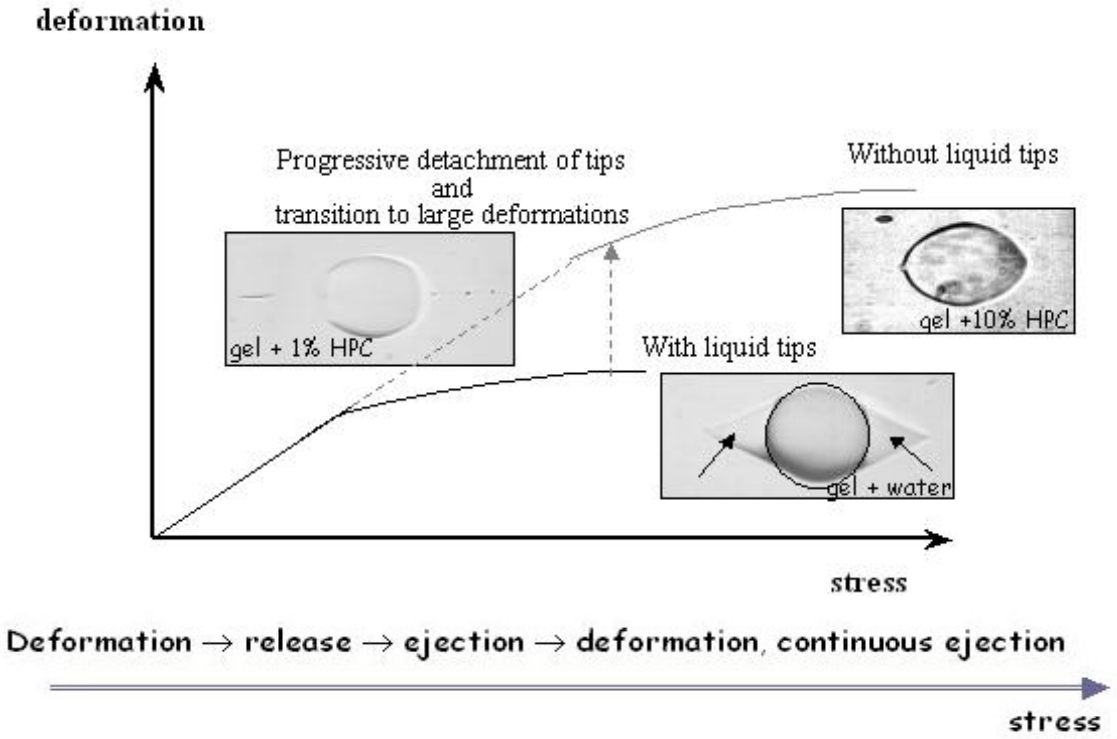

Figure 4.18: Schematic stress-deformation diagram.

Table 4.5: Overview of main parameters affecting the different phenomena observed on suspended gels

Deformation	Release	Ejection
Stress / Stress distribution	$\eta_{solvent}$	$\eta_{solvent}$ via p
Q via μ		Γ
		L_o

4.6 Conclusions

Under appropriate conditions, shear stresses induce solvent release and ejection from a suspended hydrogel particle swollen with a linear polymer solution. The particle releases some solvent at its edges as soon as the applied stress is higher than the release stress. At somewhat higher stress, droplets of solvent are detached from the tips and dispersed in the matrix.

Gel particles start to grow higher in the vorticity direction and solvent can also be released from the poles of the particle as soon as the complex modulus of the suspending fluid overcomes the shear modulus of the gel.

The polymer concentration in the gel solvent affects the release/ejection phenomena via the solvent viscosity and the solvent/matrix viscosity ratio. On the one hand, low viscosity and low polymer concentration facilitate solvent release into tips: the release stress increases with increasing solvent viscosity. On the other hand, high viscosity promotes droplet detachment from tips and dispersion into the matrix.

Interfacial tension between solvent and matrix also plays an important role for solvent detachment from the released tips: the lower the interfacial tension, the easier solvent droplets can be detached. Important reductions of the gel volume can be realised by droplet.

The release and ejection phenomena have also been observed on physical gels and on capsules with a gelly shell and can thus be considered as general phenomena. This makes these gels promising materials for carrier applications. Nevertheless, critical conditions that initiate release and ejection have to be considered when designing the process; they must not be reached before the gel particle has arrived at its target.

Résumé du Chapitre 5

Libération de solvant sous compression

Dans les deux chapitres précédents, nous avons traité le cas d'une particule de gel isolé dans une matrice d'huile silicone soumise à un cisaillement simple. Nous avons observé la sécrétion partielle de solvant aussitôt qu'un seuil de contrainte était surmonté. La compression est un autre type de sollicitation mécanique que peut rencontrer un gel lors de son application. L'étude du comportement de gel sous compression est l'objet de ce chapitre.

Des disques de gel gonflé à l'équilibre dans de l'eau ou dans une solution d'hydroxypropylcellulose ont été soumis à une compression uniaxiale. La force normale exercée par le gel sur le piston est mesurée et les dimensions du gel sont enregistrées en temps réel. Nos expériences ont montré qu'un gel gonflé à l'équilibre libère une partie de son solvant dès qu'une contrainte est exercée sur l'échantillon. Initialement, le volume du gel diminue rapidement, puis cette éjection ralentit d'à peu près un facteur 10. La vitesse de libération est limitée par la cinétique de diffusion du réseau.
L'analyse du solvant libéré par le gel gonflé dans une solution d'hydroxypropylcellulose a montré que la concentration du polymère linéaire dans le solvant libéré est la même que dans la solution initiale absorbée par le gel.

Cette diminution du volume induite par compression est également prédite par une analyse thermodynamique de la compression de gels neutres et faiblement chargés. Les pertes de volume sont petites pour des gels neutres, mais augmentent quand le nombre de groupes chargés sur le réseau augmente. A pression égale, le gel polyélectrolytique perd relativement plus de solvant que le gel non-chargé. Néanmoins, il faut considérer que le gel neutre est initialement moins gonflé.
L'allure de la perte de volume mesurée expérimentalement sur un gel fortement chargé est similaire à la forme de la courbe théorique pour les gels peu chargés.

Chapter 5

Solvent release due to gel compression

The two previous chapters treated the case of isolated gel particles suspended in oil and submitted to shear forces. We observed partial solvent release as soon as the shear stress overcame a typical value. Another type of mechanical action often encountered in applications with gels is uniaxial compression. Numerous studies on gel compression have been reported in literature. Compression tests are mostly limited to small deformations, the ratio of compressed to initial height not going below 0,8 (Gundogan et al., 2002; Okay and Durmaz, 2002; Sayil and Okay, 2001; Muniz and Geuskens, 2001; Mamytbekov et al., 1999a, b; Ilavsky et al., 1999; Dubrosvkii et al., 2001; Dubrovskii et al., 1999; Dubrovskii et al., 1997; Knaebel et al., 1997; Nisato et al., 1996; Nisato et al., 1995; Skouri et al., 1995; Schosseler et al., 1991). Compression experiments are performed either on samples immersed in a bath filled with the gel solvent (Dubrosvkii et al., 2001; Mamytbekov et al., 1999a, b; Ilavsky et al., 1999; Dubrovskii et al., 1999; Dubrovskii et al., 1997; Knaebel et al., 1997) or on samples in open air (Gundogan et al., 2002; Okay and Durmaz, 2002; Sayil and Okay, 2001; Muniz and Geuskens; Nisato et al., 1996; Nisato et al., 1995; Skouri et al., 1995; Sschosseler et al., 1991).

A swollen network immersed in solvent is a semi-open system that can exchange solvent molecules with its surroundings. It is thus supposed that the gel is in equilibrium with the solvent. A drawback of this set-up is that it becomes impossible to observe release of solvent because the solvent does not differ from the surrounding medium. The second case, compression in open air, is more complicated to analyse. Networks in open air are mostly considered closed systems in which the solvent fraction is a constant of the system. This hypothesis is only valid if the compression is executed fast enough so that the solvent has no time to diffuse out of the sample. Such system is not in equilibrium with its solvent and boundary conditions should account for the gel/air-interface created. Finally, good contact between the plates and the gel has to be assured when setting up a compression experiment. Presence of the tiniest solvent layer between plate and sample has to be avoided or taken into account since the slip caused by such layer can severely alter the results (Whiting et al., 2001).

Only few publications discuss change of gel volume due to compression. Milimouk et al. (2001) used deswelling by compression to measure the swelling pressure and diffusion coefficient of a gel. Most other experimenters do everything they can to avoid loss of solvent in order to have fully characterised samples for the duration of the experiment. This can be realised by finishing the compression experiment within a time shorter than the deswelling time of the gel (Muniz and Geuskens, 2001;

Knaebel et al., 1997; Nisato et al., 1996; Nisato et al., 1995; Skouri et al., 1995; Schosseler et al., 1991). Proceeding in this way, the gel can be considered incompressible within the experiment time (Candau et al., 1982).

In this chapter, we present results on slow continuous compression of highly swollen gels in open air. The solvent had time to diffuse out of the sample and therefore, the degree of swelling could tend to be in equilibrium with the compressive force. Both gels swollen in water and gels swollen with a linear polymer solution were tested. The gels were compressed to large deformations, sometimes reaching the failure point of the material. It was observed that under such action, the gel releases part of its solvent, as it did under shear (see **Error! Reference source not found.** and **Error! Reference source not found.**). This was observed experimentally, but volume decrease under compression was also predicted by theoretical analysis. Due to the loss of solvent, the degree of swelling is not constant. Hence, we will not draw any conclusion with respect to the gel modulus.

5.1 Data analysis

Disks cut from the synthesised gels (section **2.1.1.2**) were compressed according to the protocol described in 2.2.2. A series of images, of which a reduced version is given in Figure 5.1, was recorded during each experiment.

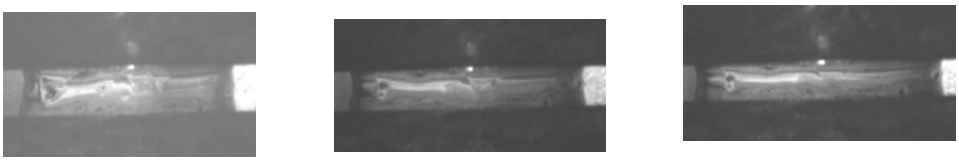

t = 535 s **t = 895 s** **t = 1079 s**

Figure 5.1: Compression of gel disk swollen with water at different times.

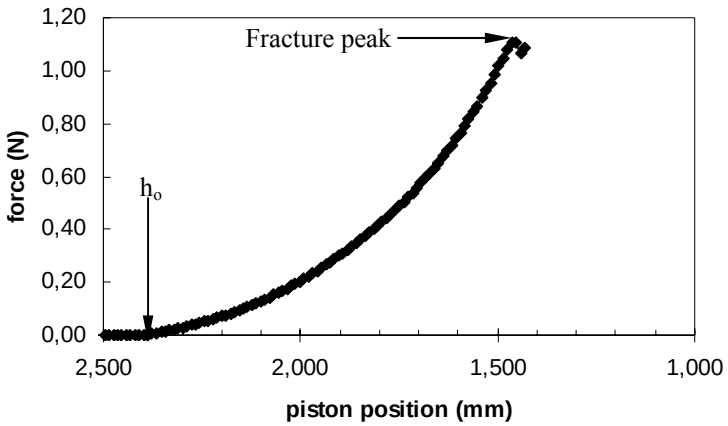

Figure 5.2: Typical force-displacement curve for gel compression experiment in open air. D_o = 9,346 mm; h_o = 2,426 mm.

The images could be related to the force – displacement data via a time code associated to each image. Figure 5.2 shows a typical force – displacement curve measured during a continuous compression experiment. No normal force is measured until the piston touches the upper face of the gel disk. This determines the initial sample height h_o. As the piston goes further down, the compressed gel exerts increasing normal forces on the piston. The force increases more than linearly (concave curve) until fracture of the gel. The fracture point is characterised by a sudden drop of the force.

The stress - strain-curve can be calculated directly from this curve. The diameter at each moment is known from the video images, so the instantaneous force can be converted into true normal stress **[5.1].**

$$\sigma_T = \frac{4F_N}{\pi D^2} \qquad \textbf{[5.1]}$$

From the knowledge of height and diameter, the volume of the cylinder can be calculated at any moment as **[5.2]**.

$$V(t) = \frac{\pi}{4} D^2(t) * h(t) \qquad \textbf{[5.2]}$$

The actual height h is converted into engineering strain ε_E according to **[5.3]**

$$\varepsilon_E = \frac{\Delta h}{h_o} = (1 - \lambda) \qquad \textbf{[5.3]}$$

Various models exist to describe the compressive behaviour of gels. A selection is given in Table 5.1. They will be used to analyse the stress-strain behaviour of the gel.

In this chapter, gel deformation and volume reduction will be considered. It should be reminded that the studied system – a gel undergoing continuous compression – is very complex and there are several reasons for which the system is not at equilibrium.

- First, since the gel is surrounded by air, there is no possibility to exchange solvent molecules with the environment in order to stay at equilibrium.
- Second, solvent is released during the experiment, entailing continuous change of the degree of swelling.

This way of testing is close to situations encountered in practical applications like squeezing a cream layer or compressing damping materials. Because of the aforementioned complexity of the system, this discussion will be limited to trends and the comparison with the theory developed in paragraph 5.5 will only be qualitative.

Table 5.1: Selection of models describing compressional stress-strain behaviour of gels

Model equation	Experimental evidence	Reference
Simplified Mooney-Rivlin (Treloar, 1975)		
$\sigma_E = \mu(\lambda - \lambda^{-2}),\ \lambda = h/h_o$ $\sigma_T = \mu(\lambda^2 - \lambda^{-1})$ **[5.4]** μ = shear modulus Constant volume: $3\mu = E$	Charged PNIPAAm*, Q ≤ 1000 g/g PAAm with PNIPAAm*, Q ≈ 5-7 g/g PVCL*, Q ≤ 40 g/g Charged PAA, Q ≤ 40 g/g PVA*, Q ≤ 20 g/g Polystyrene, Q ≤ 20 g/g	(Gundogan et al., 2002) (Muniz and Geuskens, 2001) (Ilavsky et al., 1999) (Knaebel et al., 1997) (Zrinyi and Horkay, 1984) (Bastide et al., 1981)
Model accounting for changing volume (Hasa et al., 1975)		
$\sigma_E = \mu\left(\lambda - \frac{V}{V_o}\lambda^{-2}\right)$ **[5.5]**	Charged PMAA, Q ≈ 2-20 g/g	(Hasa and Ilavsky, 1975)
Model by Blatz, Sharda and Tschoegl: BST-equation (Blatz et al., 1974)		
$\sigma_T = \frac{2E}{3n}\left[\left(\frac{D}{D_o}\right)^n - \left(\frac{D}{D_o}\right)^{-2n}\right]$ **[5.6]** E = Young's modulus n = Elasticity parameter (non-linearity)	Gelatin gels, Q ≈ 6-50 g/g	(Bot et al., 1996)
Empirical power law (Peleg and Campanella, 1989)		
$\sigma_E = k * \varepsilon_E^n,\ \varepsilon_E = 1 - \lambda$ k = rigidity constant n = degree of concavity (non-linearity) **[5.7]**	Alginate gels, Q ≈ 66-130 g/g	(Mancini et al., 1999)

* PMAA = Poly(methacrylic acid); PNIPAAm = Poly(N-isopropylacrylamide) ; PVA = Poly(vinyl acetate) ; PVCL = Poly(N-vinyl caprolactam)

5.2 Gels swollen in water

Gel disks swollen to equilibrium in water were compressed continuously. The force exerted on the piston was monitored and the observations on the disk were recorded on a videocassette.

When submitted to compression, the gel disks deformed and a certain amount of water was released. The release of water could already be observed during the experiment. The video images showed samples with concave surfaces like the ones schematised in Figure 5.3b. A cylindrical sample that is compressed would remain cylindrical in case of good sliding contact (Figure 5.3a). In case of friction, the sample surface becomes convex, as was discussed in the Materials' part. The released water must be held responsible for the apparent concave sample shape. Most of the released water accumulated on the lower plate due to gravity but part of it remained around the gel due to capillary forces. The release of water could also be noticed at the end of each experiment: droplets of water were left on the lower plate after removing the gel sample.

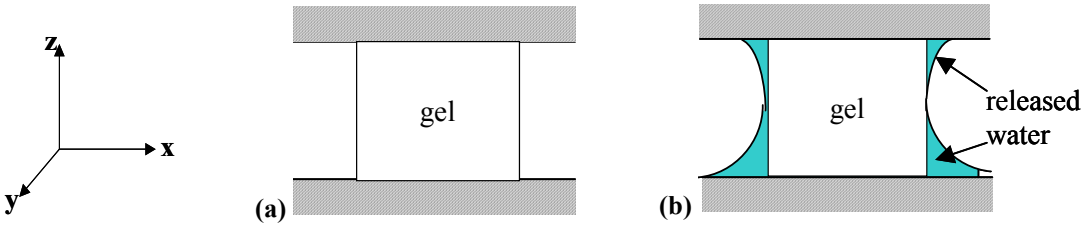

Figure 5.3: Schematic representation of a compressed gel without (a) and with (b) solvent release.

Most experiments were run until failure of the gel. The yield strain for gels swollen to equilibrium in water was ~ 0,4 at ~ 10^4 Pa.

5.2.1 Deformation

Uniaxial compression along the z-axis causes a disk to stretch uniformly in the x and y direction (biaxial extension). Under volume conservation conditions, the instantaneous diameter obeys [5.8]:

$$D(t) = D_o\sqrt{\frac{h_o}{h(t)}} \qquad \textbf{[5.8]}$$

The advantage of combining compression experiments with video recordings is that the real stretching of the disk diameter is known at each instant. The measured dependence of the relative diameter on true stress is plotted in Figure 5.4a. Data series are coincident within the range of the experimental error. The relation between (D/D_o) and true stress is linear in the studied region. Higher deformations lead to rupture of the gels.

The relative diameter is also compared to the constant volume case in Figure 5.4b. It is clear that the measured D/D_o is smaller than the constant volume prediction for all experimental cases: the disk volume decreased due to solvent release during compression. This loss of solvent was also observed on the video images.

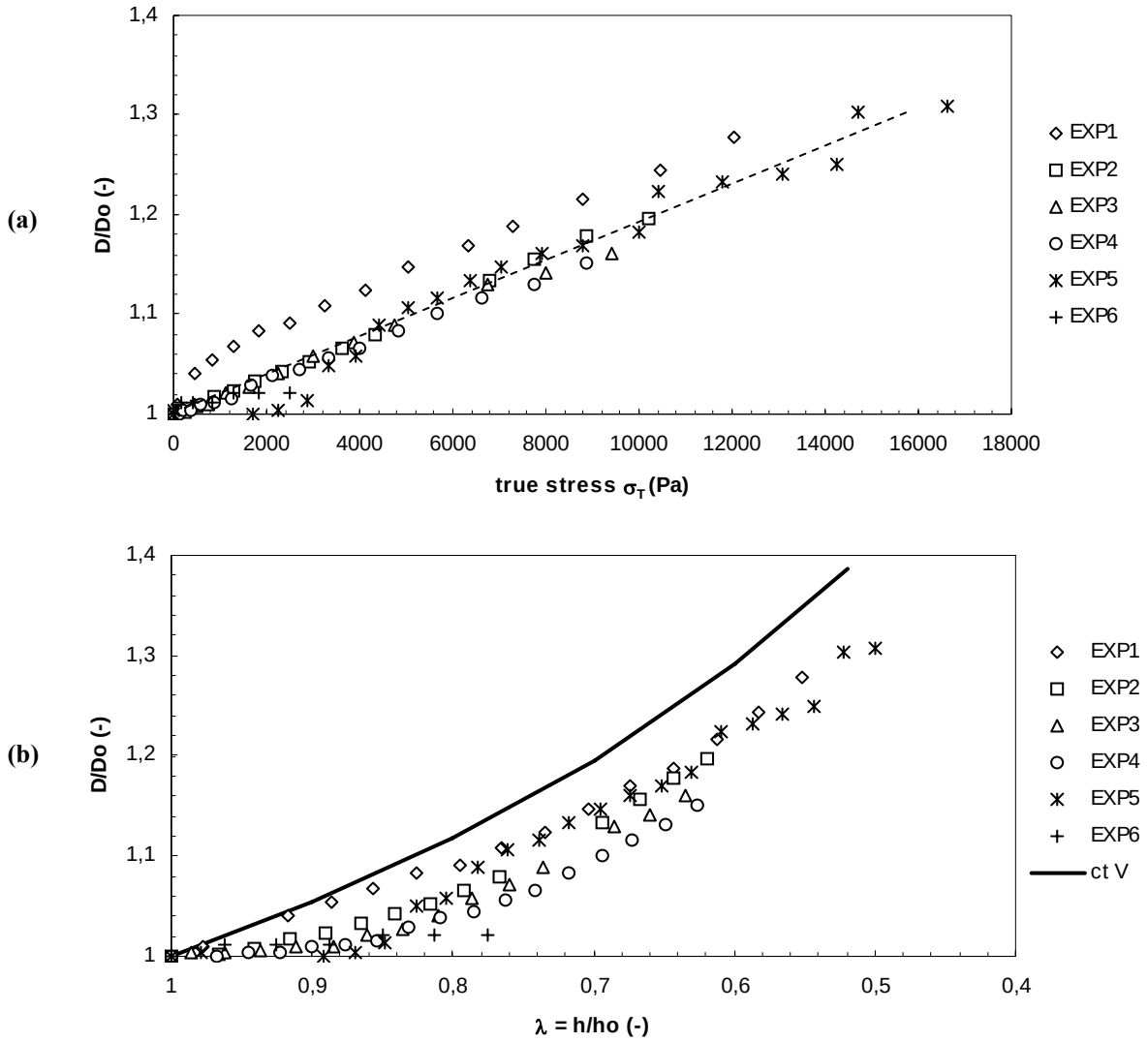

Figure 5.4: Relative diameter of a compressed gel cylinder as a function of (a) true stress and of (b) h/h_o. Dashed line in (a) is to guide the eye. The constant volume case (—) is added to (b) for comparison. Different experiments with synthesised gel initially swollen in water at Q_{eq} (200 g/g).

5.2.2 Solvent loss due to compression

It is shown in the previous section that the compressed gel disks release part of their solvent. Figure 5.5 shows the relative instantaneous volume as a function of true stress. Initial height of the disks varied between 2 and 2,5 mm and initial diameter was between 8,5 and 10 mm. In order to exclude the effect of initial size, the instantaneous volume is represented relatively to the initial volume V_o, which is the volume at equilibrium swelling in water at room temperature.

It is clear that the volume steadily decreases for all samples, which indicates that solvent is pressed out of the gel. Initially, the volume decreases rapidly giving a quite steep curve (zone A). Yet, the decrease flattens out in the second part of the curve (zone B). The reason hereof is obvious: the more solvent has been released, the farther the gel is from its equilibrium state at P = 0. Thus, the more the

remaining solvent is bound to the network and the more difficult it is to release it. As far as sodium polyacrylate gels are extremely hydrophilic, it is very difficult to extract all the water from such gels by compression alone.

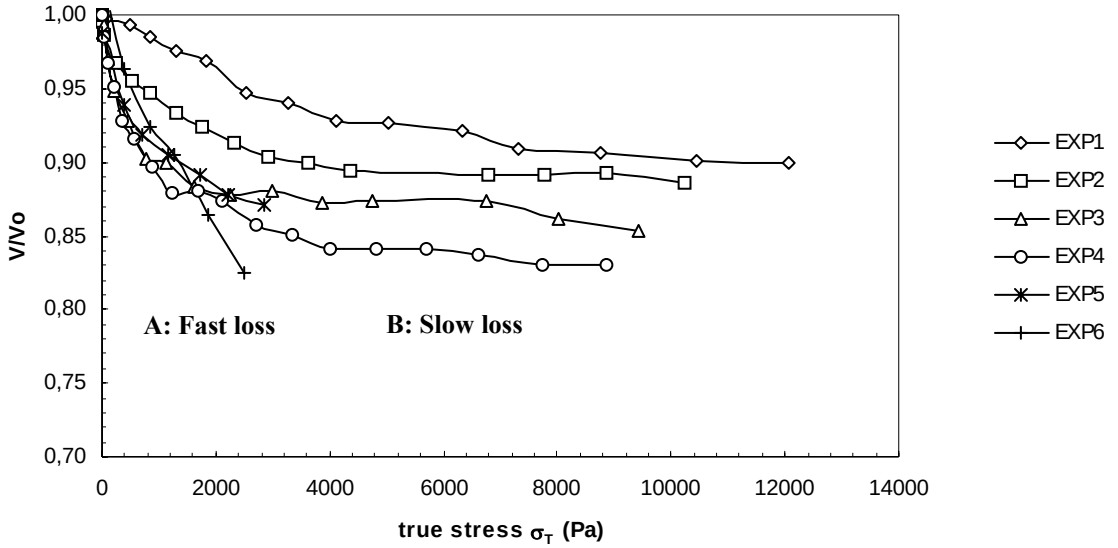

Figure 5.5: Relative volume as a function of true stress. Notice two zones differing by different slopes in the relative volume curves.

Loss of volume equally implies change of degree of swelling, according to [5.9].

$$Q = Q_o \frac{V}{V_o} \qquad \textbf{[5.9]}$$

Although all samples had the same initial degree of swelling, volume loss did not proceed in the same way for all of them. Some samples initially released their solvent faster than others (compare different series in Figure 5.5). The rate of change of volume with stress can be represented by the slope of a tangent straight line to the curve. This slope has been determined for both zones of the dependence. Slopes in zones A and B are plotted against initial jacket surface of the cylinder in Figure 5.6. The jacket surface is calculated as follows:

$$\text{Jacket surface} = \pi D h \qquad \textbf{[5.10]}$$

The diameter and height of the uncompressed disks are used to calculate the initial jacket surface.

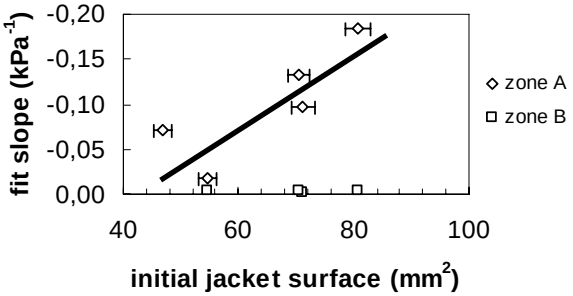

Figure 5.6: Slopes of zones A and B as a function of initial outer cylinder surface area for different sized samples.

It is clear from the figure above that the slope of zone A increases with increasing initial jacket surface. The data point out a linear relation.

$$\rightarrow \text{ slope (zone A)} = \frac{\partial\left(V/V_o\right)}{\partial\sigma_T} \sim D_o h_o \qquad \textbf{[5.11]}$$

Considering the samples are not at equilibrium during testing because of the continuous compression procedure, this figure suggests that the measured solvent release is limited by diffusion outwards.

In zone B, where $V(P)/V_o$ levels off, all curves are more or less parallel. The slope of zone B is very small, about 0,003 kPa^{-1}, and independent of initial jacket surface. The jacket surface at this instant has reduced at the onset of zone B, so it is not striking that its slope does not depend on the initial value anymore. If the onset of zone B is taken as the crossover between the tangent line to the start of the curve and the tangent to the end of the curve, this zone starts between 2000 and 4000 Pa for all cases.

Volume loss at mainly two different rates was also observed by Weyts (2001) on Stocksorb®410K gels. Those commercially available gels from Stockhausen Co. are very similar to the homemade samples used for the present work. The network is composed of 70 % Potassium acrylate and 30 % acrylamide with a maximum degree of swelling in water of about 140 g/g. The will be referred to as 'potassium gels', while the synthesised gels will be named 'sodium gels'. The tests performed by Weyts (2000) were run between sandpaper-covered plates, so measured stresses are automatically higher than the ones presented for experiments between smooth plates due to friction. Yet, apart from this point, qualitatively similar behaviour was observed on both types of gel. A comparison is given in Figure 5.7.

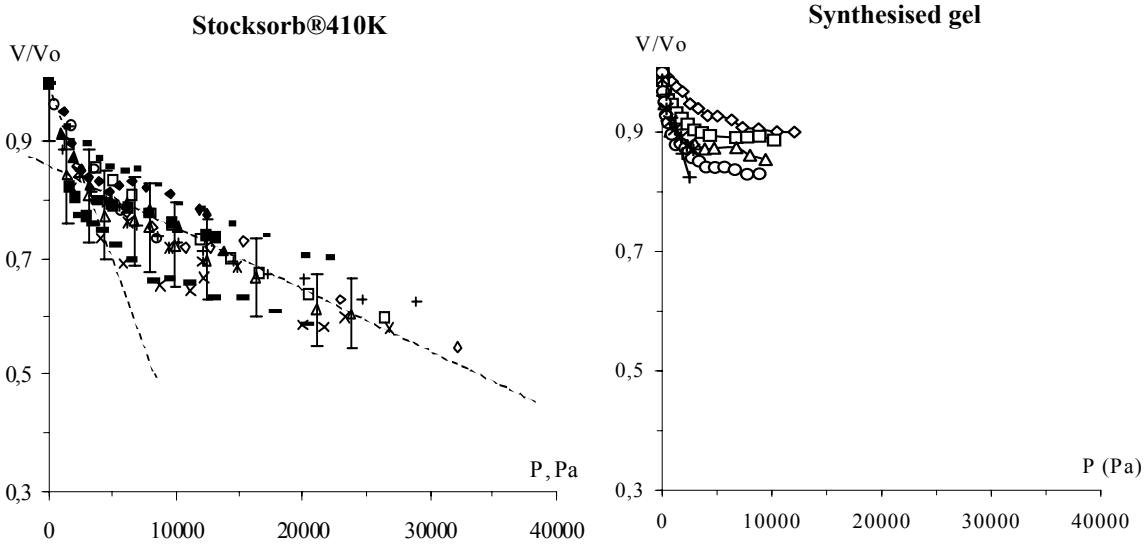

Commercial product from Stockhausen Co.
Potassium acrylate-*co*-acrylamide 70/30
Q_{max} = 140 - 150 g/g

Homemade at CEMEF
Sodium acrylate-*co*-acrylic acid 75/25
Q_{max} = 200 ± 20 g/g

Figure 5.7: Comparison of volume loss between gels of different nature.

The potassium acrylate gels could be compressed to far further extent and to higher stresses than the sodium acrylate gels. They yielded at higher deformation. The relative loss of volume at equal stress is higher with the potassium gel. Apparently, it needs less effort to induce water release from the potassium gels than from the sodium gels. Nevertheless, the deswelling behaviour of both types of gel is qualitatively the same: roughly two zones can be distinguished in each of the $V(P)/V_o$ data series of both types of gel.

5.2.3 Stress-strain curve

Calculated stress-strain curves are shown in Figure 5.8 for a series of samples of different initial size, all other things being equal. The figure represents engineering stress (a) and true stress (b). All data series are close, considering the experimental error.

Both true stress and engineering stress curves immediately show a concave upturn. No linear (Hookean) part can be distinguished in the curves. The concave upturn of the curve indicates strain hardening of the material. This behaviour probably results from a densification of the material, induced by solvent loss in the present case. Peleg and Campanella (1989) proposed to describe such non-linear stress-strain behaviour by the power-law model given in **[5.7]** where k is the rigidity constant which is a measure of stiffness and n is the degree of concavity that accounts for the deviation from linearity. If n = 1, equation **[5.7]** coincides with Hooke's law with k the elasticity modulus. $n > 1$ represents concavity, $n < 1$ describes a convex shape. Parameters k and n characterise the material. Mancini et al., (1999) found this power law satisfactorily fitting their experimental compression data on alginate gels.

Fitting the power law to our data of highly swollen polyelectrolyte gels gave the following learnings. Each of the data series (using engineering or true stresses) can be described in an accurate way by the power law. Two examples are shown in Figure 5.8 a and b to illustrate this. Average parameter sets (k; n) are ($4{,}2.10^4$; 1,66) for true stresses and ($6{,}7.10^4$; 1,82) using engineering stress. Coefficients of determination R^2 were 0,94 and 0,95 respectively. It was expected that the parameters fitted for engineering stresses are higher than for true stresses, since engineering stresses increase faster than true stresses.
The fits coincide well with the experimental points at small deformations. However, at strains above 0,4, experimental stresses clearly increase steeper than predicted by the best power law fit. The gel hardening under compression is stronger than can be described by a power law with two parameters. This observation might be explained by the observed loss of solvent. Remind that in Peleg and Campanella's model, the parameters k and n are material-dependent constants. If solvent is released by the gel, the degree of swelling is continuously changing and so do the gel properties. Therefore, the power law parameters k and n should change as well. They should be expressed as a function of Q in the power law: $n = f(Q)$ and $k = g(Q)$ with $f(x)$ and $g(x)$ unknown functions of x.

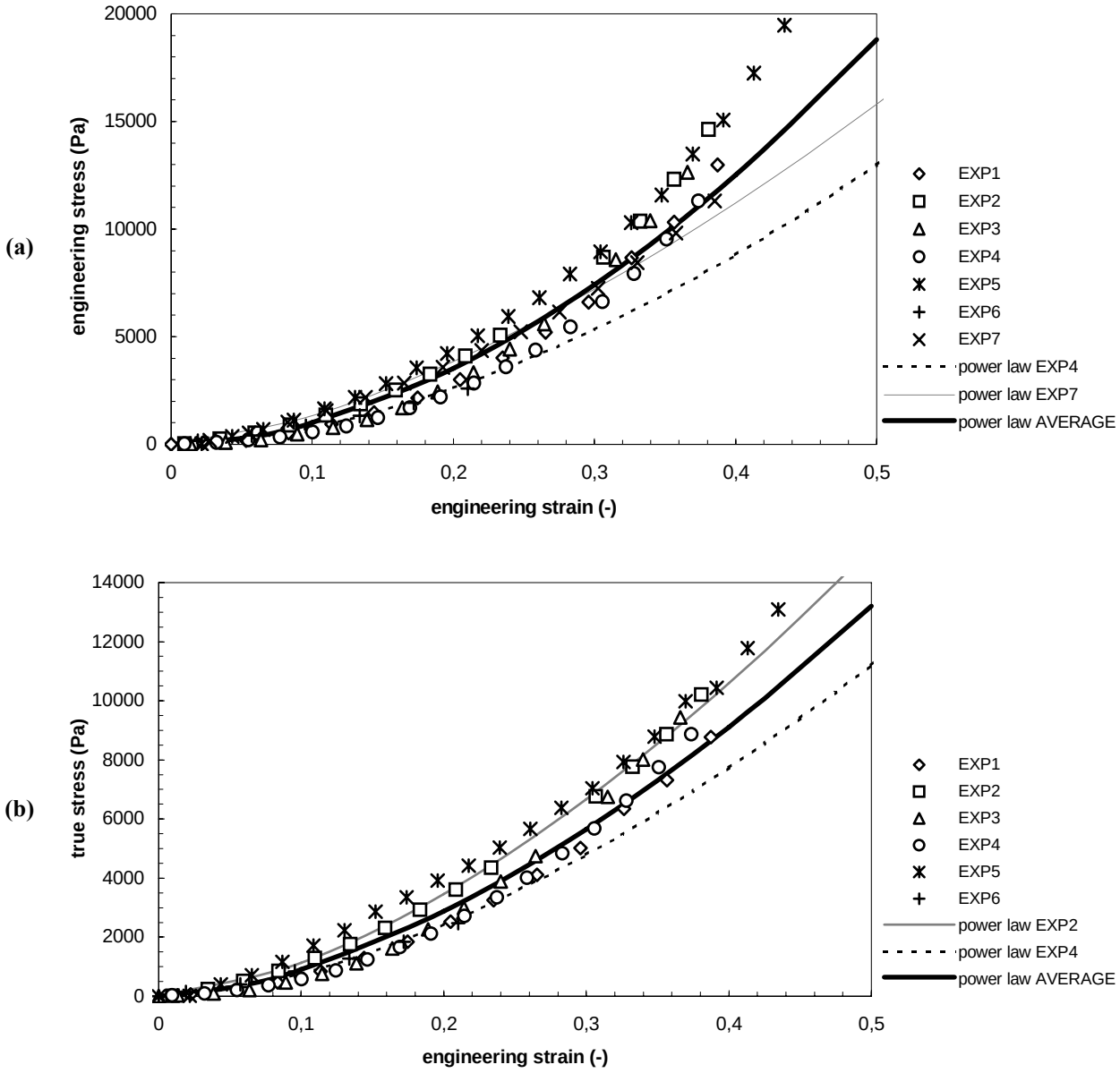

Figure 5.8: Compressive stress strain curves of gel disks expressed as engineering stress (a) or true stress (b) vs. engineering strain. Lines represent power law fits through data series. Only two fits and the overall average fit are given in order not to overload the graph.

Only one stress-strain model was found in literature that takes into account changing volume (equation **[5.5]**). It is interesting to fit our data with this model as well. Figure 5.9 shows our data in a representation adapted to the model of Hasa et al. (1975). Represented in this way, the model describes a linear relation between the combination in the abscissa and true stress.

This model was only tested for true stresses. All data series can be fitted well with a straight line. The slope of this line provides an estimate of the initial shear modulus of the gel. The fitting parameters and R^2-values for the fits are given in Table 5.2. The initial modulus of the gels is estimated as the average of the measured moduli. The high standard deviation is due to the high experimental error.

The estimate of the modulus found in this way is close to the k-parameter found from the power law fit. Dependence of the data on sample geometry could be used to identify the real compressional part of deformation. However, the data set presented here is mostly generated with samples of similar

geometry. Therefore, we were not able to draw conclusions with respect to the true compressional behaviour of these gels.

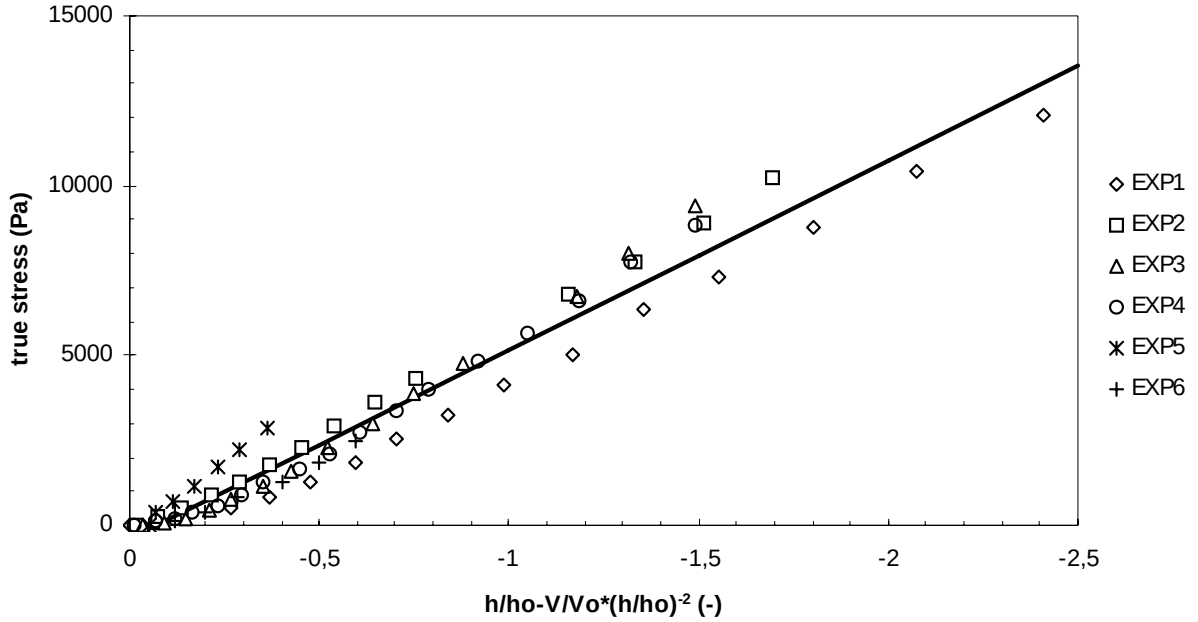

Figure 5.9: Compression data according to the model of Hasa et al. (1975), equation [5.5]. Full line is the overall best fit.

Table 5.2: Modulus determined by fitting the model of Hasa et al. (1975).

Experiment nr.	μ (kPa)	R^2
1	4,7	0,97
2	5,8	0,99
3	5,4	0,96
4	5,4	0,97
5	5,8	0,99
6	3,6	0,93
average	5,1 ± 0,8	
overall	5,5	0,97

5.3 Gels swollen in a linear polymer solution (5 % HPC)

Reminding the context of this thesis, i.e. to evaluate possibilities to implement gels as carriers of active compounds in cosmetic emulsions, compression tests were also performed on gel disks swollen in a model linear polymer solution. The solution used contained 5 % HPC. The maximum degree of swelling in this solution is 129 ± 2 g/g. The gels are swollen to this degree when the compression experiment starts. The aim of these series of experiments was twofold. First, the experiments had to show how the presence of a linear polymer in the solvent affects the rigidity of the gel and second, the

released fluid could be collected for analysis in order to learn in what concentration the HPC is released from the gel.
The comparison between gels swollen in water and gels swollen in this linear polymer solution will be treated in paragraph 5.4.

5.3.1 Deformation

Figure 5.10 shows the relative diameter as a function of stress and of relative height for four different samples. Experiments encoded as EXP5_2 and EXP5_3 were performed between smooth (uncovered) plates and EXP5_5 was executed between sandpaper-covered plates, which are rougher.

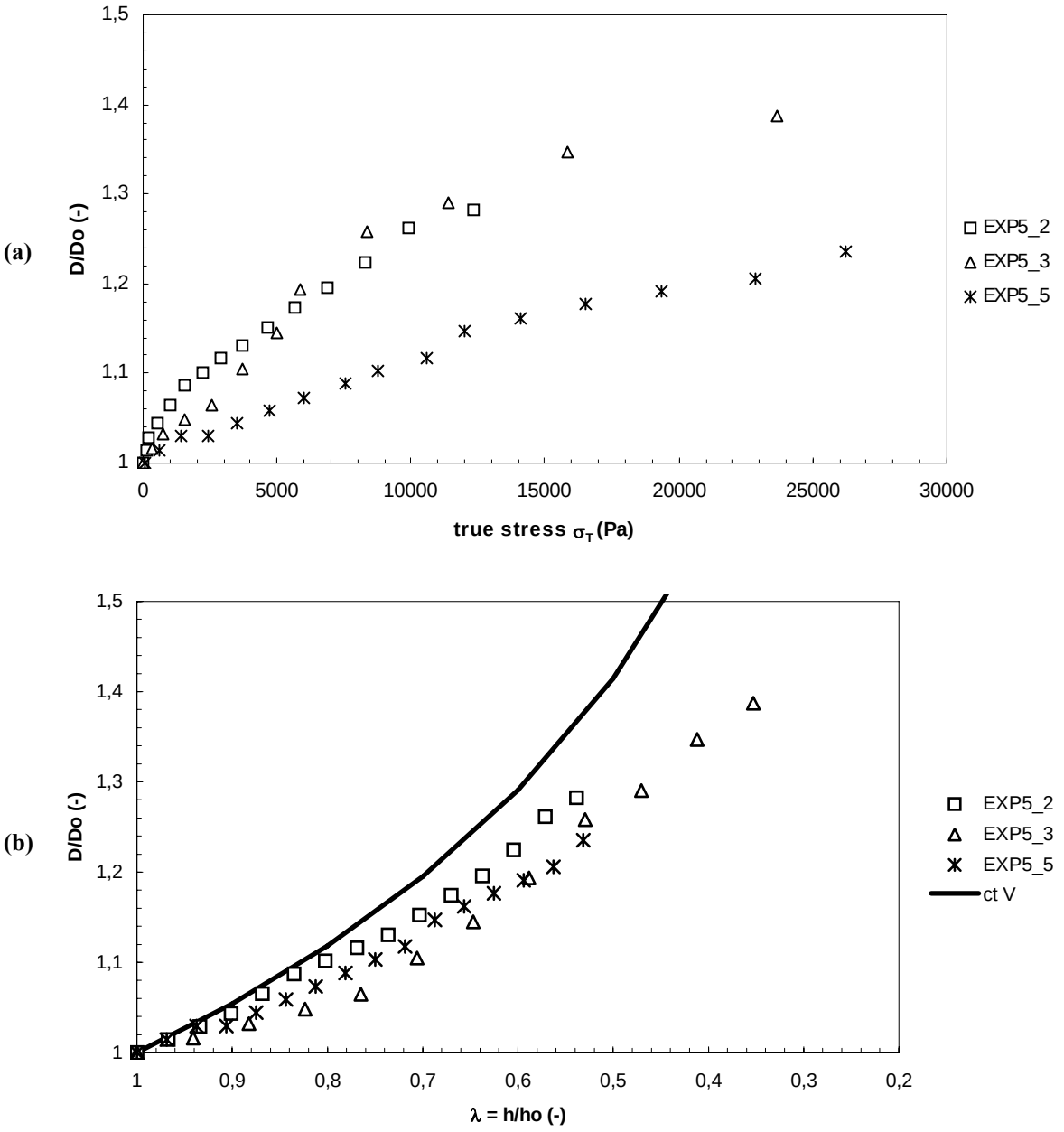

Figure 5.10: Relative diameter of gels swollen with 5 % HPC under uniaxial compression.

EXP5_5 was performed with sandpaper-covered plates. Still, it is not significantly different from the other curves in figure Figure 5.10. One should note that when sandpaper is used, the sample gets barrel-shaped under compression. The diameter is not homogeneous in this case. The diameter is therefore measured on top and bottom of the sample and at h/2. The average between these values is taken as D(h). Using this method, the sandpaper does not significantly affect the deformation as a function of h/h_o, as shows comparison with peer samples without sandpaper, yet higher stresses are needed to realise this deformation (see Figure 5.10a).
Like the gels swollen in water, the relative diameter linearly increases with increasing stress. However, at higher stresses, the increase of D/D_o flattens and seems to evolve to saturation before the sample ruptures.

The diameter evolution is also compared with the constant volume case in Figure 5.10b. It can be seen that D/D_o is always lower than the constant volume case, so the instantaneous volume is decreasing under compression as was also observed for gels swollen with water.

5.3.2 Solvent loss due to compression

The instantaneous volume of gels swollen with a 5 % HPC solution is decreasing when the gel is compressed. The dependence of the relative volume on true stress is depicted in Figure 5.11. Up to 20 % of the initial volume could be expulsed within 20 minutes experiment time. This is more than the gel could lose by evaporation only during this period (see **2.4.3**). Most solvent is released in the beginning of the compression experiments.

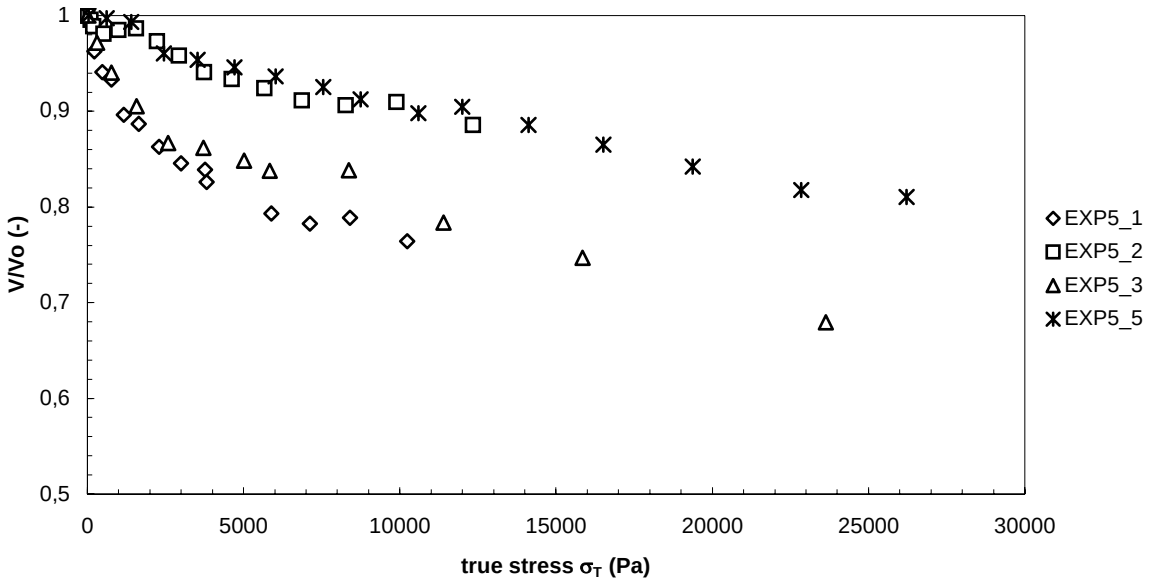

Figure 5.11: Relative volume of gels swollen with 5 % HPC solution under uniaxial compression.

The loss of solvent from gels swollen in the polymer solution qualitatively proceeds according to the same scheme as for gels swollen in water: initially fast release of solvent followed by a stage of slower release until rupture of the sample ends the experiment. However, the two zones are less pronounced. The initial slopes are less steep than for the case of gel swollen in water (-0,08 vs. -0,13 for a disk of similar dimensions swollen with water).

Two arguments can explain this difference. First, the initial degree of swelling in 5 % HPC solution is lower than in water (129 g/g compared to 200 g/g). This means that the water is stronger bound to the gel in the case of the gel swollen with the HPC solution. It is thus harder to press it out, hence the weaker slope of the dependence of V/V_o on stress. Second, deswelling is a diffusion phenomenon, which proceeds slower if the medium is more viscous. The 5 % HPC solution is more viscous than pure water (7.10^{-3} compared to 1.10^{-3} Pa.s), therefore causing slower network diffusion in the 5 % HPC solution and consequently slower decrease of the gel volume.

5.3.3 Analysis of the released liquid

The liquid released from the gel was recuperated with a Pasteur pipette and analysed by refractometry. This allowed determining the concentration of the secreted fluid by using Figure 2.6. The composition varied between 5 ± 0,5 %, which is exactly the composition of the solvent fluid. This analysis shows undoubtedly that this type of gel can be used as a true carrier of active compounds under the condition that the gel does not react with the polymer. Besides that, it releases the polymer in the concentration it has in the gel. If this tendency were true as well for higher concentrations, this type of gels would be suitable for controlled delivery systems, controlling the concentration of actives delivered by the concentration inside the gel.

5.3.4 Stress-strain curve

The stress-strain behaviour was calculated from force-displacement curves measured by the RMS 800 and from diameter measurements on the video-images. Results are plotted in Figure 5.12. Yield strain and stress were ~ 0,50 at ~ $1{,}6.10^4$ Pa for compression between smooth plates.

Series EXP5_5 shown in the figure is a typical measurement executed with sandpaper-covered plates. By covering the plates with sandpaper, the contact between gel and plate becomes sticky. This induces extra friction forces that are reflected in higher stresses at equal strain. In general, slip will underestimate stresses (Whiting et al., 2001) while friction induces overestimation. Both are undesirable. Since the tested samples did not displace on the lower plate (this was verified on the video images), we estimate slip is not an important phenomenon for these experiments. Covering the plates with paraffin oil to ensure a perfect frictionless contact could still optimise the experiment. Nevertheless, since the plates are of stainless steel and smooth and the samples are for more than 99 % composed of water, friction must be very low. This is also confirmed by the fact that the samples were cylindrical during the whole experiment and no barrelling due to surface friction was observed when using the smooth plates.

The stress-strain curves in Figure 5.12 show a concave upturning curve that can be described by the power law **[5.7]**. Parameters for experiments performed with smooth plates and with sandpaper-covered plates are given in Table 5.3. Parameter k is always higher for the rougher plates. The friction causes thus overestimation of the gel rigidity. The concavity parameter n is lower in the case with sandpaper-covered plates, owing to the fact that the same deformation range is now stretched over a broader stress interval.

Table 5.3: Average power law fitting parameters for gels swollen in 5 % HPC. Effect of plate roughness.

	Engineering stress			True stress		
	K (Pa)	n (-)	R^2	k (Pa)	n (-)	R^2
Smooth plates	6.10^4	1,85	0,96	$3,6.10^4$	1,66	0,96
Sandpaper-covered plates	1.10^5	1,55	0,98	$6,6.10^4$	1,39	0,99

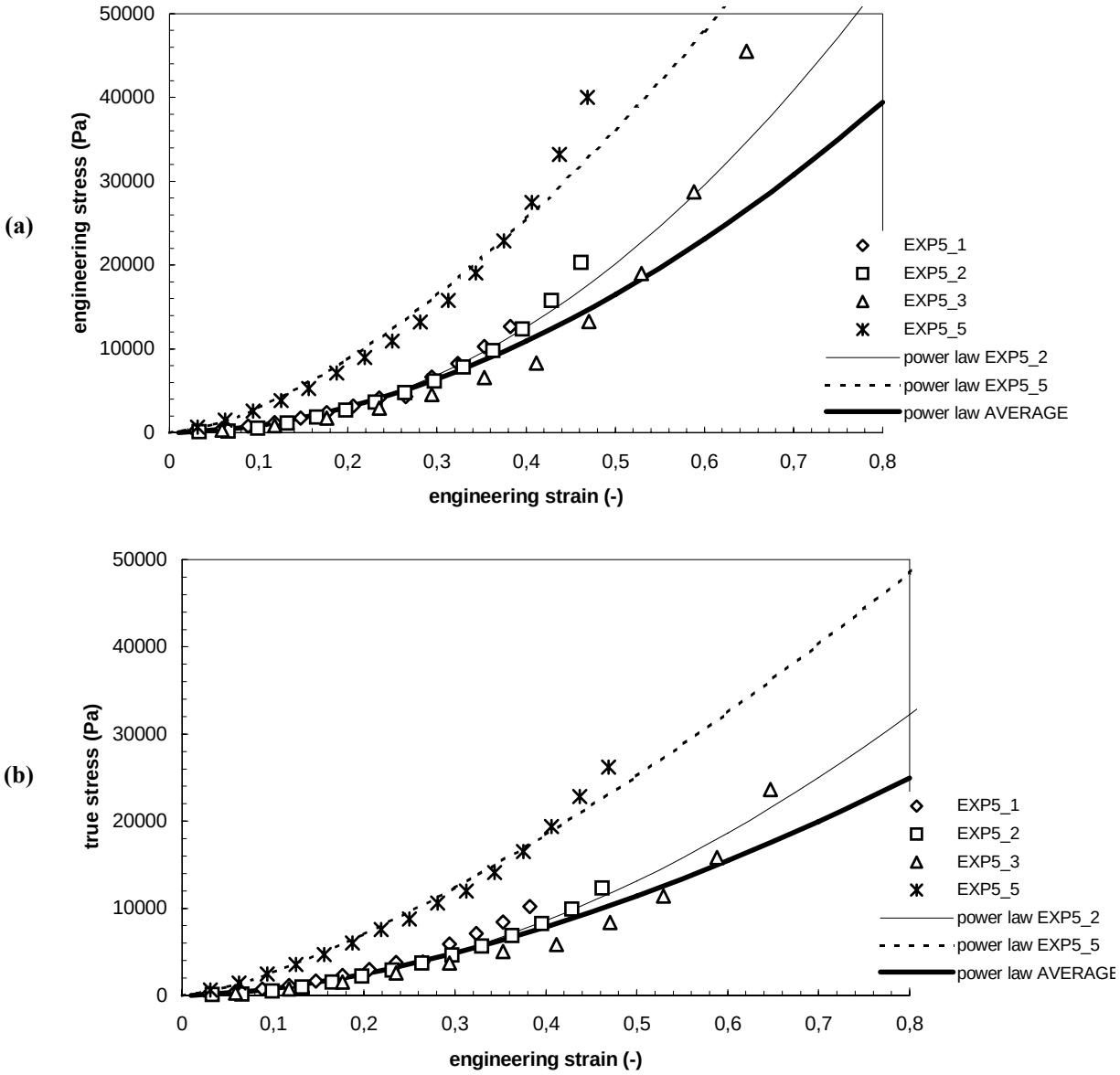

Figure 5.12: Stress-strain curves for gels swollen in 5% HPC expressed in terms of engineering stress (a) and true stress (b). Q_0= 129 g/g. Experiment 5 was run with sandpaper-covered plates. Lines represent numerical power law fits through data series. Only two fits and the average overall fit are shown to avoid overloading the graph.

The agreement between the model and the data clearly deteriorates when strain becomes higher than 0,4. The stresses recorded increase faster with strain than predicted by the model.

In the previous paragraph was found that the Hasa-model fitted the experimental data of gels swollen in water rather well. The results of the same exercise on the data for gels swollen in the 5 % HPC

solution are plotted in Figure 5.13 and the fitting parameters are given in Table 5.4. As for the gels swollen in water, the data can be fitted well by a straight line through the origin. However, the scatter of the slopes is larger than for gels swollen in water.

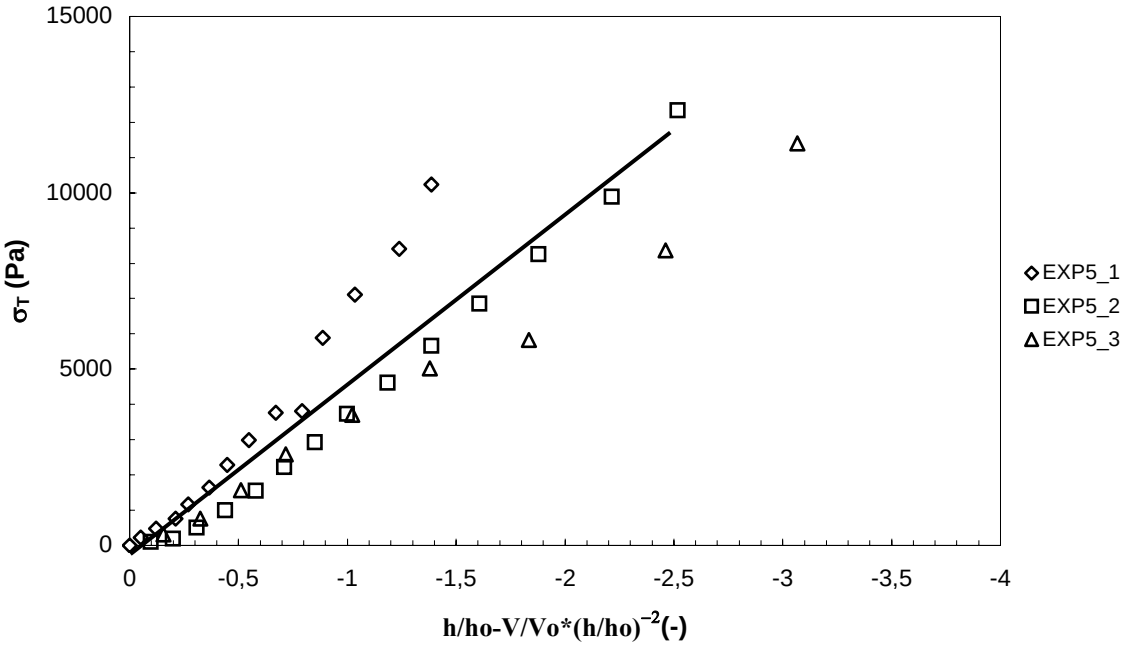

Figure 5.13: Compression data according to the model of Hasa et al. (1975).

Table 5.4: Modulus determined by fitting the model of Hasa et al. (1975).

Sample	μ (kPa)	R^2
EXP5_1	6,5	0,95
EXP5_2	5,0	0,97
EXP5_3	4,4	0,97
average	5,3 ± 1	
overall	4,3	0,93

5.4 Comparison between gels swollen in water and in 5 % HPC under compression

Figure 5.14 illustrates the differences in stress-strain behaviour between a gel swollen in water and in the aqueous polymer solution. Material properties are assembled in Table 5.5. Parameter k values indicate that the gel swollen with water is more rigid than the gel swollen with the HPC solution. If looking at the initial degree of swelling, this may be understood by the fact that the chains are less stretched in the network swollen with the HPC solution. Therefore, these chains resist less to further stretching in the x-y plane. This idea is confirmed by the higher yield strain measured on the gel swollen in 5 % HPC.

Table 5.5: Material parameters of synthesised gel samples swollen in two different solvents.

Solvent	Q_{max} (g/g)	$\eta_{solvent}$ (Pa.s)	k^* (Pa)	n^* (-)	ε_y (-)	σ_y (Pa)	μ_{Hasa} (kPa)
H_2O	200	1.10^{-3}	$4{,}6.10^4$	1,74	0,4	1.10^4	5,5
5 % HPC	130	7.10^{-3}	$3{,}6.10^4$	1,66	0,5	$1{,}6.10^4$	4,3

* Parameters determined for $\sigma_T(\varepsilon_E)$

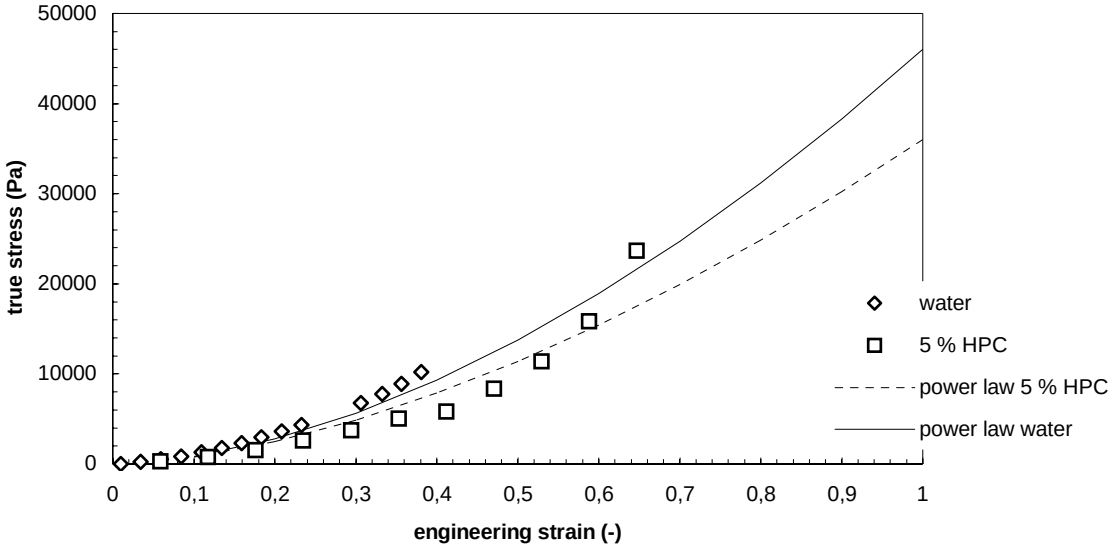

Figure 5.14: Effect of polymer solution on compression properties of synthesised gel disks. Lines are overall power law fits.

If the dry state is taken as the reference V_{ref}, then holds

$$Q \propto V/V_{ref} \qquad \textbf{[5.12]}$$

If the swelling is isotropic in all dimensions,

$$V/V_{ref} = \left(L/L_{ref}\right)^3 \Rightarrow L/L_{ref} \propto \sqrt[3]{Q} \qquad \textbf{[5.13]}$$

where L represents a distance unit.

At equilibrium swelling, indicated by the subscript "o", this becomes:

$$L_o \propto \sqrt[3]{Q_{eq}} * L_{ref} \qquad \textbf{[5.14]}$$

Yield strain is measured with respect to the completely swollen state, $\varepsilon_y = (\Delta L/L_o)_y$. To compare yield properties between gels swollen at different extent, one should consider $(\Delta L/L_{ref})_y = \varepsilon_y \sqrt[3]{Q_{eq}}$. This alternative yield strain is 2,3 for the gel swollen in water and 2,5 for the gel swollen in the HPC solution. Considering the limited precision of ε_y, one may suppose them equal. This suggests that stretching with respect to the dry state is the dominant factor for gel failure.

In literature, deswelling data are generally represented in terms of relations between pressure and degree of swelling. In order to compare our data to data published elsewhere, the relative volumes were converted into actual degree of swelling using relation [5.9]. The converted data are plotted in Figure 5.15. A first observation is that the relative amount of solvent that is released at the end of an experiment is in the same order of magnitude for both solvents. It results in a decreased degree of swelling with about 30 g/g for the applied deformations. However, it should be stressed that the deformation changes continuously and that the corresponding volumes are not equilibrium data.

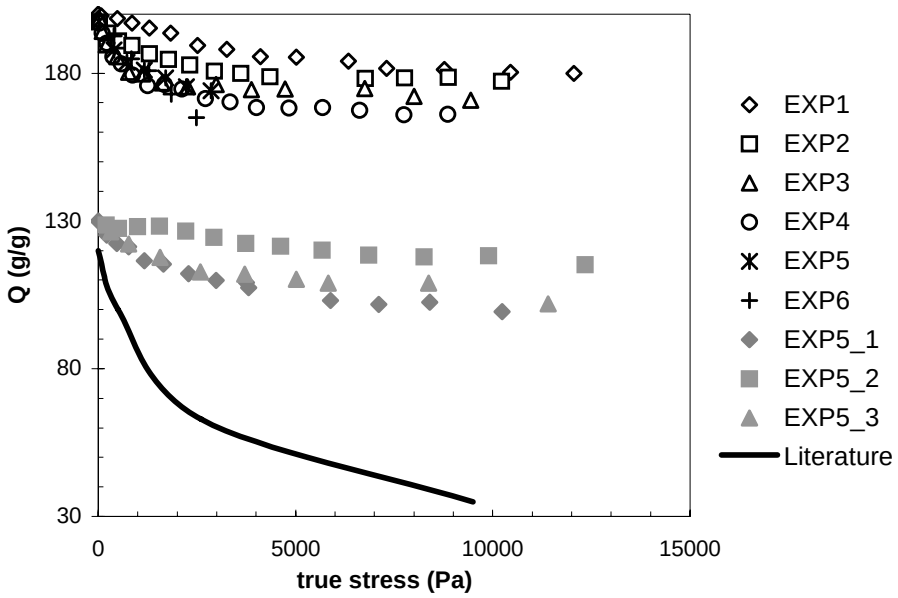

Figure 5.15: Changing degree of swelling with increasing pressure for gels swollen in water (series EXP1 to EXP6) and in 5 % HPC (series EXP5_1 to EXP5_3). Equilibrium data for a charged acrylamide gel from Lagutina and Dubrovskii (1996) are added for reasons of comparison.

Equilibrium swelling data from Lagutina and Dubrovskii (1996) for a charged polyacrylamide gel are compared to our deswelling data. Lagutina and Dubrovskii 's data show that the equilibrium degree of swelling decreases with increasing applied stress. The equilibrium degree of swelling decreases rapidly with stress when going from 0 to 3000 Pa. Above this stress value, the equilibrium degree of swelling continues to decrease with further increasing stress, but slower.

Although the initial degree of swelling is close to Q_{eq} of our gels in 5 % HPC, the equilibrium curve lies a lot lower than our experimental data as soon as some stress is applied. This is not surprising since the experiments performed in this study are continuous compression experiments. The gel has no time to reach equilibrium since the pressure is continuously increased. Therefore, the data are transitory data that are mostly governed by network diffusion. This is the limiting factor for the rate of solvent release. A gel may need several hours before reaching equilibrium (Milimouk et al., 2001; Inci et al., 2001). It appears that at the applied compression speed, and consequently the residence time of the gel at a given pressure was too short to allow release of all the solvent needed to reach the corresponding equilibrium state. Transitory volumes cannot be predicted by models like those used by Lagutina and Dubrovskii a.o. Nevertheless, both equilibrium data and transitory data show that a gel under compression does not conserve its volume. In our experiments, solvent release started just after

the piston touched the gel disk, which is within a few seconds. This means that solvent release from a gel under pressure is a true phenomenon that should be taken into account when interpreting such tests, even though it complicates the task.

5.5 Modelling of highly swollen gels under compression

The case of a highly swollen gel cylinder was also approached from a theoretical point of view. The approach presented here is based on a thermodynamic analysis developed for weakly charged polyelectrolyte gels (Kramarenko et al., 2000; Grosberg and Khokhlov, 1994). This is somewhat different from the material system in the experimental part of this chapter. The hydrogel studied experimentally was strongly charged and far from equilibrium. No theory describing the behaviour of such system has been developed yet. The proposed approach should be considered as a first step towards the solution of the problem of solvent release from a gel under compression. The comparison between theoretical predictions and experimental results will therefore be only qualitative.

Consider a cylindrical hydrogel sample swollen to equilibrium in water. The sample is immersed in an infinite vessel filled with water as represented schematically in Figure 5.16a. If no external pressure is exerted, the only pressure on the sample comes from the Laplace pressure caused by the interfacial tension.
The network is considered flawless. The average number of chain monomers between neighbouring crosslinks of the network is N. Each chain contains N/A charges separated by A monomers. The perfect network may be considered as a close packing of ν coils (de Gennes, 1979). νN/A counter-ions guarantee the electrical neutrality of the system. N/A equals zero for an uncharged gel. The system is schematically represented in Figure 5.16.

Since the final aim of this theoretical analysis is to estimate the volume change of a swollen gel under uniaxial compression and at equilibrium, the degree of swelling before and after compression will be calculated. Because of cylinder symmetry, the degree of swelling can be described alternatively by two stretching factors α along z and r-axis. $\alpha_z = H/H_{ref}$ and $\alpha_r = R/R_{ref}$ where H and R represent the height and radius of the compressed cylinder as defined in Figure 5.16c and H_{ref} and R_{ref} define the reference state.

The samples used in the experimental part were prepared in a large amount of solvent, so the reference state corresponds to the θ-condition where Gaussian chains connect neighbouring crosslinks. The radius of gyration of such chains is

$$r_g = dN^{1/2} \qquad \textbf{[5.15]}$$

with d the persistent length of the monomer. The number of internodal chains in the gel is in the order of

$$\nu = V_{ref} / r_g^3 \qquad \textbf{[5.16]}$$

with $V_{ref} = L_{ref}R_{ref}^2$ the sample volume in the reference state. The monomer concentration in the reference state is then

$$n_{ref} = \nu N / V_{ref} \qquad \textbf{[5.17]}$$

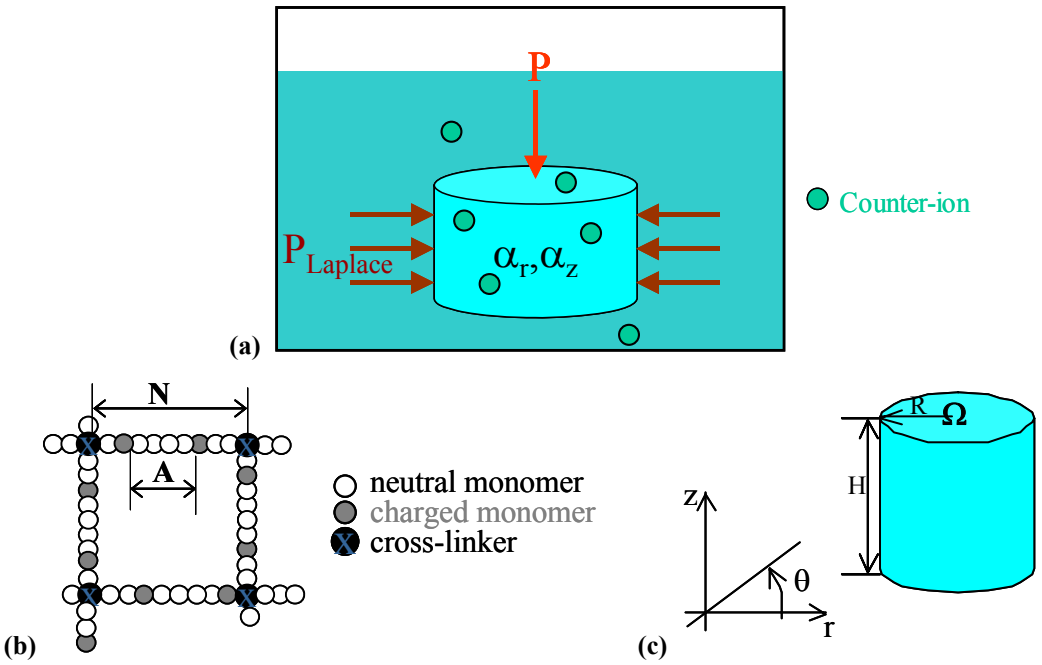

Figure 5.16: Schematic representation of modelled system. (a) force system; (b) network model; (c) sample dimensions and framework.

Substitution of **[5.15]** and **[5.16]** in **[5.17]** gives the monomer concentration in the limiting case of overlap threshold of the chains.

$$n_{ref} = d^{-3}N^{-1/2} \qquad \textbf{[5.18]}$$

The size of a freely swollen sample (zero external pressure) is defined by H_o and R_o or by swelling degrees $\alpha_{oz} = H_o/H_{ref}$ and $\alpha_{or} = R_o/R_{ref}$. α_{oz} and α_{or} may be different due to the lateral Laplace pressure.

The volume of a sample can be expressed as $V = \alpha_z\alpha_r^2 V_{ref}$, which gives $V_o = \alpha_{oz}\alpha_{or}^2 V_{ref}$ for the uncompressed volume. Relative volume [5.19] as a function of pressure will be taken as objective function in the following.

$$\frac{V(P)}{V_o} = \frac{\alpha_z\alpha_r^2}{\alpha_{oz}\alpha_{or}^2} \qquad \textbf{[5.19]}$$

Due to the axial symmetry of the problem, the stress tensor can be reduced to two components σ_{zz} and σ_{rr}. They represent the elastic response to the applied uniaxial pressure P and the lateral Laplace pressure. The dependency of α_z and α_r on P can be derived from the equilibrium between internal and external stress [5.20]:

$$\begin{cases} \text{Along z:} & \sigma_{zz} = P = \dfrac{1}{\alpha_r^2 V_{ref}} \dfrac{\partial G}{\partial \alpha_z} \\ \text{Along r:} & \sigma_{rr} = P_{Laplace} = \dfrac{1}{2\alpha_r \alpha_z V_{ref}} \dfrac{\partial G}{\partial \alpha_r} \end{cases} \quad \textbf{[5.20]}$$

where G is the free energy of the polyelectrolyte gel.
The free energy of a polyelectrolyte gel in solvent can be described as the sum of four contributions (Grosberg et al., 1994):

$$G = G_{el} + G_{int} + G_{tr} + G_C \quad \textbf{[5.21]}$$

- G_{el} is the elastic energy of a swollen network. For a weakly charged gel, it may be expressed quite accurately as the sum of elastic energies of the ν Gaussian coils that compose the sample (Zeldovich et al., 1999; Kramarenko et al., 2000):

$$G_{el} = \frac{1}{2} \nu k_B T \left[2\alpha_r^2 + \alpha_z^2 - \frac{2}{f} \ln\left(\alpha_r^2 \alpha_z\right) \right] \quad \textbf{[5.22]}$$

- G_{int} expresses van der Waals interactions between uncharged monomers. It may be written in terms of the virial expansion for a highly swollen gel:

$$G_{int} = \nu k_B T N \left[Bn + Cn^2 \right] \quad \textbf{[5.23]}$$

  where B and C are the second and third virial coefficients. The second coefficient is a measure for the deviation of the polymer system from the θ temperature $(\Delta T = T - \theta)$: $B \propto d^3 \Delta T/T$ while $C \propto d^6$. The monomer concentration n at any state is related to the monomer concentration in the reference state as $n = n_{ref} / \alpha_r^2 \alpha_z$.

- G_{tr} represents the free energy of counter-ions entrapped in the gel. The counter-ions are considered gas-like (Grosberg et al., 1994).

$$G_{tr} = k_B T \frac{\nu N}{A} \ln\left(\frac{n}{A}\right) \quad \textbf{[5.24]}$$

  The escape of counter-ions from the gel with the released solvent is neglected because of the high electric potential that arises when the electro-neutrality condition within the gel is violated. Only a very small number of ions can be released, yet will not give a dominant contribution to the free energy.

- G_{Coul} is the free energy due to electrostatic interactions between charges in the polyelectrolyte gel. It can be compared to the free energy of Coulomb interactions in electrically neutral plasma with the same concentration of charges. In the Debye-Hückel approximation, it may

be expressed as $G_{Coul} = -k_B T v \left(\frac{\ell_B}{d}\right)^{3/2} \frac{N}{A}\left(\frac{nd^3}{A}\right)^{1/2}$ where $\ell_B = \frac{e^2}{\varepsilon k_B T}$ is the Bjerrum length (Grosberg et al., 1994) with e = the protonic charge (1,6022.19^{-19} C) and ε = the dielectric constant of the solvent (78,5 for water at 25 °C, (Manning, 1969)). For the aqueous system considered here, ℓ_B = 0,7 nm at room temperature. This is the same order of magnitude as the size of the monomers in the gel, d = 0,8 nm, so we will set $\ell_B / d \cong 1$. As a result, the contribution of electrostatic interactions to the free energy of a weakly charged hydrogel can be written as:

$$G_{Coul} = -k_B T v \frac{N}{A}\left(\frac{nd}{A}\right)^{1/2} \qquad \textbf{[5.25]}$$

Substitution of equations [5.22] to [5.25] into [5.21] and using [5.20] results in following correlations between degrees of swelling and external stresses:

$$\begin{cases} P = k_B T n_{ref}\left[\frac{f\alpha_z^2 - 1}{Nf\alpha_r^2\alpha_Z} - \frac{Bn_{ref}\alpha_r^2\alpha_z + 2Cn_{ref}^2}{\alpha_r^6\alpha_z^3} - \frac{1}{A\alpha_r^2\alpha_z} - \frac{1}{2A\alpha_r^3\alpha_z^{3/2}}\left(\frac{n_{ref}d^3}{A}\right)^{1/2}\right] & \textbf{[5.26]} \\ \Gamma = P + \frac{k_B T n_{ref}}{N}\left(\frac{1}{\alpha_z} - \frac{\alpha_z}{\alpha_r^2}\right) & \textbf{[5.27]} \end{cases}$$

Note that the last term in equation [5.26] arising from the electrostatic interactions is small compared with the term related to the osmotic pressure of the counter-ions. The Laplace pressure will be set to zero in the following, supposing the interfacial tension between a gel swollen in water and water is close to zero.

The system of equations [5.26] and [5.27] now contains network parameters, two unknown, α_r and α_z, and the variable P, so it can be solved numerically. α_{or} and α_{oz} can be calculated from P = 0. Knowing these, α_r and α_z can be calculated for each value of P. The relative degrees of swelling as a function of the applied pressure follow from equation [5.19]. The results are presented in Figure 5.17 for three ratios N/A : 0 (uncharged case), 5 and 10. The polymer volume fraction in the reference state $n_{ref}d^3$ was set at 0,1 and 0,25 respectively (This means changing the number of chains in the network). The curves are calculated for network parameters N = 100 and f = 4. For these network parameters, the overlap threshold corresponds to polymer volume fraction 0,1. The considered values for the second and third virial coefficients, B = 4d^3 and C = 0,08D^6 provide a high degree of swelling.
The solution for N/A = 0 shows that a neutral gel under compression loses part of its volume. The applied pressure restricts the van der Waals repulsion between monomers, causing a decrease of the sample volume.

Increasing the ratio N/A corresponds to increasing the number of charges on the chains, resulting in higher translational entropy of counter-ions and higher electrostatic interactions (see equations [5.24] and [5.25]), leading to higher degrees of swelling in both dimensions in the stress-free state.

Figure 5.17 illustrates that the more charges per chain, the smaller the relative volume of the polyelectrolyte chain when compressed to the same pressure. A charged gel is initially swollen to a further extent than a neutral gel, but the average solvent molecule is bound in a stronger way to the neutral network.

Extrapolating these findings to the case of highly charged polyelectrolyte gels, as the ones studied in the experimental part, incites the prediction that uniaxial compression could induce noticeable decrease of the relative volume of those gels. Important loss of volume was indeed observed in the experimental part. Although this theoretical analysis is restricted to the case of weakly charged gels, the trends are in qualitative agreement with the experimental observation on highly charged systems.

The physics behind these predictions and observations of solvent release induced by compressing a hydrogel are the following. In the case of neutral gels, the applied pressure restricts van der Waals repulsion between monomers, resulting in some decrease of the sample volume. In the case of polyelectrolyte gels, a second – much stronger – phenomenon contributes to gel swelling: osmotic pressure of counter-ions. This contribution is partially compensated by the action of compression. This leads to decreased efficiency of swelling due to counter-ions, thus leading to larger solvent release than for neutral networks. The decrease of polymer concentration enhances this effect. Actually, both van der Waals repulsion of monomers and osmotic pressure of counter-ions would be diminished in this case, leading to larger compression with less lateral stretching. As a result, solvent release rises.

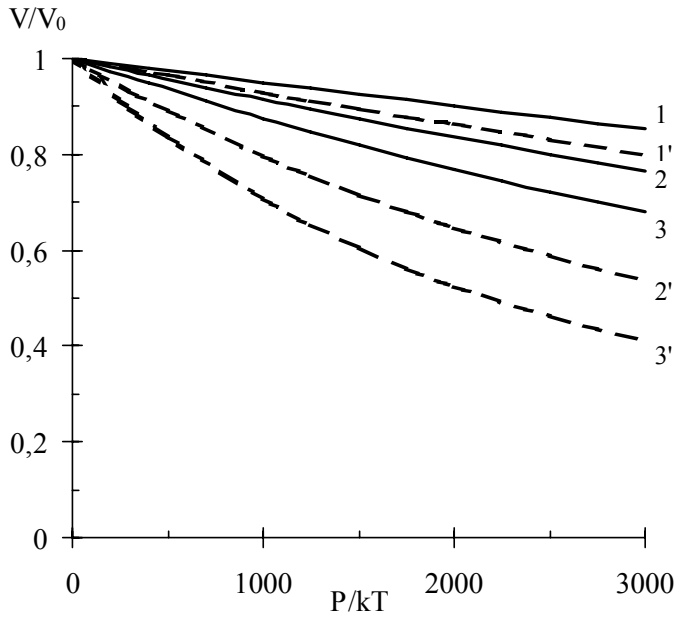

N/A	$n_{ref}d^3$ 0,1	0,25
0	1’	1
5	2’	2
10	3’	3

Figure 5.17: Theoretical predictions of the effect of applied pressure on the relative equilibrium volume of weakly charged polyelectrolyte gels for different charge densities (N/A) and initial polymer volumes ($n_{ref}d^3$). Abscissa parameter is a non-dimensional measure of pressure.

5.6 Conclusions

Homemade poly(Na-acrylate-*co*-acrylic acid) gels swollen at equilibrium in water and in an aqueous linear polymer solution were submitted to compression. It was shown that solvent is released from the gel swollen at equilibrium as soon as some pressure is exerted on the sample and it continues as compression proceeds. Two regimes could be identified: in a first stage, the gel volume decreases fast. After that, solvent ejection proceeds about 10 times slower. The rate of solvent release is limited by network diffusion kinetics.
Taking a linear polymer solution as solvent changes the equilibrium degree of swelling and consequently the mechanical properties. However, comparison of yield properties points out that failure is inherent of the stretching of the network in the studied range of degrees of swelling.
Analysis of the solvent released from the gel swollen with this polymer solution showed that the linear polymer is released in the same concentration as it was absorbed by the gel, which gives good prospective for carrier applications for hydrogels.

Thermodynamic analysis of neutral and weak polyelectrolyte gels also predicts loss of volume induced by compression. Small loss of volume was predicted for a neutral network, but the predicted loss increases as more charged groups are embedded in the network. At equal pressure, polyelectrolyte gels lose relatively more solvent than neutral-ones. Nevertheless, one should keep in mind that neutral gels are less swollen initially.
The shape of the experimentally measured loss of volume curve of highly charged gels is similar to the theoretical shape for weakly charged gels.

Conclusions

In the search for novel vectors for active substances in emulsions, hydrogels propose an original route. Encapsulation of various types of solutes has been proven to be rather easy, but release remains an important research theme nowadays. A typical aspect of cream preparation and application is the mechanical action: shear and/or compression. Release induced by this type of stimulus has not been investigated systematically before and is not well understood yet. Therefore, the purpose of this thesis was to investigate if and how active compounds will be released from a gel by the mechanical action of shear or compression.

We studied in detail the behaviour polyelectrolyte hydrogels swollen with aqueous linear hydroxypropylcellulose solutions by means of a counter-rotating rheometer and by compression tests. The reactions of a swollen gel to mechanical action were identified and the effects of system parameters including particle size, solution concentration, interfacial tension and degree of swelling were studied. Our main findings are highlighted below.

Depending on the applied shear stress, a gel particle suspended in oil can show different responses:

- At stresses below release stress, the particle is deformed into an ellipsoid with three different axes that is oriented along the flow direction and rotates around the vorticity axes. The period of rotation corresponds to the Jefferey period. Initially, deformation increases linearly with stress. Deformation before release is predicted by the Cox model modified with an elastic term.
- At stresses above release stress, some solvent comes out of the gel, but stays attached to the edges of the ellipsoid. Gel and solvent tips flow together. The solvent tips can grow very large for low viscosity solvents. The presence of large tips limits the deformation of the gel particle, whereas tiny tips hardly affect deformation. Solvent release is reversible.
- Release stress is lower for low viscosity solvents.
- At stresses above ejection stress, tiny solvent droplets are detached from the edges of the solvent tips. Due to this phenomenon, the gel particle may lose up to 20 % of its volume. The lost volume could be dramatically increased by addition of a w/o emulsifier to the suspending oil.
- Ejection stress is lower for higher viscosity ratios, for lower interfacial tension and for larger particles.
- As soon as the complex modulus of the matrix overcomes the elastic modulus of the gel, the particle height increases and eventually, solvent is released in the vorticity direction.

The behaviour of some physical gels and gel capsules based on polysaccharides under shear was also screened. These gels also demonstrated deformation, solvent release and ejection. This means that the observations made in this study on synthetic gels have a general character.

Compression tests on polyelectrolyte gel disks gave rise to the following learnings:

- Gel disks at equilibrium degree of swelling release solvent as soon as some compression force is applied. Initially, the release is rather fast, but it slows down as more solvent has been lost. The initial release rate depends on the jacket surface of the disk.
- Recovery of the released fluid allowed concluding that the gel releases the HPC solution in the concentration that it has inside the gel.
- Loss of volume due to compression has been predicted theoretically for neutral and weakly charged gels. The tendencies are qualitatively the same for the highly charged gels examined experimentally.

A common observation during shear and compression tests is that a gel reacts to increasing stress not only by deformation but also by partial release of its solvent. This observation confirms they are promising for release applications induced by mechanical action. Nevertheless, critical stresses have to be taken into account because they should not be overcome before the gel has reached its target.

Suggestions for further research

The results of this first study on release induced by mechanical action from gels swollen with a polymer solution are very promising. The possibility to release the solvent that is temporarily stored in a gel, by mechanical action has been demonstrated. This is of interest for various industries and could open the way to innovative products. Nevertheless, many issues are left open and the system is far from being fully understood. Below, we give some suggestions for further research on this subject.

- The logic continuation of this work would be to proceed with concentrated gel suspensions, which are closer to realistic cosmetic emulsions. Most probably, the phenomena observed on an isolated particle cannot be transposed straightforward to concentrated systems. Incidental collisions of two gel particles observed during our experiments showed that two particles can flow together for some time after collision. The contact altered solvent release and ejection. It was also observed that solvent could be released at stresses below the release stress if another particle passed close enough to the observed particle, which changed the local stress field.
- Industrially relevant combinations of gel and polymer must be tested. For personal care applications, it is important that no toxic materials or allergens are used. The gel container should as well be biodegradable after delivery of the active compound in order to ensure consumer comfort (no residual material layer). Moreover, active compound and container have to be combined with care. Some common tests at Cemef and Dior with Aqua Keep and aqueous solutions of dihydroxyacetone (DHA) failed because the interaction between the polyacrylic acid - polyacrylate network and DHA led to decomposition of DHA.
- The next step should be that physico-chemical effects relevant for the application (temperature, pH, physiological salts) are taken into account. This also includes the effect of

other emulsion ingredients. We already showed briefly that the addition of a w/o emulsifier to the system dramatically facilitated ejection of the aqueous solvent. Also minor ingredients like colorants or preservatives are expected to affect release and ejection.

From a more fundamental point of view, following issues deserve attention as well:

- It would be interesting to study the system at molecular scale. Knowing how the linear polymer is stabilised inside the gel, how it is distributed and how it flows outside when the appropriate stresses are applied, is important to master controlled release. It was not possible to directly measure the concentrations of the released fluid in our study although the different observations with different solvents (water versus HPC solutions and solutions at different concentrations) suggest the effect of the solvent properties on release conditions.
- The critical conditions are unique for each type of swollen gel and a large number of parameters are involved. The evaluation of each new system requires a large number of experiments. Numerical modelling and simulation of gelly objects in a viscous matrix could reduce the workload since it would allow easy variation of parameters. Before a code can be developed, one needs to know the analytical relations that describe the system. These are still to be developed.
- Another fast way to determine critical conditions could be rheometry of the gel suspension. If relations could be established between deformation - release - ejection phenomena and bulk rheology of the gel suspensions, a rheological fingerprint could be used to derive critical conditions. Moreover, knowledge of bulk rheology is also of interest for process design.

References

Almdal, K., Dyre, J., Hvidt, S., Kramer, O., Towards a phenomenological definition of the term 'gel', Polym. Gels and Networks, 1, 5-17 (1993).

Anseth, K.S., Bowman, C.N., Brannon-Peppas, L., Mechanical properties of hydrogels and their experimmental determination, Biomaterials, 17, 1647-1657 (1996).

Aqua Keep superabsorbent polymer, Sumitoko Seika, Ltd.,Osaka.

Astruc, M., Etude rhéo-optique des mécanismes de dispersion de mélanges sous cisaillement simple, Ph.D. thesis, Ecole des Mines de Paris, Sophia-Antipolis, 2001, 213p.

Astruc, M., Vervoort, S., Nouatin, H.O., Coupez, T., De Puydt, Y., Navard, P., Peuvrel-Disdier, E., Experimental and numerical study of the rotation and the erosion of fillers suspended in viscoelastic fluids under simple shear flow, Rheol. Acta, 42, 421-431 (2003).

Aqualon, Klucel hydroxypropylcellulose: propriétés physiques et chimiques.

Barrat, J.-L., Joanny, J.-F., Pincus, P., On the scattering properties of polyelectrolyte gels, J. phys. II France, 2, 1531-1544 (1992).

Bartok, W., Mason, S.G., Particle motions in sheared suspensions. VII. Internal circulation in fluid droplets (theoretical), J. Coll. Sci., 13, 293-307 (1958).

Bastide, J., Picot, C., Candau, S., The influence of pendent chains on the thermodynamic and viscoelastic properties of swollen networks, J. Polym. Sci.: Polym. Phys., 17, 1441-1456 (1979).

Bastide J., Candau, S., Leibler, L., Osmotic deswelling of gels by polymer solutions, Macromolecules, 14, 719-726 (1981).

Bastide, J., Picot, C., Candau, S., Some comments on the swelling of polymer networks in relation to their structure, J. Macromol. Sci. –Phys., B19(1), 13-34 (1981).

Bastide, J., Boué, F., Buzier, M., Swelling and deswelling of polymer networks investigated by different types of SANS experiments: comments about the structure. In: Baumgärtner, A., Picot, C.E., eds., Molecular basis of polymer networks, Proc. Phys., 42, Springer-Verlag, Heidelberg, 1989, p48-64.

Bekturov, E.A., Frolova, V.A., Mamytbekov, G.K., Swelling of poly(2-methyl-5-vinylpyridine) gel in linear sodium poly(vinylsulfonate) solution, Makromol. chem. phys ., 199, 1071-1073 (1998).

Bekturov, E.A., Frolova, V.A., Bimendina, L.A., Swelling behaviour of a non-ionic poly(N-vinyl-2-pyrrolidone) gel in a linear poly(acrylic acid) solution, Makromol. Chem. Phys., 200, 431-435 (1999).

Bell, C.L., Peppas, N.A., Equilibrium and dynamic swelling of polyacrylates, Polym. Eng. Sci., 36(14), 1856-1861 (1996).

Bikard, J., Menard, P., Peuvrel-Disdier, E., Budtova, T., 3D numerical simulation of the behaviour of a spherical particle suspended in a Newtonian fluid and submitted to a simple shear, *submitted to J. Comput. Mater. Sci., 2005*.

Blatz, P.J., Sharda, S.C., Tschoegl, N.W., Strain energy function for rubberlike materials based on a generalized measure of strain, Trans. Soc. Rheol., 18(1), 145-161 (1974).

Bot, A., van Amerongen, I.A., Groot, R.D., Hoekstra, N.L., Agterof, W.G.M., Large deformation rheology of gelatin gels, Polym. Gels and Networks, 4, 189-227 (1996).

Boyer, R.F., Deswelling of gels by high polymer solutions, J. Chem. Phys., 13 (9), 363-372 (1945).

Brochard, F., Polymer networks swollen, by a homopolymer solution, J. Physique, 42, 505-511 (1981).

Budtova, T.V., Budtov, V.P., Navard, P., Frenkel, S.Y., Rheological properties of highly swollen hydrogel suspensions, J. Appl. Polym. Sci., 5, 721-726 (1994).

Budtova, T.V., Suleimenov, I.E., Frenkel, S.Y.A., Interpolymer complex formation of some non-ionogenic polymers with linear and cross-linked polyacrylic acid, J. Polym. Sci.: Part A: Polym. Chem., 32, 281 – 284 (1994).

Budtova, T., Navard, P., Polyelectrolyte hydrogel swelling in a concentrated polymer solution, Macromolecules, 28, 1714-1716 (1995).

Budtova, T., Navard, P., Swelling dynamics of cross-linked poly(acrylic acid) and neutralised poly(acrylate-co-acrylic acid) in aqueous solutions of (hydroxypropyl)cellulose, Macromolecules, 29, 3931-3936 (1996).

Candau S., Bastide J., Delsanti M., Structural elastic, and dynamic properties of swollen polymer networks. In: Adv. Polym. Sci., 44, Springer-Verlag, Heidelberg, 1982, p. 27-71.

Carette, L., Pouchol, J.-M., Silicones, Plastiques et composites AM3, Techniques de l'ingénieur, 1996, A 3475, p. 1 to 7.

Cerf, R., Recherches théoriques et expérimentales sur l'effet Maxwell des solutions de macromolécules déformables. I. Théorie de l'effet Maxwell des suspensions de sphères élastiques, J. Chim. Phys., 48, 59-84 (1951).

Chang, K.S., Olbright, W.L., Experimental studies of the deformation and break-up of a synthetic capsule in steady and unsteady shear flow, J. Fluid Mech., 250, 609-633 (1993).

Chen J., Shen J., Swelling behaviors of polyacrylate superabsorbent in the mixtures of water and hydrophilic solvent, J. Appl. Polym. Sci., 75, 1331-1338 (2000).

Cherdhirankorn, T., Lerdwijitjarud, W., Sirivat, A., Larson, R.G., Dynamics of vorticity stretching and breakup of isolated viscoelastic droplets in an immiscible viscoelastic matrix, Rheol. Acta, 43, 246-256 (2004).

Cox, R.G., The deformation of a drop in a general time-dependent fluid flow, J. Fluid Mech., 37 (3), 601 – 623 (1969).

De Bruijn, R.A., Tip streaming of drops in simple shear flows, Chem. Eng. Sci., 47 (2), 277-284 (1993).

de Gennes, P.-G., Scaling concepts in polymer physics, Cornell University Press, Ithaca and London, 1979, Chapter 5.

Degussa Newsletter, 2003.

des Cloizeaux, A naive approach to the physics of polymer networks: remarks, questions and prospects. In: Baumgärtner, A., Picot, C.E., eds., Molecular basis of polymer networks, Proc. Phys., 42, Springer-Verlag, Heidelberg, 1989, pp. 2-10.

Dubrovskii, S.A., Lagutina, M.A., Kazanskii, K.S., Method of measuring the swelling pressure of superabsorbent gels, Polym. Gels and Networks, 2, 49-58 (1994).

Dubrovskii, S.A., Rakova, G.V., Elastic and osmotic behavior and network imperfections of nonionic and weakly ionized acrylamide-based hydrogels, Macromolecules, 30, 7478-7486 (1997).

Dubrovskii, S.A., Rakova, G.V., Lagutina, M.A., Kazanskii, K.S., Poly(ethylene oxide) hydrogels with charged groups at network junctions, Pol. Sc. Ser.A, 41, 1062-1067 (1999).

Dubrovskii, S.A., Rakova, G.V., Lagutina, M.A., Kazanskii, K.S., Osmotic properties of poly(ethylene oxide) gels with localized charged units, Polymer, 42, 8075 – 8083 (2001).

Dušek, K., Prins, W., Structure and elasticity of non-crystalline polymer networks, Adv. Polymer Sci., 6, 1-102 (1969).

Dušek, K., Dušková-Smrčková, M., Stewart, R., Kopeček, J., A model for swelling changes in a covalently crosslinked gel caused by unfolding of folded domains, Polymer Bulletin, 47, 351-358 (2001).

Erman, B., Flory, P.J., Critical phenomena and transitions in swollen polymer networks and in linear macromolecules, Macromolecules, 19, 2342-2353 (1986).

Evmenenko, G., Budtova, T., Structural changes in hydrogels immersed in a linear polymer solution studied by SANS, Polymer, 41, 4943-4947 (2000).

Fernández-Nieves, A., Fernández-Barbero, A., de las Nieves, F.J., Interfacial tension and a volume phase transition of microgel particles, Macromol. Symp., 151, 521-527 (2000).

Flory, P.J., Principles of polymer chemistry, 7th ed., Cornell University Press, Ithaca and London, 1969.

Frith, W.J., Lips, A., The rheology of concentrated suspensions of deformable particles, Adv. Colloid Interface Sci., 61, 161-189 (1995).

Geissler, E., Hecht, A.-M., Horkay, F., Zrinyi, M., Compressional modulus of swollen polyacrylamide networks, Macromolecules, 21, 2594-2599 (1988).

Ghodgaonkar, P.G., Sundararaj, U., Prediction of dispersed phase drop diameter in polymer blends: the effect of elasticity, Pol. Eng. Sci., 36 (12) 1656-1665 (1996).

Grace, H.P., Dispersion phenomena in high viscosity immiscible fluid systems and applications of static mixers as dispersion devices, Chem. Eng. Commun., 14, 225-277 (1982).

Groot, R.D., Bot, A., Agterof, W.G.M., Molecular theory of strain hardening of a polymer gel: application to gelatin, J. Chem. Phys., 104 (22), 9202-9219 (1996).

Groot, R.D., Bot, A., Agterof, W.G.M., Molecular theory of the yield behaviour of a polymer gel: application to gelatin, J. Chem. Phys., 104 (22), 9220-9233 (1996).

Grosberg, A.Y., Khokhlov, A.R., Statistical physics of macromolecules, AIP press, New York, 1994.

Guido, S., Simeone, M., Greco, F., Effects of matrix viscoelasticity on drop deformation in dilute polymer blends under slow shear flow, Polymer, 44, 467-471 (2003).

Gundogan, N., Melekeslan, D., Okay, O., Rubber elasticity of poly(*N*-isopropylacrylamide) gels at various charge densities, Macromolecules, 35, 5616-5622 (2002).

Hachani, E., Etude du comportement de gels de polymers dans de l'huile silicone et sous écoulement de cisaillement simple, Trainee report, CEMEF/Ecole des Mines de Paris, Sophia-Antipolis, 2000.

Hasa, J., Ilavsky, M., Dusek, K., Deformational, swelling, and potentiometric behavior of ionized poly(metacrylic acid) gels. I Theory, J. Polym. Sci. Polymer Physics, 13, 253-262 (1975).

Hasa, J., Ilavsky, M., Deformational, swelling, and potentiometric behavior of ionized poly(metacrylic acid) gels. II. Experimental results, J. Polym. Sci. Polymer Physics, 13, 263-274 (1975).

Hayashi, R., Takahashi, M., Yamane, H., Jinnai, H., Watanabe, H., Dynamic interfacial properties of polymer blends under large step strains: shape recovery of a single droplet, Polymer, 42, 757-764 (2001).

Hoffman, A.S., Intelligent polymers in medicine and biotechnology, Macromol. Symp., 98, 645-664 (1995).

Horkay, F., Zrinyi, M., Studies on mechanical and swelling behaviour of polymer networks on the basis of the scaling concept. 6. Gels immersed in polymer solutions, J. Macromol. Sci.-Phys., B25(3), 307-334 (1986).

Horkay, F., Geissler, E., Hecht, A.-M., Zrinyi, M., Osmotic swelling of poly(vinyl acetate) gels at θ temperature, Macromolecules, 21, 2589-2594 (1988).

Horkay, F., Hecht, A.-M., Geissler, E., Effect of cross-links on the swelling equation of state: polyacrylamide hydrogels, Macromolecules, 22, 2007-2009 (1989).

Horkay, F., Hecht, A.-M., Zrinyi, M., Geissler, E., Effect of cross-links on the structure of polymer gels, Polymer gels and networks, 4, 451-465 (1996).

Horkay, F.; Tasaki, I.; Basser, P., Osmotic swelling of polyacrylate hydrogels in physiological salt solutions, Biomacromolecules, 1, 84-90 (2000).

Ilavský, M., Mamytbekov, G., Bouchal, K., Hanyková, L., Phase transitions in swollen gels: 27. Effect of negative charge concentration on swelling and mechanical behaviour of poly(*N*-vinylcaprolactam) gels, Polymer bulletin, 43, 109-116 (1999).

Inci, M.N., Erman, B., Okay, O., Durmaz, S., Elastic behaviour of solution cross-linked poly(isobutylene) gels under large compression, Polymer, 42, 3771-3777 (2001).

Iso, Y., Koch, D.L., Cohen, C., Orientation in simple shear flow of semi-dilute fiber suspensions. 2. Highly elastic fluids, J. Non-Newt. Fluid Mech., 62, 135-153.

Janssen, J., Dynamics of liquid-liquid mixing, Ph.D. thesis, University of Technology, Eindhoven, 1993.

Jeffery, G.B., The motion of ellipsoidal particles in a viscous fluid, Proc. Royal Soc. London, A102, 161-179 (1922).

Karybiants, N.S., Philippova, O.E., Starodubtsev, S.G., Khokhlov, A.R., Conformational transitions in poly(methacrylic acid) gel/ poly(ethylene glycol) complexes. Effect of the gel cross-linking density, Macromol. Chem. Phys., 197, 2373-2378 (1996).

Katchalsky, A., Lifson, S., Eisenberg, H., Equation of swelling for polyelectrolyte gels, J. Polymer Sci. letters, 7, 571-574 (1951).

Katchalsky, A., Lifson, S., Eisenberg, H., Errata Equation of swelling for polyelectrolyte gels, J. Polymer Sci., 8, 476 (1952).

Katchalsky, A., Michaeli, I., Polyelectrolyte gels in salt solutions, J. Polym. Sci., 15, 69-86 (1955).

Kavanagh, G.M., Ross-Murphy, S.B., Rheological characterisation of polymer gels, Prog. Polym. Sci., 23, 533-562 (1998).

Kayaman, N., Okay, O., Baysal, B.M., Phase transition of polyacrylamide gels in PEG solutions, Polym. Gels and Networks, 5, 167-184 (1997).

Kayaman, N., Okay, O., Baysal, B.M., Swelling of polyacrylamide gels in polyacrylamide solutions, J. Polym. Sci., 36, 1313-1320 (1998).

Kazanskii, K.S., Dubrovskii, S.A., Chemistry and physics of “agricultural” hydrogels, Adv. Polym. Sci., 104, 97-133 (1992).

Khokhlov, A.R., Swelling and collapse of polymer networks, Polymer, 21, 376-380 (1980).

Khokhlov, A.R., Kramarenko, E.Y., Collapse of a polymer gel induced by complex formation with linear polymers, Makromol. Chem., Theory Simul., 2, 169-177 (1993).

Knaebel A., Rebre S.R., Lequeux F., Determination of the elastic modulus of superabsorbent gel beads, Polymer gels and networks, 5, 107-121 (1997).

Kramarenko, E.Y., Khokhlov, A.R., Yoshikawa, K., A three-state model for counter-ions in a dilute solution of weakly charged polyelectrolytes, Macromol. Theory Simul., 9(5), 249-256 (2000).

Kulicke, W.-M., Nottelmann, H., Structure and swelling of some synthetic, semisynthetic and biopolymer gels. In: J. E. Glass ed., Polymers in aqueous media, Adv. Chem. Series, 223, ACS, Washington DC, 1989, p. 15-44.

Lac, E., Barthès-Biesel, D., Pelekasis, N.A., Tsamopoulos, J., Spherical capsules in three-dimensional unbounded Stokes flow: effect of the membrane constitutive law and onset of buckling, J. Fluid Mech., 516, 303-334 (2004).

Lagutina M.A., Dubrovskii S.A., The swelling pressure of weakly ionic acrylamide gels, Polym. Sci. A, 38, 1059-1064 (1996).

Li Y., Tanaka T., Phase transitions of gels, Annu. Rev. Mater. Sci., 22, 243-277 (1992).

Macosko, C., Rheology: principles, measurements and applications, Wiley/VCH, Poughkeepsy, New York, 1994.

Maffetone, P.L., Minale, M., Equation of change for ellipsoidal drops in viscous flow, J. Non-Newtonian Fluid Mech., 78, 227-241 (1998).

Mamytbekov, G., Bouchal, K., Sedlakova, Z., Ilavsky, M., Phase transition in swollen gels: 25. Effect of the anionic comonomer concentration on the first-order phase transition of poly(1-vinyl-2-pyrrolidone) hydrogels, European Polym. J., 35, 451-459 (1999).

Mamytbekov, G., Bouchal, K., Ilavsky, M., Phase transition in swollen gels: 26. Effect of charge concentration on temperature dependence of swelling and mechanical behaviour of poly(*N*-vinylcaprolactam) gels, European Polym. J., 35, 1925-1933 (1999).

Mancini, M., Moresi, M., Rancini, R., Uniaxial compression and stress relaxation tests on alginate gels, J. Food Text. Stud., 30, 639-657 (1999).

Manning, G.S., Limiting laws and counterion condensation in polyelectrolyte solutions. I. Colligative properties, J. Chem. Phys., 51, 924-933 (1969).

Matzelle, T.R., Geuskens, G., Kruse, N., Elastic properties of poly(*N*-isopropylacrylamide) and poly(acrylamide) hydrogels studied by scanning force microscopy, Macromolecules, 36, 2926)2931 (2003).

Melekaslan, D., Okay, O., Swelling of strong polyelectrolyte hydrogels in polymer solutions : effect of ion pair formation on the polymer collapse, Polymer, 41, 5737-5747. (2000).

Melekaslan, D., Gundogan, N., Okay, O., Elasticity of poly(acrylamide) gel beads, Polym. Bulletin, 50, 287-294 (2003).

Momii, T., Nose, T., Concentration-dependent collapse of polymer gels in solution of incompatible polymers, Macromolecules, 22, 1384-1389 (1989).

Milimouk, I., Hecht, A.M., Beysens, D., Geissler, E., Swelling of neutralized polyelectrolyte gels, Polymer, 42, 487-494 (2001).

Minale, M., Deformation of a non-Newtonian ellipsoidal drop in a non-Newtonian matrix: extension of Maffetone-Minale model, J. Non-Newtonian Fluid Mech., 123 (2-3), 151-160 (2004).

Muniz, E.C., Geuskens, G., Compressive elastic modulus of polyacrylamide hydrogels and semi-IPNs with poly(N-isopropylacrylamide), Macromolecules, 34, 4480-4484 (2001).

Nisato, G., Skouri, R., Schosseler, F., Munch, J.-P., Candau, S.J., Elastic behaviour of salt-free polyelectrolyte gels, Faraday Discuss., 101, 133-146 (1995).

Nisato, G., Schosseler, F., Candau, S.J., Sweling equilibrium properties of partially charged gels: the effect of salt on the shear modulus, Polym. gels and networks, 4, 481-498 (1996).

Obukhov, S.P., Rubinstein, M., Colby, R.H., Network modulus and superelasticity, Macromolecules, 27, 3191-3198 (1994).

Okamoto, K., Takahashi, M., Yamane, H., Shape recovery of a dispersed droplet phase and stress relaxation after application of step shear strains in a polystyrene/polycarbonate blend melt, J. Rheol., 43 (4), 951-965 (1999).

Okay, O., Durmaz, S., Charge densitiy dependence of elastic modulus of strong polyelectrolyte hydrogels, Polymer, 43, 1215-1221 (2002).

Okuzaki, H., General theory of gel preparation. In: Osada, Y. and Kajiwara, K. eds., Gels Handbook Vol. 1, Academic Press, San Diego, 2001, p. 98-117.

Oosawa F., Polyelectrolytes, Marcel Dekker Inc., New York, 1971.

Osada, Y., Sato, M., Conversion of chemical into mechanical energy by contractile polymers performed by polymer complexation, Polymer, 21, 1057-1061 (1980).

Osada, Y., Polymer gels: crosslink formations. In: Osada, Y. and Kajiwara, K. eds., Gels handbook Vol. 1, Academic Press, San Diego, 2001, p. 13-25.

Panyukov, S.V., Scaling theory of high elasticity, Sov. Phys. JETP, 71 (2), 372 – 379 (1990).

Peleg, M., Campanella, O.H., The mechanical sensitivity of soft compressible testing machines, J. Rheol., 33 (3), 455-467 (1989).

Philippova, O.E., Starodubtzev, S.G., Intermacromolecular complexation between poly(methacrylic acid) hydrogels an poly(ethylene glycol), J.M.S.-Pure Appl. Chem., A32(11), 1893-19023 (1995).

Rallison, J.M., The deformation of small viscous drops and bubbles in shear flow, Annu. Rev. Fluid Mech., 16, 45-66 (1984).

Rhodorsil, Material Safety Data Sheet, Rhône-Poulenc, 1996.

Ross-Murphy, S.B., Formation, structure and properties of physical networks. In: Stepto, R.F. ed., Polymer networks: principles of their formation, structure and properties, Blackie Academic and Professional, London, 1998, p. 289-315.

Rubinstein, M., Colby, R.H., Dobrynin, A.V., Joanny, J.-F., Elastic modulus and equilibrium swelling of polyelectrolyte gels, Macromolecules, 29, 398-406 (1996).

Sayil, C., Okay, O., Macroporous poly(N-isopropyl)acrylamide networks: formation conditions, Polymer, 42, 7639-7652 (2001).

Schosseler, F., Ilmain, F., Candau, S.J., Structure and properties of partially neutralizef poly(acrylic acid) gels, Macromolecules, 24, 225-234 (1991).

Schröder, U.P., Opperman, W., Properties of polyelectrolyte gels. In: Cohen-Addad, J.P. ed., The physical properties of polymeric gels, John Wiley and Sons Ltd., Chichester, 1996, p. 19-38.

Seyvet, O., Etude rhéooptique de l'imprégnation et de la dispersion d'agglomérats de silice en suspension dans des polymers, Ph.D. thesis, Ecole des Mines de Paris, Sophia-Antipolis, 1999.

Shenoy, S.L, The effect of uniaxial deformation on swollen gels, Polym. gels and networks, 6, 455-470 (1998).

Sigillo, I., Di Santo, L., Guido, S., Grizutti, N., Comparative measurements of interfacial tension in a model polymer blend, Polym. Eng. Sci., 37 (9), 1540-1549 (1997).

Skouri, R., Schosseler, F., Munch, J.P., Candau, S.J., Swelling and elastic properties of polyelectrolyte gels, Macromolecules, 28, 197-210 (1995).

Tanaka, T., Collapse of gels and the critical point, Phys. Rev. Lett., 40, 820-823 (1978).

Tanaka, T., Phase transitions in gels and a single polymer, Polymer, 20, 1404 – 1412 (1979).

Tanaka, T., Fillmore, D., Sun, S.-T., Nishio, I., Swislow, G., Shah, A., Phase transitions in ionic gels, Phys. review letters, 45 (20), 1636 – 1639 (1980).

Tanaka, T., Gels, J. Ch. Soc. Am., 244, 110-123 (1981).

Taylor, G.I., The viscosity of a fluid containing small droplets of another fluid, Proc. Roy., Soc. London, A138, 41-48 (1932).

Taylor, G.I., The formation of emulsions in definable fields of flow, Proc. Roy., Soc. London, A146, 501-523 (1934).

Treloar, L.R.G., The physics of rubber elasticity, 3rd ed., Clarendon Press, Oxford, 1975, P. 74.

Tucker, C.L., Moldenaers, P., Microstructural evolution in polymer blends, Annu. Rev. Fluid Mech., 34, 177-210 (2002).

Vasilevskaya, V.V., Khokhlov, A.R., Swelling and collapse of polymer gel in polymer solutions and melts, Macromolecules, 25, 384-390 (1992).

Vervoort, S., Budtova, T., Evidence of shear-induced polymer release from a swollen gel particle, Polym. Int., 52, 553-558 (2003).

Vervoort, S., Budtova, T., Shear-induced gel widening and solvent release in the vorticity direction, Colloids and surfaces A: Physicochem. Eng. Aspects, 262, 132-138 (2005).

Vervoort, S., Patlazan, S., Weyts, J., Budtova, T., Solvent release from highly swollen gels under compression, Polymer, 46, 121-127 (2005).

Weyts, J., Mechanical properties of highly swollen gels at high deformations, Master's thesis, K.U. Leuven, 2001.

Whiting, C.J., Voice, A.M., Olmsted, P.D., McLeish, T.C.B., Shear modulus of polyelectrolyte gels under electric field, J. Phys.: Condens. Matter, 13, 1381-1393 (2001).

Whiting, C.J., Voice, A.M., The shear modulus of polyelectrolyte gels as a function of swelling degree in the lightly-swollen low-salt regime, submitted to macromolecules, (2002).

Yamane, H., Takahashi, M., Hayashi, R., Okamoto, K., Observation of deformation and recovery of poly(isobutylene) droplet in a poly(isobutylene)/poly(dimethyl siloxane) blend after application of step shear strain, J. Rheol., 42 (3), 567-580 (1998).

Yamauchi, A., Gels: Introduction. In: Osada, Y. and Kajiwara, K. eds., Gels Handbook, Vol.1, Academic Press, San Diego, 2001, p. 4-11.

Zanina, A, Budtova, T., A hydrogel particle under shear: a rheo-optical study of the particle deformation and solvent release, Macromolecules, 35, 1973-1975 (2002).

Zanina, A., Vilesov, A., Budtova, T., Shear-induced solvent release from gel particles: application to drug-delivery systems, Int. J. Pharm, 242, 137-146 (2002).

Zeldovich, K.B., Khokhlov, A.R., Osmotically active and passive counter-ions in inhomogeneous polymer gels, Macromolecules, 32, 3488-3494 (1999).

Zeo, U., Tarabukina, E., Budtova, T., Kinetics of shear-induced gel deswelling/solvent release, J. Controlled Release, *accepted*, 2005.

Zrinyi M., Horkay, F., Studies on mechanical and swelling behaviour of polymer networks on the basis of the scaling concept. 5. Crossover effects above and below the θ temperature, Macromolecules, 17, 2805-2811 (1984).

Zrinyi, M., Horkay, F., On the elastic modulus of swollen gels, Polymer, 28, 1139-1143 (1987).

Appendix A: Calculation of tip volume

Observe a gel particle with tips. The dimensions of this entity are defined in the figure below. The gel particle is characterised by its length, L, height, H, and width, W. The distance between the edges of the tips is named L', and the maximum height of the tip is denominated H_t. L, L', H and H_t. W is an unknown. The initial dimension L_o of the particle must also be known.

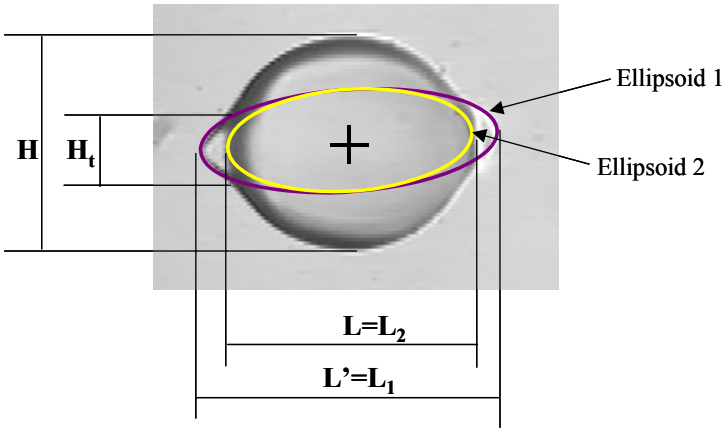

The total volume will always remain constant:

$$V_o = 2 * V_{tip} + V_{particle} \quad \textbf{[A-1]} \text{ where } V_{particle} = \frac{1}{6} L * H * W .$$

The exact volume of the tips needs complex calculations, but estimates allow building some ideas on their volume. Two different approaches are proposed below.

Approach 1

Suppose the tips are true cones with height (L'-L) and bottom surface diameter H_t.

$$V_{cone} = \frac{1}{3} \pi \frac{H_t^2}{4} \frac{(L - L')}{2} \qquad \textbf{[A-2]}$$

Supposing the two tips are identical, the total volume in the tips is then given by

$$\boxed{V_{tips} = 2 * V_{cone} = \frac{\pi}{12} H_t^2 (L - L')} \qquad \textbf{[A-3]}$$

This approach was used by Zanina and Budtova (2002).

Approach 2

Consider ellipsoids 1 and 2. Both have the same height and width, but their length is different:

$L_1 = L'$

$H_1 = H_2$

$W_1 = W_2 = W$

$L_2 = L$

First, ellipse 1 has to be characterised. In a Cartesian framework, an ellipse is generally described as

$$\frac{x^2}{a^2} + \frac{y^2}{b^2} = 1 \qquad \textbf{[A-4]}$$

'a' is the long axis and 'b' is the short axis of the ellipse. For ellipse 1 holds thus $2a = L'$ and $2b = H_1$.

Extra information we have on ellipse 1 is that at position L/2, its height is approximately H_t. The point $(L/2, H_t/2)$ lies thus on the ellipse.

$$y = \pm b\sqrt{1 - \frac{x^2}{a^2}}$$

$$H_1 = 2b = \frac{2|y|}{\sqrt{1 - \frac{x^2}{a^2}}} = \frac{H_t}{\sqrt{1 - \frac{L^2}{L'^2}}} \qquad \textbf{[A-5]}$$

The tip volume can be calculated as the volume difference between ellipsoids 1 and 2:

$$2V_{tip} = V_1 - V_2 = \frac{\pi}{6} H_1 W_1 (L' - L) \qquad \textbf{[A-6]}$$

where W_1 can be estimated using **[A-1]:**

$$V_o = V_{particle} + (V_1 - V_2)$$

$$L_o^3 = LHW_1 + H_1 W_1 (L' - L)$$

$$\Rightarrow W_1 = \frac{L_o^3}{LH + H_1 (L' - L)} \qquad \textbf{[A-7]}$$

Substitution of **[A-7]** in **[A-6]** allows calculating the volume in the tips:

$$2V_{tip} = \frac{\pi}{6} \frac{H_t}{\sqrt{1 - \frac{L'}{L}}} \frac{L_o^3}{\left[LH + \frac{H_t}{\sqrt{1 - \frac{L'}{L}}} (L' - L) \right]} (L' - L) \qquad \textbf{[A-8]}$$

Appendix B: Publications and presentations at conferences

Papers

S. Vervoort, T. Budtova, Evidence of shear-induced polymer release from a swollen gel particle, Polymer Int., 52, 553-558 (2003).

S. Vervoort, S. Patlazhan, J. Weyts, T. Budtova, Solvent release from highly swollen gels under compression, Polymer, 46, 121-127 (2005).

S. Vervoort, T. Budtova, Shear-induced gel widening and solvent release in the vorticity direction, Colloid Surfaces A: Physicochem. Eng. Aspects, 262(1-3), 132-138 (2005).

Presentations

S. Vervoort, A. Zanina, T. Budtova, Shear-induced solvent release from a highly swollen hydrogel, **Formula III**: Concepts et stratégies émergents en formulation: du laboratoire à l'industrie, 13–16 October 2001, La grande Motte, France.

S. Vervoort, T. Budtova, Libération d'une solution de polymère par cisaillement simple à partir d'une particule de gel gonflée, **Matériaux Polymères Stimulables**, workshop organised by the Groupe Français des Polymères, 12-13 November 2001, Grenoble, France.

S. Vervoort, T. Budtova, Ejection de solvant d'une particule de gel gonflé induite par cisaillement, **4èmes Journées du GFP-Méditerranée**, 29-30 April 2002, Sophia-Antipolis, France.

S. Vervoort, A. Zanina, T. Budtova, Shear-induced solvent release from a swollen gel: a rheo-optical study, **Work-shop "Controlled-release systems in cosmetic and personal care"**, May 2002, Lyon, France.

S. Vervoort, T. Budtova, Shear-induced polymer solution release from a highly swelling hydrogel, **Europolymer Conference 2002,** Polymeric gels: interesting synthetic and natural soft materials, 2-7 June 2002, Gargnano, Italy.

T. Budtova, A. Vilesov, A. Zanina, S. Vervoort, Shear-induced deformation and solvent release from microgels and capsules, **4th International Symposium "Molecular Mobility and Order in Polymer Systems"**, June 2002, St.-Petersburg, Russia.

T. Budtova , P. Navard, , A. Zanina, S. Vervoort, Shear-induced solvent release from a swollen hydrogel particle, **Polymer Networks 2002**: Functional networks and gels, 16th Polymer Networks Group meeting, 2-6 September 2002, Autrans, France.

S. Vervoort, T. Budtova, Shear induced solvent release from microgels, **3rd International Symposium on Food Rheology and Structure**, 9-13 February 2003, Zürich, Switzerland.

T. Budtova, S. Vervoort, A. Zanina, Shear-induced solvent release from microgels and capsules, **XIth International Workshop on Bioencapsulation**, 25-27 May 2003, Illkirch, France.

S. Vervoort, T. Budtova, Déformation et éjection de solvant d'un gel sous contrainte mécanique, **5ème Journée du GFP Méditerranée**, 6 June 2003, Montpellier, France.

S. Vervoort, T. Budtova, Rheo-optical study of suspended gel particles under shear flow, **Rhodia International Conference**, Third ed., 15-17 July 2003, Lyon, France.

T. Budtova, S. Patlazhan, S. Vervoort, J. Weyts, Solvent release from highly swollen gels under compression: an important phenomenon that has to be taken into account, **38eme Colloque Annuel du Groupe Française de Rhéologie**, October 2003, Brest, France.

T. Budtova, S. Patlazhan, S. Vervoort, J. Weyts, Hydrogels under mechanical stress: deformation and solvent release, **Structure Sensitive mechanics of Polymer Materials. Physical and Mechanical Aspects**, January 2004, Moscow, Russia.

S. Vervoort, A. Zanina, T. Budtova, Shear-induced microgel deformation and solvent release, **3rd Russian Kargin conference – Polymers 2004**, January 2004, Moscow, Russia.

T. Budtova, E. Tarabukina, S. Vervoort, U. Zeo, Controlled release from microgels induced by shear, **40th International Symposium on Macromolecules**, July 2004, Paris, France.

T. Budtova, S. Vervoort, Comparison between microgel and droplet behaviour under shear, **The XIVth International Congress on Rheology**, August 2004, Seoul, South Korea.

COMPORTEMENT D'HYDROGELS GONFLES DANS DES SOLUTIONS DE POLYMERES SOUS ACTION MECANIQUE

RESUME

Le comportement d'hydrogels polyélectrolytiques gonflés de solutions de polymère linéaires soumis à une contrainte mécanique (cisaillement, compression) est étudié avec des outils rhéo-optiques afin d'obtenir une meilleure compréhension du comportement de gel et d'ouvrir la voie vers des applications dans des formulations cosmétiques.

L'étude en cisaillement a été effectuée avec des particules de gel isolées suspendues dans une matrice d'huile silicone. Différents régimes ont été identifiés: a faible contrainte, la particule se déforme, mais moins qu'une goutte de son solvant. Au-delà d'un premier seuil de contrainte, nous observons le relargage de bouts de solvant dans la direction de l'écoulement. Ces bouts restent attachés à la particule. Le solvant est libéré et dispersé dans la matrice au-delà d'une deuxième contrainte seuil. Relargage et éjection ont également été observés dans la direction de la vorticité. Des volumes importants de solvant peuvent être libérés. Les effets de la taille de la particule, du degré de gonflement, de la concentration de la solution de polymère et de la tension interfaciale ont été étudiés.

L'étude en compression a été réalisée avec des disques de gels gonflés à l'équilibre d'eau ou d'une solution de polymère et entourés d'air. Le gel se déforme et relargue partiellement son solvant dès qu'il est soumis à une contrainte. L'analyse thermodynamique d'un tel système prédit que ce relargage est plus important pour des gels chargés que pour des gels neutres.

Mots clés : Hydrogel, déformation, relargage contrôlé, rhéo-optique, cisaillement simple, compression

BEHAVIOUR OF HYDROGELS SWOLLEN IN POLYMER SOLUTIONS UNDER MECHANICAL ACTION

ABSTRACT

The behaviour of highly swollen polyelectrolyte gels containing linear polymer solutions submitted to mechanical stresses (shear, compression) was studied using rheo-optical tools in order to gain understanding in gel behaviour and to open the way towards the application of hydrogels in cosmetic applications.

Shear stresses were imposed on isolated gel particles suspended in a silicone oil matrix. Different regimes were identified: at the lowest stresses, the particle only deforms, but less than a droplet of its solvent would do. Above a first threshold stress, release of some solvent is observed in the flow direction. The solvent tips stay attached to the particle. The solvent can be detached and dispersed into the matrix at stresses above a second critical stress. Release and ejection were also observed in the vorticity direction. Important volumes of solvent can be set free. The effects of particle size, degree of swelling, polymer solution concentration and interfacial tension were evaluated.

The compression tests were executed with gel disks swollen at equilibrium in water or in a polymer solution and surrounded by air. The gel deforms and releases some solvent as soon as it undergoes some stress. The thermodynamical analysis of such system predicts that release is more important for weakly charged gels than for neutral-ones.

Key words : Hydrogel, deformation, controlled release, rheo-optics, simple shear flow, compression